

**FEDERAL SERVICE FOR HYDROMETEOROLOGY AND ENVIRONMENT MONITORING**

**STATE RESEARCH CENTER OF RUSSIA  
“ARCTIC AND ANTARCTIC RESEARCH INSTITUTE”**

# **SEA ICE OBSERVATIONS**

Manual



Saint-Petersburg  
SSC RF “AARI”

2009

**Sea Ice observations. Manual– Saint-Petersburg: SSC “AARI”, 2009. – 300p.**

The manual is intended to train “ice experts – ice observers” as a main methodic document for preparing to studies or self education.

The book consists of systematical description of principles and methods of obtaining sea ice information. The methods are based on long-term experience, accumulated during expedition support and work of operational support of economical activity in freezing seas.

Manual can be used by specialists in hydrometeorology, navigators, specialists, supporting offshore platforms and terminals, established in the Arctic and freezing seas, and also to train specialists in the field of “Polar hydrometeorology”.

ISSBN

© State Scientific Center of the Russian Federation “Arctic and Antarctic Research Institute”, Saint-Petersburg. 2009.

## Content

Preface	4
Introduction	5
1. History of observations and regularities of sea ice formation	
1.1. History of sea ice observations in the Arctic and freezing seas	8
1.2. Regularities of sea ice formation depending on hydrological and meteorological conditions	21
2. Ice conditions in the Arctic and freezing seas	
2.1. Characteristics of the Baltic Sea ice condition	47
2.2. Characteristics of the White Sea ice conditions	56
2.3. Characteristic of the Barents Sea ice conditions	65
2.4. Characteristics of the Kara Sea ice conditions	74
2.5. Characteristics of the Laptev Sea ice conditions	89
2.6. Characteristics of the East-Siberian Sea ice conditions	105
2.7. Characteristic of the Chukchi Sea ice conditions	120
2.8. Characteristics of ice conditions in the Beaufort Sea	133
2.9. Characteristic of ice conditions in the Central Arctic Basin	149
2.10. Characteristic of the Bering Sea ice conditions	163
2.11. Characteristics of ice conditions in the Sea of Okhotsk	168
2.12. Characteristic of ice conditions in the Sea of Japan	174
3. Types of ice observations	
3.1. Remote sensing observations of ice cover	181
3.2. Airborne observations. General information	188
3.3. Ice observations from ships	192
3.4. Ship telemetric system for ice thickness recording	200
3.5. Dangerous ice phenomena and ice formations	209
3.6. Ice impact on engineering structures	227
Conclusion	228

## **Preface**

Training manual is intended to train “ice experts – ice observers” and to be main methodic document for self-preparing for lessons or self education.

“Ice experts – ice observers” are located in 21<sup>st</sup> classifying subdivision of All-Russian classifier of occupations OK 010-93 (corresponding to International Standard Classification of Occupations ISCO-88) as specialists of high level in the field of natural and engineering science. Activity, foreseen for this subdivision, is characterized by high complicity level of occurred work and corresponds to skill level, which is defined as having high professional education.

Training manual was prepared according to cooperation program between State Scientific Center “Arctic and Antarctic Research Institute” and company «BP Trading Limited” in 2007-2009. Program coordinators were Graham Thomas (BP) and E.U. Mironov (AARI). Head of the project is V.V. Stepanov (AARI).

Authors: E.U. Mironov – editing, preface, introduction, section 3.5.1, V.V. Stepanov – editing, sections 1.1, 3.1, conclusion, Z.M. Gudkovich - section 1.2, A.V. Yulin - sections 2.1-2.3, 2.10-2.12, V.P. Karklin - sections 2.4-2.8, S.V. Frolov - sections 2.9, 3.3, A.D. Masanov - section 3.2, A.E. Klein - section 3.4, V.Yu. Benzeman – sections 3.5.2, 3.5.3, V.A. Likhomanov - section 3.6. Yu.D.Bichenkov

Training manual is intended for specialists in hydrometeorology, ship navigators and also specialists, supporting offshore platforms and terminals in the Arctic and freezing seas.



## **Introduction**

Ice observations are the basis of ice cover condition studies and can be divided into visual and instrumental. Regular visual observations of sea ice started in the beginning of XX century, at first during ship expeditions, then during organization of stationary meteorological stations and implementation of ice reconnaissance flights.

From the middle of 30-s and till the end of 80-s airborne ice reconnaissance was one of the most essential means for obtaining information about ice conditions in the Arctic and freezing seas. Apart from that, regular ice observations in open sea were made by oceanographic expeditions “Ice patrol”, which regularly operated in all Arctic Seas. Methodic of visual ice observations was steadily improved and till the beginning of 90-s principal ice information was obtained from ice reconnaissance airplanes.

In 1961 training courses were organized at Arctic and Antarctic Research Institute (AARI) to train young specialists, especially ice observers, conducting airborne ice reconnaissance. AARI was a guidance centre in Russia, because specialists from Regional departments of hydro meteorological service took these courses.

When regular airborne reconnaissance stopped its work in 1991, images, received from Earth Observation satellites, became the most important source of sea ice information. Ice observers were obliged to re-train into specialists of satellite images interpretation.

Thus, the courses for ice observers stopped its training work due to end of regular ice reconnaissance and sharp economical changes in Russia in the 90-s. Nevertheless, increasing marine activity in the Arctic shelf and freezing seas (construction of new terminals, ice-resistant stationary platforms and increasing of navigation intensity) in the beginning of XXI century raise new requirements to quality and content of ice information. Regular ice observations are necessary in regions, where terminals and platforms are located, to provide safe navigation operations. High-quality ice observations are necessary along ship routes to work out recommendations of optimal sailing routes of container vessels, tankers and service vessels.

In accordance to this, question about renewal of courses for ice observers became really essential. In 2007 the program, directed to organization and providing of ice observers training, was developed. The following work was done within this program:

- development of a "ice expert – ice observer” training course concept;
- development of educational programs for speciality “ice expert – ice observer”;
- development of educational methodic plans for specialty “ice expert – ice observer”;
- development and preparation of science-methodic materials;
- accounting of standard- legal documents for organization of educational course;

- training of first experimental group of “ice expert – ice observer”.

Course concept is based on subject-orientated approach to studies, directed to formation of professional skills in in a degree, which allows ice experts working out recommendations, used as a basis for decision-making during conducting marine operation.

The methodic basis of the course is description of the subject through understanding of knowledge about regularities (physical processes) of ice cover formation, manifestation of its properties and their observation as phenomena (specific ice conditions).

During the course students must obtain theoretical and methodic knowledge about ice observations and sea ice mapping, and also practical skills in IT-technologies, used for ensuring activity in freezing seas.

Analysis of the first stage work results showed, that development and creation of appropriate training manual are also necessary for preparation of full set of methodic materials, and supplying courses of raising qualification level or specialists retrain. Training manual must present a document for self-preparing to studies and self-education. It must consist of summaries of brief theoretical and practical questions for self-preparing.

Main tasks of manual are the following:

- acquaintance with the history of instruments and methods of ice observations development;
- systematization of audience knowledge on formation of integrated idea of ice cover formation;
- studying sea ice types and peculiar features of its formation, depending on hydrological and meteorological conditions;
- studying ice regime regularities in the Arctic and freezing seas;
- studying international sea ice nomenclature, international and national sea ice symbolics;
- studying and understanding methods and ways of sea ice observations in the Arctic and freezing seas (aircraft – airplanes and helicopters, ship – visual and instrumental observations), and also by means of remote sensing data.

Training manual is orientated to integrate skills and knowledge, obtained by students during learning basic university disciplines by specialties, included in concept of “hydrometeorology”. It is the basis of post-graduated education and advanced professional training of specialists in new fields of hydrometeorology and related disciplines, being regulated by the following normative documents:

- Federal law from 22 of August, 1996, № 125-ФЗ "About high and post-graduated professional education" (Collected legislation of Russia Federation, 1996, № 35, p. 4135);

- Rules of development, confirmation and consummation of state educational standards of primary, secondary, secondary professional, high professional and post-graduated professional education (appr. By Government regulation of RF from 21 of January, 2005, № 36);

- Government State Standard of high professional education, direction 510900 – Hydrometeorology Degree – Magister of Hydrometeorology (approved by vice-Minister of Education of RF on 10 of March, 2000. Number of government registration 112 EH / mar);

- Government State Standard of high professional education. Government requirements to minimum content and education level of graduating student by specialty 012800 – OCEANOLOGY (Approved by vice-chairman of State Universities Commission of Russia on 7 of June, 1994).

## **1.1. History of ice conditions observations in freeze-up seas**

The history of ice observations is closely connected with Arctic exploration history. Several stages of study can be separated, every of which reflects it's own principal approach to ice observation arrangement and is connected with particular stage of observation instruments and methods development or is the cause of information demand.

The first stage – the most long-term – is connected with process of getting separate and unperiodical data about ice cover of freeze-up seas during trade of other type of activity. In the given period the process of ice data obtaining wasn't independent type of activity.

The first written evidence about sea ice is relative to 350 and 310 years B.C. It was said, that Greek Pytheas from Massalia reached a “gloomy land”, next to which “there is no sea or land or air with some mixture of all a this hanging in space”. Some separate written evidences about appearance of first Norsemen in the Arctic Seas were found.

In this period development of sea ice mapping technologies occurred independently from ice science development – ice study, and mostly came after development of seafaring in Arctic – compiling of sea navigational maps (charts). Seafarers noticed separate ship and expeditions navigation, distinguished stages of North exploration, but at the same time they hadn't always fixed information about natural phenomena and processes. First historical data about pomors, who had first settlements on the White Sea coast, was in XI century. Parallel to walrus and seal hunting they were getting an experience of ice navigating and gave it to each other as separate written notices or verbal messages. According to this evidences Lomonosov M.V. in the second half of XVIII century wrote “The brief description of different travels by Northern Seas and showing the possible route by Siberian Ocean to Eastern India”. In the third chapter of this book, called “About possibility of navigation by Siberian Ocean to Eastern India, considered by natural circumstances”, he wrote: “The main difficulty in this routing is cold, i.e. ice, made from it. So this subject must be considered very serious, because it is located to Northern Ocean and our route, and the main theory of warm and cold, and ice appearance should be fully described”.

In his research M.V. Lomonosov summarized separate data about ice characteristics and propagation in the Arctic Ocean and made some science hypothesis, summaries and forecasts, and also made public special terminology of ice science, which wasn't significantly changed till nowadays.

Specifically he wrote: “... Drifting sea ice is showing three types”:

1) Small grease ice, which like snow floats in water, sometimes it is prickly, but despite of some connection, flexible and isn't harmful for ships;

2) Mountains of irregular shape, which depth under water is from 30 to 50 sajenes, above

water part is 10 or more, cracking all the time, like wood in oven, therefore can be indentified at night or in fog, and navigators must be careful, because they are dangerous id storm, especially on shallow areas, when cracking with noise;

3) Hummocked ice or ice floes, sometimes lasting for several versts, mixed with small ice. A lot of similar ice floats and gets ships stuck. It is necessary to distinguish floating ice mountains (№2) from type which consists from broken hummocked ice.

Considered differences and amount of ice, it is necessary to observe these movements in Siberian Ocean. Bit it is impossible without having information about currents, high and low tides, which are followed by great ice, only small and thin follow the wind, and hummocked ice are moved mostly by lower water, so often opposite movements of small and great ice are seen at one place..”

This science work by Lomonosov M.V. is very valuable even at the moment, not only because it was the first general summarizing attempt of expedition observation, but because the range of thoughts, hypothesis and summaries, which became the basis of independent science direction – ice study - was given in this book.

The first through navigation on the route of Northern Sea Route was occurred by Swedish scientist A.E. Nordensheld with supply of Russian goldminer A.M. Sibiriakov, Swedish King Oscar II and manufacturer O. Dixon only in 1878.

On the boarder of XIX - XX centuries polar expedition on schooner *Zarya* headed by E.Toll was organized under management of Russian Imperial Science Academy. Expedition purpose was to investigate the Laptev Sea and Novosibirskiye islands. New materials in meteorology, polar ice, geology, geophysics, biology and zoology were received.

In 1910–1915 the Hydrographic Expedition to the Arctic Ocean was organized onboard the ships of the icebreaking type *Taymyr* and *Vaygach*, which made the epoch-making geographical discovery of the twentieth century – the Severnaya Zemlya archipelago. Observations f ice cover were episodic during expedition. Nevertheless, it was noticed, that Arctic Seas are not covered with ice ultimately, and their ice regime is not similar for different years.

However, observations were not regular and obtained data were fixed with time intervals sometimes till several years, which didn’t assist to formation of entire picture about ice origin in Arctic and ice cover dynamics in the Polar Seas and in Arctic Ocean.

*This stage of observations development, characterized by non-systematic approach to data receiving in ice science, when information about ice cover condition was obtained incidentally with occurrence of other main purpose, lasted almost till second decade of XX century.*

By the end of this period the necessity of occurrence of special organization, having wide financial and technical facilities, icebreakers and icebreaking type ships, network of radio and

meteorological stations to provide navigation in ice, became obvious. By this time (1911-1915) experience of organization radio stations in Arctic, which gave to ships meteorological and ice information, was stored. V.A. Rusanov suggested, that it was necessary to provide aerial observations using balloon, located on board.

This approach started systematical mapping of ice regime from results of special ice observations. Planes started to be used in observations for navigation support. It allowed providing regular observations of propagation, features, dynamics of sea ice and its interannual variability.

The first visual remote observations of sea ice were made in 1897 by Salomon Andree from the air balloon during his attempt to reach the North Pole. This flight demonstrated the possibility of visual remote observations of the sea ice, but simultaneously showed that balloons were not viable for this purpose.

In 1913, following the expedition onboard the icebreaking ships *Taymyr* and *Vaygach*, the possibility of using an airplane specifically for ice reconnaissance was proposed by B.A. Vilkitskiy. The Russian pilot Yan Nagursky on the hydro-airplane *Maurice Farman* implemented this idea in 1914. This is the birth of the airborne ice reconnaissance and marks the beginning of sea-ice remote sensing.

During 1918-1921 flights were not conducted.

Observational flights were provided again after and of Civil War in 20s to support transport operations in Arctic Ocean. As early as 1920, the first Siberian “bread-expedition” sailed from Arkhangelsk to the Ob’ and Yenisey River mouths and from 1921 to 1928, the Kara Sea trade-exchange expeditions were made on a regular basis. For supervising these expeditions, the Committee of the Northern Sea Route (CNSR) was set up in 1920 and the Northern Research Commercial Expedition was established, which was commissioned to conduct not only the geographical studies but also investigations in the interests of many branches of the national economy (geological exploration, fishery, hunting, etc.). During this period navigation support on Northern Sea Route was absent.

In 1925 the Northern Research Commercial Expedition was reorganized to the Research Institute on the Study of the North (from 1930, the All-Union Arctic Institute). In the sphere of activity of this institute, predominantly the oceanographic, meteorological, geophysical and geographic investigations were developed.

Parallel to it in USSR United Weather Service is establishing.

*Next stage (20s - late 40s of XX century) was the stage of beginning of regular navigation on NSR and, respectively, organization of regular system of hydro meteorological (and ice) observations.*

Constant increasing of transportation volume needed increasing of terms of polar navigation,

what was impossible without caravan steering with the help of icebreaker and regular, not episodic, air reconnaissance on route.

In these escort ice reconnaissance flights, routes were made from the ship as radial track lines with the distance from it over 50–100 km. For surveying some sea area, the sketch of the routes presented a combination of parallel and radial track lines.

Considered period of Arctic exploration coincided with development of aircraft building and their active usage in different activities – military, transport and touristic. In fact on dirigible NORGE R. Amundsen in May of 1926 first flew over the North Pole. Large aerial photography was occurred in Arctic. In 1931 German dirigible LZ-127 *Graf Tsepellin* flew with science purpose above Soviet Arctic and occurred detailed aerial photography over its territory and water area, covered with sea ice.

Flight route was Friedrichshafen (Germany) - Leningrad – Franz-Joseph Land (Tikhaya Bay) – Northern Zemlya – Taymyr peninsula – Dixon Island – Novaya Zemlya - Arkhangelsk - Leningrad - Germany.

Director of ARI Samoilovich R.L. headed science crew of specialists, accompanied flight on board of dirigible. During three days *Graf Tsepellin* had passed Franz-Joseph Land, Northern Zemlya, Taymyr peninsula and Novaya Zemlya. From the moment of departure from Leningrad and till arrival to Berlin dirigible spent 106 hours in air or 4 days and 10 hours. Aerial photography was occurred during flight. Specialists estimate, that *Graf Tsepellin* did work equivalent to 2-3 years of hard work with usage of icebreakers. 90 measurements were done from dirigible and plenty of other observations and researches. During expedition first Molchanov's spheres-radiosondes were set in Polar sky, with height of rising up to 20 km.

However, science world didn't see results of aerial photography. German officials said, that film was light-struck. There is an opinion, that materials were not lost, but were used by Germany in planning of military activities in Arctic during Great Patriotic War.

Planes were also widely used in sea ice observations, beginning from 1929 duration of air reconnaissance flights started to increase. Hydroplanes, based on water areas near harbors and polar stations, were used in ice, trade and aerial photography reconnaissance. Flights had mostly searching pattern – planes approached to ships, then went according their route and back. They sent verbal message (on radio) to captains of ships or icebreakers about ice regime and probable route. Flights routes were mostly absent on ice charts.

Development of navigation on NSR increased, and airborne reconnaissance planes needed obtaining of more précised information about ice condition and its propagation. At the same time unification of observation rules became obvious. In 1938 sector of navigation characteristics developed “Temporary navigation manual for ice airborne reconnaissance of 1938». It was

considered, that route composition must be provided by pilot. Pilots or navigators performed ice observations – visual assessment of the ice distribution and characteristics – in addition to their main duties. With no aids and instructions, the pilots themselves developed indicators characterizing ice conditions and methods for compiling the ice charts. The observers determined, assessed and plotted the ice edge position, concentration, shapes of ice floes and characteristics of their surface (level, ridged, snow puddles) on the charts.

It is necessary to note that the flight charts at that time were not quite accurate while the navigation equipment of airplanes included only a magnetic compass (operating not quite reliably under the Arctic conditions), a speedometer and a navigation cursor.

In 30s flights in Arctic didn't have particular science purpose, they were connected with ice reconnaissance, planes testing in Arctic conditions, providing medical service, exploration new routes, fur export and social tasks.

In 1932 planes were used during expedition for aerial observation of inner part of Chukchi Peninsula and total geographic and geological reconnaissance with direct science purpose.

Tactics of air reconnaissance before 1933 had episodic character. Observations occurred by navigator, and each of them contributed in development of observations methods and ice mapping.

1936 year – can be called last year of “escort aircraft” usage together with ice-breaking type ships leaders. Hydroplanes were used with this purpose, which were delivered to regions of work on ships disassembled. These ships at the same time served as airdromes – bases. Before departure hydroplane were put in water, and after landing it was taken back on board.

Main amount of hydroplanes was based in comfortable for landing and setting off closed bays, rivers or near polar stations or settlements. But they couldn't be referred to escort aviation any more. Thus, in 30s *ice observations — visual estimation of ice propagation and ice condition — were occurred by pilots or navigators as additional task to their main duties. Military and transport planes were used for observations.*

Pilots themselves developed indicators characterizing ice conditions and methods for compiling the ice charts defined decoded features by themselves, because there weren't any special documents or instructions. During ice charts compiling they used conventional designations, listed in ship instructions. The observers determined, assessed and plotted the ice edge position, concentration, shapes of ice floes and characteristics of their surface (level, ridged, snow puddles) on the charts. The development and improvement of the method of visual airborne ice observations also continued in subsequent years.

In December 1932, by the Decision of the USSR Government, the Main Administration of the Northern Sea Route (MANSR) was created. Among planning and providing of sea operations and their hydro meteorological supplement The MANSR had to be in charge for river transport in the



North, arrangement of seaports and airports, development of industry, exploration of minerals, trading, etc.

Simultaneously, the HMS system was developed and improved, its scientific center being the Arctic Research Institute. This system included: polar stations, weather bureau, ice reconnaissance aircrafts, Marine Operations Headquarters (MOH) onboard line icebreakers and service of long-range forecasting and planning of marine operations at ARI.

Marine expeditions of the Ice Patrol began regular operations in 1935–1937. They recorded the ice edge location and carried en-route oceanographic observations.

Planes had a very limited range and were not suitable for conducting ice observations and preparing ice charts onboard.

Apart from that, organization of stable ice observations had difficulties with imperfect planning of ice observations – *the quantity of planes and specialists (board observers) were not enough and conditions for mapping on board were imperfect.*

At first, in 1933 special for ice reconnaissance R. Bartini developed plane project – distant arctic reconnaissance plane. It was supposed, that it would be some kind of northern all-terrain plane. It was a flying submarine, able to set off and land on water and ice. Length of ship hull was 18,4 m and width - 2,8 m. Plane was produced in the end of 1935. Testing was occurred in Leningrad in spring of 1936. Flight duration under overloading mass 9000 kg was more than 20 hours. According to tests in MANSR it was decided to construct five vehicles, but this project wasn't finished.

In nearly the same time another specialized for Arctic plane was developed. It was named “Amphibia of northern region”. Plane was constructed in Leningrad in spring of 1935, but also wasn't produced in series.

In 1929 V.Yu. Vize suggested organizing science drifting station, which was opened in 6<sup>th</sup> of June, 1937 near the North Pole. After 9 months of drift (274 days) station was transported to the Greenland Sea. Ice floe passed more than 2000 km. Meteorological and hydrological researches about ice condition occurred on station during entire drift.

In 1938 the Department of Ice Service was created at the ARI, which was later called the Department of Ice Forecasting. From that time the pre-navigation ice reconnaissance was conducted (first, in June, then with extending navigation dates, in May and April). Based on data of these reconnaissance flights, ARI developed ice forecasts for arctic navigation and planned sea operations.

From 1939, board-observers were assigned to some ice reconnaissance aircraft. They provided uninterrupted observations during flight and didn't disturb on plane routing and other navigators duties. Such approach significantly simplified navigator's work in complicated weather

conditions, especially when planes had to move flyby. On the other hand, necessity of registering uninterrupted observations and maximum differentiating of ice characteristics made obvious necessity of creating united system of ice terminology, conventional designations and mapping, development of quantitative estimations and estimation methodic of ice cover.

Nomenclature of sea ice charts compiling was in general developed and tested to middle of 40s, and wasn't significantly changed till 50s.

Purpose of ice reconnaissance before 1940 mainly was search of most successful routes among ice for caravans of transport ships and icebreakers. Listed observations were not enough accurate to make some science summaries.

During the years of Great Patriotic War, the major part of the cargo turnover was from east to west, and main goods and food supplies were transported along the NSR.

For unification of ice reconnaissance, occurred in war period, in MANSR was validated and developed standard scheme of flight routes. Decade ice reconnaissance was occurred more or less regularly, regions and terms of navigation reconnaissance were defined and corrected depending on ice conditions and navigation regime.

The conditions for performing ice reconnaissance significantly improved after putting two-engine airplanes *LI – 2*, reequipped for purposes of ice reconnaissance. Additional fuel tanks were installed in the passenger cabins increasing the flight range and duration, and for observers, blisters were equipped considerably improving the observation conditions and a table for plotting the ice charts.

System of conventional designations in this period significantly improved. From 1941 observers began to assess the total ice concentration in tenths, which was given in a circle. In 1942 coloring of the zones in accordance with concentration gradations zone was applied, an in winter – coloring by age.

Thus, by the end of the war the terminology, scales and a system of symbols were mainly elaborated with only some minor changes and additions introduced later.

By the middle of the 1940s, ARI specialists jointly with pilots and navigators of Polar Aviation summarized this work and prepared a comparatively complete manual on visual airborne ice reconnaissance that was published in 1946.

Working technology foresaw entering results in ice air observations log. Flight conditions – altitude, visibility, wind, course, shore orientation marks and turning point coordinates – were registered in log. Then after the flight route correction, the working ice chart was prepared based on these records. Observers marked registered route parts with similar characteristics of ice cover. After plotting two or three track lines, it was generalized and zones with the same characteristics were identified by method of spatial interpolation and depicted by the adopted conventional

designations.

Observations were made in the band of 19–20 flight altitudes (ice edge, boundaries of zones of different concentration) to 2–3 altitudes (age composition), which is explained by a different reliability and, in general, possibility to determine some characteristics or other at larger observation angles. The accuracy and reliability of the assessment of sea-ice parameters and characteristics significantly depended on the conditions of illumination, horizontal visibility, meteorological conditions and the correct choice of the flight altitude under the specific conditions.

The observation data were disseminated to users in several ways.

By first one, immediately after landing at the airport combined with the MOH, the working ice chart copy was transferred to the Headquarters.

For transferring the reconnaissance results to icebreakers and ships, the method of dropping was widespread – an ice chart copy was put to a special box with a long red ribbon and a wooden buoy, which was dropped from a low-level flight to the icebreaker's or ship's deck.

The method of ice observation data transmission from board aircraft in the form of radio-telegraph ice reports – a prototype of modern formats of letter-digital ice charts was also very widespread.

Depending on the type of reconnaissance, the ice conditions were described either along the flight route or over the area – characteristics of ice zones and turning points of their boundaries were enumerated.

*Period from the beginning of 50s and till 70s was stage of most intensive usage of visual ice reconnaissance, because methods of observation and observations instruments corresponded with each other – there were methodic of providing observations on board of special equipped planes.*

During this period re-equipment of the fleet began. Three line icebreakers of the type *Captain Belousov* were built, 1960–1969 – five diesel-electric icebreakers of the *Moskva* type. In 1959 first nuclear icebreaker *Lenin* was produced with a power 44 000 h/p. Ships of the Arctic ice class ULA *Lena* type are implemented.

From 1960 helicopters, located on icebreakers' deck started to be used in Arctic air reconnaissance. As a rule, their crew consisted from pilot and board-observer (icebreaker hydrologist).

Main feature of helicopter reconnaissance is its uninterrupted connection and interaction with icebreaker or ship, because helicopter sets off, when icebreaker needs help in defining further route in complicated ice conditions.

Another feature is probability to make detailed picture of ice propagation and its condition, received from plane of air reconnaissance. When the velocity of plane is high, it is physically impossible to fix small details. Thus, ice conditions on charts of plane reconnaissance are rather

generalized. Helicopter reconnaissance presents ice regime before the caravan or icebreaker on small area. Helicopter, having less velocity and purpose to find optimal route, searches for details.

This feature of helicopter reconnaissance sometimes were considered as “optical illusion” in eyes of some navigators. They suggested that ice reconnaissance can use helicopter and powerful icebreaker only. But without plane reconnaissance, during which main features of ice regime were defined, or without image with high resolution, received from satellite, helicopter reconnaissance didn’t work.

Other feature of helicopter reconnaissance was complete dependence from local weather conditions.

Usage of helicopter in transport ships steering with leadership of powerful icebreakers and preliminary observation of ice regime from data of plane reconnaissance increases velocity of ship caravan in two times.

And, finally, helicopter and icebreaker can be used as instrument for studying ice cover composition in different spatial scales, its structure and condition, and also propagation of ice tensions and decay. In many cases icebreakers work for long time on particular limited part of route, and many aspects of ice cover variability can be studied. Disadvantage of helicopter reconnaissance is, that under large flying time only a small amount of ice charts is left, useful for science research of large water areas.

System of hydro meteorological support was developed parallel with development of air instruments of ice reconnaissance:

- About 100 polar meteorological stations worked,
- Six regional radio meteorological centers (in Amderma, on Dixon, Chelyuskin, in Tiksi, Pevek and on Cape Schmidt) worked,
- Four Arctic science-research observatories (is. Kheisa, Tiksi, Pevek, Dixon).
- Three-level system of HMS was formed;
- Central Forecasting Service in Moscow;
- Service of long-range navigation forecasting and planning at AARI on base of ARI;
- Scientific-operational groups at three Marine Operations Headquarters (Dikson, Tiksi and Pevek).

In 1964, MANSR was reorganized to the Administration of the Northern Sea Route (ANSR) of the Ministry of Marine Fleet (MMF) with surveillance functions. Transport ships and icebreakers were given to the MMF shipping companies, the Administration of Polar Aviation to the Ministry of Civil Aviation and the HMS for shipping in the Arctic and Antarctic and its operators (AARI, RRMC, a network of polar stations) were transferred to the USSR Hydro meteorological Service.

In the 1950s, visual airborne ice reconnaissance continued to be the main tool for sea-ice

monitoring and HMS of arctic navigation. Annually, 30–40 airplanes carried out 500–700 ice reconnaissance flights. However, the accuracy of visual observations did not already satisfy navigators and scientists.

Necessity of science generalization data about sea ice for purpose of analyze and forecast determined the need in receiving and systematization of data amount, which visual reconnaissance couldn't give.

*These circumstances made conditional necessity to transit to instrumental ice observations, and under direct supply of navigation. Next stage in sea ice observations (1960-1970) became stage of testing and implementation of technical instruments in sea ice observations.*

In the 1940s, aerial photography was the only airborne remote-sensing tool. Just in the end of this period AARI first did experimental planned aerial photography of sea ice, and in 1951 aerial photography group was formed. In 1967, the Laboratory of Instrumental Ice Reconnaissance was created on the basis of this group at the same department and in 1984 – an independent Department for improvement of the system and methods of ice observations was established.

Aerial photography is difficult to transport to users in appropriate terms. Film, separate cadre is impossible to proceed in faster regime, and make complicated photogrammetric proceeding of planned-prospective shots on board. Thus, aerial photography couldn't be used in operational purposes.

In 1950-1970 in addition to aerial photography new remote instruments started to be used in ice observations: panoramic radio station and a radar video-pulse meter of ice thickness, which allowed to measure ice thickness with accuracy 10 % in range 45-250 cm within limits of operational height from 200 to 2000 m.

In 1964 development of side-looking radar station started special for ice reconnaissance. In 1965 it was used in first ice observations. In September 1967 work of aerial side-looking radar station *Toros* were finished, and they equipped 2 planes AN-24 (cruising speed of 450 km/h, flight range 2700 km, operating altitudes 5000-6000 m). In the tail compartment, a topographic aerial photo camera and a device for dropping the box with the ice chart to the icebreakers and ships from a low altitude were also installed.

Radar images were screened on an operational indicator and were simultaneously registered on the photo film of the electronic photo recording device. The photo films were developed by liquid photo reagents by means of a special processing device on board providing a possibility of their operational use.

In testing period of ice observation instruments it was possible to work with large amount of data. It allowed developing methods of proceeding information and images decoding, parallel with creating instruments themselves. Already in 1970, the methodological instruction *Airborne*

*observations of the ice cover using SLAR Toros and methods for coordination were created. Analytical programs of radar images proceeding were composed.*

Nit' system was introduced into operation. The system Nit' included an airborne complex Nit'-C and the icebreaker's data receiving and processing complex Nit'-L. The system Nit'-C provided the possibility of real time translation of radar images via a special radio line to an icebreaker or any other ground-based receiving point.

Among NSR planes with Nit' C system on board were used for ice observations on entire Arctic water area.

*Next stage in development of instruments and methods of ice observations (1970 - 1980) became stage of instruments usage and implementation in operational practice information, received from space instruments of remote sensing.*

TIROS-1 satellite launched in USA in 1960 had the onboard instrumentation including TV cameras predominantly for cloud observations. First publications with the indication of possible use of satellite images for sea ice observations appeared in 1961. In 1966 the Russian satellite of the *Meteor-1* series made by-frame imaging using two TV cameras with optical axes deviated from the vertical. The information was received only by the main ground-based receiving stations (Moscow, Novosibirsk and Khabarovsk). Image study gave experience of sea ice decoding and practice of ice charts compiling from television satellite images.

In 1975, the first satellite of the *Meteor-2* series was launched. Information in the analogue format was transmitted not only to the main receiving centers, but also in the on-line transmission mode to the automated information receiving points (AIRP). Constant operation in the on-line mode allowed using the received information for addressing operational tasks while simultaneous work in the storage mode made it possible to make ice observations on a global scale. Thus, AARI could receive images from Arctic and Antarctic. From this moment quantitative methods of proceeding satellite information at users objects started to develop. In the same year, 1975, an algorithm and software for analytical geolocation using a rather imperfect computer Iskra-1250 were elaborated.

First oceanographic satellite *Seasat* was launched in the USA on 8 of June, 1978.

In 1979 began the development of the oceanographic satellite with Side-Looking Radar (SLR) *Okean* series and it was launched on September 28, 1983. The instrumentation onboard this spacecraft in addition to SLR included scanning sensors in the optical range, passive microwave radiometer RM-08 and a system for data collection and transmission from the automatic buoys. Satellite data in the on-line transmission and storage-replay modes were transmitted both to the main receiving stations and to the AIRP. The work program included not only the spacecraft creation but also the development of the methods of processing and using the received information. During the period of satellite construction, a preliminary methodological handbook was prepared.

After launch in September 1983 (space craft “Kosmos-1500”) information was successfully used for ship steering in ice.

In February 2000, the last satellite of this series (*Okean-01*, No. 7) ended active operation.

By the mid-1970s, it became obvious that operational receiving of ice and hydro meteorological information for the entire Arctic Ocean, its maximum combining and use of advanced technologies for automatic processing and analysis, taking into account constantly expanding and changing requirements of different users, is feasible only on the basis of a systems approach to solving these tasks.

In 1975-1976, AARI developed a concept of the Automated Ice-Information System for the Arctic (AIISA). It envisaged combining and correlated functioning of all main subsystems such as: information acquisition and collection, processing, analysis, calculations and forecasts, transmission and dissemination.

In 1986 system AIISA as part of AARI was exploited.

Base of measure complex till early 1990-s consisted from planes and satellite observations. Data using, received on polar stations, drifting stations “Northern Pole”, automatic ice stations and ship observations, was provided.

Analyze of technical facilities of ice observations, showed, that under their complex usage all necessary navigation data can be received with high accuracy.

Spatial resolution of board instruments of modern satellites made plane observations not necessary on entire water area of Arctic Ocean.

It is necessary to mention, that of radar imaging for operational observation of ice cover, especially in polar and near polar latitudes can facilitate. The most advantage, comparing to optical observation system, is radar imaging can be provided, e.g. from Canadian RADARSAT-1, in a day, at night, and under any weather conditions. In winter with very short light day and with large periods of unfavorable weather radar imaging can be the only technology for receiving operational information about ice cover.

In winter in the North or in mild or southern latitudes it is typical, when complete cloudiness can be observed for a week or more, which make impossible survey in optical range. Radar imaging by means of radar SAR satellite RADARSAT-1,2 gives opportunity to receive images with resolution 8, 25, 50 and 100 m. Images are used in shipment supply, ice study and ice observations.

Remote sensing information at present time can be used with strategy purposes, in marine operations, in compiling of long-term and short-term forecasts. It is obligatory used by navigators in route planning of helicopter aerial reconnaissance.

Significant advantages of space observation – occurrence of frequency of information arrival and efficiency of proceeding – make possible fixing of natural phenomena, which change rapid, in

different time periods. Automatic technologies allow dividing ice by its concentration. As a result ice charts are composed from satellite data in navigation period, and also in autumn-winter and spring period (ice formation, ice clearance).

Among ice charts, composed by satellite images, the following types can be separated:

- Large-scale charts and plans of ice cover condition with scale 1:100 000 and larger on limited territory (in gulfs, straits, harbors);
- Operational ice charts with scale 1:200 000-1:300 000;
- Observation ice charts (monthly, decade). Such charts express ice cover condition on area of several seas (with scale 1:7 500 000 and less). They are used in science study and ice forecasting;
- Special charts, characterized ice regime. E.g., charts of particular ice age type propagation, charts of average and extreme edge location and ice boundaries, charts of average hummocking, charts of decay and other. On these charts summarized results of first observational and operational charts are presented.

At present moment best construction of ice observations is searched to provide national economy activity and exploration and transportation of hydrocarbonic raw materials from territories of Russian continental shelf. Variants of creating observation system, including orbit group of specialized satellites on polar ellipse orbits, when one satellite observes Arctic Ocean water area during 4-6 hours, is considered. Specialists – decoders of remote sensing information – would play the most important roles.



## 1.2. Regularities of sea ice formation depending on hydrological and meteorological conditions

Hydrometeorological processes, which cause changes of sea ice amount, are divided into *thermal* and *dynamic* by nature of influence. Effect of thermal processes leads to increasing or decreasing of ice amount by means of aggregative transformation water↔ice (ice growth and melting), and also can lead to changes of salinity and heat content of surrounding waters. Due to this heat content and salinity in ambient water changes. Effect of dynamic processes can lead to ice mass redistribution in any water area as the result of increasing concentration, diverging and ice hummocking. Ice mass also changes due to ice exchange with neighbor water areas. Thus, these types of processes cause changes of ice balance both in the unit of region, and in entire sea.

### 1.2.1. Thermal processes in ice cover of the Arctic Seas

Thermal processes have essential features in spring-summer and autumn-winter periods. Mathematical description of these processes differs respectively.

#### 1.2.1.1. Features of thermal processes in spring-summer period

The most significant process if this period is ice melting. Ice area and mass decrease in the vast water areas of the Arctic Seas. It directly influences terms of fast ice melting, values of ice cover and ice massifs area, changes of distribution of ice concentration.

Ice melting occurs as a result of ice cover heat absorption, coming from different sources (Fig. 1.2.1.). Combined influence of this heat on ice cover can be expressed by heat balance equation:

$$\frac{\partial m}{\partial t} = \frac{1}{\rho_{\text{ice}} L} (R + \Phi + D - W_{mc}), \quad (2.1.1)$$

where  $R$  – total heat flow, caused by radiation processes;

$\Phi$  – total heat flow, caused by turbulent processes;  $D$  – total heat flow, caused by advection processes;

$W_{tc}$  – part of total heat flow, which changes ice temperature;

In equation (2.1)  $R = Q_{\text{np}} + Q_p - Q_{\text{отр}} + E_a - E_n$ ,

Where:  $Q$  – short-wave component of solar radiation  $Q_{\text{np}}$  – direct,

$Q_p$  – diffused,

$Q_{отр}$  – reflected of its parts (sum  $Q_{np} + Q_p = Q_{сум}$  is called total radiation, and  $Q_{np} + Q_p - Q_{отр} = Q_{п}$  – incident radiation;  $E$  – long-wave component

$E_{л}$  – ice cover radiation,

$E_a$  – counter radiation of atmosphere ( $E_{л} - E_a = E_{эф}$  – effective radiation).

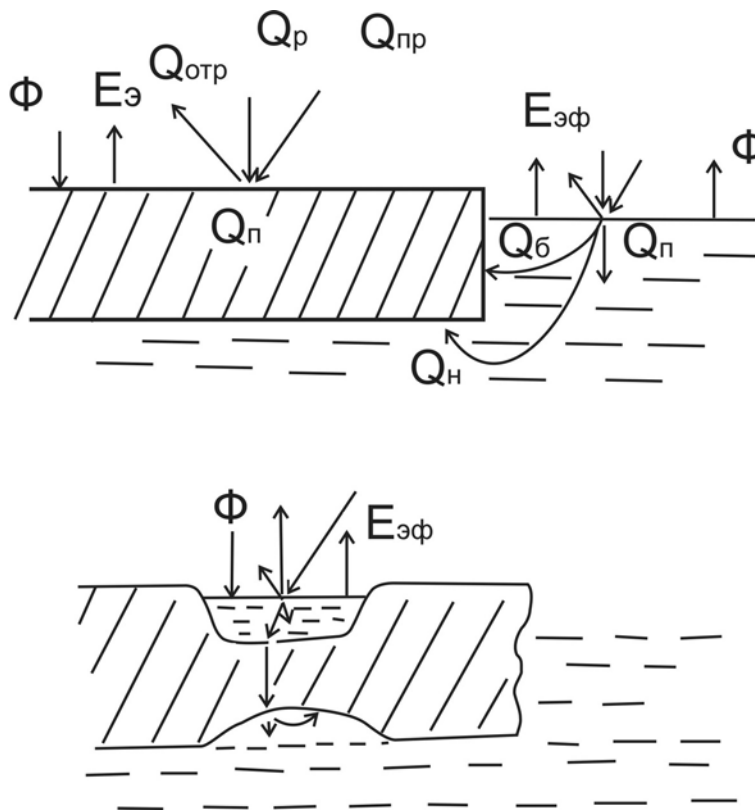


Fig. 1.2.1 – Scheme of ice cover heat balance components in summer

Turbulent processes are in effect both in atmosphere ( $\Phi_a$ ), and in water ( $\Phi_w$ ). The first ones have two components, one of which is determined by heat exchange, and the second is determined by moisture exchange, connected with changes of aggregate state water ↔ vapour and ice ↔ vapour.

Heat advection (D) in sea and atmosphere is significant within limited areas, where horizontal gradients of temperature (near ice edge) and current's velocity are high. On the larger part of the Arctic Seas this component, as well as  $W_{тс}$  value can be neglected in ice melting calculations.

Main features of other components of heat balance in spring-summer period are discussed.

Direct and diffused radiations depend on astronomical reasons (sun height above the horizon) and, thus, significantly change with latitude and during the year. Both components depend on cloudiness. However, if direct radiation decreases with the increase of cloudiness, diffused radiation, in contrary, increases. Due to this and due to small interannual variability of cloudiness in the Arctic in summer, interannual anomalies of total radiation are not large, and can be neglected in

calculation.

If  $E_{\text{пл}}$  and  $E_a$  are close in value,  $E_{\text{эф}}$  is small, changing during the year from 1,0 – 1,5 ccal/cm<sup>2</sup> in summer to approximately 2 ccal/ cm<sup>2</sup>month in winter. Interannual changes of these values don't normally exceed  $\pm 0,4$  ccal/ cm<sup>2</sup>month.

During May-September input part of heat balance exceeds its output. On average during this period  $Q_{\text{п}}$  is approximately 16 ccal/ cm<sup>2</sup>, that is enough for ice melting with thickness of 200 cm. It's the main heat source, spent on ice melting. Its interannual variability is mostly defined by albedo variability, because direct influence of cloudiness, moisture, ice ( $T_{\text{пл}}$ ) and temperature ( $T_a$ ) variability can be neglected.

Turbulent fluxes of explicit and latent heat are proportional to difference  $T_a - T_{\text{пл}}$ , at that proportional coefficients (Stanton and Dalton coefficients) depend on atmospheric stratification and wind velocity. Turbulent fluxes are normally large near coast and ice edge. In consequence of transformation  $T_a$  above melting ice (Fig. 1.2.2) with moving off the listed boundaries  $T_a$  rapidly approach to  $T_{\text{пл}}$ , that is why direct role of turbulent fluxes on the upper ice surface and its interannual variability in ice melting is not large. However, they significantly influence ice melting indirectly, defining the moment, when ice melting starts, on which albedo changes in the following time depend on.

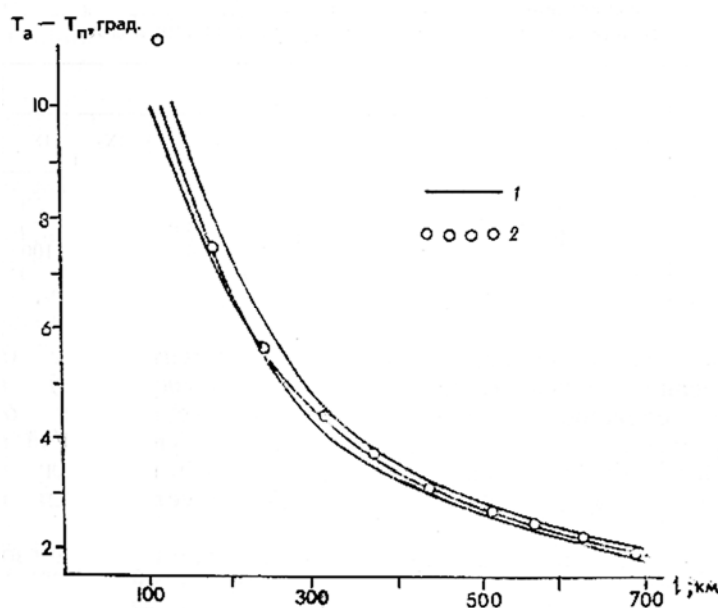


Fig. 1.2.2 – Changes of air temperature over ice cover in summer  
1 – empirical curves; 2 – their approximation

Question about albedo value of melting ice – is one of the most important in melting calculation, as  $Q_{\text{п}} = Q_{\text{сум}}(1 - A)$ . Value  $A$  depends on ice cover decay, values  $T_a$ , of initial ice thickness, thickness of melted layer, snow depth, depth and area of puddles. Relative area of puddles on average increases from 5% in the end of the first decade from the beginning of melting

to 35% in the end of third decade, after that due to melt water filtration through ice it gradually decreases to 5% in the end of eighth decade. Average area of puddles decreases with increasing hummocking and for smaller forms, and increases with reduction of ice thickness.

Simultaneous occurrence of several types of ice surface is typical for melting of ice cover. These are: snow cover, so-called dry ice zones and water surface of puddles and thaw holes. Reflectivity of these types is different. Gradual changes of radiative snow properties on average are characterized by albedo decreasing from 0,90 to 0,65. The last value is related to dry ice zones after snow cover disappearance. Further decreasing of albedo is caused by appearance and evolution of puddle area and depth (their reflectivity varies within limits of 0,10 – 0,40 depending on depth and pollution). Thus, when puddles are formed, which is close in time to ice melting beginning, albedo value and heat balance of snow-ice cover absolutely changes.

Solving equation of heat balance under condition  $T_a=T_{HT}$ ,  $T_n=0$ ,  $\partial h / \partial t = 0$ ,  $D=W_{TC}=0$ , is found from the following expression:

$$T_{hm} = \frac{0,25Q_{cym} - E_{\phi}}{0,624v} + 0,6 \quad (1.2.2)$$

From equation (1.2.2) it is found, that the bigger is  $Q_{cym}$  and the less is  $E_{\phi}$ , the lower is  $T_{HT}$  : -  $1,5 < T_{HT} < 2^{\circ}C$ .

At the moment, when  $T_a=T_{HT}$ , is term of melting beginning. From Fig. 1.2.3., on which the seasonal dependence of average and extreme air temperatures is compared to changes of  $T_{HT}$ , it is seen, that terms of melting beginning can vary from late May to early July.

On Fig. 1.2.4 annual mean dependence of decade values  $Q_{cym}$ , typical for the Arctic Seas is shown. Segment AB means period of probable terms of melting beginning. If melting begins in early terms, it'll cover period of maximum  $Q_{cym}$  values and maximum amount of solar energy will be spend on it. If melting begins in late terms, this amount will decrease twice comparing to the early terms of melting beginning. Amount of melted ice and terms of ice destruction change correspondingly.

Besides terms of melting beginning, ice cover melting (destruction) and thickness of ice, which survived summer melting, also depends on initial thickness of ice and snow.

If taking into account only melting of upper ice surface and under average conditions, ice in the south-western Kara and Chukchi Seas completely melts away to the end of second decade of August, and in the eastern East-Siberian Sea - to the middle of first decade of September.

In the other Arctic Sea regions ice doesn't completely melt away, and thickness of ice, which survived summer melting, is about 50 cm in the western East-Siberian Sea, about 60 cm in the

eastern Laptev Sea and about 100 cm in its western region and the north-eastern Kara Sea.

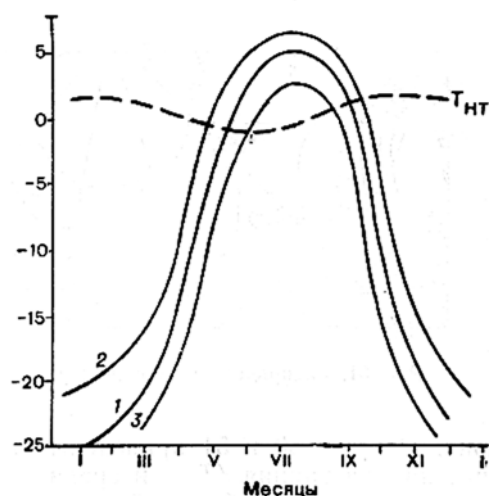


Fig. 1.2.3 – Seasonal dependence of average (1) and extreme (2,3) air temperatures in the Arctic Seas;  $T_{нт}$  – temperature of melting beginning

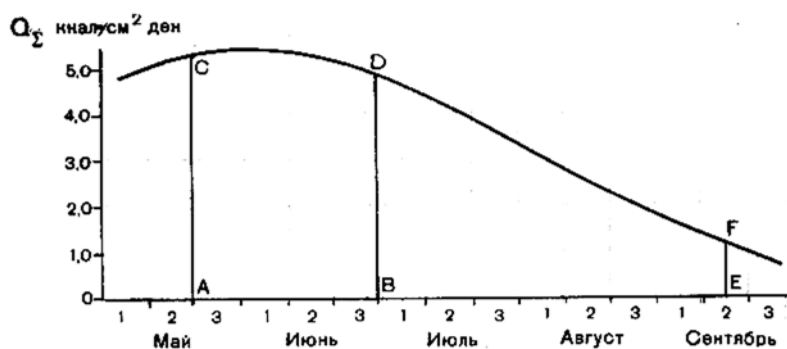


Fig. 1.2.4 – Annual mean dependence of 10-day mean values of total radiation in the Arctic Seas and terms of melting: A – earlier, B – later, E – end of melting

It is necessary to briefly consider special features of ice melting in puddles, which role in changes of ice cover albedo was shown before. Since attenuation of shortwave radiation in water ( $0,006 \text{ cm}^{-1}$ ) is about 40 times less, than in ice, significant part of solar energy reaches puddle bottom and penetrates further to ice cover bottom. This fact not only facilitates rapid increase of puddle depth, but it also creates conditions for ice bottom melting. Thus, roughness is formed on this surface, which exactly reflects upper ice surface roughness. Another process, which accelerates ice melting processes on puddle bottom, is intensive convection in puddles, connected with increasing of strongly desalinated water density during its heating. All these processes cause transition of puddles into thaw holes, which facilitate increasing area of fractures under decay of ice fields, i.e. ice cover diverging.

Melt water mainly drains under ice through thaw holes, because water level in puddles before thaw holes formation is located above sea level, but lower than upper ice surface. Ice layer is often formed in zone of its contact with salt water under ice, which temperature is lower than freezing

point of strongly desalinated melt water. Under strong drift this ice breaks and floats to the surface as shuga, partly filling thaw holes and hollow space in ice keels.

Melting from above is not the only process of ice melting in summer period. Latent melting of ice floes and, partly, from bottom, due to heat absorption by fractures are also important. It is necessary to enumerate the following circumstances to characterize this process.

- Open water among ice absorbs 2 – 4 times more heat than ice cover surface;
- One part of this heat is spent on latent melting (concentration changes), another – to melting from bottom (thickness changes), the third – to water heating;
- Observations show, that water heat content in fractures is not large (3–4 ccal/cm<sup>2</sup>); it increase, when fracture width increasing;
- The most reasonable suggestion was made by Yu.P. Doronin, is that part of heat absorbed in fractures ( $Q_{nb}$ ), which is spent on latent melting ( $Q_6$ ) and that from bottom ( $Q_n$ ) is proportional to  $N$  ( $N$  – concentration of ice cover, expressed in tenths):

$$Q_6 + Q_n = N \cdot Q_{nb} \quad (1.2.3)$$

- Question about proportion of  $Q_6/Q_n$  hasn't been solved;
- Role of  $Q_6$  in ice melting increases, when ice thickness and ice concentration decrease; for average conditions in the Arctic Seas it is comparable with the role of melting from above, proportional to value  $Q_n$ .

Only insignificant part of heat is spent on water heating before ice disappearance. Thus, maximum value of heat content depends on terms of sea surface clearance from ice. In regions, where ice cover disappeared in early terms (May-June), maximum heat content (to 18ccal/ cm<sup>2</sup>) is observed in late July-early August. Clearing terms influence insignificantly on maximum heating terms and its value. In contrary in regions, where ice cover disappears in late terms (July-August), terms of maximum heating change within limits of three decades, and its maximum value is up to 10 ccal/ cm<sup>2</sup>. Area of open water is the reliable indicator of maximum sea heat content.

Maximum value of water heating depends on its density stratification (depth of active layer). The largest depth of active layer in summer period is registered in the Kara and Chukchi Seas (up to 25-30 m). In the Laptev and East-Siberian Seas depth of this layer doesn't normally exceed 10 m. However, observations show that part of heat penetrates into pycnocline layer, where it remains even after ice formation on the surface. Further, as a result of convection and turbulent heat exchange, this heat reaches ice bottom, reducing velocity of ice growth process. In regions, where stratification is feebly marked (most part of the Barents Sea), maximum content of heat in sea exceeds 50 ccal/ cm<sup>2</sup>.

### 1.2.1.2. Peculiar Features of thermal processes in autumn-winter period

Main processes of autumn sea cooling, which in the Arctic Seas starts in late August – early September and lasts mainly during September-October, are: *effective radiation, turbulent heat exchange and evaporation* (approximately in equal parts). These fluxes in August-September are 0,5–2,5 ccal/cm<sup>2</sup>, increasing in October-November up to 2,0–4,0 ccal/cm<sup>2</sup>. Total effect of listed fluxes influence changes in space from less than 5 ccal/cm<sup>2</sup> in the Laptev and the East-Siberian Seas to 15 ccal/cm<sup>2</sup> in the western Kara Sea and in the central Chukchi Sea. Anomalies of heat loss are determined mostly by temperatures difference  $T_a - T_w$ , which normally depends on dominant wind direction.

Significant stage of ice growth process is its appearance on sea surface, free from ice cover. Following conditions have to occur on open sea surface to start stable ice formation: a) temperature of homogeneous surface water layer must decrease to water freezing point, taking into account this layer salinity; b) negative heat balance of water surface (by absolute value) must not be less than heat inflow to surface layer, caused by turbulent processes, convection and advection.

Nature of processes of heat exchange between atmosphere and sea significantly changes with the beginning of ice formation. Snow-ice cover, having high heat-insulating properties, becomes a factor, regulating this interaction. Effective radiation, which is directed from underlying surface to atmosphere during whole ice growth period due to large snow emissivity, is the main “term of expenditure” of snow-ice surface heat balance in winter period.

Turbulent fluxes  $\Phi_a$  during first winter half are also directed from ice surface to atmosphere, but as soon as values  $T_a$  и  $T_n$  become equal, they take the opposite direction.

Heat flux from ice bottom to its upper surface is itself sum of heat fluxes extracting on ice bottom under ice formation (latent crystallization heat), and heat, coming to ice bottom from underlying water layers as a result of turbulent and convectional mixing. This heat flux depends on heat-insulating properties of ice and snow. It increases with increase of temperature contrasts between lower and upper surfaces of ice cover, and decreases with ice thickening and snow height growth.

Estimations of heat fluxes, coming to ice bottom from water, significantly differ in works by different authors: above continental slope – from 4 to 6–8 ccal/cm<sup>2</sup>, above deep-water Arctic basin – from 1,0 to 1,5–3,0 ccal/cm<sup>2</sup>. Necessary to mention, that under influence of climate warming and corresponding strengthening of cyclonic activity above Arctic, not only temperature of deep Atlantic water increase, its upper boundary rise, but also salinity of upper mixed layer increase. As a result water stratification gets weaker, and heat flux from water column increases. Its changes

have to be reasonably estimated.

Large irregularity of ice cover thickness, different snow depth, and especially, occurrence of cracks, channels and leads cause irregularity in distribution of heat fluxes from underlying surface to atmosphere. In spite of rather small area of leads in compact ice cover, heat exchange with atmosphere through these formations is comparable with heat radiation of compact snow-ice cover.

Heat balance equation, similar to (1), can be used to calculate ice thickness changes in process of its growth, if substitute ice thickness  $H$  instead of ice mass  $m$ . However, accuracy of determination of components, consisting heat balance, is not high, because of their small value. Thus, other approach is used to determine ice thickness. So far as vertical heat flux through ice is proportional to ice heat conductivity  $\lambda$  and temperature gradient, and formed ice mass is proportional to crystallization heat  $L$ , heat balance equation on the ice-water boundary is given by:

$$L\rho \frac{\partial H}{\partial t} = \lambda \frac{\partial T}{\partial z} - F_w \quad (1.2.4)$$

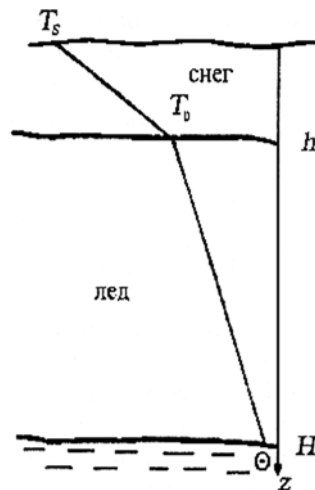


Fig. 1.2.5 – Temperature profiles for first-year ice - snow cover in winter

Expression (1.2.4) doesn't take into account almost permanent snow cover existing on ice surface, which influence ice thickness growth a lot. In order to allow for this influence, vertical temperature profile in ice and snow can be presented as broken line, coming through temperature values  $T_s$ ,  $T_0$  and  $\Theta$  (Fig. 1.2.5). It means that vertical heat flux in both mediums doesn't change, and is defined by the following equation:

$$\lambda \frac{\Theta - T_0}{H} = \lambda_s \frac{T_0 - T_s}{h} \quad (1.2.5)$$

where  $h, \lambda_s$  - snow depth and heat conductivity;



$T_0, T_s$  – temperature of ice and snow surface;

$\Theta$  - water freezing point.

From formula (1.2.5) we can derive equation for temperature on the ice-snow boundary as:

$$T_0 = \frac{H\lambda_s T_s + h\lambda\Theta}{h\lambda + H\lambda_s} \quad (1.2.6)$$

Exact solution of equation (1.2.4), taking into account (1.2.5) and (1.2.6), can't be obtained because real conditions of ice growth are complicated (inconstancy of vertical temperature gradient in ice, dependence of thermalphysic ice characteristics on temperature and salinity and etc.). Calculations using approximate formulas, obtained in some works, fit observational data. Under assumption that snow depth, and also thermalphysic characteristics of ice and snow are constant during temporal step, authors of work obtained the following formula for ice thickness calculating:

$$H = -\left(\frac{\lambda}{\lambda_s} h + \frac{F_w}{L\rho} \tau\right) + \sqrt{\left(\frac{\lambda}{\lambda_s} h + \frac{F_w}{L\rho} \tau\right)^2 + H_0^2 + \frac{2\lambda}{L\rho} (\Theta - T) \tau - \frac{2h\lambda}{\lambda_s} \left(\frac{F_w}{L\rho} \tau - H_0\right)} \quad (1.2.7)$$

calculations using formula (1.2.7) are made by method of successive approximations, according to which ice thickness, calculated on the previous step with length  $\tau$ , is entered to radicand

If put in formula (1.2.7) numeric values  $\lambda$  and  $\lambda_s$ , equal to 2,2 and 0,3 joule/msdegree respectively, and neglect heat flow from water ( $F_w$ ), simple formula can be received:

After substituting numerical values  $\lambda$  and  $\lambda_s$ , equal to 2,2 and 0,3 joule/m'sdegree respectively, in formula (1.2.7) and neglecting heat fluxes from water ( $F_w$ ), a simple formula is given by:

$$H = -7,0h + \sqrt{(7,0h + H_0)^2 + 0,00122(\Theta - T_s)\tau} \quad (1.2.8)$$

Growth of multiyear ice and ice, survived summer melting, has its own peculiar features. During melting of ice cover, especially its lower layers, content of liquid phase increases. Puddles stay on ice surface till the beginning of freezing. As a result heat sources of phase transfer occur in ice thickness, distorting quasi-linear vertical temperature changes. Under these conditions equation (1.2.8) becomes incorrect. Freezing process of puddles and liquid phase in ice depth leads to significant (sometimes for 2-3 months) delay of ice freeze-up on ice bottom. This circumstance, and also additional snow accumulation in zone of freezing puddles facilitates increase of mesoscale ice thickness irregularity. More complicated models are developed at the moment, taking into account phase transitions inside ice layer, nonlinearity of its temperature heat conductivity and heat capacity changes, depending on salinity.

Formula (1.2.8) allows calculating ice thickness in case of calm growth in the Arctic Seas in any moment of autumn-winter season – till the moment, when maximum thickness has reached, and also calculating ice thickness, formed in different time in water free from ice as a result of drift.

Reduction of ice thickening velocity with increasing its thickness, determined by thermodynamic processes, leads to idea of “equilibrium thickness”, understood as ice cover thickness, when winter ice growth is equal to summer melting. Equilibrium ice thickness and time of its reaching depend on climate conditions, especially on value of heat flux from water. According to calculations by Ivanov B.V. and Makshtas A.P., heat flux from water increasing from 2 to 8 watt/m<sup>2</sup> (from 1,5 to 6 ccal/cm<sup>2</sup>), cause equilibrium ice thickness decreases from 6 to 2 m. Ice cover thickness of the Arctic Seas doesn't normally reach equilibrium thickness, because of drift and gradual ice outflow southwards.

### **1.2.2. Dynamic processes in ice cover**

Being located on the boundary of dynamic environments – atmosphere and ocean – sea ice cover is constantly influenced by these environments, resulting in motion (drift) of ice formations. Ice cover regions, limited by area and connected with coast or sea bottom (fast ice, hummocked ice), are exceptions.

First systematical observations of ice drift, made by F. Nansen during transarctic expedition onboard *Fram* (1893–1896), allowed discovering, that ice drift in the Arctic Basin has two main components: wind component, closely connected with the local wind, and “non-wind”, which doesn't depend on the local wind at the moment of observations. The first component is caused by stresses at the upper ice cover surface, determined by relative air motion (wind), and the second is determined by different interrelated factors, such as gradient currents, sea level tilts, tidal phenomena, etc.

Direct observations of currents and water masses and different indirect methods, based on correlation of data on resulted ice drift and wind, or atmosphere pressure gradient for particular time periods, can be used to separate these components.

#### **1.2.2.1. Peculiar features of wind drift**

Velocity dependence from wind and barriers (shore, fast ice) and following to isobaric drift law are features of wind drift.

Wind drift velocity linear depends on velocity of wind, which caused it with quotient of given velocities (co-called wind coefficient,  $k$ ) on average close to 0,02. Direction of wind drift deviates

from wind direction to the right (in Northern hemisphere) on angle ( $\alpha$ ), on average close to  $30^\circ$ . Expressions for projections of wind drift velocity ( $V_x, V_y$ ) on Cartesian coordinate axis ( $x, y$ ), connecting them with corresponding wind velocity projections ( $W_x, W_y$ ), are given by:

$$\left. \begin{aligned} V_x &= k (W_x \cos \alpha + W_y \sin \alpha) \\ V_y &= k (W_y \cos \alpha - W_x \sin \alpha) \end{aligned} \right\} \quad (1.2.9)$$

Wind component of drift follows rather rapid after wind changes: ice drift gets stable normally in 3-6 hours after occurrence of stable wind.

Wind coefficient  $k$  and angle  $\alpha$  significantly change during the year: they increase from the end of winter to the middle of summer. Seasonal changes of value  $k$  are 50% of its average meaning, and changes  $\alpha$  – 40%.

Barrier occurrence (coast, fast ice) significantly influences size and direction of wind drift (normal to shore component decreases with approaching to coast).

Law of isobaric drift by N.N. Zubov is given by:

$$V_B = K \cdot (\partial P / \partial n) \quad (1.2.10)$$

Using known formulas for projections of geostrophic wind velocity on axis  $x, y$ , projections of wind drift velocity can be expressed through gradient components of atmosphere pressure:

$$\left. \begin{aligned} V_x &= K \cos \beta \left( \frac{\partial P}{\partial y} + \operatorname{tg} \beta \frac{\partial P}{\partial x} \right) \\ V_y &= K \cos \beta \left( \frac{\partial P}{\partial x} + \operatorname{tg} \beta \frac{\partial P}{\partial y} \right) \end{aligned} \right\} \quad (1.2.11)$$

Here  $K = k k_1 / \rho_a f$  – isobaric coefficient,  $\rho_a, f$  – air density and Coriolis parameter,  $k_1$  – relation of geostrophic and surface wind velocities  $\beta = \alpha + \gamma$  ( $\gamma$  – wind inclination from isobar).

Seasonal dependence of isobaric coefficient is similar to wind coefficient changes. Angle of wind ice drift velocity inclination from isobar in the middle of summer exceeds  $+20^\circ$  and decreases to the end of winter to  $-5^\circ$ .

Average values of isobaric coefficients in Arctic Seas are on 25–40% higher and angles of drift inclination from isobar on 5–10° less, than in the Arctic Basin. These differences can be explained by smaller ice thickness in the Arctic Seas, and also by influence of barotropic gradient currents, which role must increase with the reducing of sea depth and coast approaching. It is necessary to

mention, that when ice thickness is less than 100–120 cm, and in non-stationary conditions, angle  $\beta$  can take negative values with wind change not only in winter, but also in summer, which has the principal importance in processes of ice cover diverging, increasing its concentration and compacting.

#### **1.2.2.2. Peculiar features of gradient currents influence on ice drift**

The Role of gradient currents (together with tilt of level surface) in general ice drift of the Arctic Basin accounts for around 60% on average, increasing to 70%, when the ice approaches “Fram” Straight and to 90% in the Greenland Sea at latitude 74–78° N.

System of gradient currents in the Arctic Ocean (AO) is formed under influence of the following factors:

- Large-scale wind fields, determined by atmospheric circulation behavior;
- Fresh water balance of AO with its main components - river run off and overbalance of atmospheric precipitation over evaporation;
- Irregularity of water density distribution, conditional by mechanic and non-mechanic factors;
- Global inclination of level surface between the Atlantic and the Pacific Oceans;
- Water exchange conditions with neighbor oceans;
- AO morphologic features (shore configuration, bottom relief).

Effects of listed factors are closely connected with each other. At that wind fields influence on gradient currents system is affected as a result of adaptation of water mass field (water density) to resultant wind circulation. Thus, currents system in deep waters of AO is mostly baroclinic. A good stability of considered currents system is connected with this circumstance.

According to known schemes of gradient currents, large anticyclonic water circulation is located in the Amerasian subbasin, where anti cyclonic wind field dominates. On its periphery is located wide Transarctic current, which originates from the Pacific current of the Chukchi Sea and outflows from the Arctic Basin through Fram Straight. Its continuation in the Greenland Sea is the Eastern-Greenland current. In straights of the Canadian Arctic archipelago motion of surface waters is directed from the Arctic Basin to the Baffin Sea, where Labrador Current begins from. Average velocity of Transarctic current, approaching to Fram Straight, increase from 1–2 cm/s to 5–7 cm/s (in the straight) and to 18 cm/s (on latitude 72°N in the Greenland Sea).

Current velocity changes during the year: in the Arctic Basin it is maximum in summer and minimum in winter, at that in addition to annual half annual component is also noticeable in these changes – according to seasonal changes of water inflow through Bering Straight. Winter maximum of current velocity, caused by appropriate changes of dominant wind, appears in seasonal changes in Fram Straight.

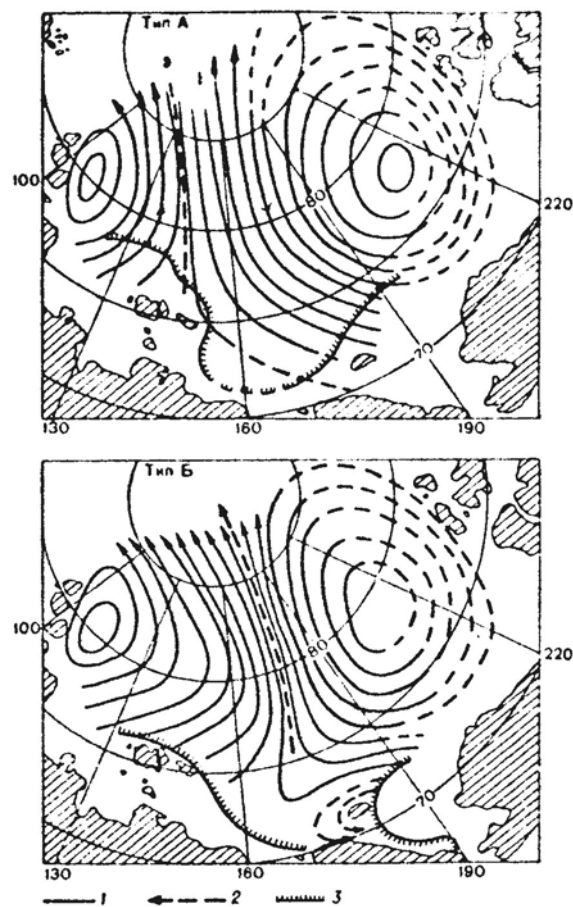


Fig. 1.2.6 – Typical dynamic maps of surface currents relative to horizon of 200: anticyclonic type (above) and cyclonic (bottom). 1 – lines of equal dynamic heights (through 20 din. mm), 2 – location of Transarctic current deep stream, 3 – average location of ice edge in August.

Oceanological surveys of the Arctic Basin, made in different years in high latitude airborne “Sever” expeditions, allowed discovering annual changes in surface current system (Fig. 1.2.6.). They are connected, firstly, with relation between areas of cyclonic and non-cyclonic circulation systems, and also with location of Transarctic current deep stream. Cyclicity with a period of 8-10 years was found in these changes. Ice conditions in the Arctic Seas, ice outflow to the Greenland Sea, inflow of Pacific waters and other indicators of hydrologic AO regime change in the same rhythms with them. Intensification of the Arctic anticyclone and its displacement to Eurasia lead to widening of anticyclonic circulation and shrinking of cyclonic. Weakening of anticyclone and its motion to American continent lead to opposite consequences. It is typical, that occurrence of similar changes in atmospheric circulation and corresponding system of barotropic currents in the Arctic Basin was confirmed in recent studies, where it was called “Arctic oscillation”.

In the shallow Arctic Seas, especially near coast, distribution of water density doesn’t reflect in full measure gradient currents structure and corresponding sea surface inclinations. Gradient

currents here are significantly barotropic. As formation time in such currents is rather short, gradient component of current, and consequently, of ice drift, correlates with wind well, being changed with the change of last one. This causes increase of empirically determined average values of wind coefficients, and their dependence on wind direction relative to coast.

In some regions of the Arctic Basin, especially in marginal seas, tidal currents significantly influence on ice drift, leading to appearance of ice drift periodic tidal component. Short-term (diurnal, semi-diurnal) and long-term (from several days to several years) tidal currents components (ice drift) are distinguished.

According to research data, direction and velocity of short-term component of tidal ice drift and tidal near surface currents practically coincide in every moment. Maximum velocity of semi-diurnal tidal currents on the large part of the Arctic Seas is 10–30 cm/s. Only in several limited areas it exceeds 1 cm/s. Maximum velocity of tidal ice drift in deep waters of the Arctic Basin doesn't normally exceed 5 cm/s. In quadrature it is 2–2,5 times less than in syzygy.

Trajectories of tidal ice drift are close to circle in most regions. Usually they are reversible only near a coast. Estimations, based on long wave's theory, show that in the most regions of the Arctic Seas maximum ice displacement by tidal wave is 2–4 km, rarely reaching 20 km, whereas in the Arctic Basin it doesn't normally exceed 1 km. However, practical importance of tidal ice drift is caused by significant spatial irregularity of its velocity, connected with increasing sea ice concentration, diverging and compacting. Tidal currents are important in process of fast ice formation.

Apart from tidal motion ice drift is affected by inertial oscillations in horizontal plane. They lead to appearance of folded trajectories with radius, depending on initial drift velocity and latitude. In the Arctic Seas, where the period of inertial oscillations is close to period of main tidal semi-diurnal waves, a radius of inertial orbits is normally about 1 km. It is rather difficult to separate inertial and tidal ice motion. Long-term and accurate observations are obligatory for this purpose.

#### **1.2.2.3. Total ice drift in the Arctic Basin**

Average velocities of total ice drift and characteristics of its variability strongly depend on time scale: if averaging period increases, average velocity of ice drift decreases from 7,5 cm/s to 2,2 cm/s for daily and annual periods respectively, i.e. almost 3,5 times. Statistical characteristics of ice drift velocity have annual variations. As seen from Fig. 1.2.7, average ice drift velocity modules for daily, 10-day and monthly periods vary within a year concordantly: the smallest mean drift velocities are observed in March, and the largest ones – at the end of summer – beginning of autumn (August-October). However, average velocity modules change little over 3-month period

throughout the year and become practically equal for 6-month periods, since seasonal velocity increase is compensated, by the end of summer, by its decreasing stability.

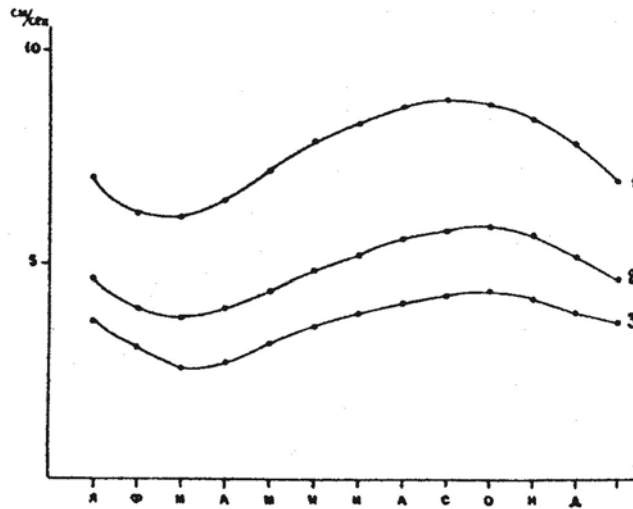


Fig. 1.2.7 – Annual dependence of average module of ice drift for daily (1), 10-day (2) and monthly (3) periods

Schemes of average resultant ice drift in the Arctic Basin for winter and summer half years, calculated from observational data of drifting expeditions and automatic buoys, using drift field approximation by two-dimensional polynomials in cube, are shown in Fig. 1.2.8 (a,b)

$$V_i = \sum_{q=0}^t \sum_{p=0}^m (a_{pq})_i X^p Y^q \quad (1.2.12)$$

Where:

i – symbol of ice drift velocity vector component on coordinate axis (x, y) and corresponding polynomial coefficients;

X, Y – coordinates of drift vectors  $\vec{V}$  beginning;

m – degree of polynomial by argument p;

t – degree of polynomial by argument q;

$a_{pq}$  – polynomial coefficient.

These patterns show the Transarctic Ice Flow that moves toward the Greenland Sea between the near-pole region and the northern margins of the Eurasian shelf seas. Large quantity of ice exported from the Russian Arctic Seas joins this flow on the left, while the anticyclonic gyre area with its center approximately at  $78^\circ \text{N}$ ,  $150^\circ \text{W}$ , adjoins it on the right. Seasonal changes are well observed in these patterns.

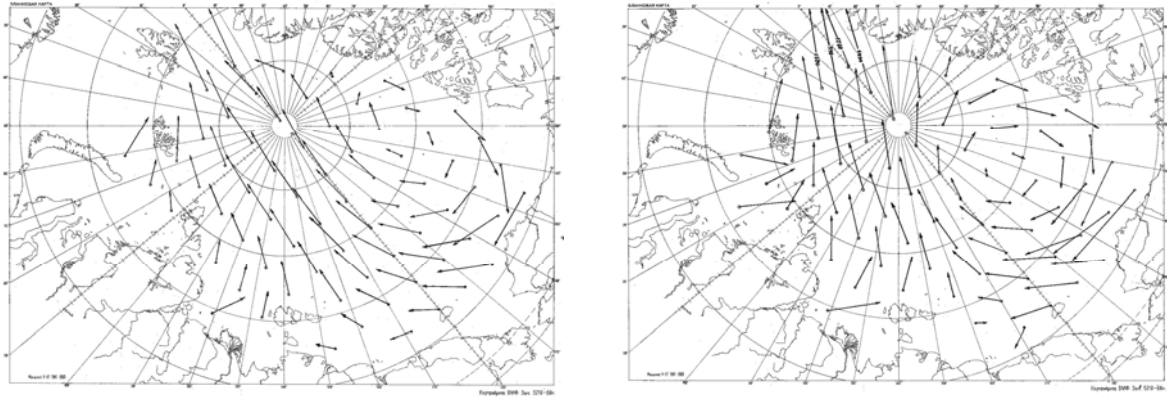


Fig. 1.2.8 – (a) – Scheme of resultant ice drift for April-September; (б) Scheme of average resultant ice drift for October-March

Ice entrained by the Transarctic Flow from the Kara Sea is exported to the Greenland Sea in 1-2 years, from the Laptev Sea – in 2-3 years, from the East-Siberian Sea – in 3-4 years, and from the Chukchi Sea – in 4-5 years. The period of ice circulation within the anticyclonic gyre changes from 4 to 10-12 years.

These schemes are used for climate forecast of different objects motion for long time periods.

### 1.2.3. Modelling of sea ice dynamics

Modelling of sea ice dynamics is based on consideration of force balance equation, which influence ice cover, called Equation of motion. In its basis – application of second Newton's law to ice dynamics: resultant value of all forces, effecting ice cover area unit, is equal to ice mass production, related to this area, on acceleration, i.e.

$$\rho_{\text{л}} H \frac{d\vec{V}}{dt} = \vec{\tau}_a + \vec{\tau}_w + \vec{C} + \vec{G}_n + \vec{G}_t + \vec{R} \quad (1.2.13)$$

Where:  $\rho_{\text{л}}$ ,  $H$  – ice density and thickness;

$\vec{V}$  – drift velocity vector;

$\tau_a$ ,  $\tau_w$  – tangent stresses on upper and lower ice surfaces;

$\vec{C}$  – Coriolis force;

$\vec{G}_n$  – gravity projection to sea surface;

$\vec{G}_t$  – horizontal component of tide-generating force;



$\vec{R}$  – force of internal interaction.

Estimations of relative force values, included into equation (1.2.13), significantly depend on average velocities, and, therefore, on motion scale.

In these models for solving equation (1.2.13) the components, composing this equation, are expressed by dependences, based on physical laws (mechanical). As a rule, such dependences include different parameters, which are defined in natural or laboratory experiments.

Models of ice cover dynamic differ by both degree accounting of acting forces and way of their expressing. In earliest models ice cover was considered as a level endless plate, to which spatially invariable tangential forces ( $\tau_a$  и  $\tau_w$ ) and Coriolis acceleration were subjected Fig. 1.2.9). In models of next level ice cover was considered to be a viscous liquid film, located between two layers of less viscous liquids – air and water. Thereby internal interaction force is connected with irregularity of ice drift velocity field in these models.

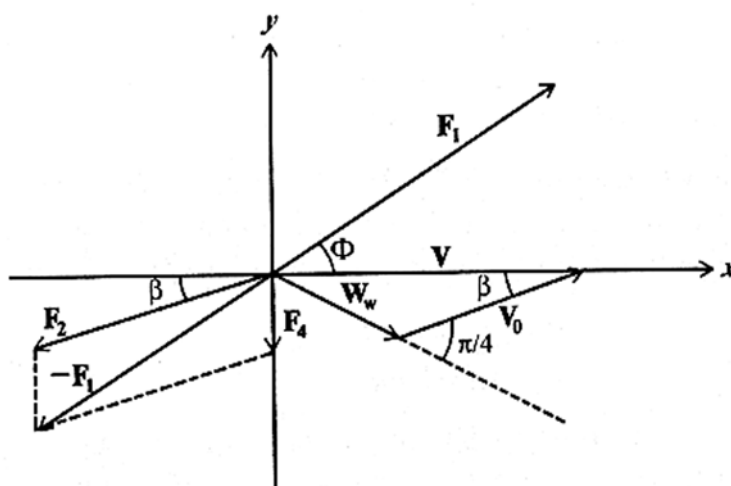


Fig. 1.2.9 – Scheme of ice drift velocity and force directions according to Shuleikin V.V.

First term of right part of equation (1.2.13), expressing tangential wind stress, is determined through vertical gradient of average wind velocity:

$$\tau_a = \rho_a k_a \frac{\partial W}{\partial z} \quad (1.2.14)$$

Under logarithmic wind profile, which is typical for atmosphere surface layer, this formula is transformed as:

$$\vec{\tau}_a = \rho_a c_a |W| (\vec{W}) \quad (1.2.15)$$

Here coefficient  $c_a$  is function of aerodynamic roughness  $z_0$ , of Karman constant and height of wind observation.

Tangential tension on lower ice surface ( $\tau_w$ ) is usually determined in the same way as  $\tau_a$ :

$$\tau_w = \rho_w c_w |\vec{V}_r| \vec{V}_r \quad (1.2.16)$$

where:  $\rho_w$  – water density;

$c_w$  – dimensionless impedance coefficient.

Calculations are complicated by circumstance that value  $V_r$  – relative velocity, which is equal to geometrical difference in vectors of drift velocity and current on lower boundary of water sublayer, where tangential drag stress changes weakly in vertical direction.

Standard expressions are used to determine third and fourth terms in equation of motion. Coriolis force, presenting horizontal projection of Earth rotation deflecting force, is given by:

$$\vec{C} = \rho_a H f \times \vec{V} \quad (1.2.17)$$

where:  $f = 2\omega \sin\varphi$  – Coriolis parameter;

$\omega$  – angular velocity of Earth rotation;

$\varphi$  – geographical latitude.

Coriolis force is directed at right angles to the right (in northern hemisphere) to the direction of ice drift velocity  $V$ . Gravity force projection to sea surface  $G_n$  is given by formula:

$$G_n = -\rho_a g H \nabla \zeta \quad (1.2.18)$$

where  $\nabla \zeta$  – tilt of level sea surface.

In most works, while determining forces of internal interaction in ice cover, expressions, similar to relations used in mechanics of continua, were used. In this case interaction force is divergence of internal stress tensor ( $\sigma_{ij}$ ):

$$\frac{1}{H} R_i = \frac{\partial \sigma_{ij}}{\partial x_j} \quad (1.2.19)$$

For determination of force  $R$  it is necessary to establish determinant equation, connecting internal stress tensor with parameters of ice cover conditions or with ice drift characteristics.

Among many works, describing sea ice evolution, there are models, describing viscous, elastic, plastic and also combined viscous-elastic, elastic-plastic or viscous-elastic-plastic properties of ice cover.

During development of ice dynamics models, it is necessary to take into account, that ice cover differently react to tangential and normal stress, to tensile and compression strain, that can simultaneously exist under ice motion. Forces of internal interaction depend on ice cover condition – its thickness, concentration, strength, forms, and also on occurrence and orientation of leads (cracks, channels) in compact ice.

Dynamic-thermodynamic models of ice cover evolution allow calculating kinematic changes of ice cover parameters. Calculations are based on differential equation, which is a result of mass conservation law. Specifically, for function of ice cover concentration it is given by:

$$\frac{\partial N}{\partial t} = -div(N\vec{V}) + S_N \quad (1.2.20)$$

Where:  $0 \leq N \leq 1$  – function of ice cover concentration;

$S_N$  – thermodynamic term.

To calculate advective changes of parameters, which do not depend on velocity divergence (e.g., level ice thickness,  $H$ ), the following equation is used:

$$\frac{\partial H}{\partial t} = V_x \frac{\partial H}{\partial x} + V_y \frac{\partial H}{\partial y} + S_H \quad (1.2.21)$$

where  $S_H$  – thermodynamic term.

If during calculations it is found that in any grid point  $N > 1$ , velocity field is corrected by means of iterations, and ice thickness correction is calculated (due to ridging). Correction is added to average (for grid point) ice thickness. The way of expressing internal resistance force in main ellipse deformation axis (only normal forces are subjected) with taking into account deformation sign - is interesting aspect to mention. Reasonable definition of boundary conditions has the main importance in ice cover models.

#### 1.2.4. Regularities of ice cover irregular motion

In studies of ice cover motion, apart from translation ice motion – actually drift, effects, which occur from changes of motion velocity in space and time, have great practical and science interest. These changes are determined by ice drift velocity field.

#### 1.2.4.1. Irregular motion types

At any moment components  $V_x$  и  $V_y$  of velocity vector  $\vec{V}$  are functions of coordinates  $x$  and  $y$ , i.e.  $V_x = V_x(x, y)$ ,  $V_y = V_y(x, y)$ .

Having chosen origin of coordinates in arbitrary point  $x_0$  and  $y_0$ , we develop these expressions in Taylor series (high-order terms are discarded):

$$V_x = V_{x0} + \left(\frac{\partial V_x}{\partial x}\right)x + \left(\frac{\partial V_x}{\partial y}\right)y \quad (1.2.22)$$

$$V_y = V_{y0} + \left(\frac{\partial V_y}{\partial x}\right)x + \left(\frac{\partial V_y}{\partial y}\right)y$$

From four spatial derivatives, contributing to equation (1.2.22), the following four characteristics of plane motion irregularity can be obtained:

$$\text{div}\vec{V} = \frac{\partial V_x}{\partial x} + \frac{\partial V_y}{\partial y} \quad (\text{divergence}) \quad (1.2.23)$$

$$\text{rot}\vec{V} = \frac{\partial V_y}{\partial x} - \frac{\partial V_x}{\partial y} \quad (\text{rotor}) \quad (1.2.24)$$

$$\text{def}_1\vec{V} = \frac{\partial V_y}{\partial x} + \frac{\partial V_x}{\partial y} \quad (\text{angular deformation}) \quad (1.2.25)$$

$$\text{def}_2\vec{V} = \frac{\partial V_x}{\partial x} - \frac{\partial V_y}{\partial y} \quad (\text{linear deformation}) \quad (1.2.26)$$

It's not complicated to prove, that expression

$$\text{def}\vec{V} = \sqrt{(\text{def}_1\vec{V})^2 + (\text{def}_2\vec{V})^2} \quad (1.2.27)$$

is invariant relative to coordinative system. That is why equalities (1.2.22) can be written as follows:

$$V_x = V_{x0} + \frac{x}{2}\text{div}\vec{V} + \frac{x}{2}\text{def}\vec{V} - \frac{y}{2}\text{rot}\vec{V} \quad (1.2.28)$$

$$V_y = V_{y0} + \frac{y}{2}\text{div}\vec{V} - \frac{y}{2}\text{def}\vec{V} + \frac{x}{2}\text{rot}\vec{V}$$

Cinematic nature of expressions (1.2.28) is that ice cover can be transferred from one location to another by means of translation (actually drift), divergence (i.e. diverging and compacting), deformation (in restricted sense this term means that body shape changes without changing size) and, finally, rotation. Common for motion, described by last three terms, is its typical spatial irregularity of velocity field. That is why, formulas (1.2.23 – 1.2.26) can serve as kinematic indicators of ice cover motion irregularities, each of them expresses rather definite and independent from each other irregularity features.

*Velocity of ice cover rotation* changes with time; its average value depends on time scale, season; it decreases with increase of ice cover concentration and increase with reduction of ice floes size.

It is known, that rotation velocity in continuum medium is connected with characteristic of cross irregularity of velocity - rotor (vorticity) as:

$$\frac{\partial \omega}{\partial t} = -\frac{1}{2} \text{rot} \vec{V} \quad (1.2.29)$$

Studies of ice cover rotary motion have not only scientific, but also large practical interest. Data about ice floe rotation allow to judge about occurrence of cross irregularity of wind and gradient ice drift. Orientation of devices, put in the ice, is changed as a result of rotation, etc. Using listed relations between ice drift velocity and gradient of atmosphere pressure, we get:

$$\text{rot} \vec{V} \approx k \text{rot} \vec{W} \approx K \nabla^2 P \quad (1.2.30)$$

Where  $\nabla^2$  – 2D Laplace operator.

Consequently, wind component of ice motion velocity rotor (and also velocity of ice cover rotation) is proportional to wind velocity rotor or atmospheric pressure Laplacian. Analysis of numerous observation data confirms validity of dependence (1.2.30).

*Divergence of ice drift velocity*, as shown before (1.2.20), is closely connected with changes of ice cover concentration. This formula can be written as follows:

$$\frac{\partial N}{\partial t} = N, \quad \text{div} \vec{V} - \vec{V} \text{grad} N \quad (1.2.31)$$

The first term of right equation part characterizes changes of concentration due to spatial irregularity of ice drift velocity, and the second – changes of concentration due to advection. divergence of ice motion velocity can be caused by the following reasons:

- spatial irregularity of currents velocity and sea level;

- spatial irregularity of wind fields;
- coast influence (or motionless ice);
- ice cover heterogeneity (its thickness, concentration, hummocking, on which upper and lower ice surface roughness, and also mass, for surface unit, depends);
- processes of horizontal diffusion;
- non-stationarity of external influence;

Velocity divergence, caused by tidal currents, depends on type, height and length of tidal wave. In case of progressive wave, divergence maximum (i.e. the largest intensity of ice cover diverging) is observed at the moment, when tidal current is changed to ebb current. In contrary, the largest converging (the largest intensity concentration increase, and with  $N=1$ - the largest compacting) must occur at the moment, when ebb current is changed into tidal. At that ice cover concentration reaches its maximum on the wave crest (high water) and minimum - at the moment of tidal current (low water). Amplitude of tidal changes of divergence under other equal conditions increase with the wave length decreasing, depended on wave period and sea depth. That is why tidal phenomena in ice cover, normally noticeable on shelf, are insignificant in deep sea.

Numerous studies show that divergence of ice drift velocity, caused by wind field irregularity, provides the major contribution in the mechanic change of ice cover concentration far from coast and ice edge. At that, both wind field irregularity and deviation of wind drift from isobaric (geostrophic) relations are important, because under isobaric ice drift  $\text{div} \vec{V} = 0$ .

The listed relations between drift velocity components, wind and pressure gradients should be used to find connection of ice motion velocity divergence with wind and pressure fields. Thus we get:

$$\text{div} \vec{V} = \frac{k \sin \beta}{\sin \gamma} \text{div} \vec{W} = K \sin \beta \nabla^2 P \quad (1.2.32)$$

The model of stationary pressure field, suggested by D.A. Drogaitsev, should be used to find out dependence of drift velocity divergence and sea ice concentration redistribution on wind fields irregularity. Such field can be described by expression:

$$P = P_o \sin \frac{2\pi}{L_x} x \sin \frac{2\pi}{L_y} y \quad (1.2.33)$$

Where:  $P$  – deviation of atmospheric pressure from some average;

$P_o$  – amplitude of pressure changes;

$L_x, L_y$  – distance parallel to coordinative axis between maximum and minimum of atmosphere pressure.

View of this field under  $P_0=10$  мб. and  $L_x=L_y=4000$  km is shown on Fig. 1.2.10

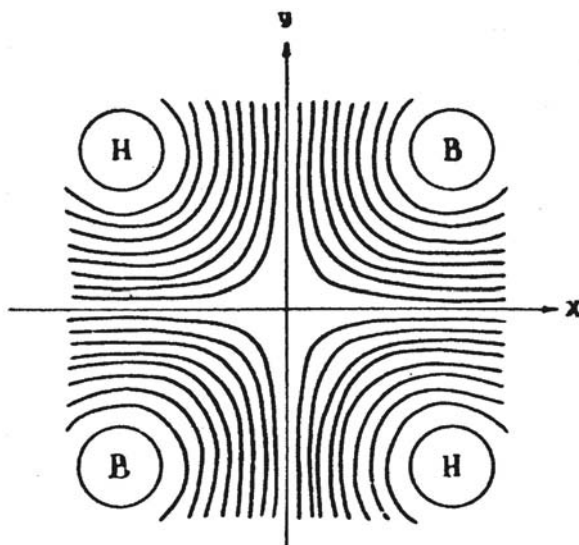


Fig. 1.2.10 – Scheme of pressure field, according to Drogaitsev D.A. (isobars – through GPa)

Ice drift components were calculated from formulas (1.2.11) with  $\beta=20^\circ$  taking into account empiric dependence of isobaric coefficient value  $K$  from gradient of atmosphere pressure. Ice concentration was calculated by using the equation (1.2.31).

Calculations results of concentration redistribution in pressure field for 10-day periods under even initial concentration, equal to 8/10-th are shown in Fig. 1.2.11. As it is seen from the figure, small changes of concentration occur close to cyclones centers (depression) and anticyclones (compaction). On axis of deformation field these changes are not large; therefore, role of nonlinearity of ice drift velocity dependence on pressure gradient has the second importance. There aren't any concentration changes in hyperbolic field point.

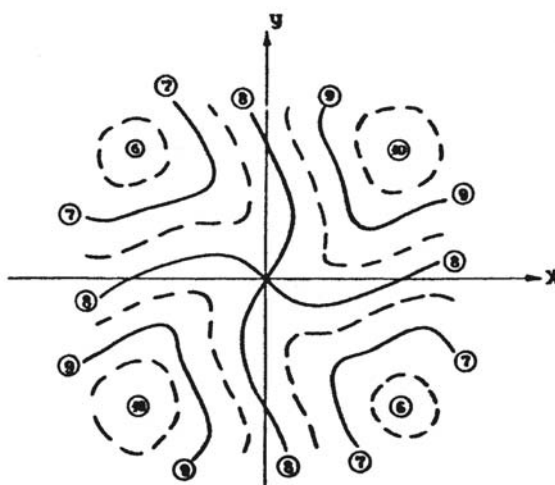


Fig. 1.2.11 – Calculated distribution of ice cover concentration in stationary pressure field (Fig. 1.2.10) with  $T_0=0,8$  (8/10-th) after 10 days

Nature of ice concentration changes, revealed in the listed calculation results, is confirmed by numerous air reconnaissance observations. In years, when cyclonic fields dominate in summer above the Arctic Basin, observers noticed significant ice cover divergence, reaching sometimes 4-6/10-th. In contrary, in years, when frequency of occurrence of arctic cyclone increased, ice cover was compact. Results of triangles and quadrangles area calculations, built according to simultaneously measured coordinates of Russian and American drifting stations and to observations from special polygons, can be considered as confirmations of these regularities.

Distribution of ice drift velocity divergence, areas of ice concentration increase and diverging in stationary baric systems was considered before. However, a number of dynamic effects is connected with non-stationarity of pressure fields – their motion in space and changes in time. Processes in moving baric systems, leading to ice concentration increase, are observed in front of cyclone, and diverging– in front of anticyclone.

It is known, that heterogeneity of ice cover thickness, and also roughness of its upper and lower surfaces, mostly depending on hummocking, cause spatial irregularity in velocity of ice drift, leading to internal strains and deformations. Large-scale heterogeneity of ice thickness is mostly noticeable in seas, where ice is transported out. There ice cover becomes gradually younger, and well-marked gradient of ice thickness occurs, directed from thick first-year ice to flaw polynyas, which in winter are rapidly covered with young ice. Large horizontal gradients of ice thickness are also observed close to multiyear ice boundary. Significant heterogeneity of hummocking can be found near external fast ice boundary in conditions, when pushing drift is dominant, and also in region of strongly broken ice, survived after summer melting.

*Ice cover deformation*, as divergence, takes place under occurrence of spatial heterogeneity of ice cover velocity motion. Dependence of deformation velocity on wind irregularity (pressure field) can be easily found, by substituting expressions (1.2.11) in formulas (1.2.23), (1.2.24) and (1.2.26).

$$def\vec{V} = K \sqrt{\left(\frac{\partial^2 P}{\partial x^2} - \frac{\partial^2 P}{\partial y^2}\right)^2 + \left(2 \frac{\partial^2 P}{\partial x \partial y}\right)^2} \quad (1.2.34)$$

As it is seen from this formula, maximum value of deformation velocity doesn't depend on angle between ice drift directions and geostrophic wind ( $\beta$ ), but is determined only by isobaric coefficient value and pressure field peculiar features. Using equation (1.2.33) for description of last expression, distribution of value  $def\vec{V}$  can be obtained (Fig. 1.2.12) in deformation pressure field similar to one shown in Fig. 1.2.10. In contrast to the last one  $L_y/L_x=0,7$  was taken, i.e. it is rather stretched along  $x$  axis.



Analysis of formula (1.2.34) shows, that deformation value, taken into account by first term of radicand, is maximum in pressure centers and equal to zero in neutral lines of pressure field. If  $L_y=L_x$  this term turns into zero, consequently, in pressure systems, close to circle, this component of deformation velocity is practically absent. Component, described by the second term of radicand (1.2.34), reaches its maximum value in hyperbolic points of pressure fields and equal to zero in centers of cyclones and anticyclones and along lines, connecting neighbor centers.

From Fig. 1.2.12 it is seen, that under moderate “elongation” of pressure systems region of maximum deformation is located in area of baric saddle, whereas in centers of cyclones and anticyclones deformation is not large. Obtained result explains regularity, known from observations: the strongest ice shearing – breaking and hummocking – are observed in areas of baric saddles, for which weak wind is typical.

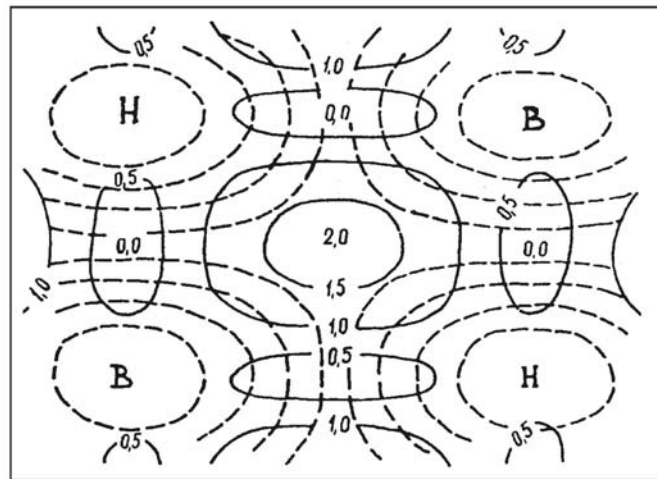


Fig. 1.2.12 – Distribution of deformation values (in  $10^{-7} \text{ c}^{-1}$ ) in pressure field

For visual presentation of deformation for any time period (or deformation velocity) it is convenient to make deformation ellipse (deformation velocity). Direction of longer ellipse axis corresponds to maximum elongation (or minimum pressure), small axe – minimum elongation (maximum pressure). From the deformation ellipse we can approximately judge about cracks direction in ice cover. Normally direction of cracks in ice cover is perpendicular to longer axis of deformation ellipses. These regularities explain typical systems of leads in sea ice cover, and other arched systems, observed while approaching to straights.

Taking into account dependence of velocities divergence and deformation from heterogeneity of ice thickness and hummocking, it can be summarized, that cracks mostly form along isolines of equal thickness, leaving thicker ice from the right, if the wind blows along these isolines. This regularity is confirmed by data of air reconnaissance: in seas, where ice thickness increases from south to north, wide leads often form in ice cover with winds of eastern quarter. Characteristic

features in ice cover deformation, connected with drift irregularity, occur also close to barriers (land, fast ice, etc). Concentric system of cracks, which is often seen in region of anticyclonic water and ice circulation northwards of the Beaufort Sea, points to significant role of sea level tilt in this region.

Thus, by means of mathematical modeling it was possible to explain, and in some cases even to predict appearing of many features in ice cover distribution, which are important for implementation of transport and other operations in sea ice cover.

## 2.1. Baltic Sea Ice Condition Characteristics

### 2.1.1. General aspects

The Baltic Sea (beginning from ancient times and till XVII century was known in Russia as “Varangian sea”) – is an inland marginal sea. The Baltic Sea is located in Northern Europe and belongs to the Arctic Ocean water basin (Fig. 2.1.1.).

The northernmost point of the Baltic Sea is located near Polar circle ( $65^{\circ}40'$  N, and the southernmost – near Vismar ( $53^{\circ}45'$  N). The westernmost point is situated in the Flensbourg area ( $9^{\circ}10'$  E), and the easternmost – in the Saint-Petersburg area ( $30^{\circ}15'$  E). The Sea area is 415 000 km<sup>2</sup>, its average depth is 52 m, and maximum depth is 459 m.

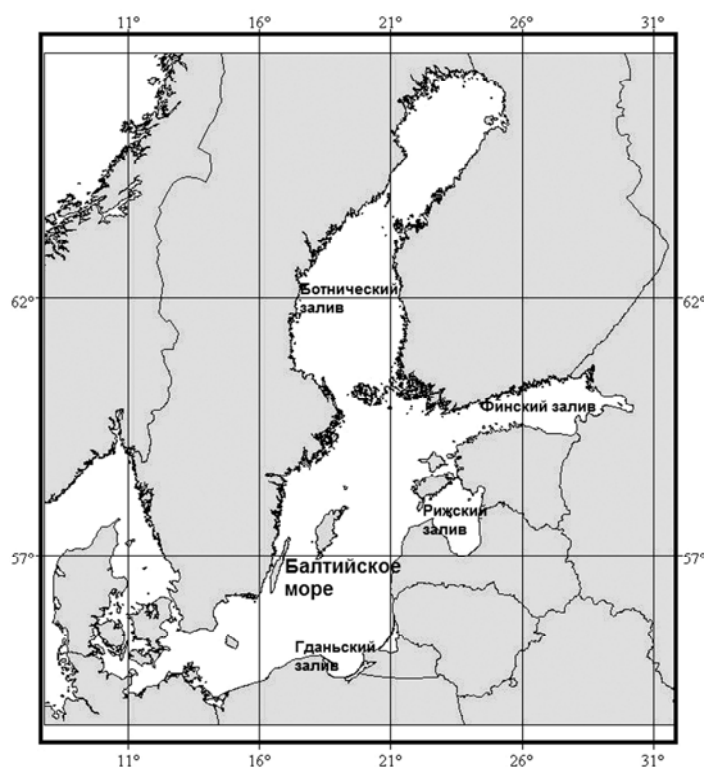


Fig. 2.1.1 The Baltic Sea division into zones

Significant variability and variety of ice conditions is the characteristic feature of the Gulf of Finland and the whole Baltic Sea. More unfavorable conditions are observed in its northern part, comparing to the southern and central Baltic.

The Baltic Sea ice regime is determined by geographical location and climatic conditions, water desalination under influence of coastal discharge, heat exchange intensity of open sea with its gulfs and with the Northern Sea.

### 2.1.2. Ice formation

On average, ice appears in the northernmost part of the Gulf of Bothnia in late November. Then, in late November – early December ice appears in the Gulf of Finland upper part and in the Gulf of Vyborg (Fig. 2.1.2).

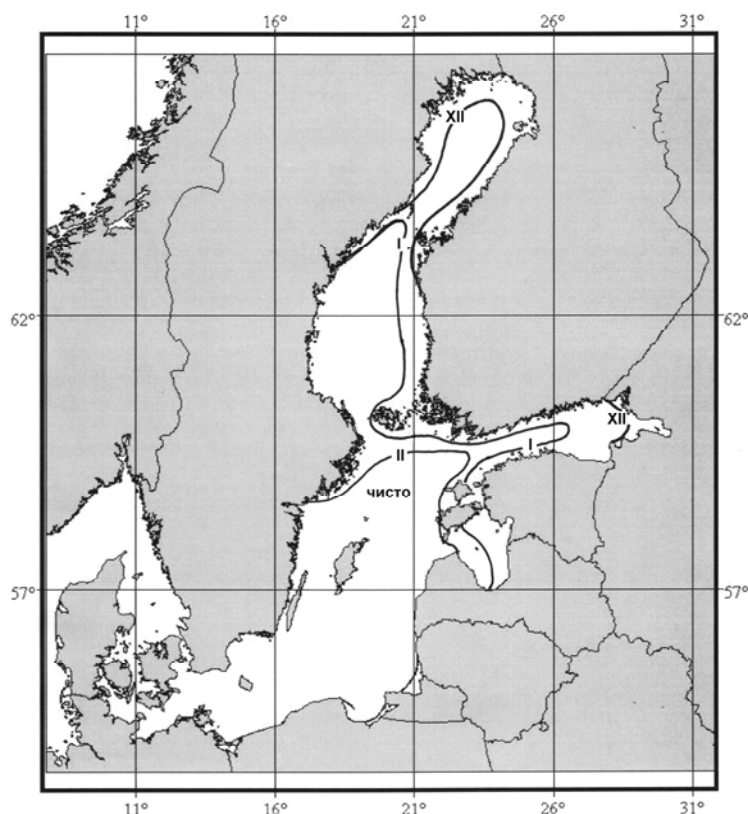


Fig. 2.1.2 Annual mean ice distribution in early December

Under unfavorable development of ice conditions, ice formation in the northern part of the Gulf of Bothnia starts in late October. In November ice formation involves the whole Gulf of Bothnia northern part and can be seen along the whole northern sea shore. In the middle of December new and young ice are observed in the whole water basin of the Gulf of Bothnia and the Gulf of Finland (Fig. 2.1.3 a, b, c).

### 2.1.3. Ice cover

The ice area in the Baltic Sea changes in wide range from 50 to 420 000 km<sup>2</sup>, when the whole sea is covered with ice. Ice cover of the Baltic Sea and it's large regions is closely connected with the sums of freezing degree-days, with correlation coefficients of 0.9 and higher.

Repetition of mild, moderate and severe winters in different sea areas doesn't always coincide. The most characteristic example of disagreement of winter type in the open Baltic, Gulf of Finland and German coast is considered to be winter of 2002/2003. It was very severe in the Gulf of Finland, moderate, a bit less than norm in the Gulf of Bothnia, and mild along the German coast.

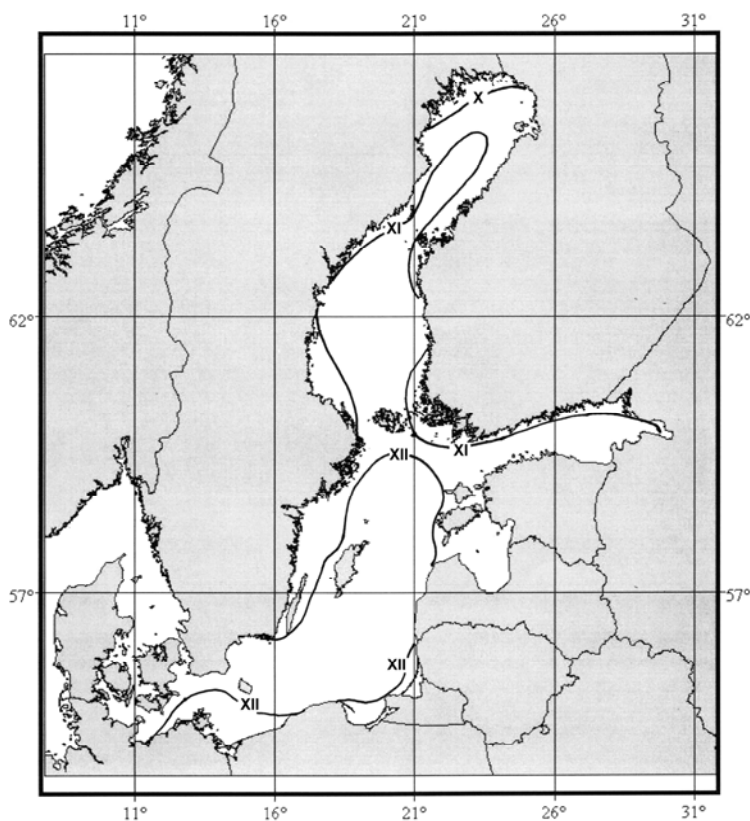


Fig. 2.1.3 Stable ice formation processes development in unfavorable years

Ice cover develops to its maximum in the period between late February and the middle of March. The most difficult ice conditions are observed in the northern part of the Gulf of Bothnia and in the eastern part of the Gulf of Finland. The most significant difficulty criterion for the Gulf of Bothnia and the Gulf of Finland is not ice area but ice volume, which allows taking into consideration both ice area and ice thickness.

In severe years ice thickness reaches 80-100 cm in the northern part of the Gulf of Bothnia, and 90cm in the Gulf of Finland in period of maximum ice cover growth.

Fast ice is formed along the Baltic Sea eastern coast with the width reaching 20 km in the north, up to 10 km in the south; drifting ice consists mostly from grey and grey-white ice. According to eastern sea coast hydro meteorological stations data maximum ice thickness varies from 10-30 cm in mild winters up to maximum of 40-60 cm in severe winters. In very severe winter 1941/42 ice, frozen up together, formed hummocked ice zone along coast with thickness 50—60 cm. Cleansing from ice takes place in the 3<sup>rd</sup> decade of April, and in northern part, in the area of

Saaremaa and Hiiumaa islands, separate ice strips and ice patches can be observed in the 1<sup>st</sup> decade of May. In very mild winters ice along Baltic Sea eastern coast is absent.

Southern parts of the Baltic Sea don't usually freeze in mild winters. Floating ice of small capacity is formed along Polish, German and Denmark coasts in mild and severe winters. Thus, near an eastern Germany coast even in severe winters sea is covered with ice only for 30-45 days, and usual ice thickness is 30-40 cm.

In southern coastal areas of Baltic the largest amount of ice is observed in late January – February. Ice cake and small floe are predominant ice forms. On average the ice thickness doesn't exceed 20-30 cm, the maximum thickness is 50-60 cm. Ultimate clearing from ice takes place in mild winters in the middle of February, in severe winters – in early March.

Fast ice melting and destruction usually starts in the second half of March – early April. In the Gulf of Finland in its first half the first wave of ice fracturing sequentially reaches areas of Gogland, Moshchniy, Seskar Islands. In the second half of April fast ice fracturing occurs southward of Moshchniy and Seskar Islands, and in Luzhskaya Bay. In late April – early May complete ice cleansing is noticed in the Sestroretsk shallow areas and in the Gulf of Vyborg. However, during winter season and in some months terms and boundaries of ice distribution can significantly differ from the conditions, described above.

In the Gulf of Bothnia ice disappears in late April – early May. Ice cover distribution in years with average ice conditions is shown in Fig. 2.1.4.

#### **2.1.4. Typical ice conditions**

Under average multiyear conditions ice cover in the Gulf of Finland in December is about 10%, but in February-March it reaches 80% of Gulf area (Fig. 2.1.5.). In April ice cover decrease to 49%, and in May is just about 4%. Fast ice thickness under normal conditions in the area of hydro meteorological station Ozerki in December is equal to 10 cm, in March reaches 50 cm, and decrease in April to 40 cm (Fig. 2.1.6.). Air temperature annual variation is characterized by stable transition to negative values in the middle of November, decrease in January – February up to -7.5 – -8,5°C and stable transition to positive values in early April.

Increasing of ice cover in December to 24%, in February, March and April – to 100%, and reducing in May – to 13% are characteristic for unfavorable conditions. Fast ice thickness on its seasonal maximum under unfavorable conditions reaches 75 cm.

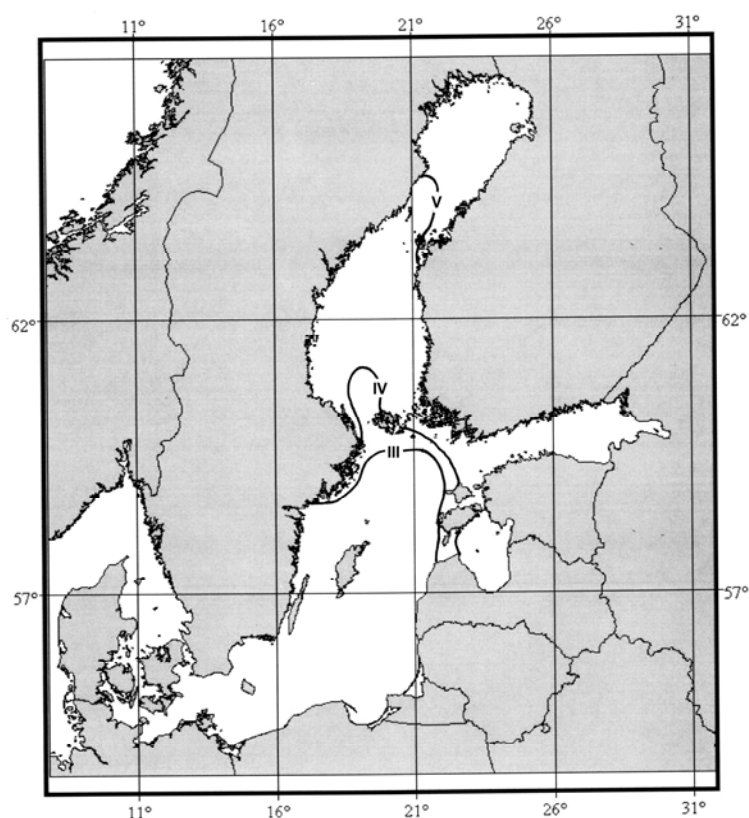


Fig. 2.1.4. Ice cover development in years with average ice conditions

Autumn transition of air temperature to negative values was noticed in the first decade of November, the most negative temperature values, about  $-19 - -20^{\circ}\text{C}$ , were observed in January, and spring transition to its positive values occurred in the first decade of April.

For favorable conditions small ice quantity in December and April, insignificant ice cover – in February are typical. Ice thickness under the same conditions in March normally doesn't exceed 30 cm. Accordingly air temperature transition to negative values in Saint-Petersburg occurs with delay to the third decade of November, and respectively its transition to positive values is observed earlier, in the third decade of March

### 2.1.5. Ice drift

Wind has a determinative effect on ice drift in the Gulf of Finland due to its limited size. Under stable southern winds ice accumulates near its northern coast. Spring ice melting in this area and in adjoining route areas slows down. With the change of wind direction to northern ice is moved to the central and southern parts of gulf, where it melts rapidly in spring.

The average ice drift speed is not big, about 15 cm/s. Depending on wind speed, ice concentration, size and shape of ice floes this speed varies in wide range from 2-5 to 90 cm/s, and

even more during severe storms. Steady ice motion is established in 1-2 hours after beginning of the wind. An angle of ice drift deviation from wind direction is 1-7° on average.

### 2.1.6. Ice conditions multiyear variability

Studies of ice cover seasonal changes in the Gulf of Finland showed, that water basin area covered by ice can rapidly reach 100% by the middle of winter. Therefore, if considering multiyear variability, it's more reasonable to use the largest seasonal area of the Baltic Sea ice, which from year to year varies in very wide range from 50000 to 420000 km<sup>2</sup>, when the whole sea area is covered by ice (Fig. 2.1.7.).

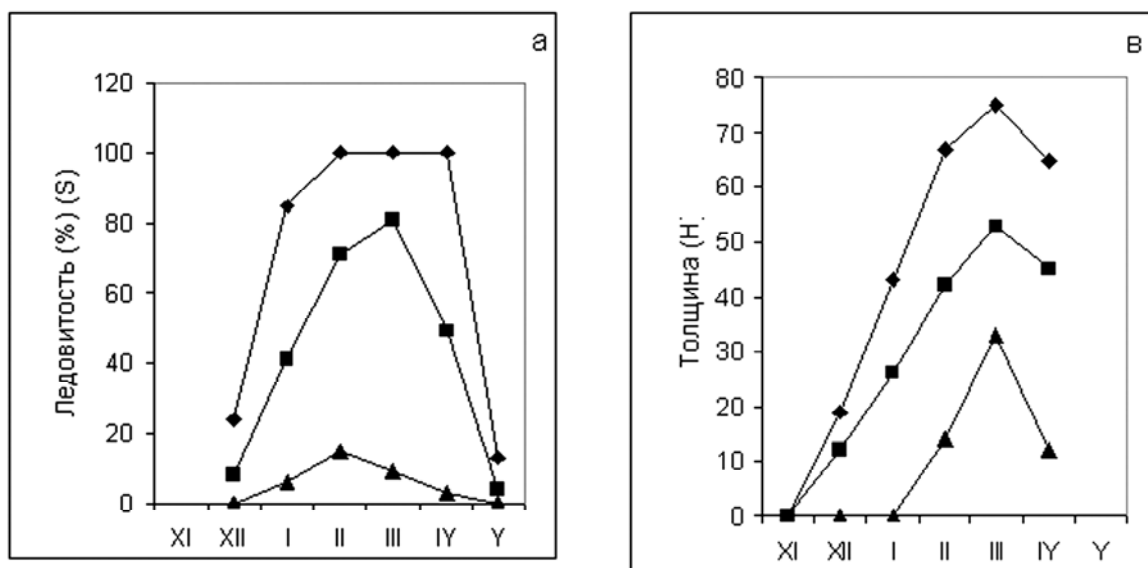
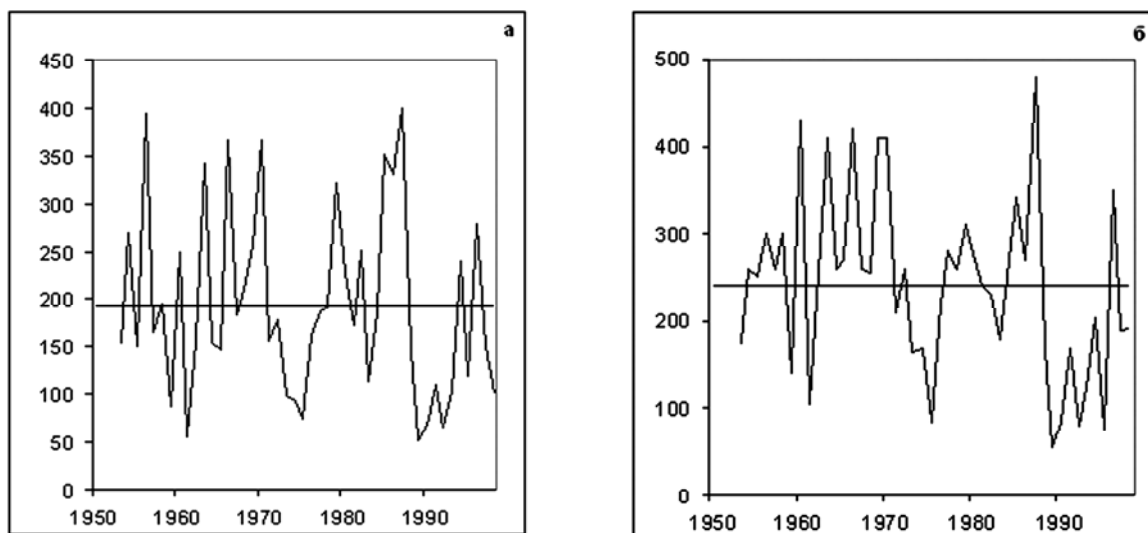


Fig. 2.1.5–Typical ice distribution in March in years with easy (a) and heavy (b) ice conditions





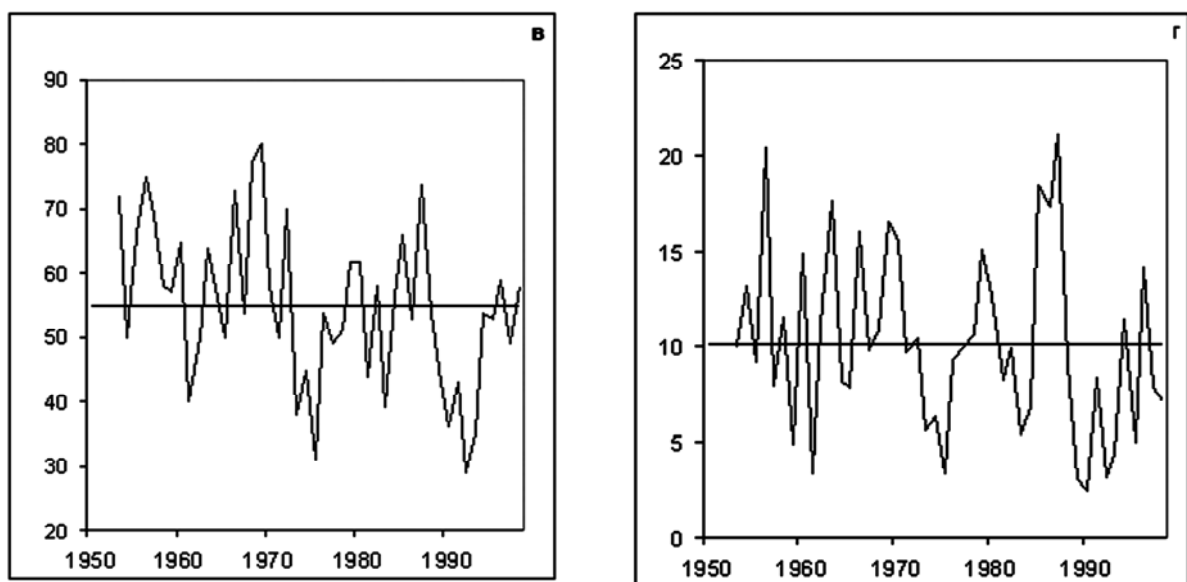


Fig. 2.1.6– Seasonal variability of ice cover and ice thickness in the Gulf of Finland (a – the Gulf of Finland ice cover (%); b – ice thickness (cm) in Ozerki)

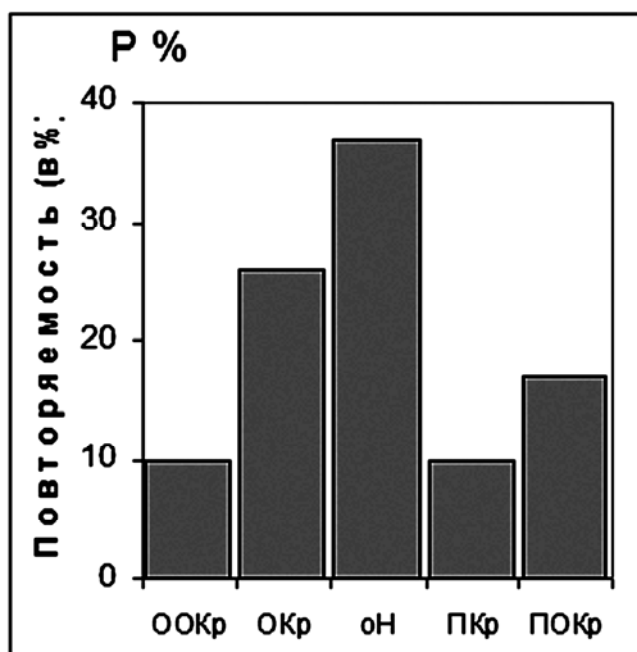


Fig. 2.1.7.– Interannual changes of ice cover, ice route length and ice thickness for the period 1953 - 1998 (a – the Baltic Sea ice cover (103 km<sup>2</sup>) on it's seasonal maximum; b – the longest route length (n.m.) in ice along fairway; c - maximum ice thickness (cm) in Ozerki; d – ice volume (km<sup>3</sup>) in the Gulf of Finland).

On Picture 2.1.7 it is noticeable, that largest by size and single-valued relative to norm deviations are repeated for different characteristics, mostly in the same years. And really in the most unfavorable years, which are 1956, 1963, 1966, 1969 and 1987, the Baltic Sea ice cover on it's

seasonal maximum exceeded 300000 km<sup>2</sup> and the largest route length in ice was more than 370 miles. In the same years ice thicknesses on its seasonal maximum were more than 70 cm and the largest ice volume in gulf exceeded 16 km<sup>3</sup>. It's interesting, that according to all chosen indicators, unfavorable 1987 year is the most extreme for the considered time period.

To the most favorable winters by the match of single-valued norm deviations were referred winters of 1961, 1975, 1989, 1990, 1992 with the Baltic sea ice cover less than 60 000 km<sup>2</sup> and route length in ice on seasonal maximum less than 85 miles. Ice thickness in Ozerki and ice volume in the Gulf were less than 40 cm and 3,2 km<sup>3</sup>, respectively.

Maximum position of ice edge and fast ice boundaries are normally connected with severe and very severe winters. In the period from 1901 to 2000 the most severe sea ice conditions in the Baltic, with the Baltic Sea ice area changed from 350000 to 420000 km<sup>2</sup>, were observed 13 times, i.e. the most severe winters in XX century occurred once in 7-8 years.

During seasonal maximum, which normally is in the late February – early March, ice distribution area in Baltic Sea can vary in very wide limits from 50000 to 420000 km<sup>2</sup>. Under the most favorable conditions ice processes develop mainly in eastern part of the Gulf of Finland, as well as in central and northern parts of the Gulf of Bothnia. However, under very unfavorable conditions almost all Baltic Sea including its gulfs are covered by ice in very severe winters.

Main ice cover statistical characteristics are shown in Table 2.1.1. Some insignificant reduction of values from more long-term to more short-term periods is characteristic for them. The given result indicates certain temporal stability of main statistical parameters of used Baltic Sea ice area data sets.

Table 2.1.1 – Statistical characteristics of the Baltic Sea ice area variability (10<sup>3</sup> km<sup>2</sup>) on its seasonal maximum for the different periods

Period, characteristic	1900-1999	1950-2005
Average	190	188
Standard deviation ( $\delta$ )	104	96
Maximum	420	402 (1987)
Minimum	52 (1989)	52 (1989)
Range	368	350

For general characteristics of the Baltic ice conditions it is important to estimate severe winter types repeatability (Table 2.1.2.) and repeatability probability, %, of particular winter type N years in succession (Table 2.1.3.).

Table 2.1.2 –Frequency of occurrence of winter severity type (%) based on three gradations of Baltic Sea ice area (km<sup>2</sup>) for the period from 1900 to 2005.

№	Type of winter severity	Sea ice area, km <sup>2</sup>	Number of cases, N	Repeatability, %
1	Mild	60-180	144	50,9
2	Moderate	181-300	62	21,9
3	Severe	301-420	77	27,2
TOTAL		60-420	283	100,0

Severe winters repeatability was shown to be significant and is about 27,2 %. From the Table 2.1.3 it is seen, that probability of severe winter occurrence during two successive years is not big (5%), which confirms the harmonic nature of ice cover changes with a period of 2-3 years.

Table 2.1.3 – Typification of winter severity types and particular winter type repeatability (%) in the Baltic Sea and Gulf of Finland during N successive years for the period from 1719/1720 to 2004/2005

Winter type	Ice area gradation, km <sup>2</sup>	N years				
		1	2	3	4	5
Mild	60 - 180	50,9	30,4	2,1	1,4	1,1
Moderate	181 - 300	21,9	0,7	-	-	-
Severe	301 - 420	27,2	5,0	1,8	1,1	-
TOTAL		100,0	-	-	-	-

Tendency of the Baltic Sea ice area reduction in 30s and 50s of the last century is probably connected with earlier climatic warming in the Arctic and subarctic (the Barents and Greenland Seas). Ice area enlargement in 1953-1988 reflected modern climate cooling, and finally, short-term but intensive tendency of ice area reduction in 1988-1998 was accompanied by flash of new climate warming. As a whole, all studied 100-year period was characterized by ice area reduction tendency and general climate warming.

## 2.10. Characteristic of the Bering Sea ice conditions

### 2.10.1. General aspects

The Bering Sea – is a sea in the northern Pacific Ocean, separated by Islands Aleut and Commander. The Bering Sea is joined with the Chukchi Sea and Arctic Ocean by Bering Strait. The sea washes coast of Russia and the USA (Fig. 2.10.1). Its area is 2,304 000 km<sup>2</sup>. Average depth - 1600 m, maximum — 4773 m. Air temperature over the water basin is +7, +10 °C in summer and –1, –23 °C in winter. Salinity 33,0-34,7 pro mille.

Conditions of ice formation and ice melting in the Bering Sea significantly differ from other Siberian Arctic shelf seas. The sea is located in moderate latitudes. Such location defines softer climate conditions. Relatively warm Pacific waters come through southern sea border to its central part, so ice isn't formed here. In most severe winters only half of the sea is covered with ice.



Fig. 2.10.1. The Bering Sea and its main islands and gulfs.

### 2.10.1. Ice formation

Ice formation is the result of interaction of factors, forming heat accumulation in the sea in the heating period and intensity of heat emission in the cooling period. The beginning of the sea cooling process coincides in time with the maximum heat accumulation in the surface layer. New ice appears in ice-free areas.

Ice formation in the Bering Sea, as a rule, occurs in open water and starts in peaks of gulfs and bays in the northern sea region, where ice usually appears in the middle of October (Fig. 2.10.2). Main “wave” of ice formation comes from the Chukchi Sea through Bering Strait in second 10-day period of November (Fig. 2.10.3).

In December all places of ice formation join together in one ice massif. Boundary of ice

propagation gets wedge-shaped. Its peak at first is directed to Gulf of Anadir, and then moves to Cape Navarin (Fig. 2.10.4). Velocity of stable ice formation increases till late December and decreases with approaching to deep water sea region with large depth of convection layer. Ice formation lasts on average till late April. Ice edge is stable in zone of isobath about 3000 m.

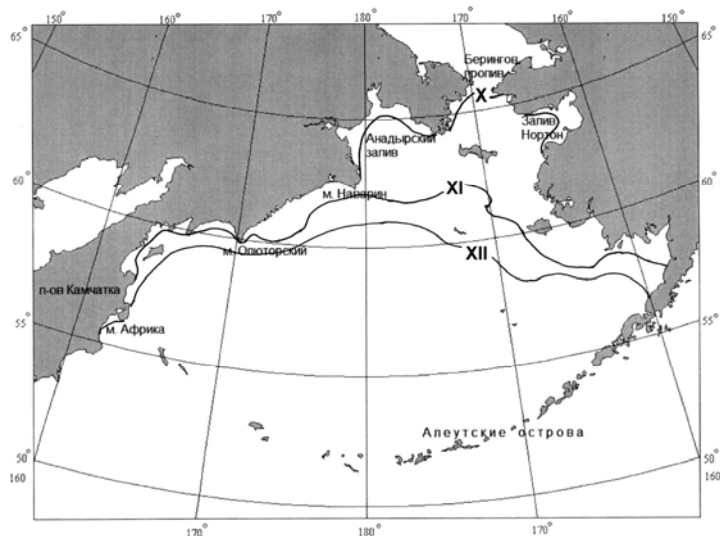


Fig. 10.2. Annual mean beginning of stable ice formation in October

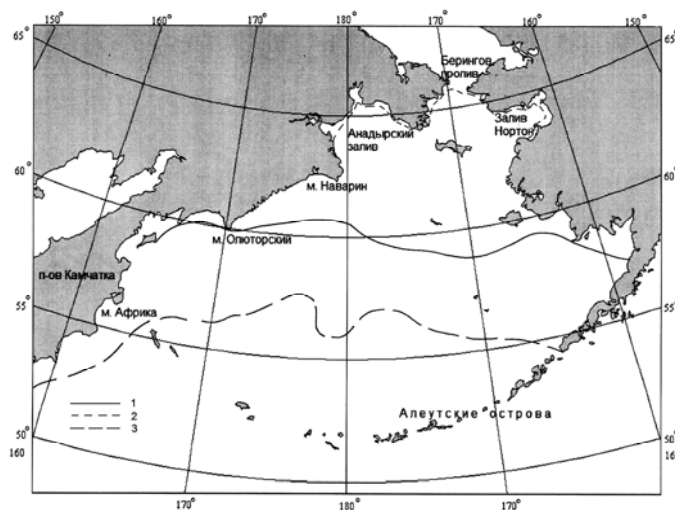


Fig. 10.3. Annual mean propagation of drift ice in November

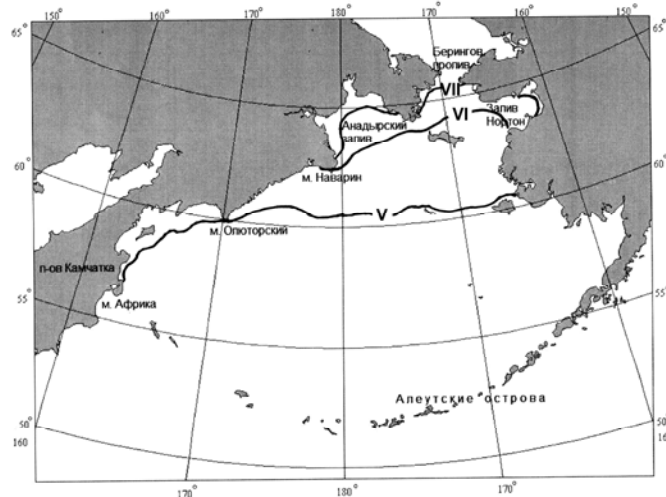


Fig. 10.4. Propagation of ice formation "wave" in December

Terms of stable ice formation depend on meteorological and ice-hydrologic conditions of spring-summer and autumn periods. These conditions have significant interannual changes. Therefore terms of stable ice formation can significantly differ from average ones. Terms variability of stable ice formation is expressed by amplitudes of terms of stable ice formation. Regime peculiarities of cooling water conditions of the Arctic Seas, which precede freezing, in significant measure are expressed by spatial distribution of amplitude values.

Early ice formation can start in the middle of September in cold autumn, and in warm - delay till early November. Thus, amplitude of stable ice formation terms in the Bering Sea on average is about month and a half.

#### 2.10.2. Ice cover in winter period

Boundary of drift ice in the Bering Sea during ice growth can move in direction of open water. Ice propagation in sea occurs till the middle of April. Location of ice edge during freezing coincides with isochrones location of stable ice formation terms.

Velocity of ice propagation in sea rapidly increases from November to December – on 13% (Fig. 2.10.4), and then it slows down with moving to the central sea regions. The central sea regions have high heat storage. To the end of ice growth period, in April, ice cover in the Bering Sea approaches on average 37%.

However, the largest ice propagation in the Bering Sea during soft and severe conditions doesn't occur simultaneously. Thus, in warm years ice maximum can be approached in February and can be only 20%. During moderate and severe winters ice cover reaches its maximum values 38 and 56% in April.

In Table 2.10.1 ice cover changes in the Bering Sea by months for different complicated types of ice conditions are presented. In moderate years ice cover is less than 40%, in severe years ice occupies more than a half of the sea water area. Difference in sea ice in warm and severe winters can reach 49%.

Table 2.10.1 – Ice changes in the Bering Sea during freeze-up period, %

Characteristic	Months						
	X	XI	XII	I	II	III	IV
Average	1	5	18	27	33	35	38
Maximum	4	8	28	38	45	52	56
Minimum	0	1	7	15	20	18	16

Ice cover in the Bering Sea is highly dynamic. Typical feature of ice cover development for

the entire sea is a sharp increase of a compact ice (10/10-th) frequency of occurrence in winter months (December-February) and decrease of concentration in April-May.

Increasing of thin first-year ice during winter period is typical for the Bering Sea. Young ice during winter decreases and in April is close to zero.

To early December frequency of occurrence of thin first-year ice is about 20%, then it slowly increases and in middle of February reaches its first maximum— 80-100%. Then frequency of occurrence of thin first-year ice decreases on 10-20% mostly till late March, that obviously depends on deep anticyclones coming over the Bering Sea. April is characterized by new increasing of frequency of occurrence of thin first-year ice to its maximum due to intensive melting of new and young ice.

Different ice forms are observed during entire cold year period in the northern region. Ice cake and small floes prevail during early ice formation, but large and medium ice floes appear in December. From January to the end of ice growth period ice mostly consists from large and medium floes. In zone of ice edge with width 30-90 miles broken ice prevails till second half of January. Ice cake and small floes are observed in zone of ice edge till the end of summer melting.

Zones with high ridging are stable in Bering Strait near Cape Navarin and in internal part of Gulf of Karagin in the first winter half. In water area ridging mostly approaches 1-2.

General increasing of ridging (2-3) is observed in March. In April reformation of ridging zones occurs due to change of general drift direction from western to northern. Ridging increases in northern regions, and in the south hummocks also disappear due to ice melting.

Several regions with stable ice compacting are observed in the sea. They are: internal part of Gulf of Karagin, western part of Anadir Strait, northern part of Bristol Strait and western part of Bering Strait.

Strong ice compacting in open sea occurs, when deep cyclones come to the south-western and southern Bering Sea.

Four zones with high snow cover are determined in the Bering Sea. In December snow areas (more than 2 marks) are formed in the western part of Gulf of Anadir, eastwards from Gulf of St. Lawrence to Bering Strait in internal parts of Gulf of Karagin and Norton-Saundo. Large amount of snow on ice is observed in Anadir liman and Gulf of Crest. Amount of snow on ice increases in late March. General decreasing of snow on ice is noticed in May due to intensive melting.

### 2.10.3. Ice cover melting and sea clearing from ice

Ice melting in the Bering Sea occurs from middle of April to June. Places of sea clearing are

near ice edge zone, river mouth zones and also stable polynyas. Ice melting intensively occurs in near ice edge zone.

Open water, areas of open and very open ice (concentration 4-6-th and 1-3-th, respectively) appear due to start of melting and under influence of dynamic processes. Sea water area, covered with all types of ice concentration (ice cover), decreases due to ice melting.

In April and May melting intensity is rather small, and ice edge in central sea region moves northwards on one degree of latitude (in the centre of sea to latitude 60° N). During July ice melting intensively increases, and open water areas approach to Bering Strait and to Gulf of Norton-Sauno. Absolute disappearance of drift ice in the Bering Sea occurs in early June.

Drift ice absolutely disappears in the Bering Sea under favorable conditions in June.

In Table 2.10.2 ice cover changes in the Bering Sea are presented by months for different complicated types of ice conditions in summer.

Table 2.10.2 – Ice changes in the Bering Sea during melting period, %

Characteristic	Months				
	V	VI	VII	VIII	IX
Average	20	5	0	0	0
Maximum	35	16	4	1	1
Minimum	6	0	0	0	0

Under average conditions ice cover of the Bering Sea approaches 20% in May, ice remains by this time in the northern sea region and absolutely melts away only in July. Ice can remain in the western half of Bering Strait from Ratmanov Island to Providence Bay till August and even September after winter with large ice cover and unfavorable ice conditions. In separate years ice can be observed in the Bering Sea during entire year under unfavorable development of ice processes in summer.



## 2.11 Characteristics of ice conditions in the Sea of Okhotsk

### 2.11.1. General aspects

The Sea of Okhotsk – is a sea in the north-western Pacific Ocean, separated by Kamchatka peninsula, Kuril Islands and Island Hokkaido. The sea washes coasts of Japan and Russia (Fig. 2.11.1).

Sea area is 1,603 000 km<sup>2</sup>. Average depth is 1780 m, maximum depth approaches 3521 m. Western sea region with small depth is located on continental shelf. Hollow of Derugin (in the south) and TINRO trough are located in the sea centre. Kurilskaya hollow with maximum depth is located in the eastern sea region.

Northern coast is strongly indented. Gulf of Shelikhov (the largest sea gulf) is located in the north-eastern Sea of Okhotsk. Coast line of Kamchatka peninsula practically doesn't have any gulfs in the east. Gulf of Aniva and Terpeniya Bay are the largest in the south-west.

From October to May-June northern sea region is covered with ice. South-eastern region is practically ice-free.

Main harbors: on continent – Magadan, Ayan, Okhotsk (harbor point), De-Castri (harbor point); on Sakhalin Island – Korsakov, on Kuril Islands – North-Kurilsk.



Fig. 2.11.1. The Sea of Okhotsk map

### 2.11.2. Ice formation

Stable ice formation normally starts in the north-western sea region in November, and in mouth parts, where water is desalinated, – in second half of October. Ice sequentially propagates

southwards along western and eastern coast and then to the open sea region. In late November and in early December northern and north-western sea regions are cooling so strong, that intensive ice formation starts on large open sea areas (Fig. 2.11.2). In December and January stable ice formation in sea intensively propagates. Ice formation in sea is observed till the first half of March.

In December extensive motionless fast ice is formed in gulfs and bays.

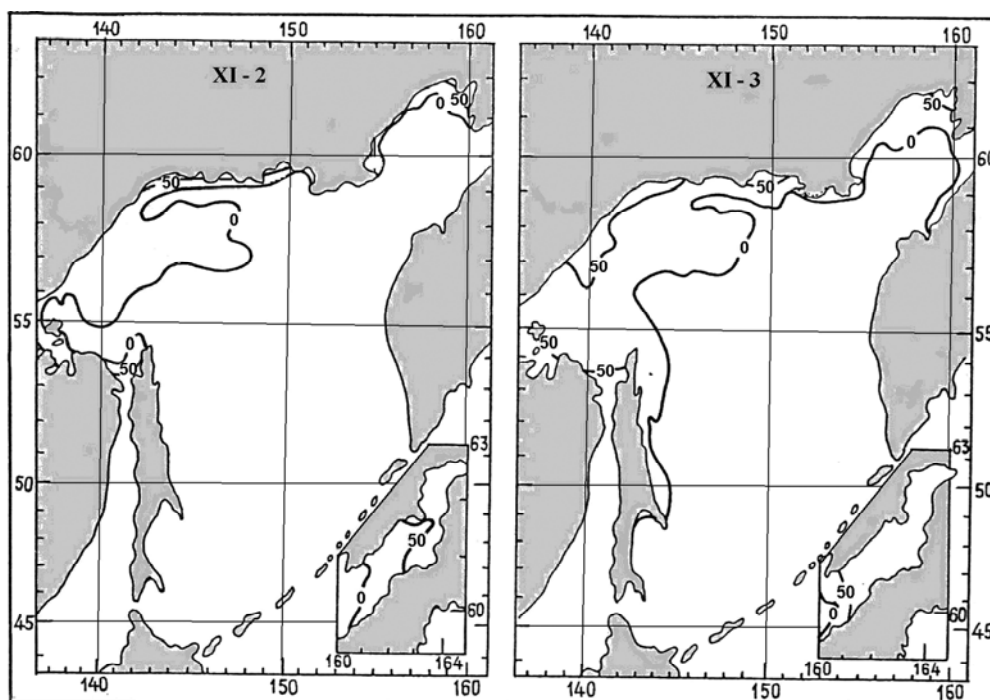


Fig. 2.11.2. Propagation of stable ice formation in the Sea of Okhotsk in November

### 2.11.3. Ice growth in winter and age composition of drift ice

Long-term winters with strong frosts lead to sea surface cooling, accompanied by intensive ice formation and ice growth mostly in all sea regions. During winter drift ice of different age is observed in most sea area. Propagation maximum of ice cover is observed in the first half of March. By this time sea is normally ice-free only in the south-western sea region (about 20% of sea area) (Fig. 2.11.3)

The Sea ice has only local origin. In general, the Sea of Okhotsk can be compared to the Arctic Seas by severity of ice conditions. Average duration of ice period in the north-western sea region is 250 days, in northern regions and near coast of Sakhalin Island - 190-200, and in the south – 110-120 days a year. Maximum duration of ice period in most severe winters can reach 290 days.

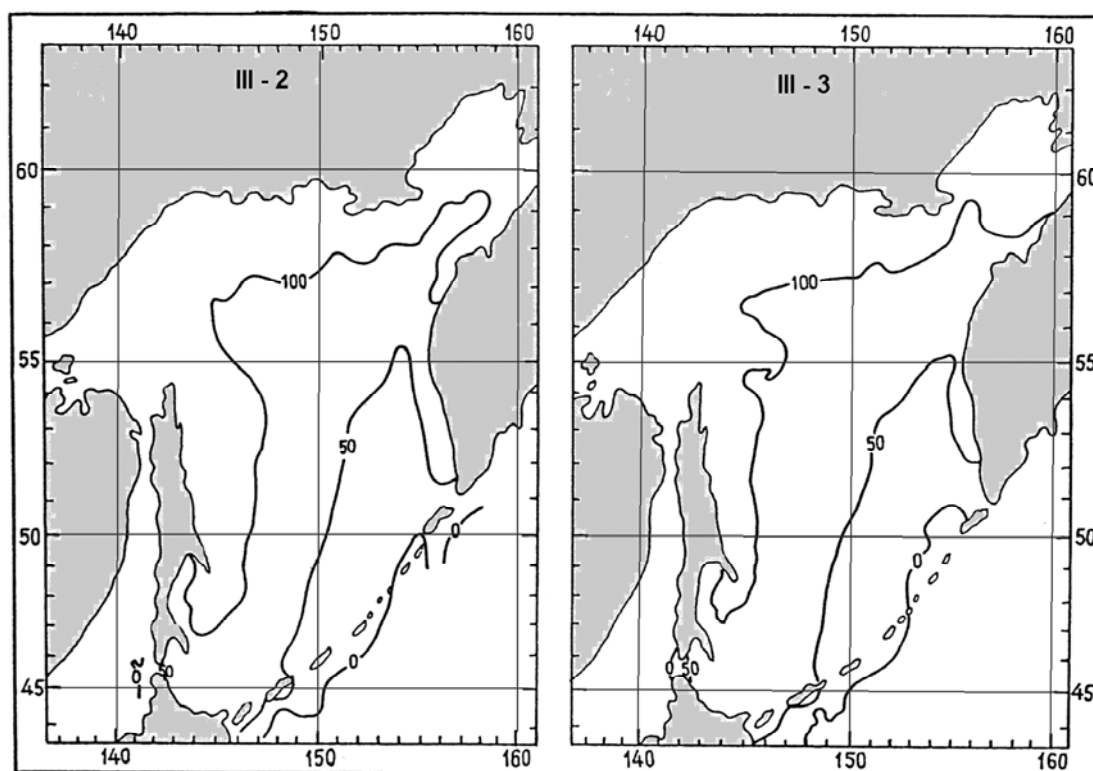


Fig. 2.11.3. Probability of ice observation (%) in the Sea of Okhotsk in period of its maximum propagation

Sea ice is about 80% (Table 2.11.1). In most severe winters ice cover occupies up to 97% of entire sea area. Only along ridge of Kuril Islands there is a narrow stripe of open water. In mild winters about 57% of sea area is covered with ice.

Table 2.11.1 – Average values of ice cover (%) in the Sea of Okhotsk in the middle of month

Characteristic	Month					
	December	January	February	March	April	May
Average	20	54	74	82	67	27
Standard deviation	6	13	12	9	12	10

Low temperatures of wind and air influence new ice compacting, freezing and rafting. Ice growth occurs rapidly, and forms of young ice appear – grey and grey-white.

In Amur liman and in peak of Penzhinskaya Bay new ice transforms into grey and grey-white in the middle of November. In December thin first-year ice is observed in these zones. Medium first-year ice is normally observed in the mid-February. It propagates to Hokkaido Island and blocks La Perouse Strait.

Ice thickness (if not accounting ridging) in coastal and shallow zones approaches 40-50 cm in January and December, in Gulf of Shelikhov and along Kamchatka coast - 30-40 cm, in open sea (average conditions of winter severity) - 40-70 cm. Maximum values of ice thickness (90-160 cm) are observed in severe winters in Gulf of Sakhalin and in zone north-eastwards from Elizabeth Cape (Northern Sakhalin).

Hummock height in open sea is less than 1 m. In separate gulfs with intensive ridging, in Gulf of Sakhalin, Yamskaya and Penzhinskaya Bays, it increases up to 1,5-3,0 m. Ice ridging in the Sea of Okhotsk is caused by stormy winds, tidal currents and horizontal ice motion forced by wind and currents. Stormy wind is caused by cyclones, coming to the Sea of Okhotsk from the south. As a result such type of ridging is mostly observed in the southern and eastern sea regions. Ridging under effect of tidal currents is typical for Penzhinskaya Bay and ware areas, adjoining to Gulf of Sakhalin.

The strongest ice compacting occurs under total effect of wind, currents and tidal currents. Gulf of Sakhalin and Yamskaya Bay can be related to these regions. In Gulf of Sakhalin zone with high ridging up to 3 is formed in January. In listed regions, and also near northern coast of eastern Sakhalin grounded hummocks are formed on depth up to 20 m.

In March drift ice mostly propagates southwards and south-eastwards. At this time very compact ice (up to 10-th) is observed everywhere.

Drift ice in the Sea of Okhotsk is presented by all age types during its development in winter, including thick first-year ice (Fig. 2.11.4). In the end of growth period ice thickness reaches its maximum - 120-140 cm (Gulf of Sakhalin). Ice reaches thickness of thick first-year ice (30-70 cm) in 2,5-3 10-day periods (from the beginning of ice formation), and thickness of medium first-year ice (70-120 cm) – in 7 10-day periods.

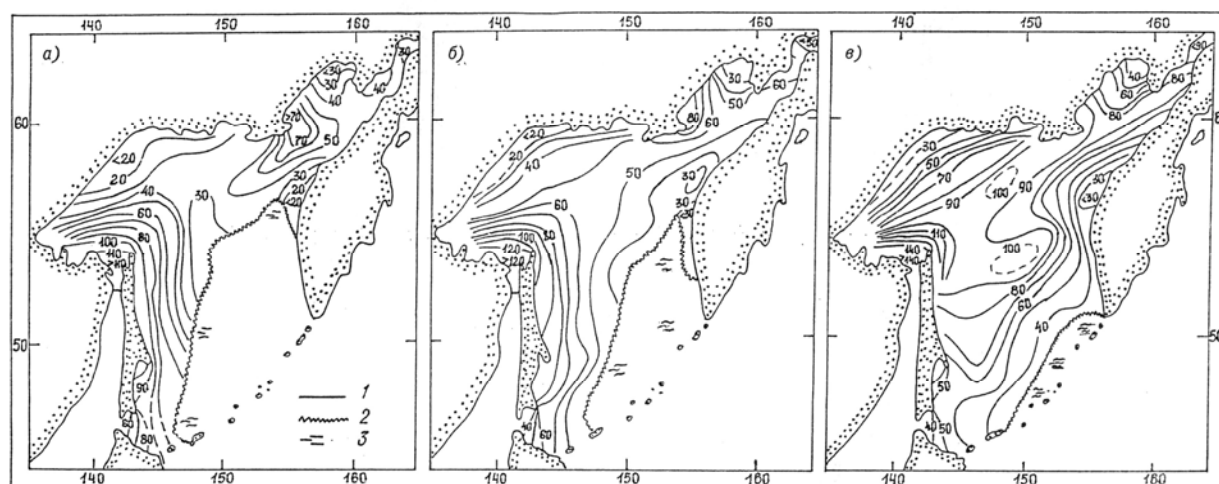


Fig. 2.11.4. Calculated ice thickness in the Sea of Okhotsk in period of its maximum development in mild (a), moderate (б) and severe winters (в) 1 – isolines of ice thickness, 2 – edge of drift ice, 3 – open water)

Ice transforms into thick first-year (more than 120 cm) in 12 10-day periods after beginning of ice formation, though in most severe winters it can occur 2 10-day periods earlier (Table 2.11.2).

Table 2.11.2 – Period between stable ice formation and reaching particular age with formation of ice cover under different conditions

Ice age	Number of 10-day periods between stable ice formation and reaching different age under ice formation								
	In open water			Among open ice			Among compact ice		
	average	Max.	Min.	average	Max.	Min.	average	Max.	Min.
Grey-white	1	2	0	0	1,5	0	0	1	0
Thin first-year	2,5	4,5	1,0	2,5	3	1	0	1,5	0

Dominant ice forms are changed with ice cover development in winter. Maximum prevalence of large ice forms occurs from January to March. In listed period broken ice is observed only near the drifting ice boundary as a narrow, 30-60 miles wide stripe. In north-western sea region vast ice floes with linear size up to 10 km are observed among dominant big floes in February. In March big ice floes are also dominate along Sakhalin Island. In April intensive destruction of ice brecchia floes, which form vast ice floes, begins and amount of smaller ice floes (broken ice) increases.

Snow cover of the Sea of Okhotsk is propagated irregularly. In December snow cover is significantly developed in some sea regions. These are zones of Gulf of Sakhalin, Yamskaya and Penzhinskaya Bays. Snow cover in these zones reaches 2 marks.

In January snow cover increases in sea in general. In March total ice cover reaches its maximum. It is a natural process, connected with frequent occurrence of cyclones and with fall of large number of dry precipitations. Zone with snow cover of 3 marks is observed near Shantar Islands, Gulf of Sakhalin and propagates to the eastern coast of Sakhalin almost to Hokkaido Island. In April snow melting starts on ice surface and snow cover decreases everywhere.

#### 2.11.4. Ice melting in summer and sea clearing

Beginning of ice melting is noticed in April. Ice starts melting in the southern sea regions on the boundary with the ocean. Beginning from April, ice edge moves northwards and total amount of ice decreases. More than half of sea area is ice-free to the middle of May (Table 2.11.1).

Eastern and western halves of the central Sea of Okhotsk are sharply distinguished by ice period duration and by type of ice conditions changes. Ice melting occurs during long period from April to June. In the north-western sea region ice remains till July. Southern coast of Kamchatka, central and northern Kuril Islands are distinguished by small ice cover and rather short terms of ice cover occurrence.

Melting processes intensively occur in May. Young ice and thin first-year ice melt first. In late May the most Sea of Okhotsk water area is normally ice-free.

Residual thick first-year ice can be observed in some sea regions for a long time. In June separate points of ice can be observed along north-eastern coast of Sakhalin Island, in zone of Shantar Islands, in Yamskaya and Penzhinskaya Bays (Fig. 2.11.5). It is parts of floes of thick first-year ice and broken fast ice, which is distinguished by large thickness and ridging. They melt slower due to their high capacity.

Sea absolutely clears from ice in July. But after severe and very severe winters stripes and points of drift ice can be observed in the second half of August south-westwards from Shantar Islands.

During entire period of observations the Sea of Okhotsk always got ice-free during summer. Ice, survived summer melting, which remains in sea till new stable ice formation, wasn't observed.

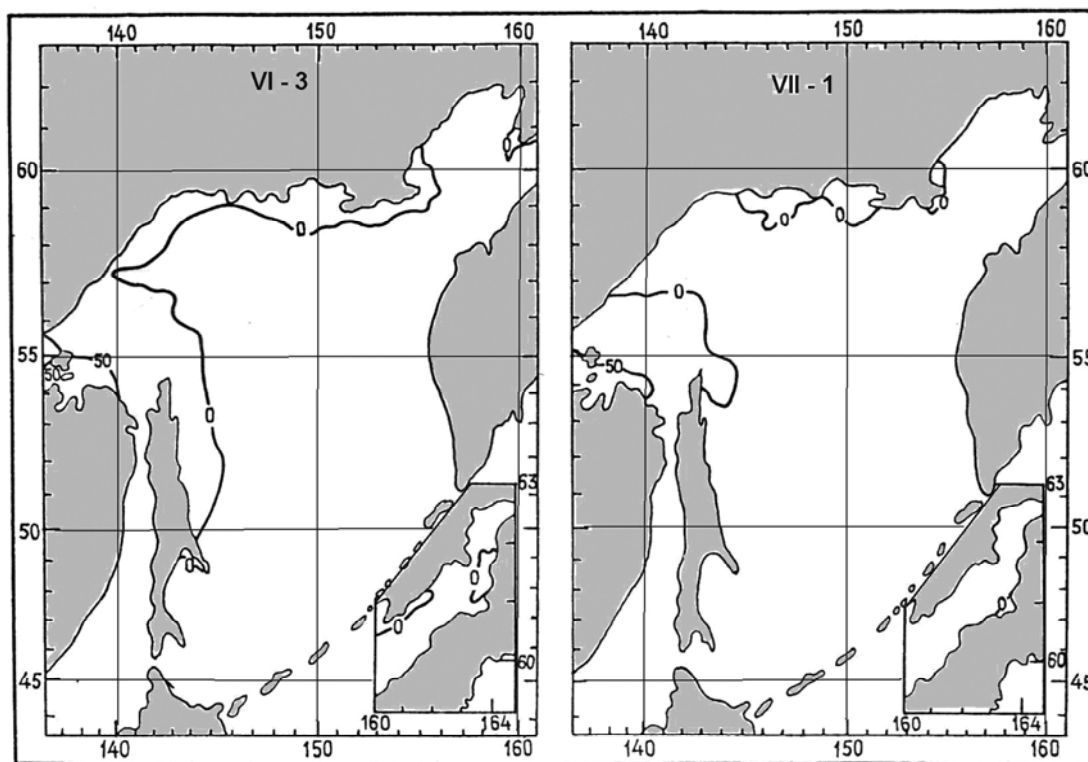


Fig. 2.11.5. Probability of ice observation (%) in the Sea of Okhotsk in period of clearing

## 2.12. Characteristic of ice conditions in the Sea of Japan

### 2.12.1. General aspects

The Sea of Japan - is a sea in the north-western Pacific Ocean, separated by Japanese Islands and Island Sakhalin. The sea is considered to be a marginal oceanic sea by its physical-geographical location. It is fenced off from adjoining water basins by shallow barriers. In the north and north-east it is connected with the Sea of Okhotsk by Straights of Nevel and La Perouse (Soya), in the east – with the Pacific Ocean by Sangar Strait (Tsugaru), in the south – with the East-Chinese Sea by Korean Gulf (Tsushima) (Fig. 2.12.1). The most shallow straight among them is Nevel Strait with maximum depth 10 m, and the deepest is Sangar Strait – about 200 m. In the south branch of warm current Kuroshio flows into the sea.

Sea area is 1,062 000 km<sup>2</sup>. Average depth is 1535 m. The largest depth reaches 3742 m. Northern and western coastal regions of the sea freeze every winter.

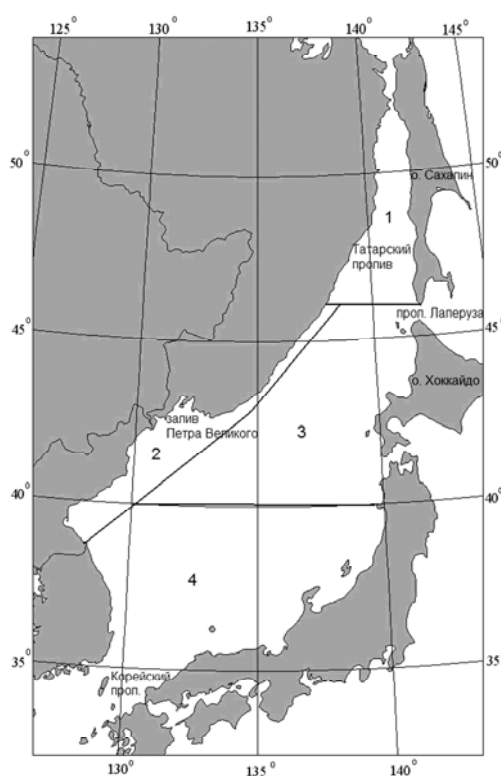


Fig. 2.12.1. Chart of the Sea of Japan with isobath

The Sea of Japan is located in two climatic zones: subtropical and moderate. Within these limits two sectors with different climatic and hydrologic conditions are separated: severe cold northern (partly covered with ice in winter) and mild warm adjoining to Japanese and Korean Coasts. Main factor, forming sea climate, is monsoon atmosphere circulation.

Ice conditions in the Sea of Japan are rather heterogeneous due to large sea extent in latitude direction and peculiar features of meteorological and hydrologic regimes. Three sea regions can be separated by ice conditions: Tatar Strait, western coastal region and Gulf of Peter the Great.

In winter ice is constantly observed only in Tatar Straight and in Gulf of Peter the Great. In other parts of water area ice, except closed gulfs and bays, hardly ever occurs. The coldest region in the Sea of Japan is Tatar Straight; where more than 90% of total ice is formed in winter.

Annual mean duration of ice period in Gulf of Peter the Great is about 120 days, and in Tatar Straight, due to its large meridian extent, from 40-80 days in the southern part of straight to 140-170 days in its northern part.

#### 2.12.2. Ice formation

Stable ice formation is observed in early November in isolated, deeply run inland, bays in the northern part of Tatar Straight. During November young ice rapidly propagates to open water area of Tatar Straight.

In moderate winters stable ice formation in Tatar Straight, in Gulfs of Soviet Harbor, Chikhachev and in Nevel Straight normally starts in the first 10-day period of November. In Gulf of Peter the Great ice formation normally starts in the second 10-day period of November.

When ice formation is early, ice appears in Tatar Straight in the second half of October. In Gulf of Peter the Great (Gulf of Amur) early ice formation is observed in early November. Late terms of ice formation occur in late November.

In early December ice propagation along Sakhalin Island occurs more rapid, than along continental coast. To late December ice amount on the eastern and western periphery becomes equal, and direction of ice edge changes, after reaching parallel of Cape Surcum. Decreasing of ice edge motion (initial ice) and intensive motion of ice formation “wave” along continental coast are observed along Sakhalin coast. In late January ice occupies entire northern part of Tatar Straight.

Amplitude of terms of stable ice formation reaches 30 days.

#### 2.12.3. Ice cover in autumn-winter period

During January and February stable ice propagation is observed in the sea freezing regions. Ice in the Sea of Japan has mostly local formation. Ice, coming from the Okhotsk Sea through Strait of La Perouse, is rarely observed.

In the Sea of Japan ice cover reaches its maximum propagation in the middle of February. On average, about 52% of Tatar Straight area and 56% of Gulf of Peter the Great area are covered with ice. In Tatar Straight absolute maximum of ice cover was registered (86,8% from area) in winter of 1950 – 51. In Gulf of Peter the Great this maximum approached in winter of 1969 – 70 (95% of area). Ice cover minimum in Tatar Straight was observed in 1991 (23,7%



from area).

Ice edge takes its extreme southern location in February, when ice cover is maximum. In mild winters it is less than 2,7 %, in moderate - 5,4 %, and in severe winters increases up to 10,3 % from sea surface area (from total sea area, 1062000 km<sup>2</sup>). Seasonal propagation of ice cover is presented on Fig. 2.12.2.

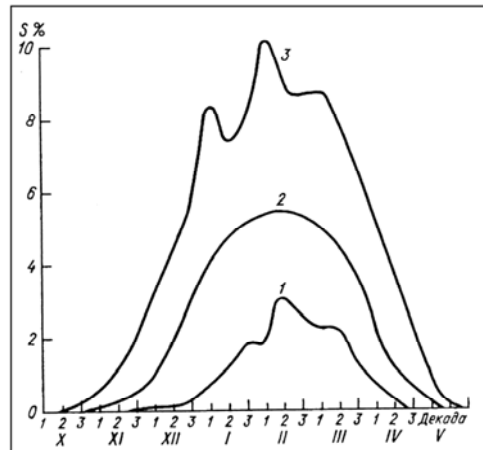


Fig. 2.12.2. Seasonal course of ice cover changes in the Sea of Japan (1 – favorable conditions, 2 – moderate conditions, 3 – unfavorable conditions)

Ice edge in period of its maximum propagation, which occurs in February, in the west moves down to 39° N, and in the east – to 43° N. Frequency of occurrence of different types of ice seasons is: 14% - minimum ice, 72% - close to norm and 14% - seasons of maximum ice.

In mild and moderate winters ice is observed only in Gulf of Peter the Great and Tatar Strait. On Fig. 2.12.3 different probabilities of ice observing in February are shown. Probabilities of 50% correspond with average boundary of ice location. Probabilities of 25% and 75% correspond with location of ice boundary under rather mild and severe conditions.

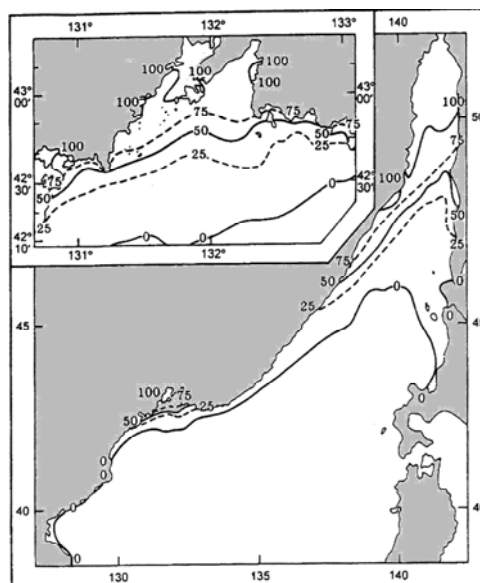


Fig. 2.12.3. Probability of ice observation in February

Ice of the Sea of Japan has different age composition during entire winter, depending on ice growth. Grey and grey-white ice is observed in the northern part of Tatar Strait in late November. Young ice reaches stage of thin first-year in late January – early February. Ice rafting, ridging and small ice cake are observed in coastal sea parts due to dynamic processes (offshore and onshore winds). Low temperatures facilitate its freeze up. That is why, ice with thickness up to 100 cm can be observed in separate coastal regions.

In spite of low air temperatures average thickness of drift ice in open parts of Tatar Strait is about 40 cm, but it can reach 60-80 cm in more severe years.

In the peak of Gulf of Amur grey ice is observed in late November, in the first 10-day period of December it transits to stage of grey-white ice. In January grey-white ice is observed in entire water area of Gulf of Peter the Great. Thin first-year ice is observed in the northern parts of gulf on the boundary with fast ice and in closed bays.

Annual mean ice boundary, which ice can approach with winds and currents from the north, approximately comes along Strait Posiet by the western sea coast to Cape Kamui at Hokkaido Island, deeply run to the north to 46 parallel. Northwards from this line ice is observed annually, southwards it hardly ever appears in the open sea. Only shuga, broken ice and slush ice are observed in small bays of western coast in very cold winters. Slush ice, shuga and broken ice are normally observed to 46° N. Northwards 46° N ice becomes more compact, its thickness increases up 30–60 cm; after 48° N its concentration increases a lot, especially along coast, where ice thickness on level floes reaches 50–80 cm. Ice cover of the Sea of Japan is extremely unstable. As a result of strong north-western winds, dominant in winter, ice uninterruptedly breaks and drifts south-westwards and southwards, especially in the central sea region, where strong ice motion and wide fracturing are observed during the most winter. Ice moves to Sakhalin coast by the same reason, forming here solid hummock ridges up to six meters height. During long-term south-eastern wind hummocks are formed along continental coast, but with less height, to 2 – 3 m.

It is necessary to mention, that ice cover in the eastern parts of Tatar Strait and Gulf of Peter the Great is less, than in western water areas. According to long-term data duration of ice period in Gulf of Peter the Great is about 120 days. In Tatar Strait (due to its large meridian extent) it is from 40 – 80 days in the southern part of straight to 140-170 days in the northern part.

In spite of relatively small area, occupied by ice in the Sea of Japan, concentration, age and ice forms significantly differ by spatial and time variability. E.g., ice is transported to the central and eastern parts of Tatar Strait under strong and long-term western and north-western winds. At the same time polynya is formed along western coast with width up to 5-10 miles, where

intensive producing of initial ice occurs in its term. Under long-term storms with northern winds ice depression takes place, and under southern ones - ice compacting in the central part of straight, leading to ice edge retreat northwards.

In Tatar Straight dominant concentration of ice cover in period of ice formation and intensive ice growth (November-December) is - 7-9-th, under maximum possible values of concentration - 9-10-th; in period of maximum ice propagation (February) -9-10-th, under average possible values of concentration – 10-th. In March and in April average concentration starts to decrease.

Ice ridging in Tatar Straight propagates irregularly. Low ridging is observed in the central part of straight, compared to the western and eastern parts of straight, where ridging is higher. In November, when nilas and grey ice prevail, where ice rafting occurs instead of ridging, ice ridging is equal to zero. Starting from grey-white ice, motions and compacting of all age types lead to occurrence of hummocks. Average ridging in December – January (dominant grey-white ice) is 1-2, in February – April (dominant medium first-year ice) average ridging is 2. The highest ridging, reaching 3-4, is observed in the north-eastern part of straight (Fig. 2.12.4).

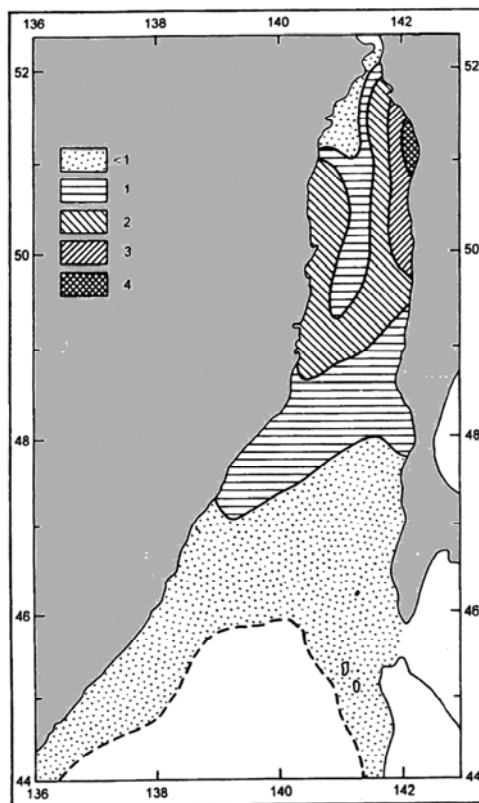


Fig. 2.12.4. Average ridging in Tatar Strait in period of maximum propagation of ice (marks)

Dominant size of ice floes changes during autumn-winter period. In November and December ice cake and small floes prevail. Decreasing of air temperature leads to rapid freezing of broken ice forms into large and medium floes. In January-March large and medium ice floes dominate in straight (Fig. 2.12.5). Large and giant floes can be observed in some rare cases. In

April large ice forms start to melt. Dominant broken ice is observed in the straight.

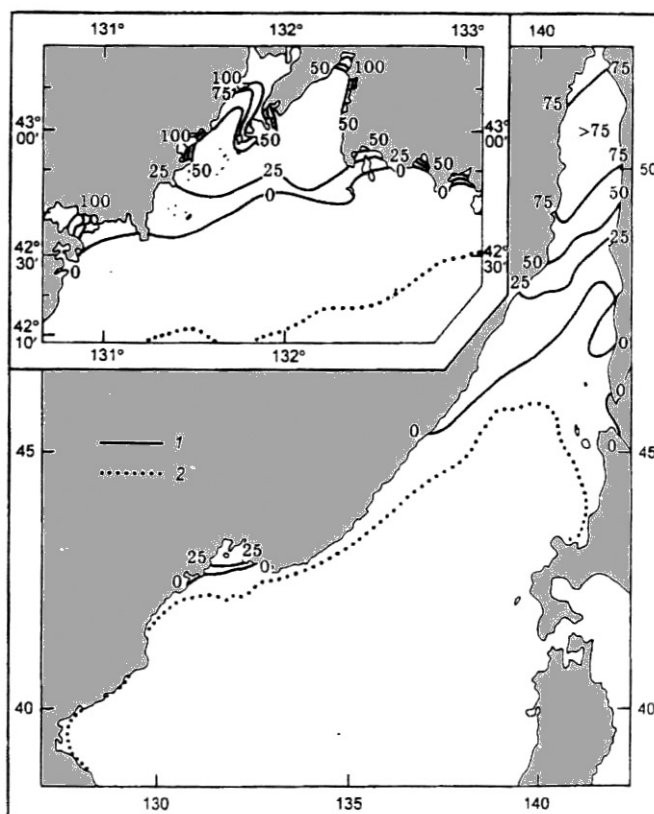


Fig. 2.12.5. Frequency of occurrence of large ice forms (large and medium floes) in period of maximum propagation of ice cover. (1 – frequency of occurrence isolines; 2 – boundary of the largest ice propagation)

Ice compacting in straight depends on velocity and direction of wind and tidal currents. When wind velocity is 15 m/s and more, role of wind component in compacting is dominating compared to tidal component. Ice compacting is normally observed under ice concentration 9 and 9-10-th. In zones, where large and giant floes prevail, ice compacting can start under concentration 7-8-th. As a rule, compacting occurs along coast, where ice suffers from off shore wind. Study of observations and climate estimations allows suggesting, that average intensity of compacting is 1. Maximum values of compacting can reach 2-3. Compacting is not observed in November, when young ice prevail and its concentration on average is less than 7-8-th, and in April, when average ice concentration decreases to 3-6-th.

In Gulf of Peter the Great and in the eastern and northern parts of Gulf of Amur and in Posiet Gulf ice areas with concentration 7-9-th dominate to mid-November. In bays and gulfs ice concentration is less than 6-th and only in Preobrazheniya Bay and harbor Tihkaya Pristan' ice concentration can reach 9-10-th.

Propagation of ice age types has its own regularities. In the most northern part of straight grey ice zone with concentration 0 marks is observed as a rule. Southwards this zone there is a massif of compact grey-white and thin first-year ice. In zone near ice edge with width 10-15

miles broken grey-white ice dominates. In mild winters heavier ice accumulates along western and south-western coast, and in winters close to norm – concentrates along Sakhalin coast. Latitude propagation of age ice zones corresponds with severe winters: from Nevel Strait young ice sequentially transforms into old types, and only near ice edge frequency of occurrence of young ice increases again.

Amur and Ussuriysk Gulfs are mostly covered with grey and grey-white ice with concentration 7-9-th in January – February. Decreasing of temperature facilitates freezing of small ice forms into floes of frozen ice, which, beginning from January, are observed in the entire water area of Amur and Ussuriysk Gulfs. In spring ice concentration rapidly decreases due to intensive melting, all types of young ice disappear and percentage of older ice content increases. In the middle of March compact ice can be observed only in the northern half of Amur Gulf and in the eastern parts of Ussuriysk Gulf. During one or two 10-day periods ice concentration decreases to 1-3 to absolute clearing.

#### 2.12.4. Ice cover in spring period

Spring processes, facilitating ice melting, start in late February, but especially sharp in March and April. Ice edge moves northwards and in mildest years ice absolutely disappears to late April. After very severe winters separate parts of ice can be observed near Nevel Strait even in late May. Early clearing from ice in the Sea of Japan occurs in second 10-day period of April, later – late May – early June (Fig. 2.12.2).

Sea absolutely clears from ice. Ice has never survived even after very severe winters.

## 2.2. Characteristics of the White Sea ice conditions

### 2.2.1. General aspects

The White Sea, located in the north of European part of Russia, is connected with the Barents Sea and belongs to the Arctic Ocean water area, and in structural-geomorphologic relation it is marginal shelf sea.

Geographical location, morphometric features, river flow and advection influence of warm Barents water are characteristic features of hydrologic and ice regime of the White Sea. Some elements of its continental climate are defined by its inland location, which brings it closer to the Arctic Seas under hydrologic and ice regime. Negative water temperatures are kept in sea column even in summer, and compact ice cover is formed in winter.

Though rather small water area (about 90 000 km<sup>2</sup>), the White Sea was strongly dismembered and divided into several regions with their own names (Fig. 2.2.1).

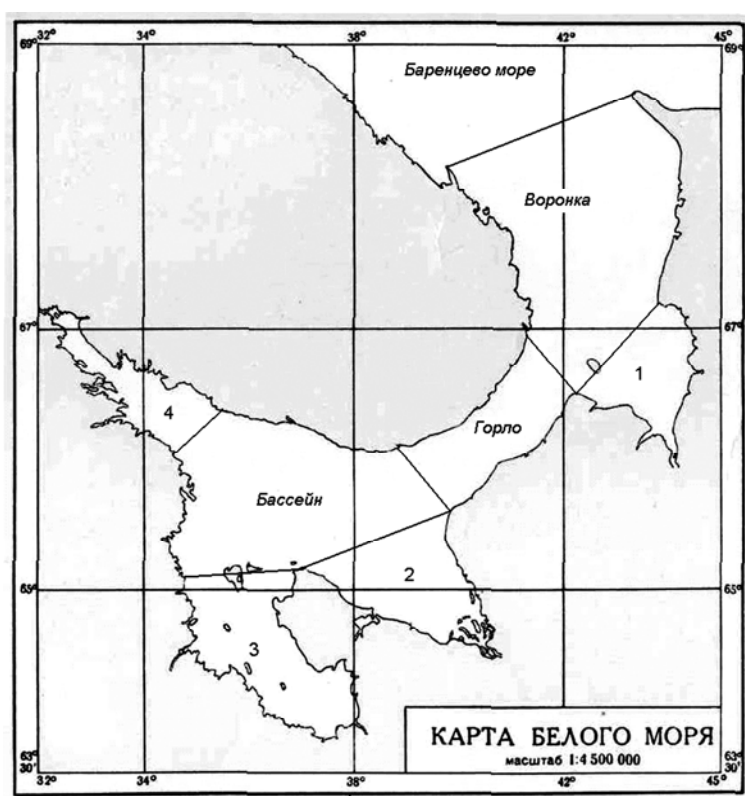


Fig. 2.2.1– The White Sea division into zones

Maximum depth of the White Sea is 343 m. On the large part of Voronka (funnel) and Gulf of Mezen depth doesn't reach 50 m. The deepest part of the White Sea is its Basin. About 2/3 of its area is occupied by cavity with depth more than 100 m. This cavity with width 15-40 miles lasts from Gulf of Kandalaksha south-eastwards to entrance of Gulf of Dvina.

Gulf of Kandalaksha is the most deep-water among all sea gulfs. Its depth peak is 50 m. In Onega Bay depth of 10-25 m is dominant.

### 2.2.2. Ice formation

Sea ice formation starts in the first numbers of November in the gulf's peaks. In December ice formation intensively propagate from gulfs to central sea regions. In the middle of December ice formation starts in Gorlo (throat), and in early January – in Basin (Fig. 2.2.2).

Fig. 2.2.2. Annual mean terms of stable ice formation in the White Sea

In January new and young ice are propagated to entire water basin, except north-western part of Voronka. In this region processes of ice formation are held back by warm flow of the Barents Sea water and by western winds, that move formed ice to eastern parts of Voronka.

Drift ice can cover the White Sea water basin ultimately and even come out of its boundary to the Barents Sea in severe winters.

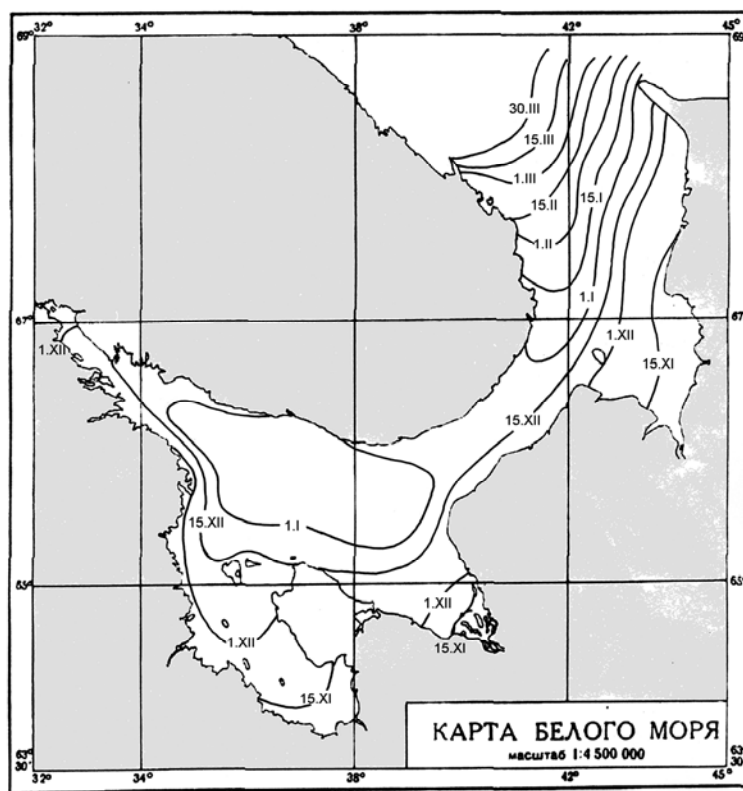


Fig. 2.2.2 – Ice growth and age composition of drifting ice

When stable ice formation is propagated, drifting ice edge in the White Sea moves to deep-water basin, then through Gorlo to Voronka and further to the Barents Sea boundary.

The White Sea ice has only local origin, that is why winter severity plays the most important role in formation of ice thickness and ice amount in the White Sea. Severity criterion of winter is air temperature and frost degree-days summary. Variability range of air temperature between mild and severe winters is more than 7°C in January-February (Fig. 2.2.3).

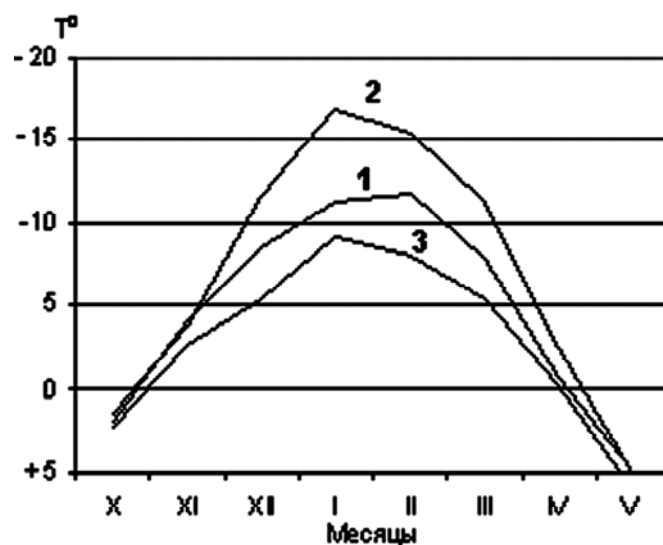


Fig. 2.2.3 – Average air temperatures in the White Sea in moderate (1), severe (2) and mild winters (3).

From data for 40 years observational period mild winters frequency of occurrence is - 20%, moderate - 63% and severe – 17%. Duration of ice period in the White Sea in heavier years is 8 months, 2 months more than in average years.

Ice edge location in freeze-up period is close to location of isochrones of terms of stable ice formation. Ice edge location significantly differs in sea, depending on winter severity. In moderate winters ice edge moves from gulf basins to open sea regions in December (Fig. 2.2.4), in severe – in November (Fig. 2.2.5), and in mild – only in January (Fig. 2.2.6).

Apart from the Arctic Seas, open ice and very open ice is completely absent in the White Sea (1-6).

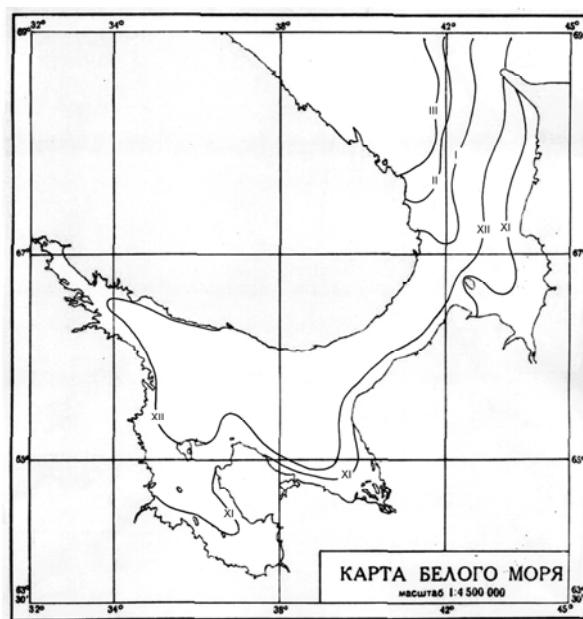


Fig. 2.2.4 – Ice edge location in the White Sea in moderate winter



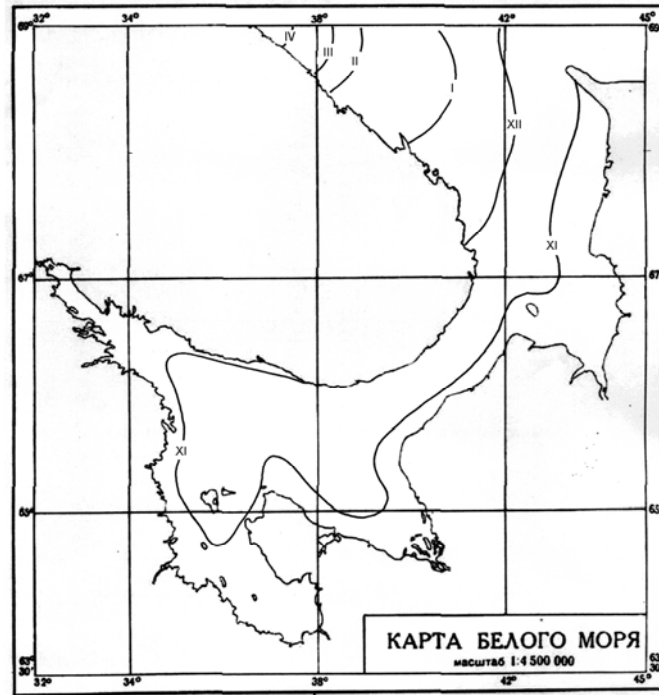


Fig. 2.2.5 – Ice edge location in the White Sea in severe winters

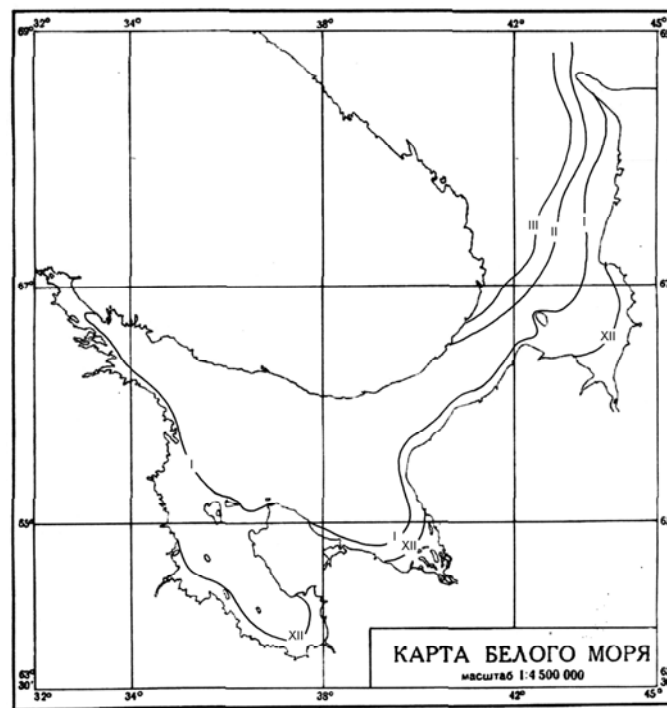


Fig. 2.2.6 – Ice edge location in the White Sea in mild winters

In severe winters ice edge comes out of sea limits in January, and ice cover formation continues till April (Fig. 2.2.5). In moderate and mild winters ice cover formation lasts till March (Fig. 2.2.4, 2.2.6). In mild winter about half of Voronka is free from ice, and in moderate – only edged north-western part.

In December first ice and nilas are seen in sea, grey ice starts to occur. Ice can be observed in Gulf of Onega, Gulf of Mezen and Gulf of Dvina.

From the middle of January all ice types are presented in sea, however, grey-white and thin first-year ice are dominant. Concentration of grey-white and first-year ice increases from 3 marks in Voronka, to 5 marks in Gorlo and to 7 marks in Basin. Grey ice and nilas have rest 3-7 marks.

Compact first-year ice and grey-white ice are observed in sea in February. The most amount of thin first-year ice (60 cm thickness) is located in sea Gorlo – up to 6 marks, 4 marks – in Voronka, and 2 marks – in Basin.

In March-early April compact first-year ice prevails in most water basin (Table 2.2.1), except western sea regions. Near western continental coast and western coast of Gulf (Karelia, Pomor, Letniy) polynyas are formed in summer under effect of prevailing south-western winds. Polynyas are filled in by young and less compact ice. In mild winters ice in polynyas is able not to form.

In February-March new ice and nilas can absolutely disappear as a result of long-term thaws.

Drifting sea ice doesn't exceed age of thin first-year ice even in most severe winters (medium first-year ice is rarely formed in small amount). Sea ice is formed in December, two months earlier than in mild winters, in February-March its concentration reaches 9-10 marks. Age ice composition in period of maximum propagation is presented in Table 2.2.1.

Zones of ice, formed as a result of stratification, are observed practically in entire sea basin. Their thickness significantly exceed level ice thickness, formed only under effect of thermal factors, and can reach 1,5 m. Snow cover on sea routes doesn't depend on winter severity, and in January on average it doesn't reach 1-2 marks. It increases to 2-3 marks till March and in April decreases to 1-2 marks.

Table 2.2.1 –Ice age composition in the White Sea during period of its maximum propagation (March), from data for the period 1951-1985

Ice age	Ice thickness	Amount, %
Initial ice type	≤5 cm	1
Nilas	<10 cm	7
Grey ice	10-15 cm	10
Grey-white ice	15-30 cm	18
Thin first-year ice	30-70 cm	43
Channels, polynyas	-	21

#### **2.2.4. Ice drift**

Dynamics of water and ice in the White Sea are defined by morphometric sea features, river flow, wind regime and tidal phenomena. Scheme of general ice drift in the White Sea is defined by system of constant currents and prevailing from November to March south-western winds (Fig. 2.2.7).

Velocity of windy ice drift depends on wind velocity. If wind velocity is equal to 10-15 m/s, ice drift speed in Gorlo is 0,4-0,5 knots. Maximum velocity of total drift (wind and tidal both) in Gorlo can reach 2.5-4.2 knots.

In general exporting drift is typical for the Barents Sea. According to different estimations annual export is from 35 to 70% from the total ice volume of the White Sea.

Maximum velocity of ice drift in Gorlo was observed within limits of 20-25 miles/day, for other regions - 10-15 miles/day.

#### **2.2.5. Fast ice and flaw polynyas**

In the White Sea formation of fast ice starts on average in the second half of November from ice freeze-up in river mouth parts, flowing into seas. Fast ice establishment in gulf regions of sea occurs in late December – early January. Fast ice is formed in the second half of January along open coast. Maximum propagation of fast ice occurs in late February. By this time fast ice is edging almost entire sea coast, becoming wider in gulf peaks. In late winter total area of fast ice normally doesn't reach 10% from sea area.

Fast ice reaches its most propagation in Gulf of Kandalaksha, Onega and Dvina (Fig. 2.2.7). In Gulf of Kandalaksha, depending on severity of winter conditions, maximum fast ice thickness varies in range of 45-65 miles.

In Gulf of Onega fast ice width changes in range of 9-13 miles, in Gulf of Dvina - 13-18 miles. In Gulf of Mezen fast ice develops sequentially, and its width on average doesn't exceed 1-1,5 miles. Fast ice is located from several hundreds meters to a mile from open coast.

In Gulf of Onega fast ice width changes in range of 9-13 miles, in Gulf of Dvina - 13-18 miles. In Gulf of Mezen fast ice propagates sequentially, and its width on average doesn't exceed 1-1,5 miles. Fast ice is located from several hundreds meters to a mile from open coast.

Every year fast ice is formed round Solovetskie Islands.

During winter the largest thickness of level fast ice near coast is on average 60-70 cm, and in severe winters is close to 100 cm (two times bigger than ice thickness in late mild winter).

Practically entire fast ice of Gulf of Onega, Mezen, southern part of Voronka is strongly hummocked and grounded hummocked. Ice ridging in some places can reach 4-5 marks.

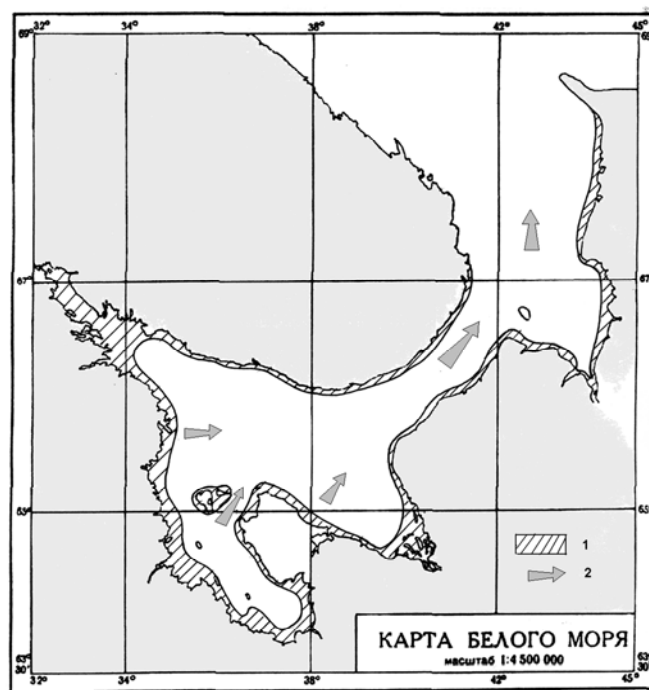


Fig. 2.2.7 – Maximum propagation of fast ice (1) and general ice drift direction (2) in the White Sea

The White Sea polynyas are rather dynamic. Their occurrence usually lasts several days and depends on wind force and duration, and also cooling intensity. Prevailing of western, south-western winds in winter leads to flaw polynyas occurrence and formation of depression zones, located mostly along Tersk (eastern) coast of Gorlo, and also along southern coasts of the White Sea Gulfs.

### 2.2.6. Compacting and ice ridging

Ice compacting is typical for entire sea basin, because ice constantly moves under tidal drift and wind effect. Tidal in the White Sea are semidiurnal. Tidal deviations of level from average position can reach in Voronka 3,5 m, in Gulf of Mezen – 10 m, in Gorlo – 3 m, in Gulf of Onega peak – 3,2 m. Tidal are significant for occurrence ice drift depression and zones of compacting in these regions (Fig. 2.2.8).

Ice cover in the White Sea is mostly ridged. Level floes of nilas and young ice partly can be seen in basin, Gulfs of Dvine and Kandalaksha and in Voronka, but they don't exist long.

Grounded hummocking is typical for shallow regions of the White Sea. The largest amount is observed in Gulfs of Onega and Mezen. Thickness of hummock ridges in piles and barriers and grounded hummocks can exceed 10-15 m.

Ice ridging increases in course of general ice drift from Basin to Voronka in any winter month. At the same time seasonal increasing of ice ridging is observed on almost entire sea basin from January to April.

In January ice ridging in water basin is 0-1 marks, in throat – 1-2 marks, on the bigger part of Voronka (along Kaninsk coast) – 2-3 marks. In the north-easternest Gulf of Mezen ridging reaches 3-4 marks. Ice along Onega coast was ridged to 2-3 marks.

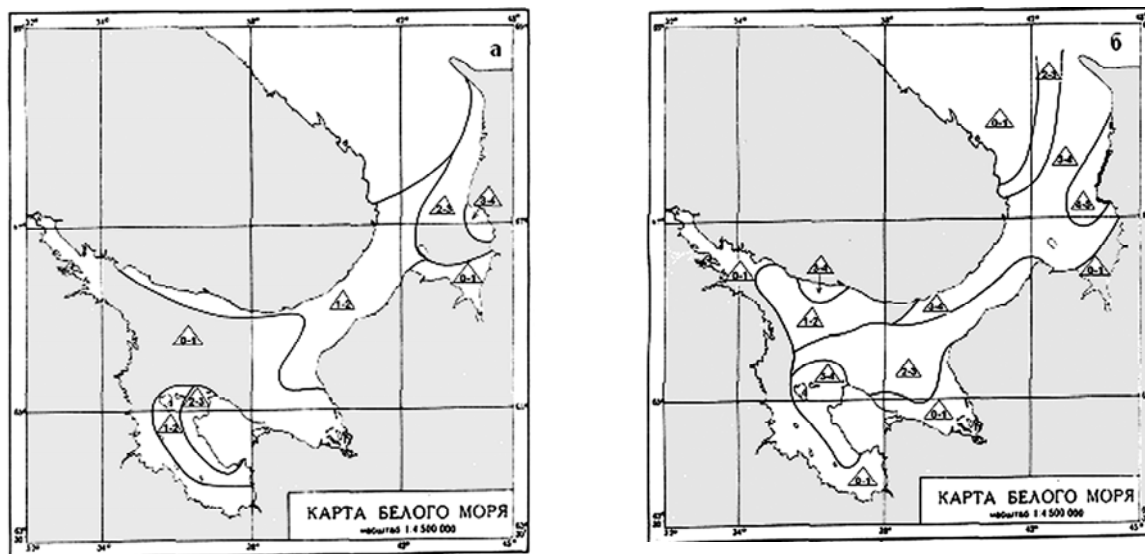


Fig. 2.2.8 – Ice ridging in the White Sea in January (a), and in April (b)

In April ice volume reaches its seasonal maximum on the most White Sea basin. Ridging of main mass, accumulated in Voronka and Gorlo, reaches 3-4 marks. Coastal region with ice 4-5-marks is widening along southern region of Kaninsk. Ice with ridging 2-3 marks occupies almost half of basin. Ice ridging increases to 3-4 marks along Onega coast. At the same time rather level ice mass is increasing (hummocks 0-1 marks) along Kandalaksha and Pomor coasts, including Gulf of Onega peak. It can be explained by small hummocking of young ice in polynyas, formed as a result of offshore wind and constant exporting ice drift for this sea region.

It is necessary to mention, that the most level ice (ridging not more than 1 mark) is kept near Karel and Pomor coasts during almost all winter, and in Gulf of Kandalaksha during all period. Similar ice ridging is observed on the biggest part of Gulf of Dvine basin (except March) and in Gulf of Mezen peak.

### 2.2.7. Drift ice

Ice floes are mostly typical for regions with weak tidal currents: in Basin, in Gulf of Kandalaksha and Gulf of Dvine. Broken ice with high ridging prevails in Gorlo and Voronka as a result of exporting ice drift, strong tidal currents. Co-called “kotli” – round-shape ice floes with contiguous high barriers of hummocks on edge, comparatively level in central parts, are often observed.

Ice cake and small broken floes are formed mostly due to ice floes decay and their parts. In

April-March broken ice prevails.

To the end of winter small ice cake is often observed, which occurs at the same time with broken ice formation. Small ice cake under compacting can reach 3-4 m and more. Amount of small ice cake gradually increases in direction from Basin to Voronka.

#### **2.2.8. Ice melting and ice-free sea**

Melting intensity increases after stable air temperature transition through 0°C to positive values, that on average occurs in the second decade of April. Firstly, young ice, covering polynyas region, melts away, and depression ice zones appear. Thin first-year ice, dominant in sea, is exported from Gulfs of Kandalaksha, Onega, Dvine into basin and further through Gorlo to Voronka under western winds. At that, they are accumulated and ridged mostly in eastern parts of gulfs, Gorlo and Voronka.

More intensive process of clearing from ice occurs in May. In early May all drift ice is divided into three parts. One part of depression broken ice is usually located in the north-western Gulf of Onega, another – in Gulf of Kandalaksha and north-western part of basin. Third part of more compact ice is in region of Gorlo and Voronka near Tersk coast and north-western Gulf of Mezen. First two ice regions intensively melt away and are transported to centre of basin. Ice melting and decreasing of its concentration in third region occur slower, what is connected with its large power and volume, increased while ridging. By the same reason, this ice region is safe to late May – early July. It is also a result of wind changing into eastern, what prevents ice transportation from sea.

Final clearing of the White Sea from ice occurs as a rule in the first decade of June after final fast ice break up.

#### **2.2.9. Fast ice break up and decay**

First fast ice break up in the White Sea occurs in the end of second decade of April near Abram coast of Gulf of Mezen and Letniy coast of Gulf of Dvine, and also near Kandalaksha coast. Fast ice starts to break up along Kanin coast in the middle of third decade of April. Later than others, fast ice break up occurs in Gulf of Kandalaksha and along Tersk coast.

Final decay of fast ice normally occurs in May. In the first decade of May fast ice in Gulf of Onega and Gulf of Dvine finally breaks up, and in the second decade – in Gulf of Mezen and round Solovetskie Islands. Fast ice in Gulf of Kandalaksha is the latest; it breaks up in the third decade of May.

Broken fast ice partly melts away, where it was located, and partly is transported to open sea regions, where they ultimately disappear.

## 2.3. Characteristic of the Barents Sea ice conditions

### 2.3.1. General aspects

Ice formation and decay conditions in the Barents Sea significantly differ from conditions of the Siberian Arctic shelf seas due to advection of Atlantic water, transported by the Gulfstream Current system. As a result of this effect the Barents Sea is not covered with ice completely even in severe winters, whereas all other Arctic Seas in winter period are covered by ice with concentration of 9-10/10-th.

The Barents Sea is subdivided by its ice-hydrologic features into three regions: western, north-eastern and south-eastern parts (Fig. 2.3.1.). Western region occupies about 53% of water area, north-eastern - 29% and south-eastern – about 18. The Pechora Sea - water area eastwards from Kolguev Island to the boundary with the Kara Sea is often separated within the limits of its south-eastern part.

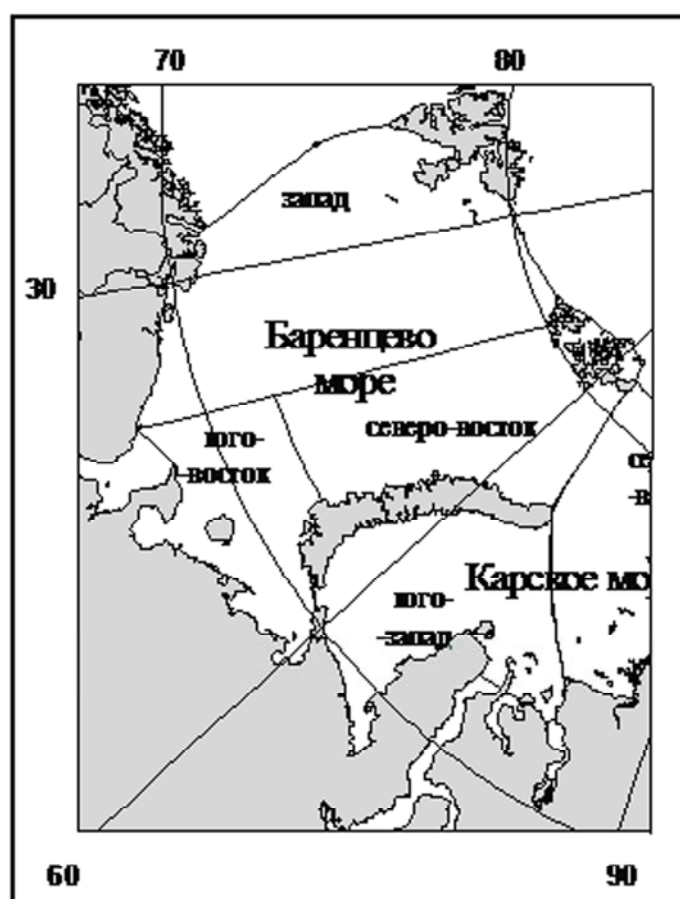


Fig. 2.3.1 – The Barents Sea division into zones

Ice formation in the Barents Sea starts from the second half of September and lasts for 7 months; melting period is 5 months. Maximum development of ice cover occurs in April. Minimum ice amount is observed in August-September.

In period of maximum development of ice cover (March-April), ice area in the Barents

Sea usually comprises 55-60%, and the rest 40-45% of water area is ice-free. Under favorable conditions in winter period ice cover occupies only 30-35%, and under unfavorable conditions 85-90% of sea area.

In summer period ice cover (relative ice area) in the Barents Sea is only 5-10%. Under favorable summer conditions sea ice in the Barents Sea almost completely disappears, and under unfavorable conditions ice cover in the Barents Sea is 20-25% by the end of melting.

Existing of non-freezing sea parts means that in winter period zone of zero heat budget is located here. To the south and west from this zone continuous in-flow of warm water to surface water layers compensates for radiation cooling and cold advection by air transport, which prevents ice formation.

To the north and east from this area there aren't such strong in-flow of warm water to surface layers, heat losses by means of infrared radiation cause active cooling of sea surface, and, as a result, ice formation.

### **2.3.2. Ice formation**

Stable ice formation in the Barents Sea starts in late August on the boundary with the Arctic basin. First of all, Straights of France-Joseph Land and Svalbard archipelagoes freeze up. Gradually, at the same time with cooling of sea regions with large heat content, ice formation wave propagates to the south up to the latitude of the northern extremity of Novaya Zemlya. As it is seen from location of isochrones of stable ice formation terms, further the process of ice formation, propagating to the south in central sea parts, at the same time occupies water area to the west from Novaya Zemlya coast (Fig. 2.3.2).

According to annual mean data ice formation in the Barents Sea stops in the middle of April on the boundary of zone with water of high heat content. All water column to west and south from isochrones "April, 15" has rather high temperature that is why, heat in-flow from water depth in process of autumn-winter convection not only compensates its outflow to atmosphere, but keeps positive temperature on the sea surface. Further ice spreading in the sea is ceased. As a result of it, on average, 35% of the Barents Sea area is free from ice. 47% of this water area is located in the western sea part, 14% - in the north-eastern part and 30% in the south-eastern (Fig. 2.3.2).

In sea area, limited from south by isoline of 100% probability of ice occurrence, annual amplitude of stable ice formation terms on northern sea boundary is 40 days and it increases in direction of ice edge to 120 days (Fig. 2.3.3.). Such variability can be explained by both interannual variability of hydro meteorological factors in period, before ice formation, and conditions of heat exchange between sea and atmosphere in period of its cooling.



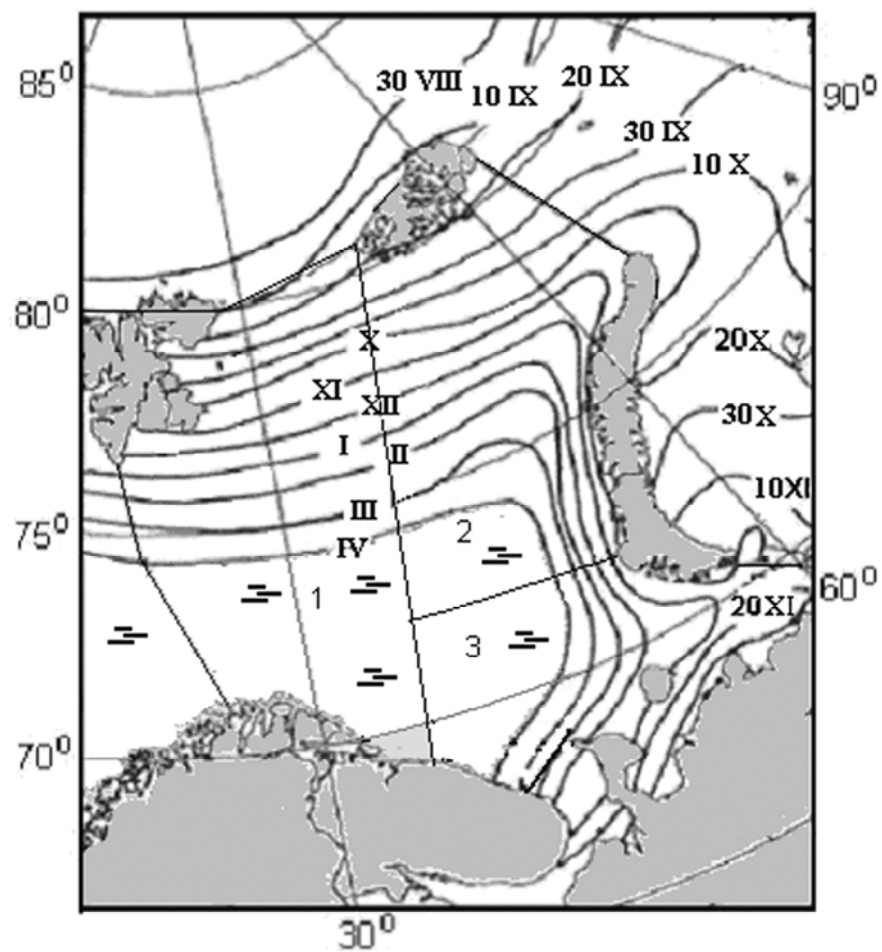


Fig. 2.3.2 – Average terms of stable ice formation in the Arctic seas

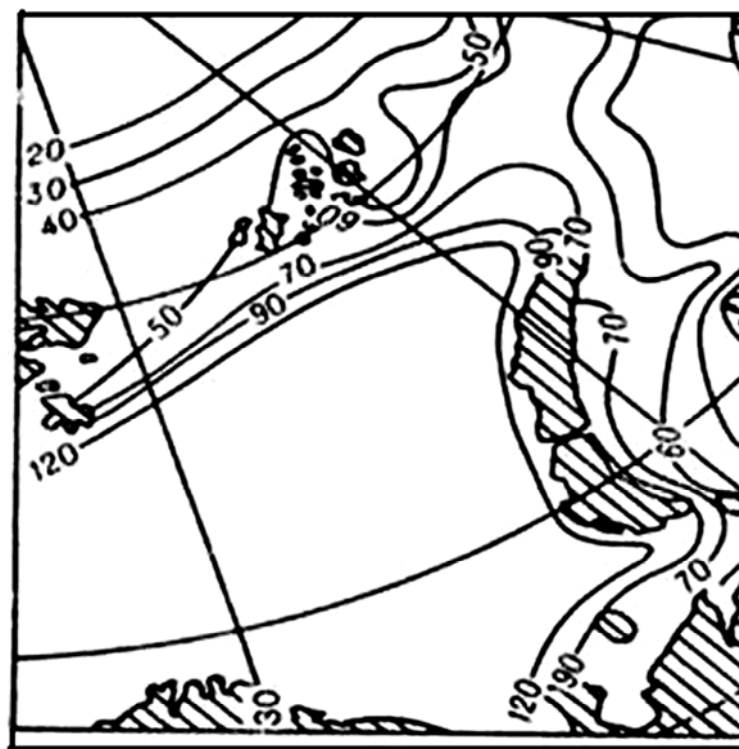


Fig. 2.3.3 – Amplitudes (days) of stable ice formation terms

### 2.3.3. Ice cover in winter period

Transition of new ice types to first-year ice occurs after stable ice formation, and ice edge gradually moves to open parts of the Barents Sea from north to south and from east to west.

This process lasts till April inclusive. At the moment of maximum development of ice cover in year with average ice conditions, ice edge is situated southwards from Svalbard near Medvezhiy Island, and gradually inclines to south-east, and reaches 45° E at 74° N. Then ice edge usually sharply turns to south-west and comes to continent coast in the area of Cape Svyatoi Nos (Fig. 2.3.2).

*Fast ice.* The Barents Sea fast ice isn't distributed much, which distinguishes it from other Siberian Arctic shelf seas. It occupies only about 2% of the sea area. Stable fast ice is normally formed in peaks of bays and fjords in Svalbard, and in straits of Franz-Joseph Land, in bays of Novaya Zemlya, and near coast of Beliy, Victoria, Kolguev Islands, and also in several gulfs of the southern coast (Pechora Bay, Khaipudirskaya Bay and others). Along open coast of Novaya Zemlya and continent from Yugorskiy Shar Straight to Cape Kanin Nos fast ice width usually doesn't exceed several hundred meters, at that it often breaks.

*Drifting ice.* The Barents Sea drifting ice is usually formed within the limits of the sea. But in some winters multiyear ice is transported from the Arctic Basin through straight between Svalbard and Franz-Joseph Land to its western part, and ice from the northern Kara Sea moves to the north-eastern part.

According to multiyear observational data (visual and instrumental aerial and satellite), supplemented with calculations, ice of different age in the Barents Sea has zonal distribution. Near ice edge there is a zone of young ice with thickness of 10-30 cm, and zones of thicker ice are located northward and eastward of. In November, Two months after ice formation beginning, thin first-year ice is formed in sea besides young ice.

When ice formation occupies new sea regions, ice transits to grade with higher thickness. This process lasts till maximum development of ice cover. At that areas of different ice types change (Table 2.3.1.).

In November thickness of drifting ice in all parts of the Barents Sea do not exceed 50-55 cm. At that in south-eastern sea part all formed ice is in stage of young ice with thickness up to 30 cm.

In February in western and north-western sea parts three age stages of ice are presented, from young to medium ice. Thin first-year ice prevails in south-eastern sea part, occupying 52% of its area. In April this ice medium first-year ice and its thickness reaches 70-80 cm. North-

eastern sea part is occupied mostly by this ice (but with thickness of 90-120 cm), and areas of young and thin ice. In western sea part thin first-year ice and young ice is occupied in about quarter of its area and another quarter is occupied by medium ice (Table 2.3.1).

Table 2.3.1 – Ice age composition in the autumn-winter period in the Barents Sea regions under mean annual conditions, in % from the region area

Part	Months														
	XI	II	IV	XI	II	IV	XI	II	IV	XI	II	IV	XI	II	IV
	No ice			Young ice			Thin first-year			Medium first-year			Thick first-year		
<b>West</b>	75	54	47	20	10	8	5	24	15	-	12	24	-	-	7
<b>North-west</b>	59	25	14	14	4	2	27	16	6	-	55	70	-	-	8
<b>South-west</b>	93	39	30	7	9	8	-	52	21	-	-	41	-	-	-

Thick first-year ice with thickness of 130-150 cm is formed only in the north of western and north-western parts and occupies about 7-8% of their areas (Table 2.3.1).

Level drift ice thickness on all age stages is close to ice thickness on polar stations.

As a result of hummocking ice thickness of any age can increase on average to 20% in winter period.

*Sea ice cover in the freeze-up period.* Along with ice edge, ice cover is important characteristic of sea ice state– sea area or its zone covered by ice of any concentration. The highest speed of ice cover propagation is observed in November-December, on average 12% of the sea area is covered by ice. When ice edge shifts to zones with higher heat content of water, ice cover spreading in the sea slows down, and ice cover increase is 3-5% of its area from March to April (Table 2.3.2).

*Ice drift in autumn-winter period.* Main features of ice drift in the Barents Sea are determined by atmospheric circulation over sea and system of currents (Fig. 2.3.4). From October to April southern and south-eastern winds dominate in sea, and only on the boundary with Arctic basin from January to April eastern and north-eastern winds are observed. That is why, in winter period ice drift in the Barents Sea is directed to its northern parts, where strong pressures and ice hummockings take place under counter flow from the Arctic basin and the Kara Sea.

Table 2.3.2 –Variability of the ice cover in the Barents Sea and its parts in the freeze-up period under mean annual conditions, in, % of its water area

Part	Months						
	X	XI	XII	I	II	III	IV
Entire sea	15	27	39	49	57	62	65
Western	15	25	34	41	46	49	53
North-eastern	27	41	55	66	75	81	86
South-eastern	0	7	26	45	61	67	70

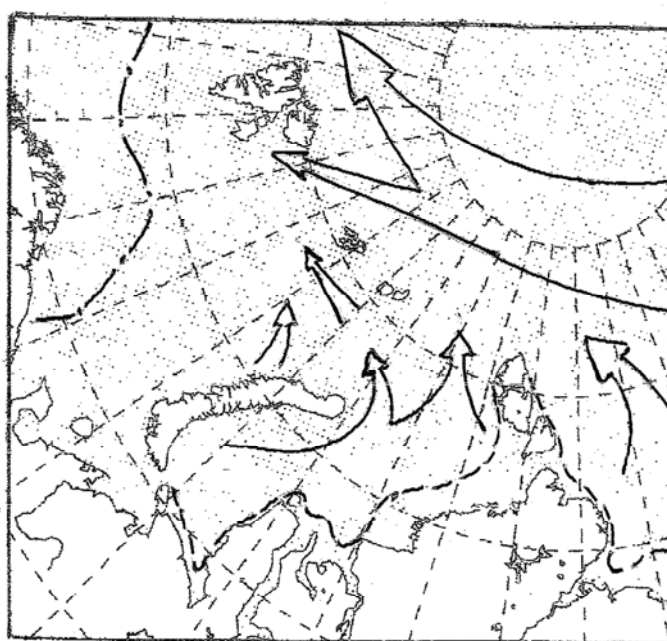


Fig. 2.3.4 – . Scheme of ice drift in winter period

*Flaw polynyas.* Formation and development of flaw polynyas depend on wind direction and its stability. Offshore wind is the cause of polynyas. Depending on their occurrence, polynyas are classified to as stationary, stable and episodic. Polynyas with a frequency of occurrence from 75% and more – are stationary, from 50% to 74% - stable, and less than 50% - episodic.

In the Barents Sea polynyas are formed near the southern and south-eastern coasts of Franz-Joseph Land, along the coast of Novaya Zemlya, near Kolguev and Vaigach Islands.

There are some characteristics of flaw polynyas of Franz-Joseph Land, obtained from ice reconnaissance data (Table 2.3.3.). According to table data, western and north-western polynyas of Franz-Joseph Land are stable. South-eastern polynya is episodic, if considering its frequency of occurrence.

Polynyas, formed along the entire southern coast of the Pechora Sea, are episodic. They exist from 1 to 22 days. On average duration of polynyas varies from 2 to 4 days in different parts of the coast.

Table 2.3.3 – Characteristics of polynyas of Franz-Joseph Land archipelago

Polynyas	Frequency of occurrence %	Average width, km
North-eastern	60	24
South-eastern	50	15
Western	74	60

#### 2.3.4. Ice cover melting and ice clearing in the sea

In May-June under effect of solar radiation and heat, transport by currents, processes of melting and destruction start. First features of melting are puddles, appearing on ice surface. According to data of polar stations ice melting starts in the south of the south-eastern Barents Sea and gradually propagates to the north. Average terms of melting beginning in Yugorsky Shar region, are in the end of third decade of May, and in straits of Franz-Joseph - on 20<sup>th</sup> of June. Process of ice disappearance finishes in September.

*Melting intensity and ice disappearance.* Intensity of melting in the Barents Sea regions significantly differs and increases from north to south because of its significant latitude extent. Thus, if to the end of June in Franz-Joseph Land area ice thickness decreases for 10 cm, ice thickness near the western coast of Novaya Zemlya – for 50 cm, and in Vaigach Island area - for 70 cm.

Under average melting conditions ice in open parts of the Barents Sea disappears faster, than in Seas of Siberian shelf, due to both thermal and dynamic current effect. Ice edge moves back to north and to coast of Novaya Zemlya. Western coast of Novaya Zemlya is free from ice in July; also ice disappears in the south-eastern sea part. In August ice edge reaches Svalbard and Franz-Joseph Land (Fig. 2.3.5.).

ice edge retreat to the north and to the east occurs mostly due to thinner ice melting. All young ice and partly thin first-year ice in the south of the north-eastern Barents Sea melts in May. In June thin ice zone almost disappears in all regions, and significant part of medium ice in south-eastern part and north-eastern sea parts is melted. In western sea part this ice still exist. South-eastern sea part and bigger part to the west from Novaya Zemlya are clear from ice in July. The rest of medium ice is located to the north from line Svalbard - Franz-Joseph Land in

August. Melting process lasts till September and ends up among thick ice in straight between Svalbard - and Franz-Joseph Land.

Ice disappearance during period of melting occurs heterogeneously. Speed of ice edge retreat to the north in the central part (40°E) increases from April to July, and then slows down. Thus, in May it is equal to 60 miles a months, in June – 90 miles, in July – 110 miles, in August – 70 miles (Fig. 2.3.5).

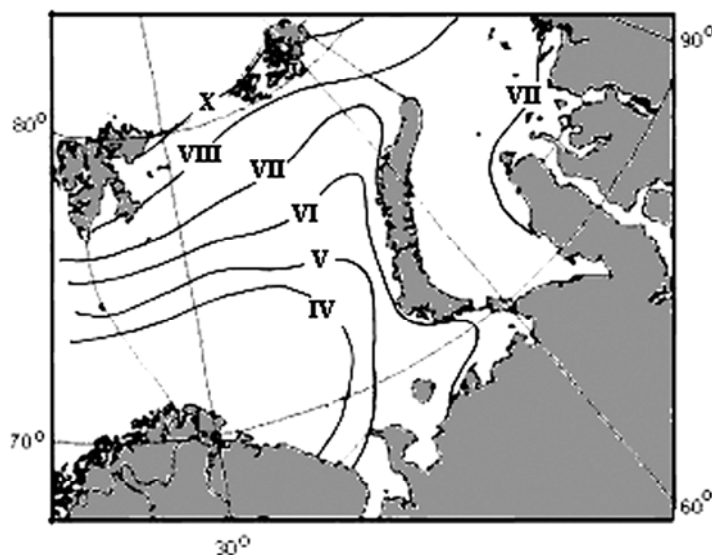


Fig. 2.3.5 – Location of drifting ice edge in summer period.

*Sea ice cover in melting period.* Changes of sea ice cover correspond with ice edge motion from month to month. In May (comparing to April) 7% of sea area clears from ice, and in June - 21%. Then velocity of clearing decreases, and in September amounts to 3% (Table 2.3.4). Similar pattern is observed in the western and north-western sea parts. Maximum clearing of the south-eastern part occurs in July, when 33% of the area is free from ice, and in August ice absolutely disappears. Ice, survived after melting, occupies 7-8% of the northern parts of western and north-eastern sea parts by the beginning of ice formation (Table 2.3.4).

Table 2.3.4 –Variability of the ice cover in the Barents Sea and its parts in the melting period, in, % of its water area

Part	Months					
	IV	V	VI	VII	VIII	IX
Entire sea	65	58	43	24	11	8
Western	53	47	39	24	11	7
North-western	86	79	62	36	20	15
South-western	70	55	22	3	0	0

*Ice drift in melting period.* Process of the Barents Sea clearing from ice occurs under the influence of both thermal and dynamic processes as a result of ice drift. In May-August northern winds prevail in the Sea. These winds force ice drift to the south to warmed water, where they melt faster (Fig. 2.3.6).

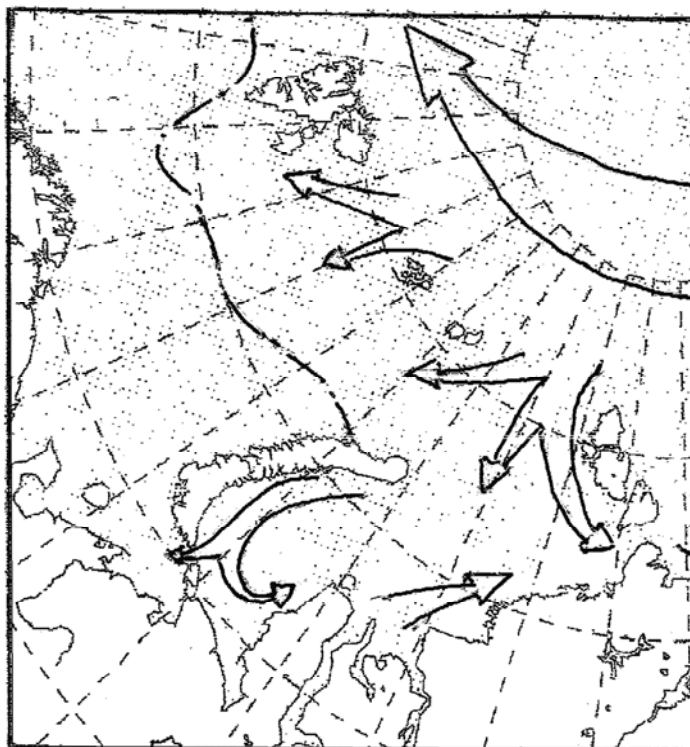


Fig. 2.3.6 – Scheme of ice drift in summer period

*Icebergs.* Icebergs observed in the Barents Sea calve from glaciers of Franz-Joseph Land, Svalbard and Novaya Zemlya in spring-summer period. Their largest amount can be observed in waters near Svalbard. The estimated volume of icebergs, produced by Svalbard glaciers, amounts to 5 km<sup>3</sup> a year, by Novaya Zemlya glaciers – 2 km<sup>3</sup> and Franz-Joseph Land glaciers – 1,5 km<sup>3</sup>. Size of these icebergs is not large, (average length, width and height of their above water part are, respectively, 64, 46 and 11 meters), that is why they mostly destructed in fjords, where they were formed, the rest part drift to central sea part under wind and currents effect. Separate icebergs and bergy bits were observed in the southern sea part in some years.

Analysis of interannual changes of ice cover of the Barents Sea was made on the basis of annual mean data. It is necessary to mention, that ice conditions in the Barents Sea are characterized by significant interannual variability, and ice area can change in limits 50-90% of its water area.

## 2.4. Characteristics of the Kara Sea ice conditions

### 2.4.1. Physic-geographical sea characteristics

*Borders, depths.* The Kara Sea is a marginal sea of the Arctic Ocean, which has borders with the Arctic basin in the north, in the west – with the Barents Sea, in the east – with the Laptev Sea. Coast line is indented, with large gulfs (Baidaratskaya, Obstkaya, Gidanskaya Bays, Gulf of Enisey), deeply run into continent shore (Fig. 2.4.1).



Fig. 2.4.1 – Geographical location of the Kara Sea

The Kara Sea is divided into two parts: south-western and north-eastern. Conventional border between them is on the line of Cape Zhelaniya – Dixon Island (Fig. 2.4.2). Such division into zones is provided taking into account geographical location, hydro meteorological and ice conditions, which are more severe in north-eastern area.

Main morphometric characteristics of the Kara Sea:

- Total area – 830 000 km<sup>2</sup>
- North-eastern part area – 495 000 km<sup>2</sup>;
- South-western part area – 335 000 km<sup>2</sup>
- Average depth: 111 m; the largest depth - 600 m.

Deep water parts of the Kara Sea (with depth more that 500 m) occupy more than 1% of the total ground.

*Climate.* The Kara Sea is located northwards of the Polar circle and is situated under influence of the Arctic basin and Asian continent from the south.

From September-October the Kara Sea is under influence of narrow of Icelandic depression and Asian anticyclone. During this period southern winds dominate over the sea.

In April reconstruction of baric field occurs. The narrow of Icelandic depression decreases,



above Asian continent extensive depression is established. In summer period northern winds dominate over the sea.

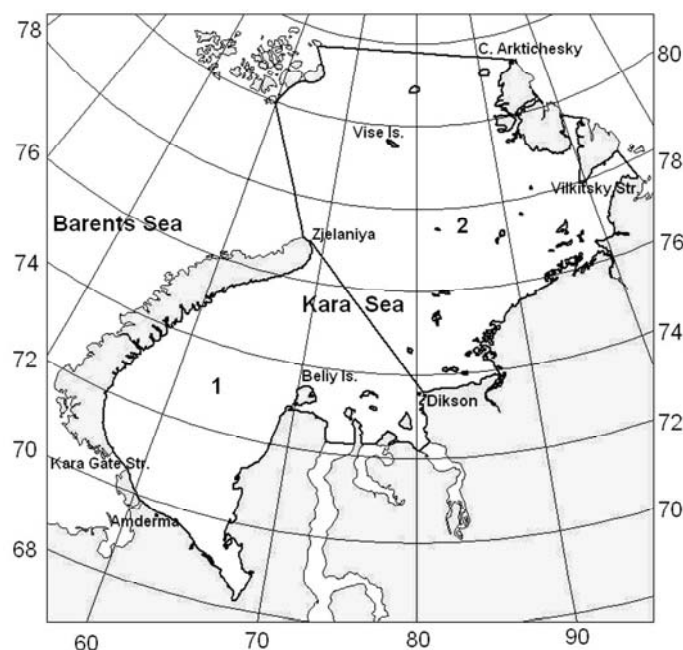


Fig. 2.4.2 – The Kara Sea division into zones: 1 – south-western and 2 – north-eastern regions

Significant sea length and peculiarities of atmosphere circulation cause differences in thermal regime. Average annual temperature above the south-western sea part is 6-7° higher, than above the north-eastern. In January air temperature in the south-western part of the sea changes from -17 to -20°C, and in the north-eastern – from -28 to -30°C.

From April to March air temperature starts to increase. In July air temperature above sea is positive everywhere: above south-western part it is 4-6°C, above north-eastern - 0-2°C. At the same time in the Ob'-Yenisey district it can reach 6-12°C.

Warm period duration lasts from 50 days in northern sea parts to 120 days near southern coast.

Wind currents with unstable directions and changeable velocity dominate in shallow areas of the Kara Sea. Gradient and tidal currents in general are weak.

More or less stable water flows are typical for summer period. In the south-western part they form cyclonic circulation from relatively warm Yamal current, moving from Kara Gate Straight to the north-east, and relatively to cool Eastern-Novozemelsky current, moving to the south along the eastern coast of Novaya Zemlya (Fig. 2.4.3).

#### **2.4.2. Characteristic of sea ice cover in period of its growth**

The most part of year the Kara Sea is covered with compact ice. In the south-western sea part ice is observed during 7-8 months, from November to June-July. The north-eastern sea part in summer period isn't absolutely ice-free.

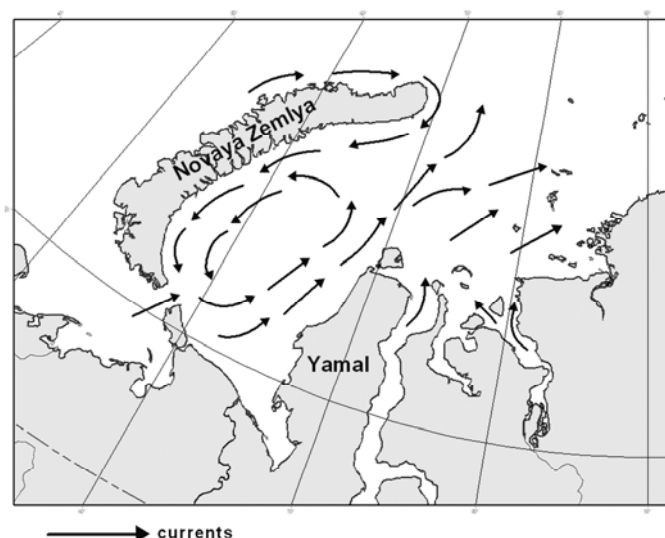


Fig. 2.4.3 – Scheme of quasi constant currents in the south-western Kara Sea

*Ice formation.* Ice formation in the Kara Sea starts in late August – early September on northern sea boundary, often among ice, survived after summer melting. In late September ice formation propagates to the most areas of the north-eastern sea part. Ice formation processes at the same time occupy large water areas, and in first decade of October new ice is observed in the whole north-eastern sea part (Fig. 2.4.4).

During October and first half of November “wave” of ice formation propagates to most part of coastal and open regions of the south-western sea part (Yamal and Novozemelskiy coasts, Baidaratskaya Bay), and on 20<sup>th</sup> -25<sup>th</sup> of November new ice appear in Kara Gate Strait (Fig. 2.4.4).

Thus on average, sea completely freezes up during two months and 20 days. At that, half of this period falls on the south-western sea part which area is 1,5 times less. It can be a result of summer warming of water in this area, and inflow of warmer water from the Barents Sea through Kara Gate Strait. In accordance with this isochrones of average terms of stable ice formation form arches, stretching to the north (Fig. 2.4.4).

*Ice growth.* Ice thickness increase takes place at the same time as ice formation processes develops in the sea. In the middle of September only 17% of the north-eastern sea region is free from ice, 60% of its area is covered with young (to 30 cm), 15% – with thin first-year ice (30-70 cm). Medium first-year ice (70-120 cm) forms in its northern part. At the same time young ice appears only on 40% of the south-western sea region, on the rest part ice formation hasn't started yet (Table 2.4.1). In the end of ice growth period, in May, most part of the Sea is covered with thick first-year ice (thickness more than 120 cm). 80% of this ice is located in north-eastern sea region and 60% – in northern parts of south-western region. Medium first-year ice (70-120 cm) covers southern parts of the south-western sea region (Fig. 2. 4.5).

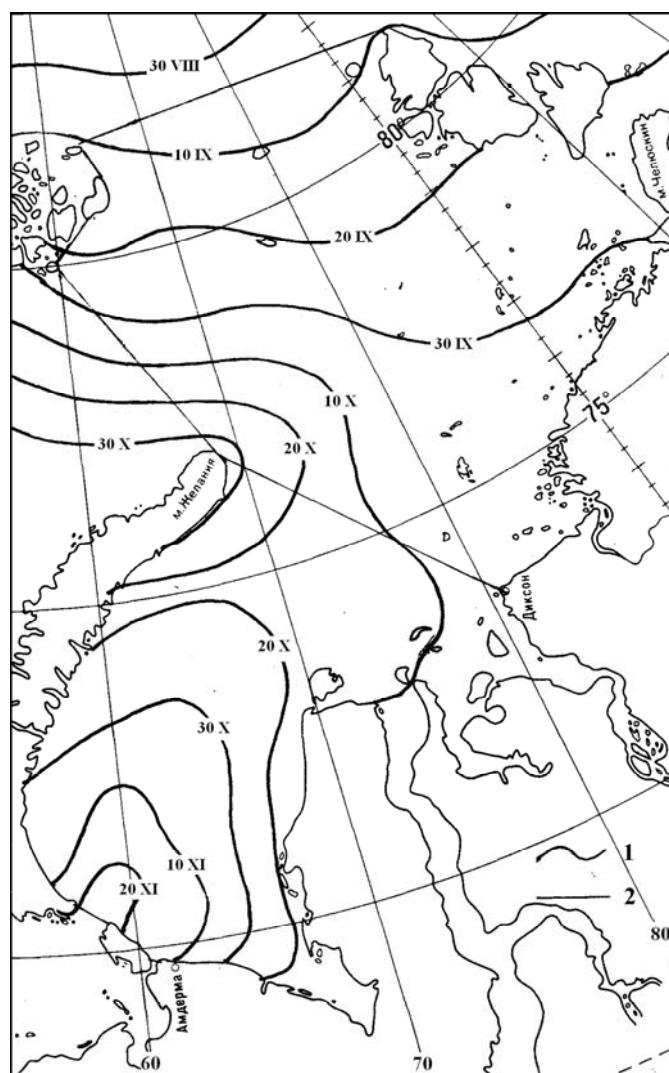


Fig. 2.4.4 – Isochrones of average terms of stable ice formation in the Kara Sea

Table 2.4.1 – Composition of ice age in the Kara Sea regions in autumn-winter period, %

Sea regions	Ice age																	
	No ice			Young			Thin first-year			Medium first-year			Thick first-year			Second-year, multiyear		
	Months																	
X	II	V	X	II	V	X	II	V	X	II	V	X	II	V	X	II	V	
South-western	60	0	0	40	12	15	0	35	3	0	53	20	0	0	62	0	0	0
North-eastern	17	0	0	60	2	6	15	10	5	8	20	5	0	65	81	6	3	3

Drifting ice is presented by ice objects of different linear sizes from ice cake to floes. In straights and coastal zones behind fast ice, ice is presented by small forms, medium floes and broken ice. In sea zones floes and medium floes prevail. Ice thickness in zones of thick first-year

ice is 1.4-1.8 m (Table 2.4.2). In the half of the sea area (as a result of drift) ice is hummocked, and hummocking increases to the end of ice cover growth period (April-May).

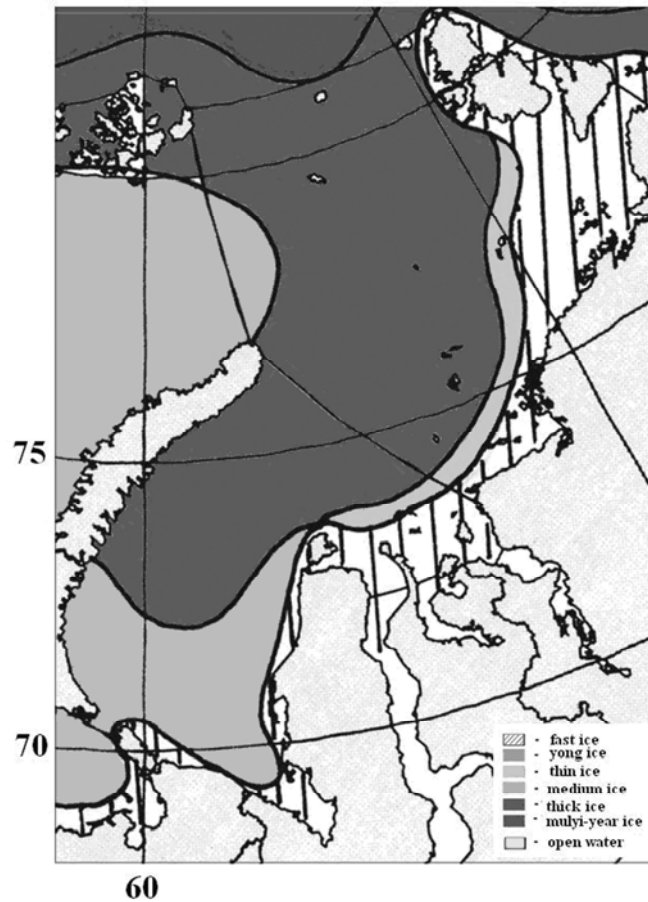


Fig 2.4.5 – Average distribution of different ice types in the Kara Sea in the end of sea ice growth period

Table 2.4.2 – Characteristics of drifting ice in the Kara Sea regions

Characteristic	Average values	
	South-western	North-eastern
Length of ice floes, m	3000-6000	4000-6000
Thickness of ice floes, m	1.4-1.6	1.6-1.8
Hummocking, marks	2-3	3
Month with the most hummocking	April-May	April-May
Average sail of hummocks, m	1.3-1.5	1.5-1.8
Maximum sail of hummocks, m	4.0-6.0	5.0-6.0

Drift and ice cover motion in autumn-winter period lead to interaction between ice floes and to occurrence of cracks and fractures in ice cover, or to ice compacting. Ice compacting leads to formation of hummocks and grounded hummocks (near fast ice zone).

In winter period ice outflow from the Kara Sea to the Arctic basin through its northern boundary and to the Barents Sea through Kara Gate Strait, prevails. During winter half-year (from October to March) more than 138 000 km<sup>2</sup> of ice cover is transported from the Kara Sea to

the north, and in summer half-year (from April to September) on average 24 000 km<sup>2</sup> of ice comes from the Arctic basin. Thus, about 115 000 km<sup>2</sup> of ice is transported to the north from the sea during the year, which is about 14% from total sea area or 23% from area of its north-eastern part.

*Fast ice.* When young ice reaches thickness of 10-30 cm fast ice is formed along continental and island coasts. In period of its maximum development boundary of fast ice is located along 10-20 m isobath.

Fast ice development in the Kara Sea can occur in the period from late September in its northern part to late January near Amderma Coast and Vaigach Island. According to satellite observation data variability of multiyear terms of fast ice development in the Kara Sea region varies is from 4 to 8 weeks. Average date of fast ice development in most sea part is less reliable (Table 2.4.3).

Estimation of probable terms of fast ice development is more reliable. With probability of about 70% fast ice development occurs in period of second-third decades of October in western approach to Vilkitsky Strait and along southern coast of north-eastern sea region (Table 2.4.3). Terms of fast ice development are less variable in desalinated waters of Ob'-Yenisey region. In more than 80% of cases fast ice is formed here in third decade of October – first decade of November

Table 2.4.3 – Probability of stable fast ice formation terms in the Kara Sea regions from the satellite data for the period 1980-2005, %

Regions	Months												
	IX	X			XI			XII			I		
	Decades												
	3	1	2	3	1	2	3	1	2	3	1	2	3
Severnaya Zemlya	33	17	12	28	11	–	–	–	–	–	–	–	–
Approaches to Vilkitskiy Strait	–	–	24	44	22	10	–	–	–	–	–	–	–
Piasinskiy gulf – Nordenskjold Islands	–	9	26	41	14	5	4	–	–	–	–	–	–
Ob-Enisey	–		8	53	31	4	4	–	–	–	–	–	–
Yamal coast	–		4	16	28	29	23	–	–	–	–	–	–
Amderma coast	–	–	–	–	–	4	26	10	8	20	16	10	6

The closer to Kara Gate, the more stretched is the period of probable fast ice formation. Thus, fast ice formation along Yamal coast is equiprobable in any decade of December. 80% of fast ice formation cases are in this month. (Table 2.4.3).

The largest variability in terms of fast ice formation is observed near Amderma coast and Vaigach Island, where it reaches 8 weeks: from the middle of November to late January. Fast ice here can be formed here in any of 8 weeks.

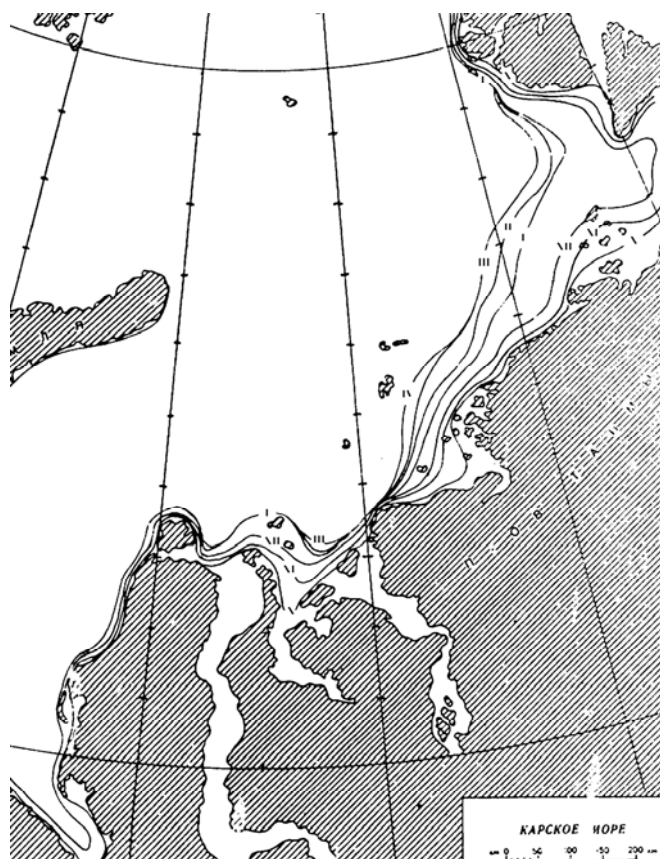


Fig. 2.4.6 – Average location of fast ice boundaries in the Kara Sea in period of ice growth from satellite data for the period 1980-2005

Development of fast ice intensively occurs till January, then its boundary slowly moves to open sea and is established in March - early April (Fig. 2.4.6).

As it can be seen from Fig. 2.4.6, the largest area of fast ice is in the north-eastern sea region. Fast ice develops in shallow southern and eastern parts, involves all groups of islands and comes along entire coast of Severnaya Zemlya archipelago. On average fast ice here occupies 26% of the area (with multiyear range 9-33%). Fast ice width to north-west from Taimyr coast can reach 250 km.

Fast ice area in the south-western sea part on average is 14% (with range 10-26%). Its most development is in the Ob-Yenisey region and in Baidaratskaya Bay. Near coast of Yamal peninsula its width doesn't exceed 20 km, near Amderma coast – 5 km. Ice Thickness of fast ice in south-western part reaches 1,6 m, in north-eastern part – 1,8–2,0 m.

Increasing of fast ice area in the Kara Sea is during 7-8 months from October to late May – early April. During April-May fast ice area is getting stable, its gradual melting starts in May (Fig. 2.4.7).

Fast ice in the Kara Sea consists mostly of first-year ice of autumn formation. In fast ice near Severnaya Zemlya archipelago inserting of second-year or multiyear ice formed here from ice,

survived last summer melting, is possible.

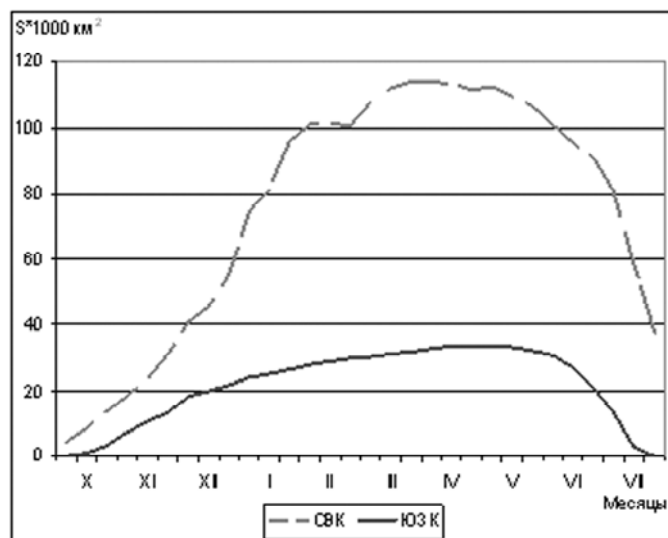


Fig. 2.4.7 – Seasonal changes of fast ice area in the north-eastern (NE) and south-western (SW) Kara Sea

*Flaw polynyas.* Flaw polynyas are formed behind fast ice during whole winter period. Flaw polynyas are areas with open water and young ice with thickness up to 30 cm. Their formation depends on direction of winds and their stability.

Frequency of occurrence of polynyas behind fast ice of Novaya Zemlya Islands is about 50%. Stable polynyas (with frequency of occurrence about 75%) are observed behind fast ice of Amderma and Yamal coasts, in Ob'-Enisey region and behind fast ice in the north-eastern sea region (Fig. 2.4.8).

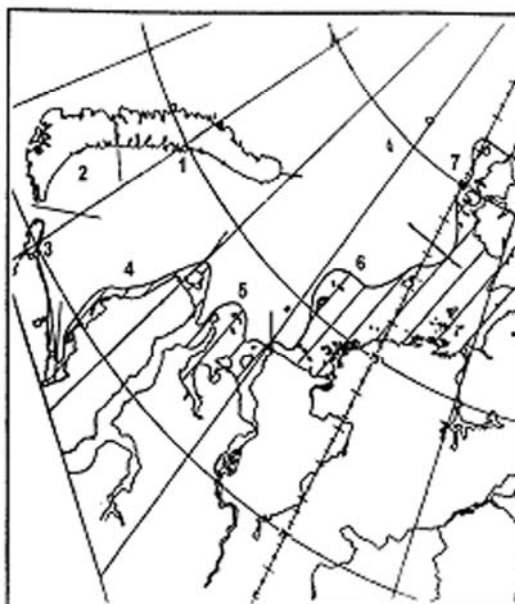


Fig. 2.4.8 – Areas of flaw polynya formation in the Kara Sea. 1-Northern Novozemelskaya; 2-Southern Novozemelskaya; 3-Amderminskaya; 4-Yamalskaya; 5-Ob'-Yeniseyskaya; 6-Central Kara; 7-Western Severozemelskaya.

Total average length of polynyas is about 2000 km, maximum more than 4000 km (Table 4). If all polynyas of the Kara Sea occur at the same time, their average area will be about 9% of the

Kara Sea area.

Table 2.4.4 – Average frequency of occurrence (P, %) and size of the Kara Sea flaw polynyas in October-June from satellite data for the period 1980-2008.

№	Polynya name	P, %	Characteristic					
			Length, km		Width, km		Area, km <sup>2</sup>	
			average	range	average	range	average	range
1	Northern Novozemelskaya	59	341	50-630	28	2-110	10,0	0,5-66
2	Southern Novozemelskaya	58	271	60-350	42	2-160	10,4	0,5-45
3	Amderminskaya	73	287	40-470	32	2-127	10,5	0,4-58
4	Yamalskaya	76	420	80-670	28	2-137	12,3	0,6-70
5	Ob'-Eniseyskaya	88	281	50-560	44	2-190	12,9	0,4-65
6	Central Kara	80	479	50-920	36	2-138	20,9	1,0-144
7	Western Severozemelskaya	66	259	50-620	29	2-170	8,0	0,4-56

Polynyas are formed under influence of offshore (from fast ice boundaries) winds. Under western or eastern air flows above the south-western sea region polynyas, formed behind fast ice of Yamal and Novaya Zemlya coasts, react opposite. Under western flows frequency of occurrence of Novozemelskaya polynyas increases and that of Yamal polynyas decreases. Change of directions of air flows to opposite seems to be favorable for Yamal polynya development and unfavorable for polynyas on the opposite coast. It can be observed rather well from comparing average monthly frequency of occurrence of Southern Novozemelskaya and Yamal polynyas in Fig. 2.4.9: with increasing of Yamal polynya frequency of occurrence –frequency of occurrence of Southern Novozemelskaya polynya decreases and vice versa.

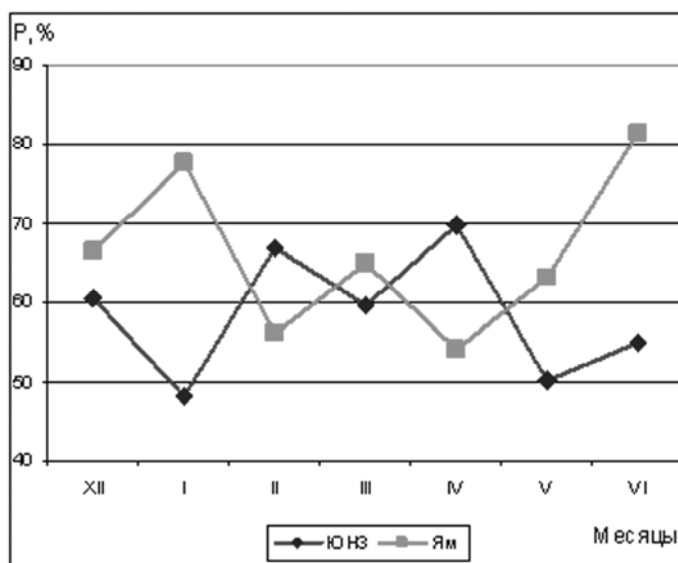


Fig. 2.4.9 – Average monthly frequency of occurrence of Southern Novozemelskaya and Yamalskaya polynyas



Finish of winter season, when ice cover becomes thicker, can be considered as time, when ice formation stops in polynyas, and from this moment polynyas become heat accumulators and areas of sea clearance from ice.

### 2.4.3. Characteristics of sea ice cover during its melting period

*Melting and sea clearing from ice.* Occurrence of puddles on ice is first feature of melting, which occurs normally when air temperature is  $-1,2^{\circ}$ . Ice cover melting starts in the south-western Kara Sea in late May. As a result of thermal and dynamic effect in early June about 10% of the south-western region area is free from ice (Table 2.4.5).

Ice melting and clearing of the north-eastern sea part during whole summer season occurs slower, than in south-western sea part, and this area isn't absolutely clear from ice (Table 2.4.5).

Table 2.4.5 – Area of the Kara Sea ice-free regions in the melting period, %

Sea region	June			July			August			September		
	1	2	3	1	2	3	1	2	3	1	2	3
South-western	8	11	12	22	38	48	80	91	94	100	100	100
North-eastern	4	6	7	9	11	12	18	23	36	53	52	54

Velocity of cleaning from ice in south-western sea part increases in July. By this time ice cover is influenced by dynamic processes and melting, and as a result of this process - fast ice breaks up and changes into drift ice of different size.

Break up of fast ice. Fast ice starts melting the earliest in Amderma region, where in 80% of cases it completely melts during June. Mostly in the first half of July fast ice breaks up along Yamal coast and the Ob'-Enisey region (Table 2.4.6). Range of multiyear terms of absolute fast ice melting in Amderma and Yamal regions is about one month, in Ob'-Enisey region – two decades (Table 2.4.6).

Table 2.4.6 – Terms of ultimate fast ice melting in the south-western regions of the Kara Sea

Terms	Parts		
	Amderma	Yamal	Ob'-Enisey
Average	23.06	6.07	17.07
Early	8.06	18.06	8.07
Late	5.07	14.07	27.07

In the north-eastern sea part break up of fast ice starts on average in early June from the fast ice

edge side. Most area of fast ice breaks up during July and by end of month fast ice exists only in narrow coastal part between Minin skerry and southern part of Nordensheld archipelago and in straits of Severozemelskiy archipelago (Fig. 2.4.10).

Range of multiyear terms of absolute break up of fast ice is one month in north-eastern sea region (Table 2.4.7). Thus, if fast ice is formed during 7-8 months in sea, its complete melting will occur during 2 months.



Fig. 2.4.10 – Isochrones of average terms of fast ice ultimate melting in the north-eastern Kara Sea

Table 2.4.7 –Terms of ultimate fast ice melting in the north-eastern regions of the Kara Sea

Terms	Date
Average	30.07
Early	15.07
Late	14.08

*Ice distribution in melting period.* In late July half of south-eastern sea part clears from ice under influence of thermal and dynamic process, and in this district only very open ice and open ice remain most often (Table 2.4.5). In late August – early September in 80% of cases this district is completely free from ice (Fig. 2.4.11).

Cleaning of south-western sea part starts from peninsula Yamal and distributes in western direction most often. Initial point of cleaning is Yamal flaw polynya.

Ice melting in north-eastern sea part occurs slower, and to the end of melting period (in September) about half of the region is still covered with ice, survived summer melting (Fig. 2.4.11).

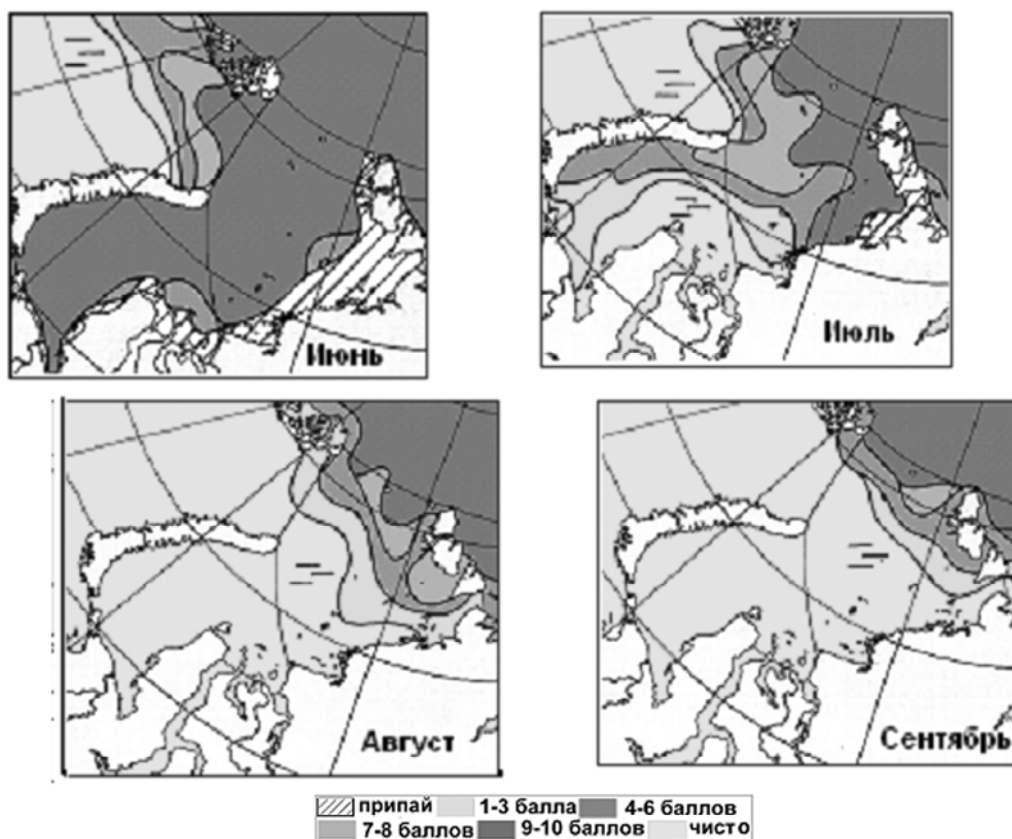


Fig. 2.4.11 – Ice distribution in the Kara Sea in June-September (with probability of 50%)

At the same time with melting of compact ice area of very open and open ice increases, and in late September their areas in north-eastern sea part are approximately equal (Fig. 2.4.12).

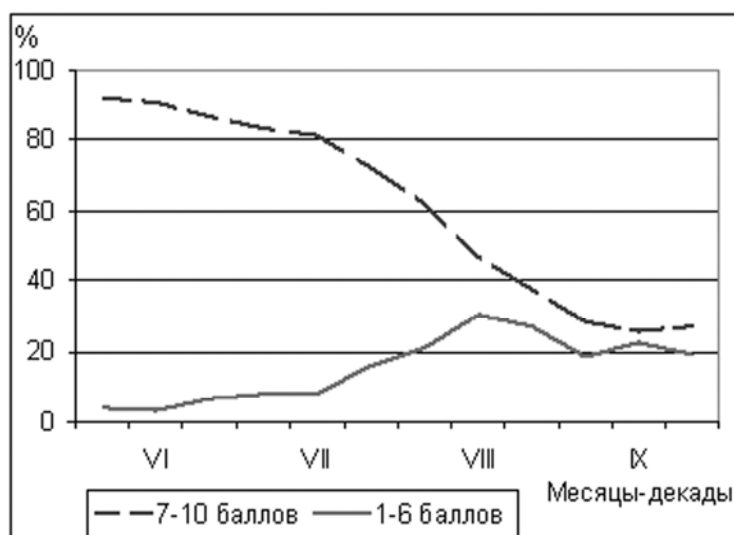


Fig. 2.4.12 – Changes of close (7-10/10-th), very open, and open (1-6/10-th) ice areas in the north-eastern Kara Sea in melting period, %

As it is seen from ice edge location in Fig. 2.4.13, sea cleaning is the most intensive in July and

August. In late August only about 60% of sea water area is ice-free, mainly due to south-western sea region. In September melting processes continue. During September 10-15% of sea is clear from ice as a result of melting and ice drift (Table 2.4.8). In northern sea regions ice formation starts at the same time.

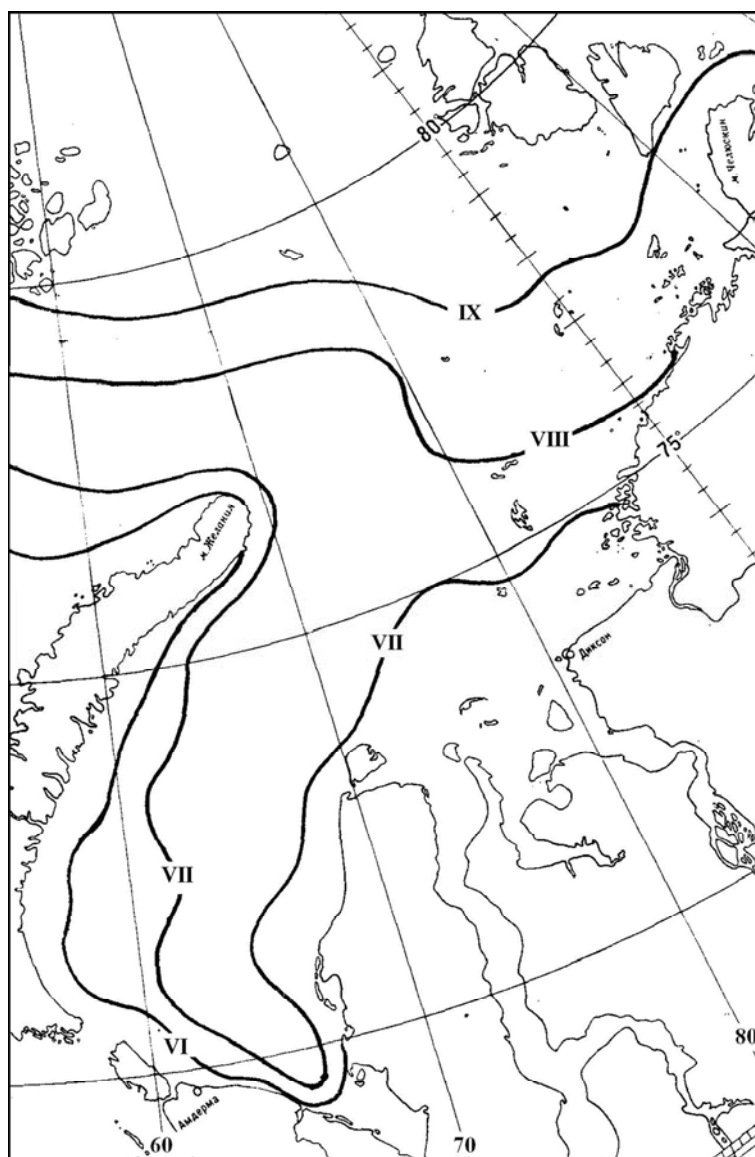


Fig. 2.4.13 – Location of ice edge in the Kara Sea in late June-September

Under average melting conditions by the end of summer melting period all age types of ice, except of thick first-year ice are melted. Its thickness can decrease to 20-40 cm. Ice melting in very compact ice cover (9-10/10) occurs slower, and in late September their thickness in north-eastern sea part is about 100 cm.

Table 2.4.8 –The Kara Sea ice-free areas in melting period, %

June			July			August			September		
1	2	3	1	2	3	1	2	3	1	2	3
6	8	9	14	22	26	43	50	59	72	71	73

*Ice massifs.* Compact sea ice (7-10/10) is localized into ice massifs in melting period:

Novozemelsky massif in the south-western sea part, and Severozemelsky and Northern Kara - in the north-eastern sea part (Fig. 2.4.14).

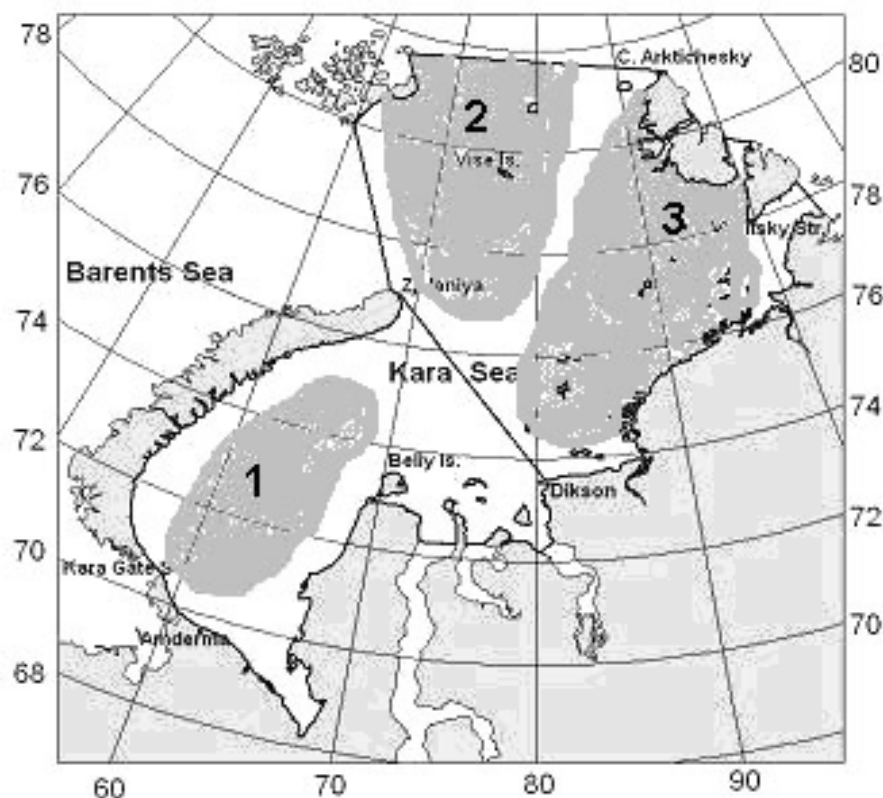


Fig. 2.4.14 – Scheme of ice massif location in the Kara Sea. 1 – Novozemelsky, 2 – Northern Kara, and 3 – Severozemelsky

Novozemelsky ice massif consists of first-year and young ice (in places of polynyas formation). In sea clearing period it can take central, western and eastern location. Western location is observed most often, when the massif is pressed to Novaya Zemlya and blocks Kara Gate Strait. In the middle of July massif occupies about 50% of the south-western Kara Sea area, and in August ice massif intensively melts and in the end of month in 80% of cases it disappears (Fig. 2.4.15).

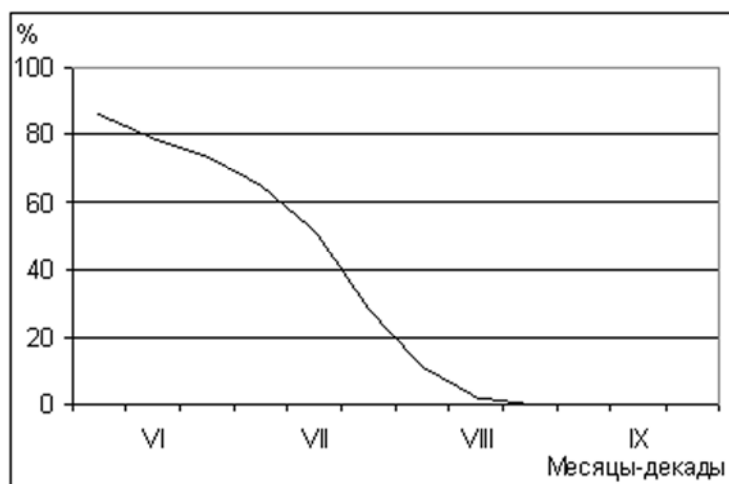


Fig. 2.4.15 – Change of the Novozemelsky ice massif area in melting period.

Severozemelsky ice massif is formed from local fast ice and is situated on navigable route between Dixon Island and Vilkitsky Strait.

Northern Kara ice massif is a branch of oceanic ice massif and occupies north-western sea parts. Mainly it consists from first-year ice, and only in northern part second-year and multiyear ice can be observed.

Division of compact ice of north-eastern sea part into two massifs occurs in the middle of August in most years. Northern Kara massif melts slower than other ice massifs, and up to 40% if its area don't melt in summer period. Severozemelsky ice massif blocks western approaches to Severnaya Zemlya archipelago and to Vilkitsky Strait most part of summer period, and on average up to 20-25% of massif is preserved in the beginning of ice formation (Fig. 2.4.16).

Fig. 2.4.16

*Grounded hummocks.* As a result of onshore ice drift in zone of fast ice, and its loading to fast ice in the depth up to 20 m grounded hummocks are formed (Fig. 2.4.17). Observed maximum values of geometry of grounded hummocks are – sail height 10-15 m, keel depth 20-25 m.

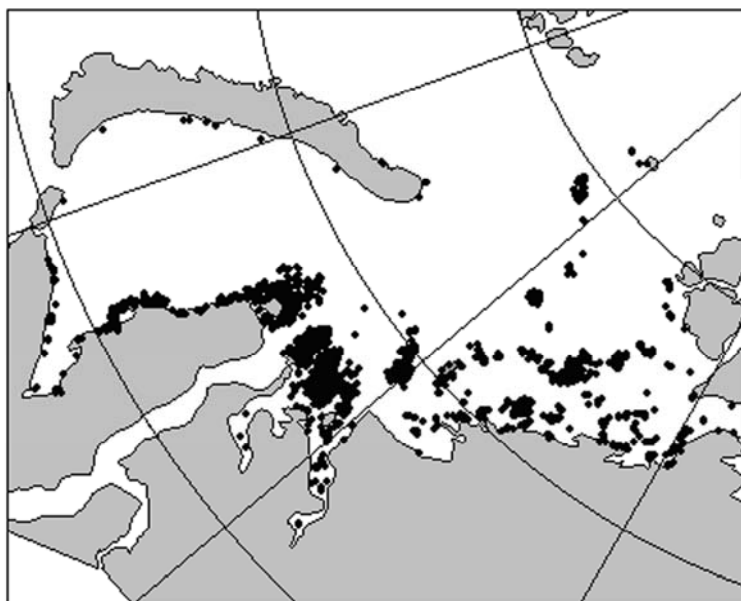


Fig. 2.4.17 – Zone of grounded hummocks formation in the Kara Sea according to data for 1962-1991

*Icebergs.* Icebergs are observed near north-eastern coast of Novaya Zemlya and western coast of Severnaya Zemlya archipelagos. In southern coastal parts icebergs are not observed.

## 2.5. Characteristics of the Laptev Sea ice conditions

### 2.5.1. Physic-geographical characteristics of sea

*Boarders, depth.* The Laptev Sea is free connected with Arctic water basin. Its northern boundary virtually runs from Cape Arctic to meridian point of northern extremity of Kotelniy Island ( $139^{\circ}$  E) with edge of continental shallow district ( $79^{\circ}$ N  $139^{\circ}$  E). Eastern boundary – from given point to Cape Anisiy, further to western coast of Kotelny Island, by western boarder of Sannikov Strait, round western coast of Islands Bolshoi and Maliy Lyakhovskie and then goes by eastern boundary of Laptev Strait. Western sea boundary goes from Cape Arctic by eastern coast of Severnaya Zemlya Islands, then by eastern boundary of Vilkitskogo Strait, and further by continental coast to Gulf of Khatanga peak. Southern boundary goes by continental coast from Cape Svyatoy Nos to Gulf of Khatanga peak (Fig. 2.5.1).

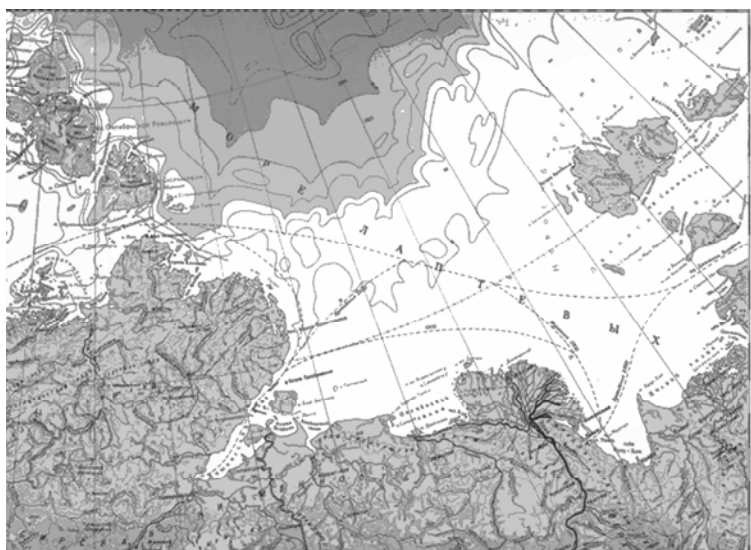


Fig. 2.5.1 – Geographical location of the Laptev Sea

Large variability of depth is seen in the Laptev Sea. In its southern region average depth is within limits 15-25 m. Sharp depth dump, beginning from 100 m and finishing about 3000 m, divides sea into northern and southern regions by parallel of Vilkitsky Strait. Depth less than 50 is observed on about 54% of sea basin (Fig. 2.5.1).

Beginning from time of active research in Arctic (30s XX century), ice observations were made in changed boundaries: northern boundary goes from Cape Berg in point  $78^{\circ}$ N  $139^{\circ}$  E. Sea area is 536000 km<sup>2</sup> (Gulf of Khatanga is not included). Western and eastern sea regions significantly differ by their ice-hydrologic characteristics, virtual boundary between them is in  $125^{\circ}$  E (Fig. 2.5.2). Area of western region is 249000 km<sup>2</sup>, eastern - 287000 km<sup>2</sup>.

*Climate.* Climate in The Laptev Sea is rather severe, because of its high latitude location ( $71^{\circ}$ – $81^{\circ}$  N) and atmospheric circulation features. From October to March the bigger part of basin is

influenced by narrow Icelandic depression. At the same time weather in south-eastern and eastern sea regions is defined by spur of powerful Siberian maximum and western periphery of Arctic anticyclone. Southern air flows prevail in winter.

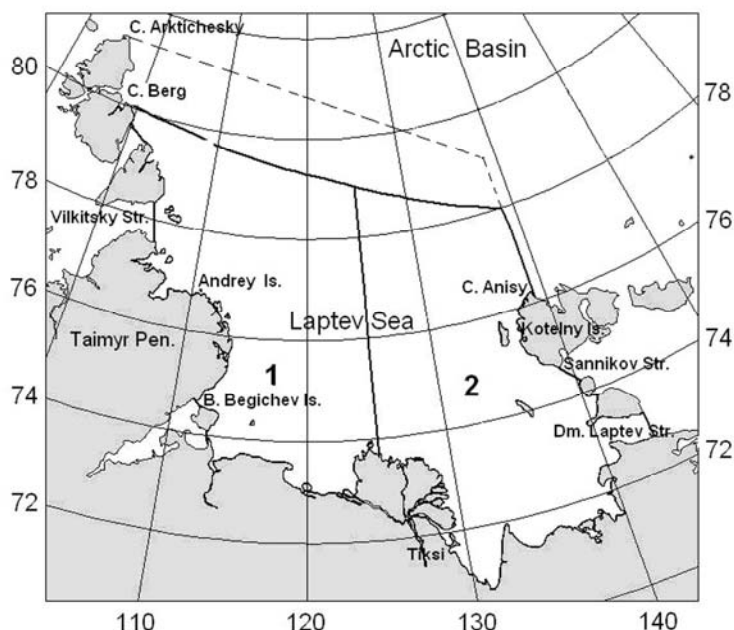


Fig. 2.5.2 – The Laptev Sea division into zones 1 –western and 2 –eastern regions

Reconstruction of atmospheric circulation starts in April, and in summer cyclonic processes dominate over the sea.

Abnormal character of air temperature propagation in winter – the warmest is northern sea part, the coolest – in southern, is main feature of thermal sea regime. In winter (January-February) air temperature along coast is  $-30\div-32^{\circ}\text{C}$ , and in northern region is about  $-29^{\circ}\text{C}$ . Air temperature under influence of radiation factor changes from  $-21\div-22^{\circ}\text{C}$  to  $-19\div-20^{\circ}\text{C}$  from north to south, beginning from April.

In summer period air temperature is close to zero over the bigger part of water area. In the south air temperature reaches  $8^{\circ}\text{C}$  near coasts, but in coastal district it rapidly decreases up to  $2^{\circ}\text{C}$  in July and August. The highest summer temperatures do not exceed  $12\text{--}15^{\circ}\text{C}$  in the north and  $26\text{--}28^{\circ}\text{C}$  in the south of sea basin.

Cyclonic water circulation is typical for the Laptev Sea. Near most northern Severnaya Zemlya Eastern-Taymyr current is separating from Transarctic current, which moves down along eastern coast of Severnaya Zemlya and Taymyr peninsula to the south. Along southern continent water is transported from west to east, where coastal flow is forced by Lensky current. Its bigger part inclines northwards and north-eastwards and as a Novosibirsky current comes out of sea limits, joining with Transarctic current, which moves north-westwards. The smallest water part goes through Sannikov Straight into the East-Siberian Sea.



### 2.5.2. Characteristics of sea ice cover in period of its growth

Almost nine months (October-June) the Laptev Sea is ultimately covered with ice.

*Ice formation.* Stable ice formation starts near northern boundaries of the Laptev Sea in first numbers of September and sequentially propagates to the south (Fig. 2.5.3). Western sea region covers with ice more intensive, than eastern, because ice formation here often starts among ice, survived after summer melting. In the first numbers of October ice formation processes propagate to southern coastal zones of western sea region, and on 5–7 of October zone, ice-free before, near delta of Lena river freezes up. Thus, sea freezes up on average during one month.

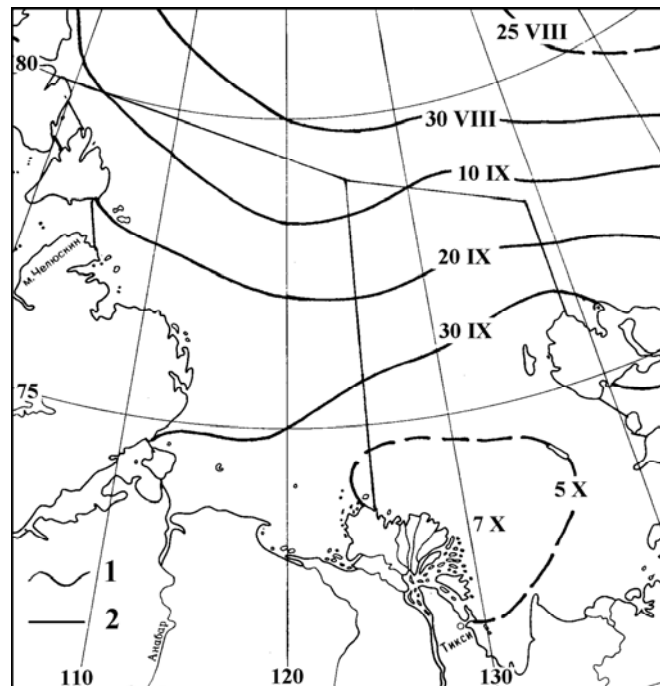


Fig. 2.5.3 – . Isochrones of Average terms of stable ice formation in the Laptev Sea. 1 – isochrones, 2 – sea and regions boundaries

*Ice growth.* When ice formation processes propagate to southern sea regions, intensive ice growth occurs in its northern and central parts, and to late October about 10% of drifting ice is thin first-year ice (30-70 cm) and approximately same percentage – medium first-year ice (70-120 cm). Ice, survived after summer melting, occupies up to 10% of western region area and about 5% of eastern region (Table 2.5.1). Some ice transforms into two-year ice stage, and some is transported out sea limits.

Ice cover thickness growth occurs rather intensive, and in the middle of winter period (February) about 60% of sea basin is occupied by thick first-year ice. To the end of ice cover growth period (May) thick first-year ice occupies about 86% of eastern sea region and 73% – of western.

Table 2.5.1 – Composition of ice age in the Laptev Sea regions in autumn-winter period,  
(% from region area)

Sea regions	Ice age														
	Young			Thin one-year			Medium one-year			Thick one-year			two-year, multiyear		
	months														
	X	II	V	X	II	V	X	II	V	X	II	V	X	II	V
Western	60	10	8	10	5	3	5	26	8	0	50	73	10	9	8
Eastern	74	3	7	8	5	3	3	20	4	0	71	86	3	1	0

In general, before melting (in May) thick first-year ice prevails in sea (thickness more than 120 cm), occupying 80% of sea water basin, young (thickness up to 30 cm) and thin ice (thickness 30-70 cm), formed mostly in polynyas, occupies about 10% (Fig. 2.5.4).

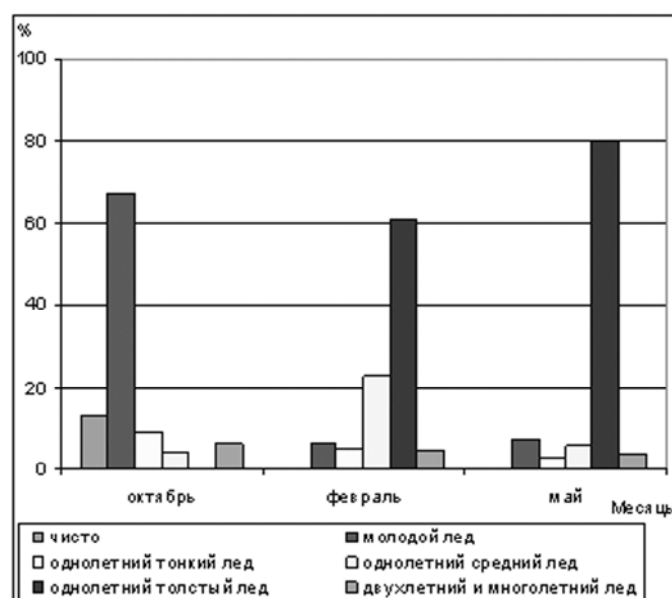


Fig. 2.5.4 – Distribution histogram of different ice age in the Laptev Sea in period of ice cover growth

Location of fast ice zones and drifting ice of different age in the Laptev Sea in the end of ice cover growth period (May) are shown on Fig. 2.5.5.

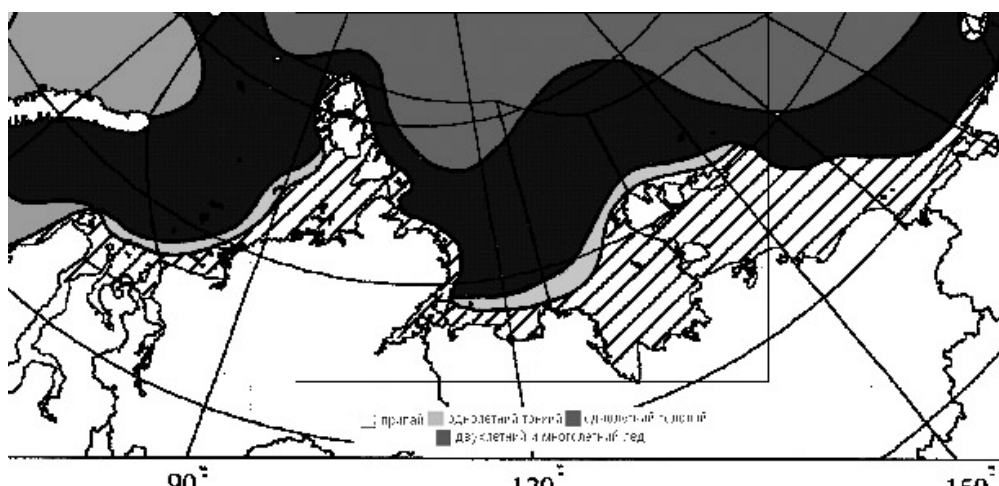


Fig. 2.5.5 – Average propagation of different ice age in the Laptev Sea in the end of ice growth period

Drifting ice mostly presented by large ice floes (extent up to 5000-10000 km, thickness up to 1,5-2,0 m) and their separate parts. Sea ice is little ridged, and ridging is 1–2 marks. Ridged ice ridge height is – 1,0–2,0 m, but hummock ridges are observed with maximum height up to 5-6 m (Table 2.5.2).

Table 2.5.2 – Characteristics of drifting ice in the Laptev Sea regions

Characteristic	Minimum and maximum values	
	Sea west	Sea east
Length of ice floes, m	10000-15000	5000-10000
Thickness of ice floes, m	1.4-1.6	1.6-1.8
Ridging, marks	3	2-3
Month with the most ridging	April-May	April-May
Average sail of hummocks, m	1.0-1.5	2.5
Maximum sail of hummocks, m	1.5-2.0	5.0-6.0
Hummock ridges width, m	5.0-7.5	7.5-10.0
Thickness of two-year ice floes, m	2.4-2.8	2.8-3.2

Drifting ice is transported to Arctic basin during entire period as a result of atmospheric circulation. In winter half year (October-May) on average about 280000 km<sup>2</sup> of ice is transported from sea to Arctic basin, which can be compared with area of eastern sea region.

*Fast ice.* Fast ice in the Laptev Sea is one of two largest and most solid (by ice thickness) in the Siberian Arctic shelf seas. The largest fast ice is in the East-Siberian Sea. Sea fast ice is formed in 10–15 days after stable ice formation along continental and island coast line. By this time ice thickness reaches 10-20 cm. From 60 to 100 % of cases fast ice formation occurs in October. However, 7 regions can be separated, if consider them by time range of probable fast ice formation terms (Table 2.5.3). In most regions fast ice formation is most probable (45-55%) in third decade of October.

Table 2.5.3 – Probability of stable fast ice formation terms in the Laptev Sea regions from the satellite data for the period 1980-2005, %

Regions	Months						
	X	X			XI		
	Decades						
	3	1	2	3	1	2	3
Severozemelskoye and Taymyr coast	12	13	21	46	8		
Entrance from Gulf of Khatanga			12	50	35	4	
Anabaro-Olenekskoye coast		15	13	51	20		
Lenskoye coast		37	41	22			
Gulf of Buor-Khaya		15	37	35	8	6	
Gulf of Yansk		18	37	45			
Novosibirskiye and Lyakhovskiye Islands		17	15	55	9	4	

The earliest fast ice development is observed in third decade of September along Severnaya Zemlya and Taymyr coast. Later, than in other sea regions, fast ice can be formed in the approach to Gulf of Khatanga (Severny Strait, Preobrazheniya Island) in the second decade of October. But fast ice formation can be delayed to the second decade of November in the same region, as in Gulf of Buor-Khay and along eastern island coast (Table 2.5.3). Multiyear variability in terms of fast ice formation is observed on Lensky coastal waters and in Gulf of Yansk – three decades, and in other regions it is stretched for 4-5 decades (Table 2.5.3).

On average almost 80% of fast ice in the Laptev Sea is formed in its shallow eastern region and only 20% – in western region.

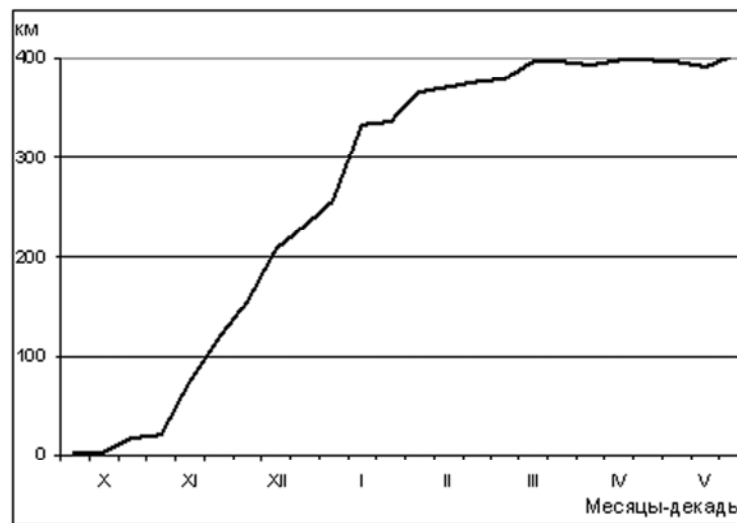


Fig. 2.5.6 – Seasonal changes of fast ice width in the eastern Laptev Sea.

Fast ice width in eastern sea region (north-western direction from coast of Gulf of Yansk) reaches on average 400 km (Fig. 2.5.6). As it is seen from Fig. 2.5.6, intensive fast ice development occurs till January, then it slows down and finishes in March-April, when fast ice propagation reaches its maximum.

Considering location fast ice boundaries (Fig. 2.5.7), in western sea region fast ice formation occurs significantly slower, and its width in the widest part from the north of Gulf of Oleneksky to the end of growth period is on average 170 km.

If fast ice boundaries move - its area changes. Intensive increasing of fast ice area occurs to January - early February in both sea regions (Fig. 2.5.8). By this time about 80% of fast ice area is formed in the western Laptev Sea and 90% – in the eastern.

Fast ice is rather resistant to interannual changes of hydro meteorological conditions in eastern sea region. From satellite data for 1980-2005, fast ice minimum area in the end of its ice cover growth period is 88% from its maximum area, ever observed.

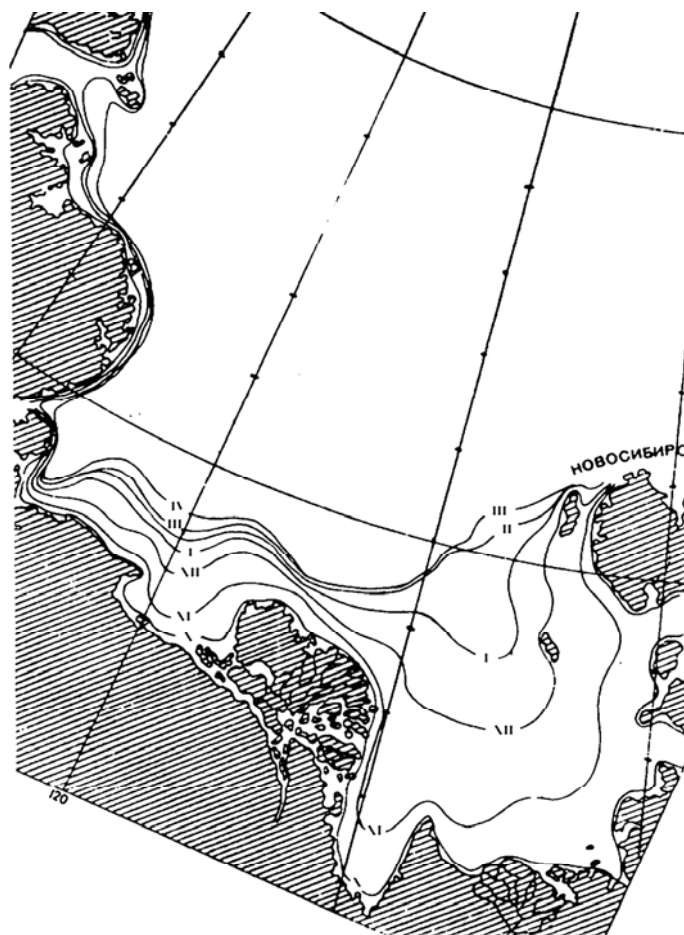


Fig. 2.5.7 – Average location of fast ice boundaries in period of its formation in the Laptev Sea from satellite data for 1980-2005

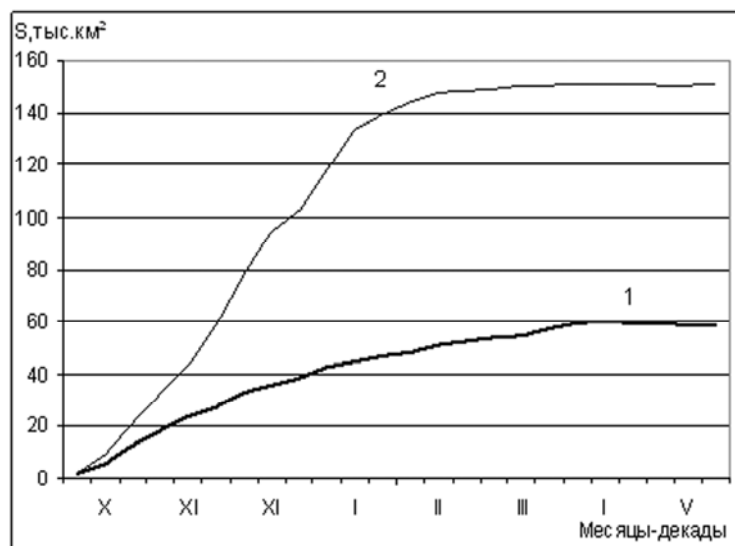


Fig. 2.5.8 – Seasonal changes of fast ice area in the western (1) and eastern (2) Laptev Sea

Range of interannual variability in fast ice area is 9% from region area or about 20 000 km<sup>2</sup> (Table 2.5.4). Fast ice area can significantly change in western sea region. Range of interannual changes in fast ice area is 19% from region area or about 47 000 km<sup>2</sup> (Table 2.5.4).

Table 2.5.4 – Average and maximum fast ice areas in the Laptev Sea regions, %

Regions	Fast ice area		
	average	maximum	minimum
Sea west	24	37	18
Sea east	53	57	48
Entire sea	40	47	35

As mentioned, Icelandic cyclones mostly influence on western sea regions, which make conditional softer winter conditions, resulting in less fast ice thickness, than in eastern sea region (Table 2.5.5). Fast ice thickness in eastern sea region exceeds 2 m.

Table 2.5.5 – Average fast ice thickness in the Laptev Sea regions in the end of month, cm

Regions	Months							
	X	XI	XII	I	II	III	IV	V
Sea west	24	61	98	128	148	170	184	192
Sea east	32	73	110	145	175	195	208	215

*Flaw polynyas.* Areas with open water and young ice with thickness up to 30 cm are formed under permanent ice transportation from the Laptev Sea – flaw polynyas. They are called by place of formation: Eastern Severozemelskaya, Eastern Taymyrskaya, Anabaro-Lenskaya and Western Novosibirskaya (Fig. 2.5.9).

Two of five polynyas of the Laptev Sea, Anabaro-Lenskaya and Western Novosibirskaya, are stationary, their average frequency of occurrence is more than 75% (Table 2.5.6).

Table 2.5.6 – Average frequency of occurrence (P, %) and size of the Laptev Sea flaw polynyas in November-June from satellite data for the period 1980-2005.

Polynya name	P, %	Characteristic					
		Length, km		Width, km		Area, km <sup>2</sup>	
		average	range	average	range	average	range
Eastern Novozemelskaya	64	323	50-540	26	5-75	9,1	0,4-53,3
North-western Taymyrskaya	70	180	50-350	36	5-165	6,4	0,3-36,3
Eastern Taymyrskaya	57	209	30-430	26	5-165	5,5	0,4-35,8
Anabaro-Lenskaya	84	371	60-750	40	5-200	14,7	0,4-71,1
Western Novosibirskaya	80	381	70-1170	42	6-235	16,6	0,8-82,2

These polynyas have continuity northwards from Novosibirskiye Islands - Northern Novosibirskaya polynyas, which are stationary most winter. Analyses of satellite data shows, that in 80% of cases all three stationary polynyas exist simultaneously and in years, which are favorable for development, can form pass-through behind fast ice with length more than 2000 km. These polynyas form “Great Siberian polynya”.

Size and area of polynyas significantly change. Polynyas, well-developed by their size, occur ten times more than polynyas, formed in periods unfavorable for their development. (Table 2.5.6).

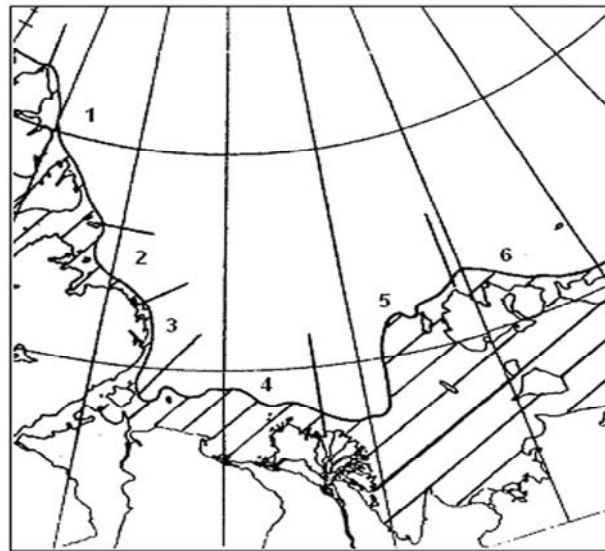


Fig. 2.5.9 – Areas of flaw polynyas formation in the Laptev Sea  
Eastern Severozemelskaya (1), North-eastern Taymyrskaya (2), Eastern Taymyrskaya (3), Anabaro-Lenskaya (4), Western Novosibirskaya (5), Northern Novosibirskaya (6)

Polynyas area depends on seasonal alterations of atmosphere circulation over the sea. Total area of the Laptev Sea flaw polynyas on average is close to 50 000 km<sup>2</sup> during their occurrence in period of ice cover growth, when polynyas are involved in process of sea ice productivity. It is about 10% of sea area.

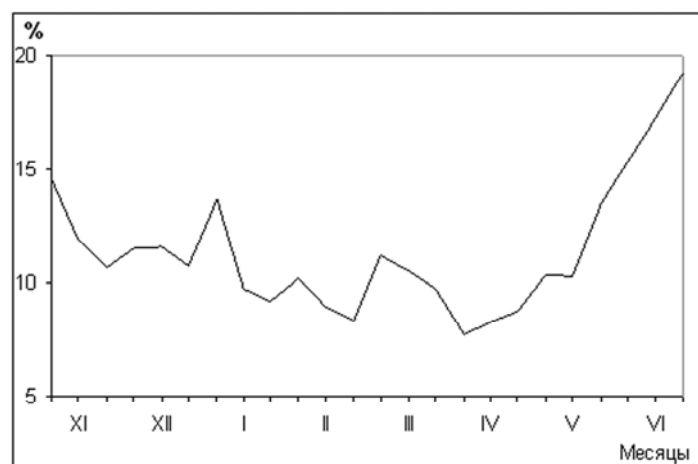


Fig. 2.5.10 – Seasonal changes of total flaw polynyas area in the Laptev Sea, %

In winter period, when polynyas are involved in process of sea ice productivity, and, despite of rather small total area, almost half ice, transported from sea, is reproduced due to polynyas.

Sharp increase of polynya area (20% of sea area) is observed in June (Fig. 2.5.10). However, ice cover starts melting in this time, and ice in polynyas stops its formation. Polynyas in this period are heat accumulators, and, consequently, ice-free areas in sea.

Correlation of polynya, fast ice and drifting ice area in the Laptev Sea is presented on Fig. 2.5.11. Drifting ice occupies 60% of sea area in the beginning of winter season and to 50% – in late May and in June.

### 2.5.3. Characteristics of ice cover during its melting period

*Melting and sea clearing from ice.* Ice cover melting starts in southern sea regions and on average occur on 5-10 of June. Ice formation stops in polynyas by this time, and they become heat accumulators and ice-free areas in sea. Clearing of southern sea regions starts under influence of warm advection in the middle of June.

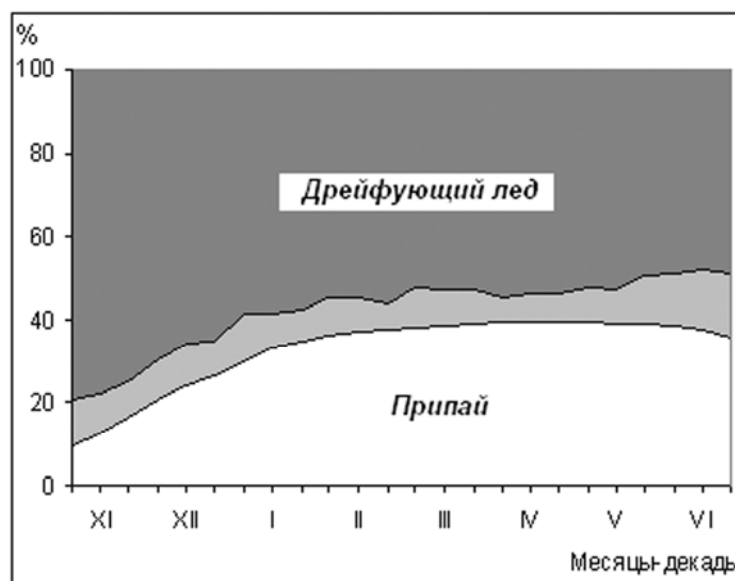


Fig. 2.5.11 – Seasonal changes of fast ice area, total polynyas area and drifting ice in the Laptev Sea

The Laptev Sea clearing from ice. About 10% of sea basin is free from ice to late June. Ice melting and clearing from ice of eastern sea region occurs more intensive during whole summer season, than in western sea region, and more than 80% of region is free from ice (Table 2.5.7).

Fast ice break up occurs in the Laptev Sea on average in late June. Gradual fast ice break up occurs during month, and fast ice completely disappears in late July, rarely in late August. On Fig. 2.5.12. average location of fast ice boundaries is presented (isochrones) in period of ice melting.



Table 2.5.7 – Area of the Laptev Sea ice-free regions in the melting period, %

Sea region	June			July			August			September		
	1	2	3	1	2	3	1	2	3	1	2	3
Sea west	6	9	11	13	16	23	32	41	46	49	50	48
Sea east	7	10	12	16	21	31	47	64	74	79	83	84

Clearing velocity increases in July after complete fast ice break up and change into drift ice of different size.

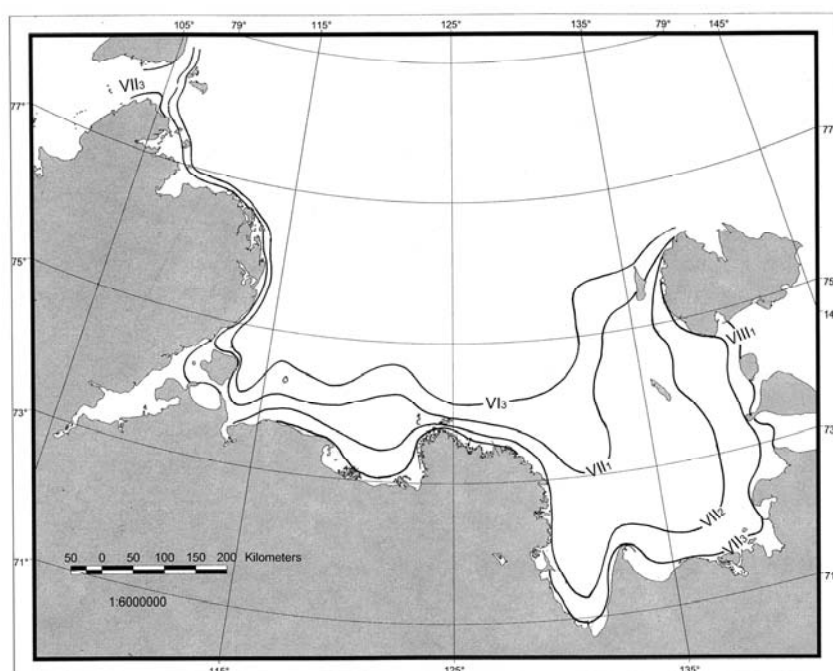


Fig. 2.5.12 – . Isochrones of average terms of fast ice melting in the Laptev Sea from satellite data for 1980-2005

On average fast ice break up occurs in eastern sea region several days earlier, than in western region. Multiyear range of ultimate fast ice break up is about month and a half in western sea region, and about two months - in eastern region (Table 2.5.8).

Table 2.5.8 – Terms of ultimate fast ice melting in the Laptev Sea

Terms	Regions	
	Sea west	Sea east
Average	21.07	18.07
Early	4.07	29.06
Late	16.08	25.08

Ultimate fast ice melting occurs in both sea regions in the second decade of July most often. In general, about 90% of total fast ice break up cases occur in July (Table 2.5.9).

Character of fast ice break up differs in sea. As it is seen from Fig. 2.5.13, fast ice area sequentially decreases from May till ultimate melting in early August in western sea region.

Table 2.5.9 – Terms of ultimate fast ice melting frequency of occurrence in the Laptev Sea, %

Sea region	June			August		
	1	2	3	1	2	3
Sea west	11	43	38	7	2	
Sea east	19	53	23	3	2	1

Small changes occur in fast ice area practically till late June in eastern region, and fast ice ultimately disappears during July.

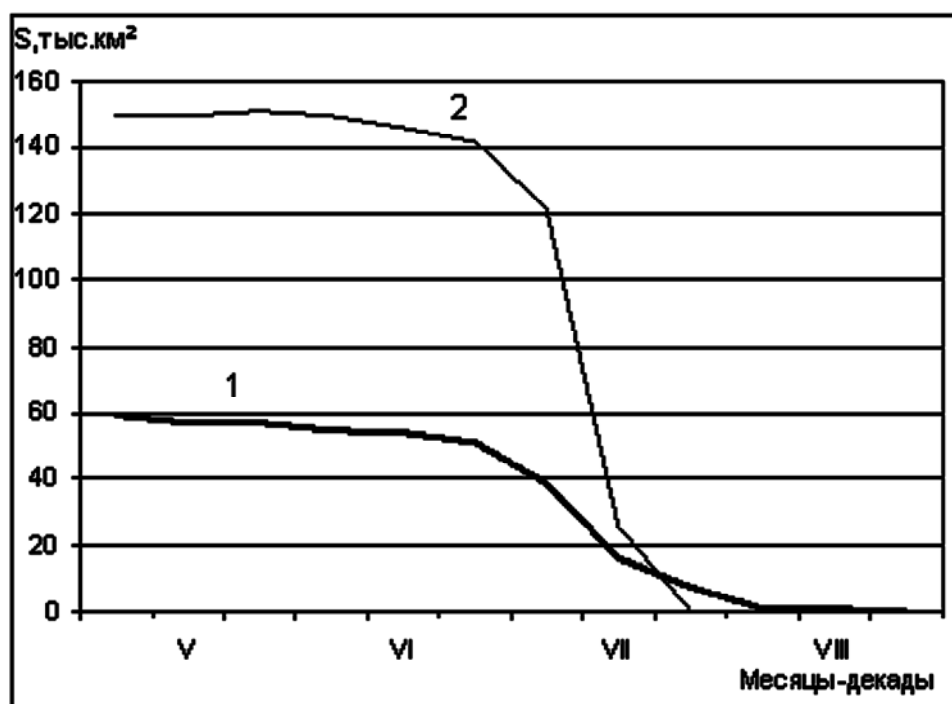


Fig. 2.5.13 – Changes of fast ice area in the western (1) and eastern (2) Laptev Sea in its melting period

Process of sea clearing occurs near fast ice more intensive. About half of western sea region and  $\frac{3}{4}$  – of eastern on average are free from ice in late August (Table 2.5.7). Totally about 70% of sea water basin is free from ice to late September (Table 2.5.7). Ice edge in eastern sea region is located northwards Novosibirskiye Islands during this time and moves down south-westwards to eastern coast of Taymyr peninsula. In September melting processes slow down, ice edge moves northwards and locates in western sea region on latitude of Vilkitsky Straight (Fig. 2.5.14).

Amount of compact ice (7-10) decreases and amount of open ice and very open ice (1-6) increases during processes of melting and ice cover decay (Fig. 2.5.15).

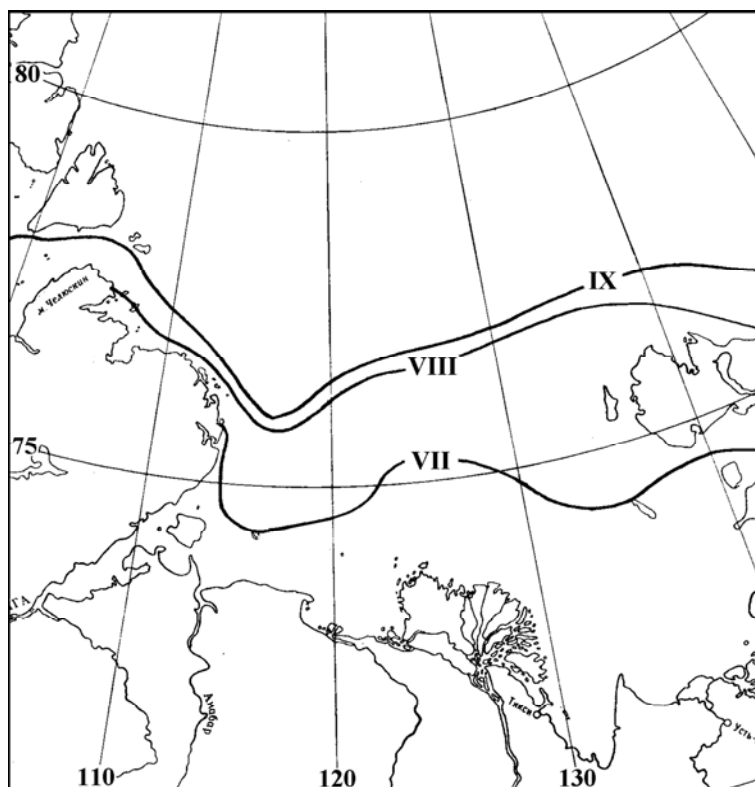


Fig. 2.5.14 – Location of ice edge in late June-September in the Laptev Sea

Amount of very open ice stays within limits of 17-19% beginning from late July, when area of compact sea decreases on average to 15% (Table 2.5.10).

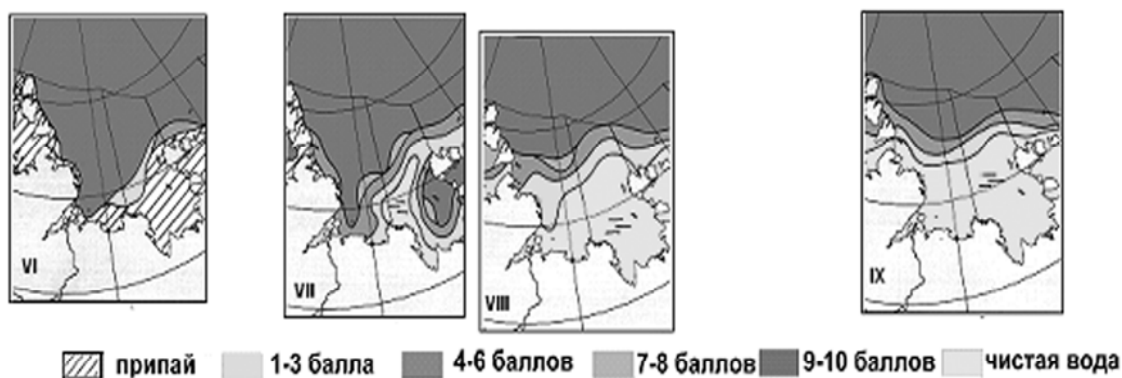


Fig. 2.5.15 – Propagation of ice with different concentration in the Laptev Sea in June-September (probability 50%)

Table 2.5.10 – Amount of compact (7-10), open and very open ice (1-6) and open water in the Laptev Sea in melting period

Ice compactness, marks	June			July			August			September		
	1	2	3	1	2	3	1	2	3	1	2	3
7-10	92	90	88	79	67	54	41	29	20	18	17	15
1-6	1	1	1	7	14	19	19	17	19	17	16	18
No ice	7	9	11	15	19	27	40	53	61	65	67	67

*Ice massifs.* Compact ice (7-10) is located in two ice massifs – Yansk and Taymyr in period of melting and ice cover decay (Fig. 2.5.16).

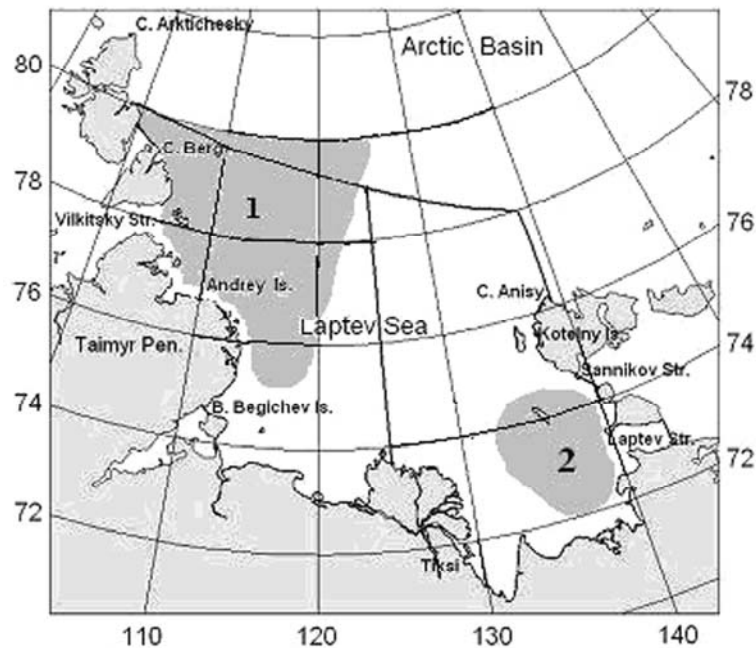


Fig. 2.5.16 – Location of ice massifs in the Laptev Sea. 1 – Taymyr and 2 – Yansk ice massifs

Yansk ice massif is formed from broken fast ice. It is located in Gulf of Yansk and near Straights Sannikov and Dmitriy Laptev. Yansk ice massif ice disappears during August-September for observational period (1938-2007) in more than 80% of cases (Fig. 2.5.17). At that, frequency of occurrence for such cases is same for August and September (41 and 43%, respectively). In some years this ice massif doesn't disappear till late summer. It hardens navigation in Gulf of Yansk and blocks Novosibirsky gulfs from western side.

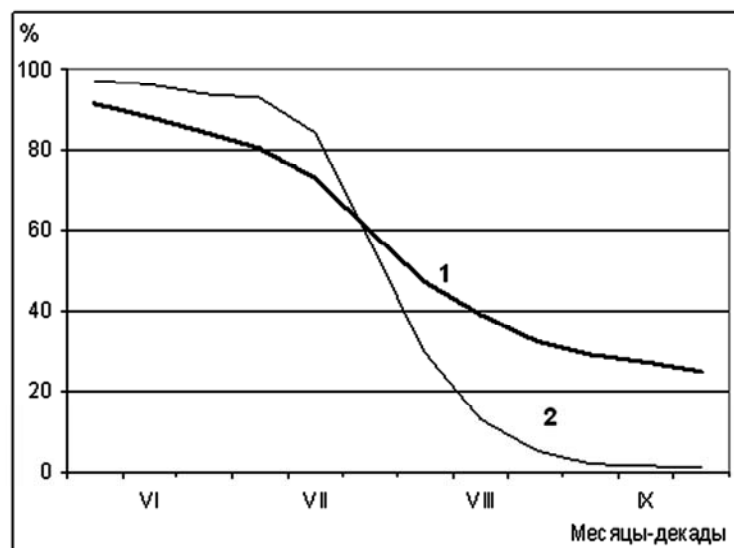


Fig. 2.5.17 – Area changes of Taymyr (1) and Yansk (2) ice massifs in of June-September, %

Taymyr ice massif is formed from compact ice of western sea region, which in summer period is supplied by ice, transported from Arctic basin with Eastern-Taymyr current. Taymyr massif is one of the most significant spur oceanic massifs with large area. On average Taymyr massif in the middle of July occupies about 60% of the western Laptev Sea, and in late September – 25% (Fig.2.5.17). However, in 10% of cases 50-70% of massif compact ice doesn't melt till the beginning of ice formation. Taymyr massif often blocks Vilkitsky Straight from eastern side and hardens ship navigation.

Taymyr ice massif rarely disappears completely to the end of melting period. From data for 1938-2007 it happened in 15% of cases, at that 5% of cases were in August.

*Grounded hummocks.* Grounded hummocks are observed in summer near coast on depth 10 m and less or in shoals in open sea. Grounded hummocks are rest of fast ice or strongly ridged drifting ice floes, settled on the ground. Their draft changes from 1,6 to 22,0 m. Grounded hummocks normally disappears to late August. The biggest propagation of fast ice boundary is shown on Fig. 2.5.18.

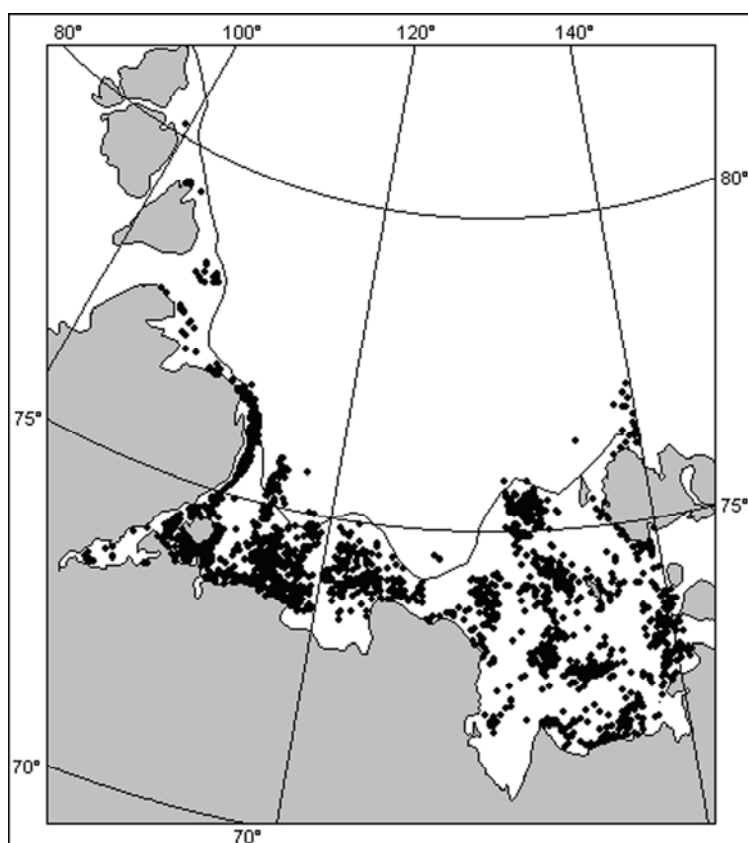


Fig. 2.5.18 – Location of grounded hummocks and their largest propagation boundary from air reconnaissance data for 1962-1991

*Icebergs.* Small amount of icebergs is produced to the sea from islands of Severnaya Zemlya. The biggest amount is observed near northern island among archipelago islands. They propagate

southwards along Taymyr coast under influence of winds and Eastern-Taymyr current. Separate icebergs were found near Island Preobragzeniya in some cases. Mostly icebergs propagate to western sea region, and only in separate cases small icebergs were observed in eastern sea regions.

## 2.6. Characteristics of the East-Siberian Sea ice conditions

### 2.6.1. Physical-geographical sea characteristic

*Borders, depth.* The East-Siberian Sea is one of the Siberian shelf seas. It has an open border with Arctic basin in the north, with the Laptev Sea - in the west, with the Chukchi Sea - in east. The East-Siberian Sea is a shallow water basin with extremely level bottom, generally inclining north-eastwards. Level and sloping coast smoothly changes into sea bottom. Dominant depth in western sea region is 10–20 m, in eastern region – 30–40 m (Fig. 2.6.1).

Siberian rivers Indigirka and Kolyma flow into sea.



Fig. 2.6.1. Geographical location of the East-Siberian Sea

Northern sea boundary, accepted by AARI, goes a bit northwards isobath 50 m by line:  $78^{\circ}$  N  $139^{\circ}$  E –  $78^{\circ}$  N  $160^{\circ}$  E –  $73^{\circ}$  N  $180^{\circ}$ . Western border:  $78^{\circ}$  N  $139^{\circ}$  E – Cape Anysiy – northern, eastern and southern coasts of Islands Kotelnii and Fadeevsky – Sannikov Strait – eastern coast of Lyakhovskiy Island – Dm. Lapteva Strait. Eastern border:  $73^{\circ}$  N  $180^{\circ}$  E – by  $180^{\circ}$  to Vrangeli Island – north-western coast of Vrangeli Island – Cape Blossom – Cape Yakan (Fig. 2.6.2).

Taking into account physical-geographical features (bottom relief, ice and hydrologic regime) sea is divided into two regions – western and eastern, with virtual border between them by meridian  $160^{\circ}$  E (Fig. 2.6.2). In accepted borders total sea area is 770000 km<sup>2</sup>, western region – 363000 km<sup>2</sup>, eastern region - 407000 km<sup>2</sup>.

*Climate.* Peculiarities of the East-Siberian Sea climate are caused by its high latitude location between  $69$  and  $78^{\circ}$  N and influence of cool Arctic basin from one side, and large Asian continent – from the other.

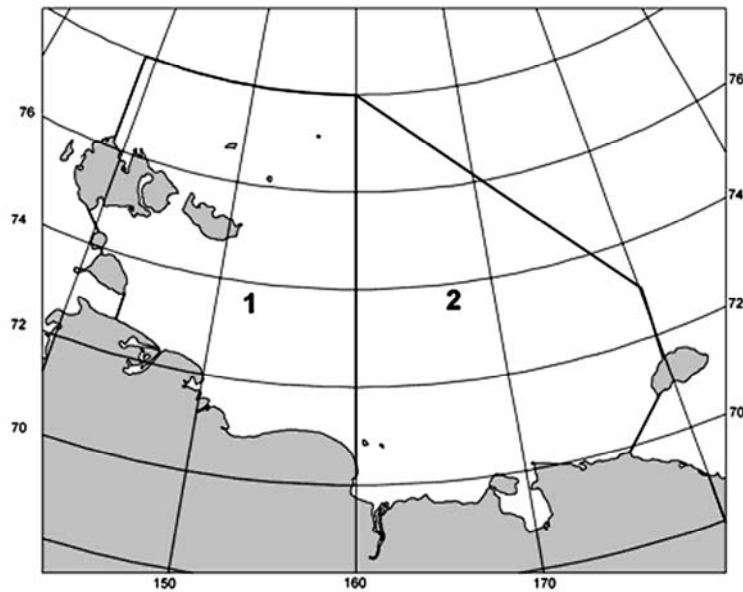


Fig. 2.6.2. Borders and regions of the East-Siberian Sea. 1 – western region, 2 – eastern region;

From November to March, atmosphere circulation over the sea is determined by small gradient field of atmosphere pressure, which is formed between Siberian and Canadian anticyclones and Aleut depression (in the eastern sea). Wind fluxes are less stable at this time. Western fluxes prevail insignificantly in western sea region.

In spring alteration of atmosphere circulation occurs in April-May. Siberian and Canadian anticyclones disappear, Aleut depression becomes weaker. At the same time northwards the Beaufort Sea arctic anticyclone is formed, branch of which defines circulation regime over the sea. Eastern fluxes also prevail over the sea, becoming northern with move off from continent, what is typical for summer period.

Low pressure hollow, connected with Siberian depression and coming along Arctic coast, influences circulation regime over the sea. Atmosphere circulation changes into winter type in September-October. At this time southern fluxes prevail insignificantly in western sea region, in the east – northern.

Most year negative air temperatures are observed over the sea. Average daily temperatures are positive less than 2 months in northern sea region, and 3–3,5 months – in southern. Over the northern sea region stable air temperature about  $0^{\circ}\text{C}$  is observed in July-August, near coast it is  $4\text{--}5^{\circ}\text{C}$ , and in gulfs and bays, juttied into continent, temperature reaches  $7\text{--}8^{\circ}\text{C}$ . The highest air temperatures in summer months are less than  $15^{\circ}\text{C}$  in northern sea half and reach  $25\text{--}30^{\circ}\text{C}$  near coast.

Changes of level and currents in the East-Siberian Sea are caused mostly by hydro meteorological factors (wind, atmosphere pressure, water exchange with Arctic basin and neighbor seas, river flow). Constant current coincides in the northern region with main



Transarctic current and ice drift westwards and north-westwards. Direction of currents is variable west-eastern. Eastern coastal current is observed in eastern sea region, which has a constant pattern till Cape Billings and further through Long Strait. The highest current velocity is observed in straits and in shallow sea regions.

#### 2.6.2. Characteristics of sea ice cover in period of its growth

The East-Siberian Sea is ultimately covered with ice from October to May-June (eight-nine month a year).

*Ice formation.* Stable ice formation starts among compact ice on the northern sea boundary on 25-30<sup>th</sup> of August. Ice formation processes propagate southwards during September, and on 5<sup>th</sup> of October young ice forms in coastal zone. Thus, sea ultimately freezes up during on average 35 days (Fig. 2.6.3).

Ice mostly has local origin in western sea region and in Novosibirsk Straits. Transformation of ice, survived summer melting, into two-year ice is observed in some years. In eastern sea region ice cover consist from new formed ice, multiyear ice, located in central and northern regions, and ice, survived summer melting.

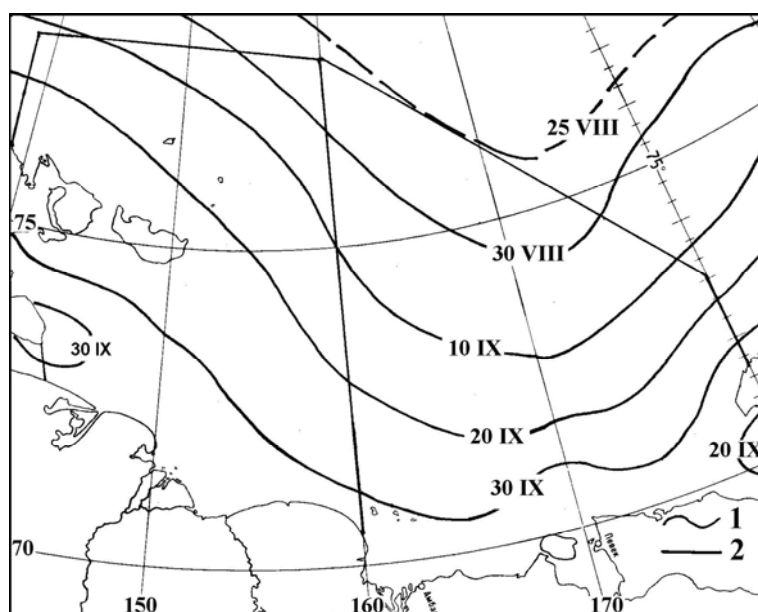


Fig. 2.6.3. Isochrones of average terms of stable ice formation in the East-Siberian Sea. 1 – isochrones, 2 – sea and region boundaries

*Ice growth.* Ice thickness rather intensive increases in sea. All ice age stages are already presented in October: thick first-year (thickness more than 120 cm); more than half of sea is occupied by young ice (thickness less than 30 cm), thin first-year ice (30-70 cm) and medium first-year ice (70-120 cm) occupies about 6% of area. In the East-Siberian Sea about 24% of ice, survived melting, with inclusion of multiyear ice occurs after summer period in contrary to other Arctic Seas. Most ice (about 30%) is located in the eastern sea region (Table 2.6.1).

Таблица 2.6.1 – Возрастной состав льда в районах Восточно-Сибирского моря в осенне-зимний период, (% от площади районов)

Районы моря	Возраст льда														
	Молодой			Однолетний тонкий			Однолетний средний			Однолетний толстый			2-летний, многолетний		
	М е с я ц ы														
	X	II	V	X	II	V	X	II	V	X	II	V	X	II	V
Запад моря	64	5	4	4	3	2	5	17	2	0	60	80	17	15	12
Восток моря	47	2	2	8	2	1	6	10	2	0	54	65	30	32	30
Все море	55	3	3	6	2	1	6	13	2	0	57	72	24	24	22

Thick first-year ice is formed till February in most water area, and amount of two-year and multiyear ice isn't practically changed (Table 2.6.1, Fig. 2.6.4).

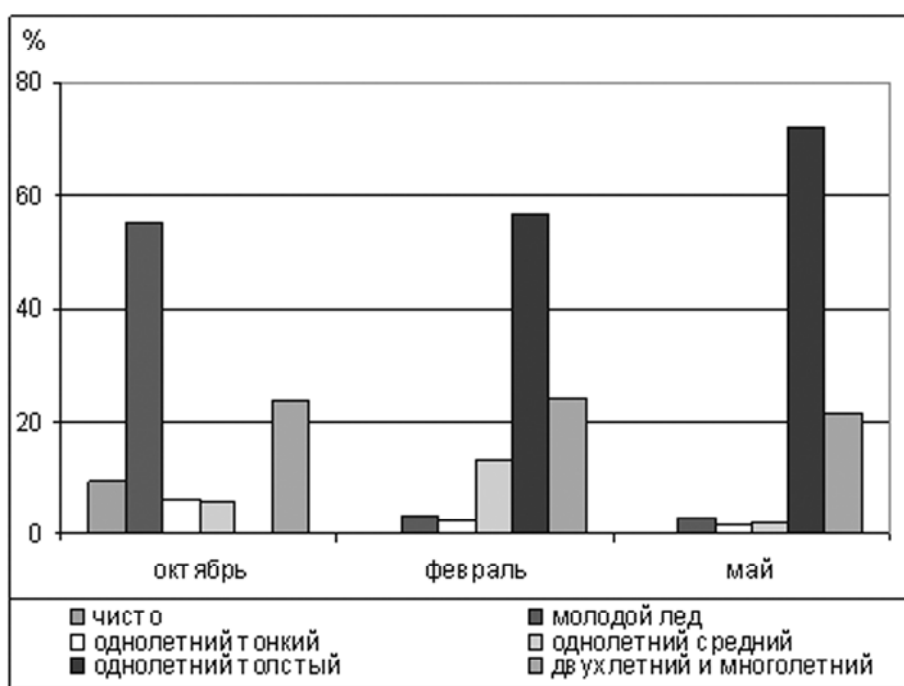


Fig. 2.6.4. Histograms of different ice age propagation in the East-Siberian Sea in ice growth period

In the end of winter ice cover consists from fast ice and drift ice, formed by thick first-year ice, two-year and multiyear ice, located in 30% of eastern sea area (Fig. 2.6.5, Table 2.6.1).

*Fast ice.* Fast ice in the East-Siberian Sea is the widest and largest among Arctic Seas. The most extensive fast ice forms mainly in the western part, which is relatively shallow (Fig. 2.6.5). As a rule, fast ice in the East Siberian Sea forms in open water. However, in the years when residual ice remains in the sea, fast ice forms with inclusion of this ice.

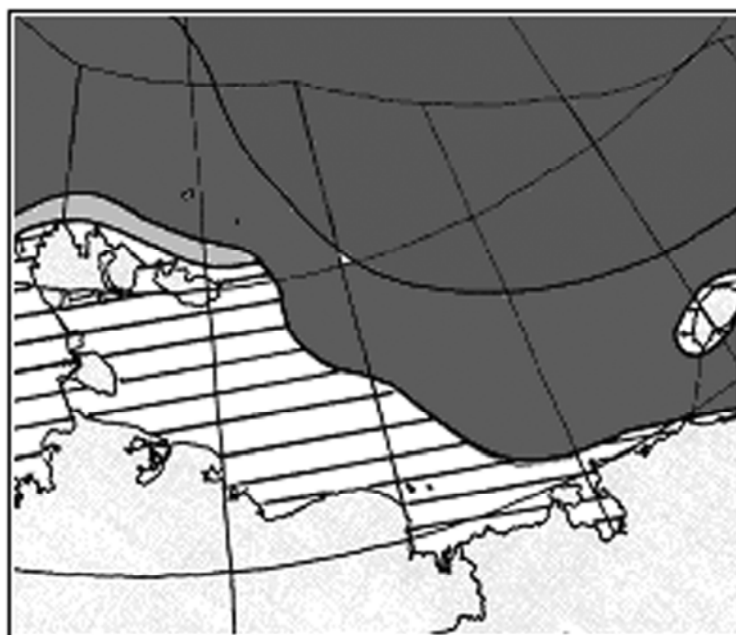


Fig. 2.6.5. Average propagation of different ice age in the East-Siberian Sea in ice growth period

Interannual changes of terms of fast ice formation are 5-6 decades in sea regions. Early terms are in the first decade of October, late ones – in the last decade of November (Table 2.6.2). From 70 to 90% of cases fast ice formation occurs in October. However, frequency of occurrence terms of fast ice formation occurs inside month in different decades in each region (Table 2.6.2).

Таблица 2.6.2 – Вероятность сроков образования устойчивого припая в районах Восточно-Сибирского моря по данным ИСЗ за 1980-2007 гг., %

Районы моря	Октябрь			Ноябрь		
	Декады					
	1	2	3	1	2	3
Новосибирские о-ва, проливы Санникова, Дм. Лаптева	15	19	48	11	5	2
Южный берег западной части моря	41	28	23	6	2	
Колыма – о.Айон	16	34	38	5	7	
Чукотское побережье	21	21	29	19	7	3

In region, including New Siberian Islands and Sannikov and Dm. Laptev Straights, fast ice forms in the third 10-day period of October (about half of all cases). In coastal sea region three zones are separated. Along southern coast of western region (zone from Dm. Laptev Strait to Kolyma mouth) fast ice is mostly formed in the first 10-day period of October. In zone from Kolyma mouth to Ayonsky Island fast ice with equal probability can form in the second and

third 10-day periods. Most unstable terms of fast ice formation are along the Chukchi Sea coast. Here, fast ice with equal probability can form in any 10-day period of October (Table 2.6.2).

Interannual changes of terms of fast ice formation depend on hydro meteorological and ice conditions variability, occurred before stable ice formation in sea, autumn conditions in periods of ice formation and growth, necessary for fast ice formation. Fast ice forms on average in 10-15 days after stable ice formation. On Fig. 2.6.6 comparison between terms of stable ice formation and fast ice formation in Sannikov Strait is shown. As it is seen from Fig. if most probable terms of stable ice formation - in the first 10-day period of October - occur, fast ice forms in two 10-day periods – in the third 10-day period of month.

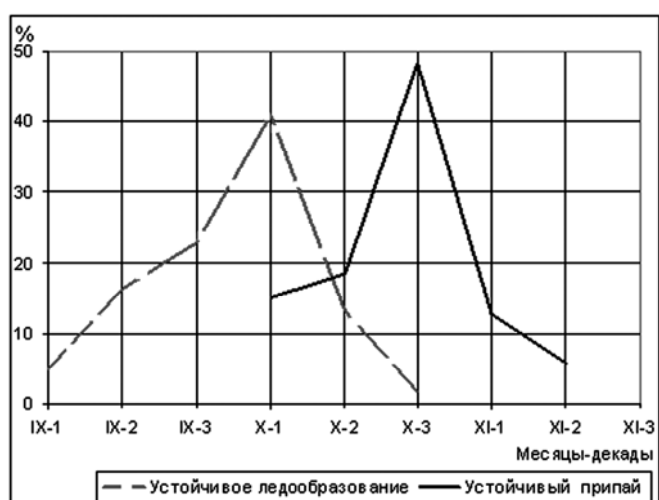


Fig. 2.6.6. Frequency of occurrence of terms of stable ice and fast ice formation in Sannikov Strait zone, %

From the moment of stable fast ice formation, its boundary moves seaward and, depending on winter conditions, reaches its maximum extent from the coast in April (sometimes in May) In some regions its external boundary is retained by stamukhas formed during the periods of strong onshore winds.

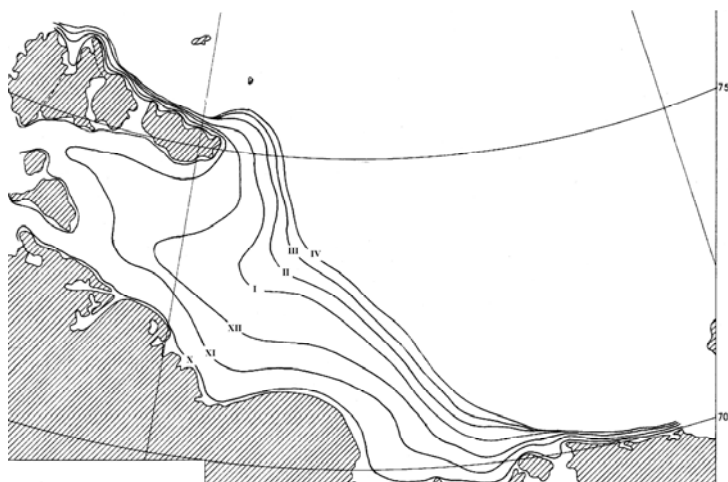


Fig. 2.6.7. Average location of fast ice boundaries in period of its growth in the East-Siberian Sea from satellite data for 1980-2005

After fast ice establishment in Dm. Laptev and Sannikov Straights its boundary moves eastwards. The most intensive fast ice formation in the East-Siberian Sea occur from October to January, at that, the largest growth of fast ice is observed in December-January (Fig. 2.6.7). From November to December on Sannikov Straight latitude boundary on average moves for 300 km. Then fast ice boundary motion decreases and in March its position stabilizes near northern coast of New Siberian Islands and Chukchi coast, and in April – in central sea regions (Fig. 2.6.7).

On average, the distance between the fast ice boundary and the Indigirka mouth in the northeastern direction comprise 285 km. To the north of the New Siberian Islands, the maximum distance of the fast ice boundary from the coast during the period of its greatest development (March–May) comprises 50–80 km. On average it extends not more than 25–30 km from the Chukchi coast.

If fast ice boundaries move seaward, its area changes. In western sea region intensive increasing of fast ice area occurs till January-early February, then it slows down, in eastern sea region fast ice area equally increases during whole growth period (Fig. 2.6.8).

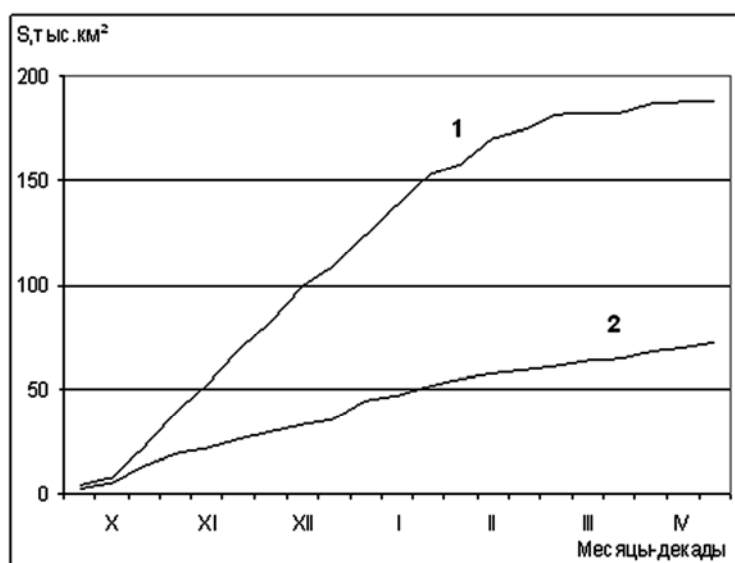


Fig. 2.6.8. Changes of fast ice area in the western (1) and eastern (2) East-Siberian Sea in ice growth period

Average area of fast ice in entire sea is 260 000 km<sup>2</sup>. Interannual changes of fast ice area occurs within limits 154-354 000 km<sup>2</sup>, i.e. fast ice in the East-Siberian Sea can occupy from 20 to 46% of its water area.

Offshore winds are often observed in winter in the East-Siberian Sea. They facilitate ice exporting from Arctic basin to eastern sea region. However, part of ice, moving along fast ice boundary north-westwards, is transported to Arctic basin, where it is involved in Transarctic drift northwards New Siberian Islands.

In summer frequency of occurrence of transporting winds in the East-Siberian Sea significantly increases, and area of ice, transported from sea is on average 100 000 km<sup>2</sup>.

Ice ridging in sea is 2 marks and increases near fast ice boundary up to 3 marks.

*Flaw polynyas.* The East-Siberian Sea polynyas, formed behind fast ice, are mostly unstable and can be referred to episodic polynyas (frequency of occurrence less than 50%). Exception is Northern Novosibirskaya polynya, formed behind fast ice northwards New Siberian Islands (Table 2.6.9). This polynya is stable, its frequency of occurrence is more than 75%, and under favorable conditions its width can reach tens of kilometers.

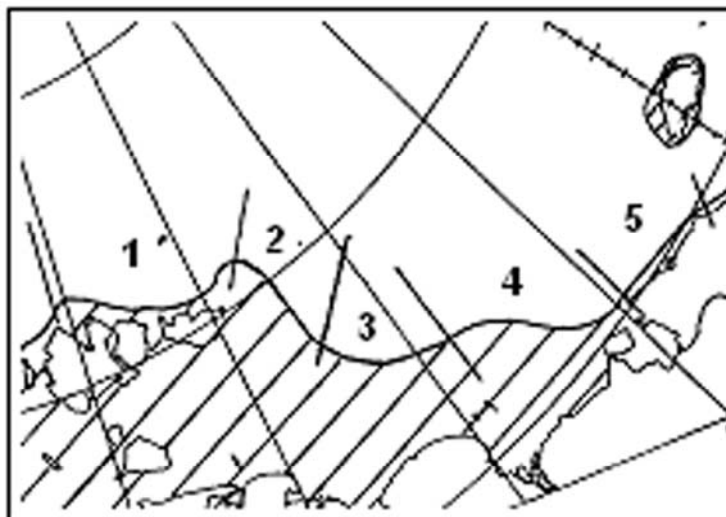


Fig. 2.6.9. Location of flaw polynyas in the East-Siberian Sea 1 - Northern Novosibirskaya; 2- Eastern Novosibirskaya (west); 3 - Eastern Novosibirskaya (east); 4 - Ayonsky; 5 - Western Chukchi

The Northern Novosibirskaya polynya was first detected at the beginning of the 19<sup>th</sup> century by the Russian Hydrographic Expedition. The expedition participants were thunderstruck when they saw open water during winter at such high latitudes. Their observations resulted in the idea of the open Northern Ocean to the north of the New Siberian Islands – an idea that was refuted only in the early 1880s by the participants who stayed alive during the *Zhannetta* drift under the command of De Long. It became obvious that the open water space over fast ice is formed under the offshore wind influence and presents a “Siberian polynya”.

The flaw polynyas of the East Siberian Sea to the north of the New Siberian Islands are formed episodically. Their average frequency of occurrence decreases from 44% to 25% with advance to the Chukchi coast. However, in some months, the polynyas exist stably and their frequency of occurrence is slightly more than 50%. Thus, Eastern Novosibirskaya (west) polynya can be referred to stable polynyas in December and June, Western Chukchi – in June (Table 2.6.4).

Таблица 2.6.3 – Характеристика заприпайных полыней Восточно-Сибирского моря

Название полыней	Характеристика						
	Р, %	Длина, км		Ширина, км		Площадь, тыс. км <sup>2</sup>	
		средняя	диапазон	средняя	диапазон	средняя	диапазон
Северная Новосибирская	80	321	50-480	32	5-125	10,6	0,4-44,4
Восточная Новосибирская (запад)	44	244	30-650	25	5-187	6,7	0,5-69,2
Восточная Новосибирская (восток)	37	297	80-530	24	5-163	7,7	0,5-58,8
Айонская	38	225	50-440	24	5-108	5,4	0,4-26,9
Западная Чукотская	25	182	40-440	21	5-73	4,1	0,3-16,6

Таблица 2.6.4 – Средняя месячная повторяемость заприпайных полыней Восточно-Сибирского моря по данным ИСЗ за период 1979-2005 гг., %

Название полыней	М е с я ц ы							
	XI	XII	I	II	III	IV	V	VI
Северная Новосибирская	67	87	67	64	77	76	90	91
Восточная Новосибирская (запад)	32	57	44	43	49	46	29	50
Восточная Новосибирская (восток)	28	42	32	42	46	44	34	38
Айонская	22	41	42	38	45	39	29	44
Западная Чукотская	18	10	20	20	19	28	30	51

Total area of polynyas is about 5% of sea area. Total area of polynyas changes within 3 to 8%. Minimum values occur in late January-early March (Fig. 2.6.10).

### 2.6.3. Characteristics of sea ice cover in period of melting

*Melting and sea clearing from ice.* Beginning from July and till late September ice cover melts and sea clears from ice under thermal and dynamic processes. Clearing occurs in near-mouth areas of rivers Indigirka and Kolyma, which significantly influence ice regime of shallow western sea region. Sea clearing occurs slower, than in other Arctic Seas. Clearing velocity increases in August after ultimate fast ice break up.

Fast ice starts melting in the edge zone on average in late May-early June. Its break up occurs during two months, and fast ice ultimately disappears in late July, rarely in early August. On Fig. 2.6.11 location of average fast ice boundaries (isochrones) in melting period is shown.

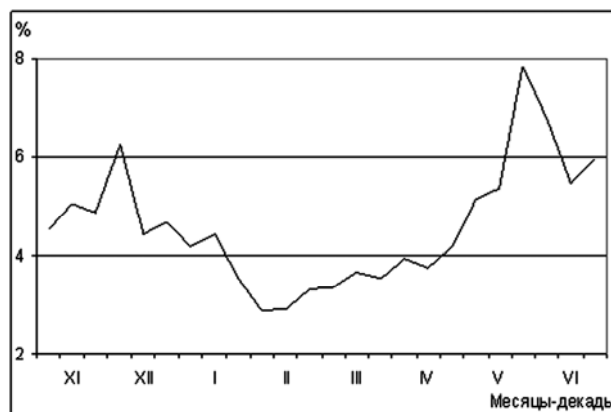


Fig. 2.6.10. Seasonal changes of total flaw polynyas area in the East-Siberian Sea

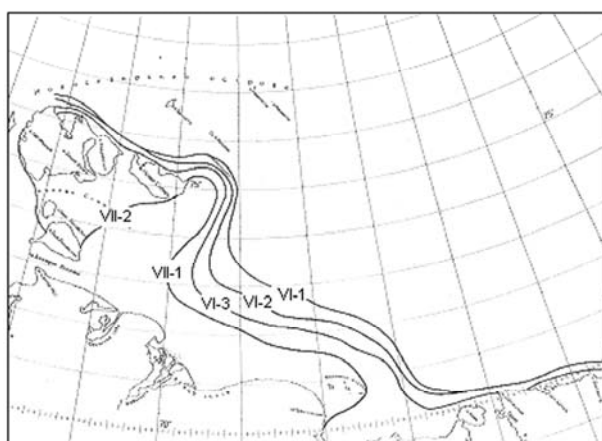


Fig. 2.6.11. Location of fast ice boundaries in the East-Siberian Sea in period of its melting (probability 50%)

Fast ice boundary slowly moves off during June. Its most part melts and becomes drift ice during July (Fig. 2.6.11, 2.6.12).

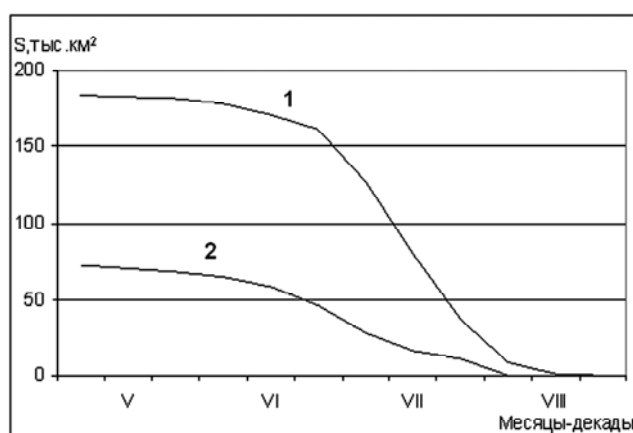


Fig. 2.6.12. Changes of fast ice area in the western (1) and eastern (2) East-Siberian Sea in melting period



Ultimate fast ice melting (fast ice breaks drift floes) depends on stage of its development in autumn-winter period. As it is seen from Fig. 2.6.13, ultimate fast ice melting in the western sea region, when its area is maximum, occurs in the second 10-day period of August, and when fast ice area is minimum - in early July. When fast ice size is close to average (50% probability), it ultimately disappears in late June.

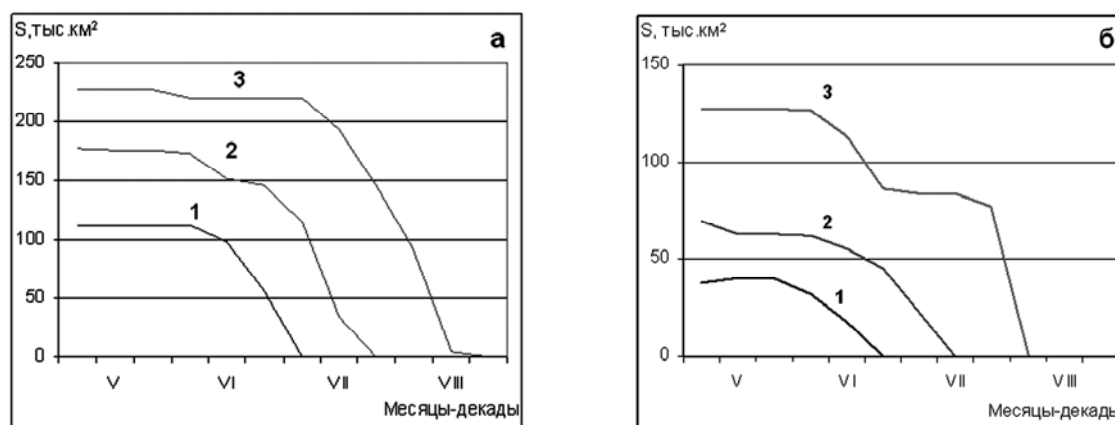


Fig. 2.6.13. Changes of fast ice area in the western (a) and eastern (б) East-Siberian Sea in melting period with different development stage: 1-minimum, 2-average, 3-maximum

Interannual changes of terms of ultimate fast ice melting are about one month in the East-Siberian Sea regions. In Table 2.6.5 characteristics of fast ice break up terms are shown in the most important for navigation regions: in approaches to Sannikov and Dm. Laptev Straights and to Kolyma river shoal.

Таблица 2.6.5 – Характеристика сроков взлома припая в районах Восточно-Сибирского моря за период 1980-2007 гг.

Район	Сроки взлома			Размах колебаний, сутки
	средние	поздние	ранние	
Подходы к проливу Санникова	22 VII	3 VIII	6 VII	28
Пролив Санникова	22 VII	9 VIII	7 VII	33
Подходы к проливу Дм.Лаптева	19 VII	31 VII	3 VII	28
Участок бар реки Колымы – о.Айон	9 VII	27 VII	21 VI	36

According to general regularity of fast ice melting (Fig. 2.6.10) the earliest break up occurs in zone of Kolyma river shoal – Ayonsky Island, it occurs on average two weeks earlier than in zone of straights. The earliest terms of fast ice break up occur in the beginning of third 10-day period of June, and in zone of straights – in the first 10-day period of July (Table 2.6.5).

Drift ice of different concentration is observed in sea after fast ice break up. In late July only 10% of water basin is free from ice (Table 2.6.6), and ice edge locates close to continent coast and islands (Fig. 2.6.14). During entire melting period eastern sea region gets ice-free two times slower, than western. Before ice formation in September, more than sea half is free from ice, and eastern part – less than a third (Table 2.6.6).

Таблица 2.6.6 – Площади акваторий в районах Восточно-Сибирского моря, освобождающиеся ото льда в период таяния ледяного покрова, %

Район моря	Июнь			Июль			Август			Сентябрь		
	Декады											
	1	2	3	1	2	3	1	2	3	1	2	3
Запад моря	4	4	6	8	10	14	24	34	44	51	54	56
Восток моря	1	1	2	3	4	7	10	14	20	26	30	31

The most intensive ice melting and sea clearing occur in August. 40% of western sea part and 20% of eastern part are ice free in the end of month. Sannikov Strait is free from ice in August.

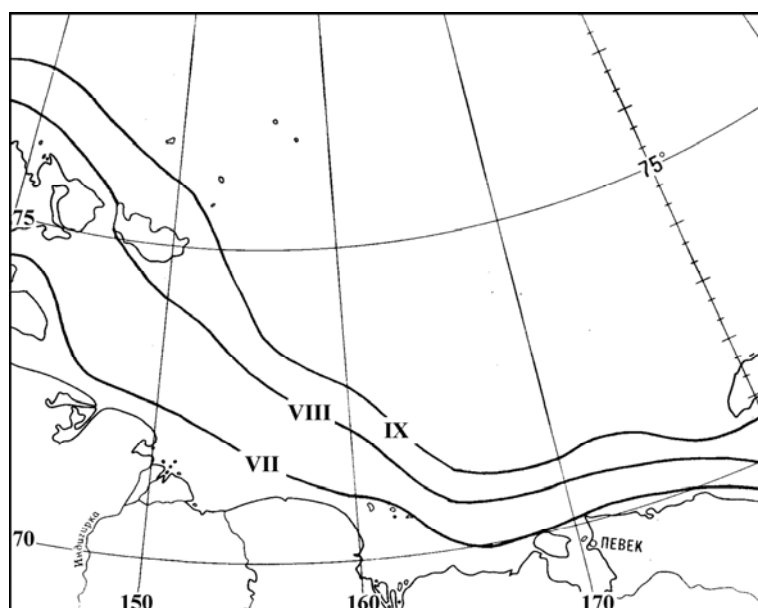


Fig. 2.6.14. Ice edge location in the East-Siberian Sea in late June-September

In September sea clearing finishes. Ice edge in western sea region locates 60-90 miles northwards New Siberian Islands. In the east – comes through Long Strait under southern coast of Vranghel Island (Fig. 2.6.13). Only 30% of eastern sea region and only about 50% – of western are ice-free before new freeze-up.

During processes of melting and ice cover decay amount of compact (7-10-th) ice decreases and amount of open and very open (1-6-th) ice increases (Fig. 2.6.15). Open and very open ice is

formed both as a result of melting and compact ice decay, and dynamic influence, resulting in partly ice transporting of sea limits (Table 2.6.7).

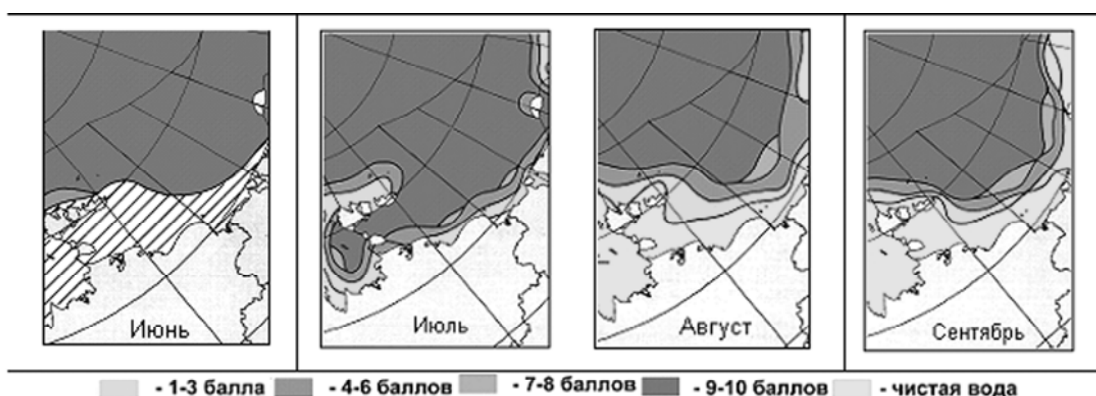


Fig. 2.6.15. Ice propagation of different concentration in June-September (probability 50%)

In late September about 40% of sea area is absolutely free from ice. Compact ice stays on more than a third of water basin, mainly due to of eastern sea region (Table 2.6.7).

Таблица 2.6.7– Количество сплоченных (7-10 баллов), редких и разреженных льдов (1-6 баллов) и чистой воды в Восточно-Сибирском море в период таяния

Сплоченность льда, баллы	Июнь			Июль			Август			Сентябрь		
	1	2	3	1	2	3	1	2	3	1	2	3
7-10	98	98	97	91	84	76	66	56	45	41	38	36
1-6	2	2	3	9	16	13	17	20	23	21	21	21
чисто	0	0	0	0	0	10	17	23	32	38	42	43

*Ice massifs.* Quasistationary accumulations of compact ice in the East-Siberian Sea form two ice massifs: Novosibirsky, occupying southern part of western sea region, and Ayonsky (Fig. 2.6.16).

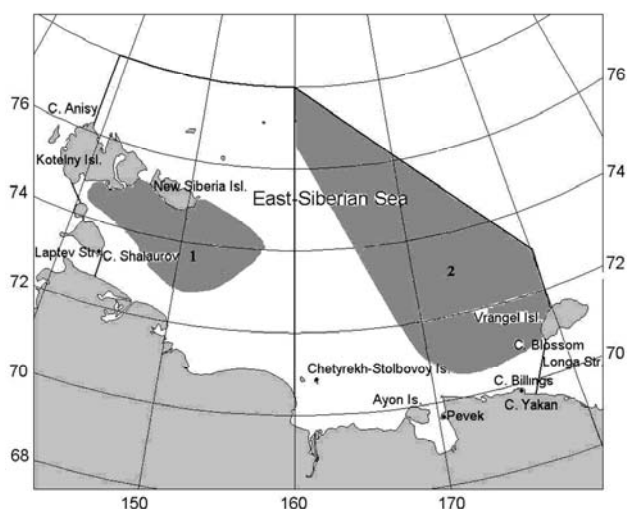


Fig. 2.6.16. Scheme of ice massifs location in the East-Siberian Sea. 1 – Novosibirsky and 2 – Ayonsky massifs

Novosibirsky ice massif is comprised from broken fast ice first-year floes of local formation. In some years inclusions of multiyear ice are observed in ice massif. In June-August ice massifs block eastern approaches to Sannikov and Dm. Laptev Straights. In most cases ice massif ultimately melts away during September (Fig. 2.6.17, Table 2.6.8). In separate years Novosibirsky ice massif can join with Ayonsky and stay till the end of melting period.

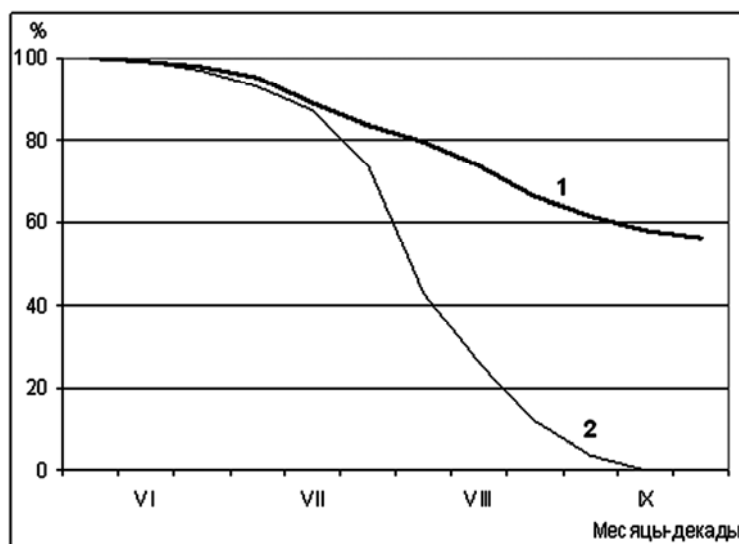


Fig. 2.6.17. Area changes of Ayonsky (1) and Novosibirsky (2) ice massifs (probability 50%) in June-September, %

The Ayonsky ice massif is the largest spur massif in the Arctic Seas. It is located in the eastern East Siberian Sea. Depending on its location (western, central or eastern), the massif blocks the central sea areas or Long Strait from the west. It is comprised due to local first-year ice of different age and multiyear ice, transporting from Arctic basin. Massif is characterized by high ice capacity and low decay in summer. Normally about 50% of ice massif doesn't melt till the end of ice formation start (Fig. 2.6.17).

Ayonsky ice massif almost never disappears, but Novosibirsky ice massif is less stable and can disappear in any of 10-day periods, beginning from third 10-day period of July (Table 2.6.8).

Таблица 2.6.8 – Число случаев полного исчезновения ледяных массивов Восточно-Сибирского моря за период 1973-2007 гг., %

Массивы	Июль			Август			Сентябрь		
	Декады								
	1	2	3	1	2	3	1	2	3
Новосибирский	-	-	3	3	13	29	39	52	52
Айонский	-	-	-	-	3	3	3	-	-

*Grounded hummocks.* Grounded hummocks are formed in fast ice zone, and sometimes out of its limits (Fig. 2.6.18). Rather often grounded hummocks reach giant sizes and are seen in entire fast ice sea zone on depth up to 20 m (sometimes up to 30 m).

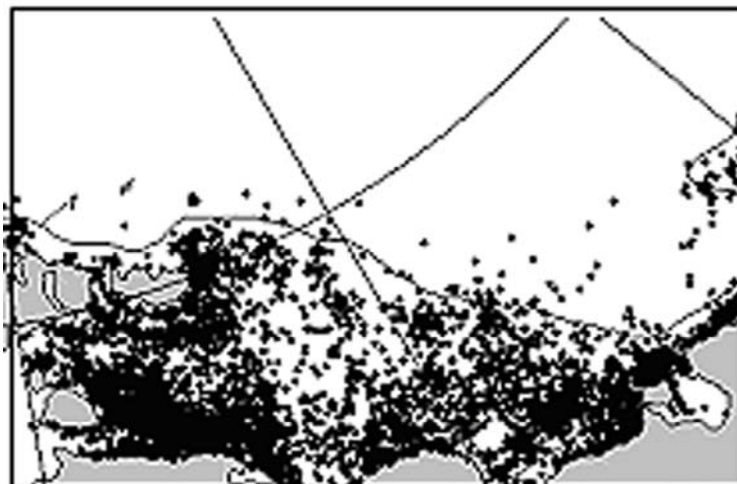


Fig. 2.6.18. Location of grounded hummocks in late winter from data for 1962-1995

*Icebergs.* Small icebergs and ice islands are sometimes observed in sea. Insignificant quantity of small icebergs comes down in sea from Genrietta and Benetta Islands, and also can be transported from other regions.

## 2.7. Characteristic of the Chukchi Sea ice conditions

### 2.7.1. Physical-geographical sea characteristic

*Depth, borders.* The Chukchi Sea is located between the two continents: Asia and America. It has a northern boundary with the East-Siberian Sea, in the most extreme north-east – with the Beaufort Sea, in south through Bering Strait it is connected with the Bering Sea. In the north, the sea has an open boundary with Arctic Basin. It conventionally comes along the edge of continental shelf between meridian  $180^\circ$  in the west and Cape Barrow meridian in the east (Fig. 2.7.1).



Fig. 2.7.1. Geographical location of the Chukchi Sea

Western sea border comes from crossing point of meridian  $180^\circ$  with northern coast of Wrangel Island, along its northern, eastern and southern coasts to Cape Blossom, then it comes along conventional line to Cape Yakan, further - along Chukchi Peninsula coast to Bering Strait. Eastern border comes along meridian of Cape Barrow, further - along Alaska coast to Bering Strait. The Sea border in Bering Strait comes between Capes Dezhnev and Prince of Wales.

Dominant depth in the Chukchi Sea reaches 50 m. Shoal Gerald with depth of 20-30 m is located in the northern sea region (on latitude of Wrangel Island). Between shoal and Gerald Island shelf is crossed by Gerald trough (depth up to 90 m). In the north-eastern Chukchi Sea Barrow trough is located on a depth of more than 50 m, approaching to Cape Franklin.

During all observational history AARI provided ice-hydrologic observations not in entire water basin, but within sea borders, limited from the north by  $73^\circ$  N and from the east by meridian of Cape Lisburn. These boundaries are located along the line  $73^\circ$  N  $180^\circ$  –  $73^\circ$  N  $166^\circ$

W in the north, then southwards to Cape Lisbern – along coast to Cape Hop – then to Cape Espenberg, and further to Bering Strait (Fig. 2.7.2).

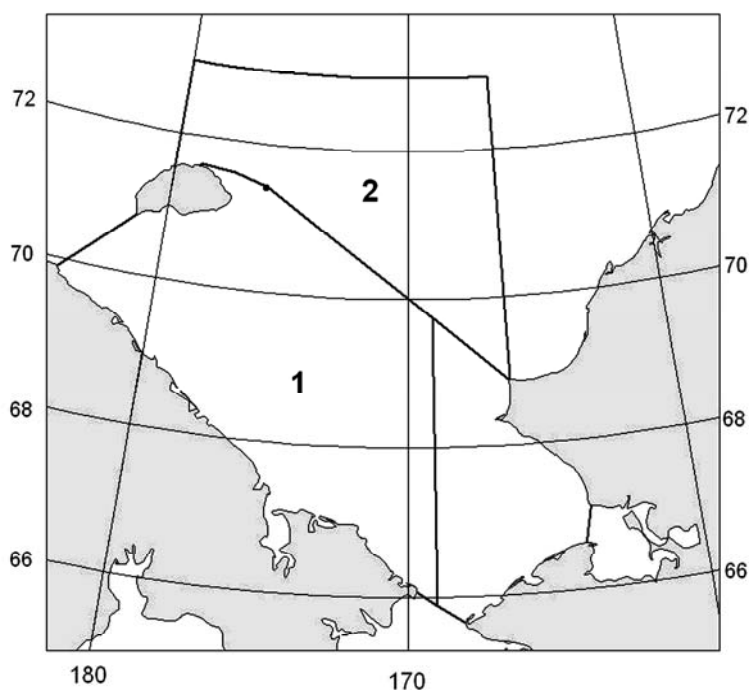


Fig. 2.7.2. Borders and regions of the Chukchi Sea. 1 – south-western region, 2 – northern region;

Northwards from Wrangel Island border with the East-Siberian Sea comes along the line  $73^{\circ}$  N – by  $180^{\circ}$  meridian to island coast. Two sea regions are separated in borders, accepted by AARI: south-western and northern. Area of south-western sea region is  $176000 \text{ km}^2$ , northern sea region –  $132000 \text{ km}^2$  (Fig. 2.7.2). Routes of the eastern Northern Sea Route come through south-western sea regions.

*Climate.* The Chukchi Sea climate is caused both by its high latitude location and influence of two oceans – Arctic and Pacific, and two continents – Asia and America. Solar radiation is essential for the Chukchi Sea climate, but baric-circulation regime plays the most significant role. It is determined by interaction of three atmosphere centers: Arctic anticyclone (which is replaced by depression in summer) and Aleut depression.

Dominance of air fluxes of eastern direction over the Chukchi Sea is determined by seasonal changes of atmosphere circulation over the Pacific sector of the Arctic. In autumn and winter eastern fluxes have northern component. In June-July south-western fluxes are observed over the sea, and in the area of Bering Strait – southern.

Negative air temperatures are observed over the Chukchi Sea during most of the year. Period with positive temperatures lasts from 4 months in the area of Bering Strait to 1 month in the northern sea region. In winter average monthly air temperature changes from  $-18 \div -22^{\circ}\text{C}$  in the Bering Strait area and to  $-26 \div -28^{\circ}\text{C}$  in its northern region.

In spring (April-May) air temperature rapidly increases from  $-8\div-18^{\circ}\text{C}$  in April to  $-2\div-8^{\circ}\text{C}$  in May.

Average air temperature in July-August changes from  $3-4^{\circ}\text{C}$  in the southern sea region to  $0\div-1^{\circ}\text{C}$  in the northern sea periphery. In October sea is rapidly cooling, and in its northern region average temperature reaches  $-10\div-12^{\circ}\text{C}$ .

The lowest temperatures, ever observed in winter, are equal to  $-40\div-45^{\circ}\text{C}$ . The highest air temperatures in coastal zone and in Bering Strait reach  $28-30^{\circ}\text{C}$ , in open sea they are less than  $15-20^{\circ}\text{C}$ .

Pacific waters are transported by the Bering current through Bering Strait to the Chukchi Sea. Further they propagate by three branches: Alaska, Gerald and Long. Role of these waters is significant in hydrologic and ice regimes. Heat content of the warm Pacific waters is enough for complete ice melting in approximately half of the sea area. Coastal Chukchi current is located near Asian coast zone, coming through Long Strait from the East-Siberian Sea south-eastwards. Sea ice is transported by this current from the Chukchi Sea to the Bering Sea through western part of Bering Strait (Fig.2.7.3).

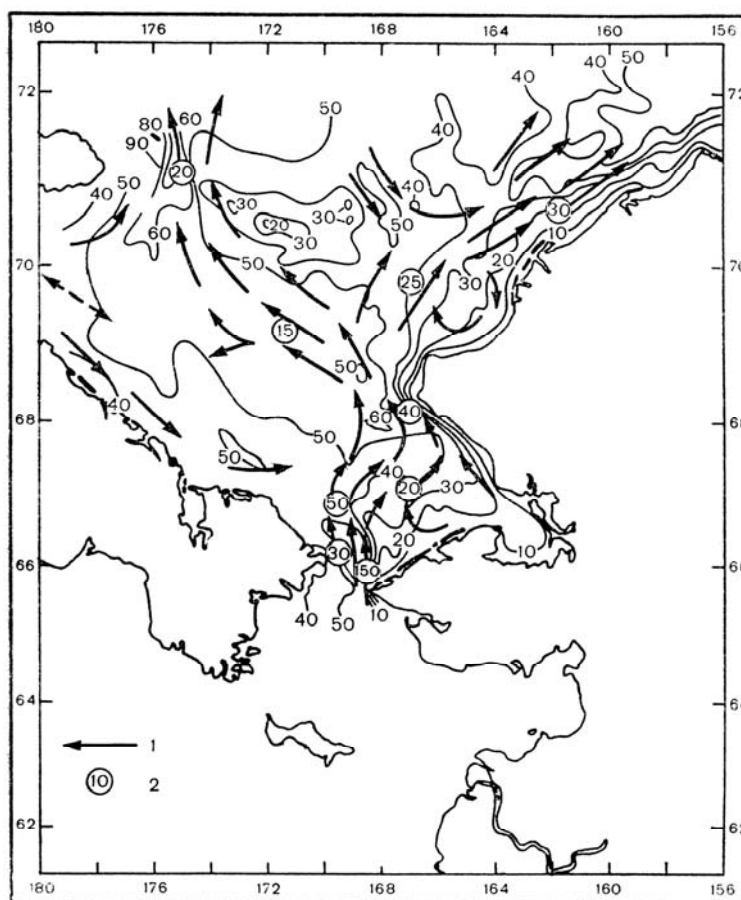


Fig. 2.7.3. Scheme of surface currents in the Chukchi Sea. 1 – currents, 2 – velocity in cm/s.  
Depth in m.



### 2.7.2. Sea ice characteristic in period of its growth

The Chukchi Sea has the most southern location among the Arctic Seas, nevertheless, from November to May it is completely covered with ice. Ice regime of the Chukchi Sea is formed, from one hand, under influence of the Arctic Basin due to open border, and from the other hand, under influence of advection of rather warm Bering Sea water, coming through Bering Strait.

South-western region of the Chukchi Sea is separated by ice conditions peculiarities (Fig. 2.7.2). In this region melting starts earlier than in other Siberian Arctic shelf seas under influence of Gerald and Long branches of Bering current.

*Ice formation.* Stable ice formation starts in the mid-September on its northern and north-western boundaries among compact (9-10/10-th) ice. Then it propagates southwards to zone of open and very open ice (4-6/10-th and 1-3/10-th), and then ice formation continues in open water. In coastal sea parts and in Long Straight ice formation on average starts on 5-10<sup>th</sup> of October. Large heat content of the sea, formed during summer and supplied by inflow of the Bering Sea waters, restrain cooling processes in the central and southern sea regions, and on average, the sea freezes completely only in mid-November. Direction of the Bering Sea current meanders form typical for this sea bend of isochrones of stable freeze-up terms (Fig. 2.7.4).

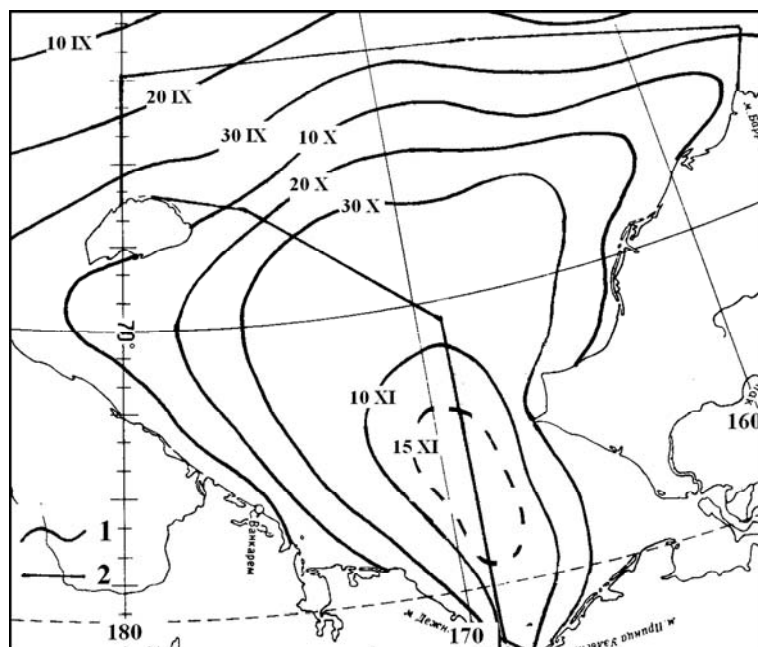


Fig. 2.7.4. Isochrones of average terms of stable ice formation in the Chukchi Sea.

*Ice growth.* In the Chukchi Sea ice forms slower than in other Arctic Seas as a result of later freeze up. In February, when in other seas thick first-year ice prevails (more than 120 cm), less than a half of south-western sea region is occupied by medium first-year ice (70-120 cm) (Table 2.7.1).

Table 2.7.1 – Composition of ice age in the Chukchi Sea regions in autumn-winter period, (% from region area)

No ice			Ice age														
			Young			Thin first-year			Medium first-year			Thick first-year			Second-year, multiyear		
X	II	V	X	II	V	X	II	V	X	II	V	X	II	V	X	II	V
63	0	0	24	3	2	5	5	1	0	45	8	0	35	73	8	12	16

Second-year and multiyear ice is transported to northern sea region from the Arctic Basin. This ice occupies on average 20% of sea in the end of ice growth period, the same area is occupied by thin first-year and medium ice, located mostly behind fast ice along Alaska coast. About 60% of sea basin is normally occupied by thick first-year ice (Fig. 2.7.5).

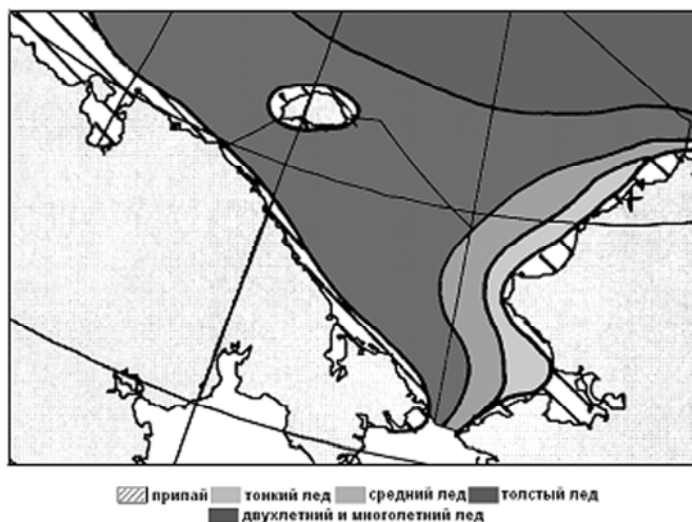


Fig. 2.7.5. Average propagation of different ice age in the Chukchi Sea in ice growth period

*Fast ice.* Interannual changes of terms of stable fast ice formation in coastal zones of the southwestern Chukchi Sea are 7-10 weeks (Table 2.7.2). At that, the biggest probability of fast ice formation on largest part of coast from Cape Yakan to Cape Heart Stone is less than 20-30% (as a rule in the first 10-day period of November). In most extreme eastern coast fast ice formation starts two 10-day periods later, and most often fast ice is formed in third 10-day period of November with probability 56% (Table 2.7.2).

Such variability of terms is caused by interannual changes of terms of stable ice formation in the Chukchi Sea. As it is shown on Fig. 2.7.6, multiyear range of terms of stable ice formation along coast in south-western sea region is more than two months.

Table 2.7.2 – Probability of stable fast ice formation terms in coastal regions of the south-western Chukchi Sea from the satellite data for 10-day periods 1980-2007, %

Coast regions	October			November			December			January
	10-day periods									
	1	2	3	1	2	3	1	2	3	1
C. Yakan – C. Vankarem	11	15	11	31	14	9	10	0	0	0
C. Vankarem – C. Heart Stone	9	9	9	20	13	6	20	5	5	3
C. Heart Stone - C. Dezhnev	0	0	6	7	15	56	7	3	3	3

They mostly occur in the first 10-day period of October, and the largest frequency of occurrence of terms of fast ice establishment is observed in a month (Fig. 2.7.6).

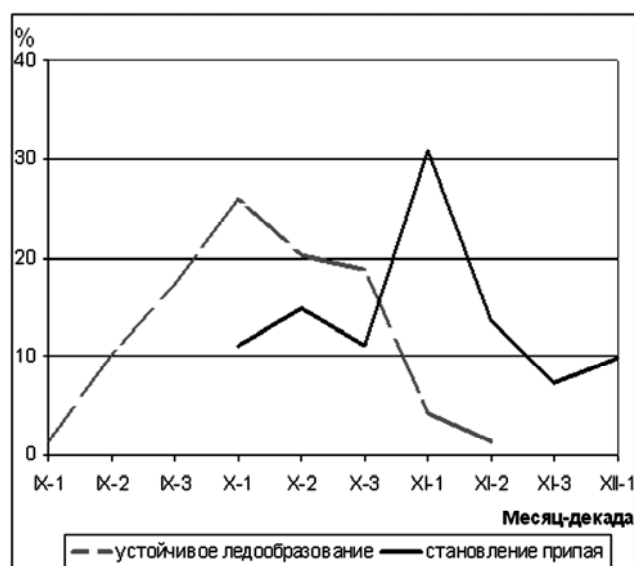


Fig. 2.7.6. Frequency of occurrence of terms of stable ice and fast ice formation in zone Cape Yakan - Cape Vancarem, %

From Table 2.7.2 it is known, that fast ice establishes along Chukchi coast in November more often, than in other autumn-winter months (Table 2.7.3).

Table 2.7.3 – Probability of stable fast ice formation terms in coastal regions of the south-western Chukchi Sea from the satellite data in autumn-winter months for 1980-2007, %

Coast regions	Months			
	X	XI	XII	I
C. Yakan – C. Vankarem	37	53	10	0
C. Vankarem – C. Heart Stone	28	39	30	3
C. Heart Stone - C. Dezhnev	6	78	13	3

Fast ice is less developed in the Chukchi Sea because of deep water coastal zone (Fig. 2.7.7). Maximum fast ice development is observed in March-April. Its width along south-western sea coast changes within 10-30 km. Long-term range of fast ice width changes within 5-70 km.

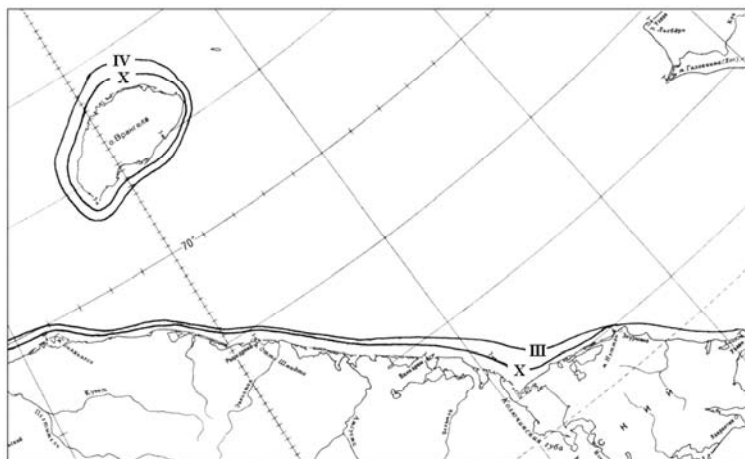


Fig. 2.7.7. Average location of fast ice boundaries in period of its growth in the Chukchi Sea

The fast ice area near the Chukchi coast after achieving about 7 thousand km<sup>2</sup> in early November slowly increases to about 11 thousand km<sup>2</sup> in March, preserving this size until the beginning of melting. In the years favorable for the fast ice development, its area is more than twice greater than the average value (Table 2.7.4).

Table 2.7.4 – Average and maximum areas of fast ice in period of its growth in the south-western Chukchi Sea in the middle of month from satellite data for 1980-2007, km<sup>2</sup>

Area	Months							
	X	XI	XII	I	II	III	IV	V
Average	5,7	7,3	7,6	9,8	10,6	10,9	10,9	10,9
Maximum	8,8	14,3	15,5	17,2	18,7	23,4	23,4	23,4
Minimum	2,3	2,5	2	4,7	5,1	5,1	5,1	5,1

The average area of the Chukchi fast ice at the end of its development comprises 6% of the southwestern sea area. It can occupy 13% and only 3% of the sea area in the years of its maximum and minimum development, respectively.

Fast ice around Wrangel Island is more developed compared to that along the Chukchi coast. Its maximum development is achieved in the second 10-day period of April. Its average width comprises 23 km near the northwest coast (changing within 10–110 km), 33 km – near the northern coast (20–55 km) and 13 km – along the southern coast of the island (7–22 km).

Mean multiyear area of fast ice around Wrangel Island during the maximum development is equal to 9.0 thousand km<sup>2</sup>, which comprises 5% of the area of the southwestern Chukchi Sea and can achieve 14% in extreme years.

Near the Alaskan coast, between the Cape Hope and Cape Barrow, the fast ice formation begins in the middle of October, on average. In the third 10-day period of October, it spreads to the regions adjoining Kotsebu Bay and Bering Strait. By the time of its maximum development, the fast ice width along the section from Bering Strait to Cape Lisbern can comprise 5 to 65 km, and farther northward to Cape Barrow – 10–40 km.

*Flaw polynyas.* Eastern Chukchotskaya polynya is episodically formed behind fast ice along the Chukchi Sea coast (with frequency of occurrence less than 50%). This mostly narrow and long polynya is also called the Chukchi flaw lead. Lead rapidly closes, when western winds become northern. Its average frequency of occurrence is less than 30% (Table 2.7.5). The lead is the most stable in the second half of June. Its frequency of occurrence in June reaches 60% (Table 2.7.6). In the years of active shipping along the NSR, the flaw lead was used for early routing of the ship convoys to Pevek and Kolyma.

Table 2.7.5 – Average frequency of occurrence (P, %) and characteristic of the Chukchi Sea flaw polynyas from satellite data for the period 1980-2005.

Polynya name	P, %	Characteristic					
		Length, km		Width, km		Area, km <sup>2</sup>	
		average	range	average	range	average	range
Eastern Chukchi (flaw polynya)	29	350	9-780	22	1-126	9,3	0,4-98,3
Chukchi lead	76	485	50-1040	24	4-52	13,9	1,0-45,6

In the eastern Chukchi Sea near the Alaskan coast, a stationary polynya is formed that was called the Chukchi lead (frequency of occurrence more than 75%). The stability of this polynya slightly decreases in January (to 50%), when the frequency of occurrence of the easterly winds decreases. In April–May, its frequency of occurrence is greater than 80% (Table 2.7.6), and it often serves as an initial ice-clearance source in the Chukchi Sea.

Table 2.7.6 – Average frequency of occurrence of the Chukchi Sea flaw polynyas from satellite data for the period 1979-2005, %

Polynya name	Months							
	XI	XII	I	II	III	IV	V	VI
Eastern Chukchi (flaw polynya)	24	23	19	28	26	18	38	61
Chukchi lead	-	76	50	79	72	86	85	-

In winter south-western and south-eastern ice drifts prevail in the Chukchi Sea, when large ice floes (length up to 5000-10000 m) are transported from the Arctic Basin to northern sea regions. In south-western sea region ice floes with length 3000-5000 m and their pieces are sometimes observed.

The most ridged ice is observed in south-western sea region in winter period, its ridging is 3 marks. In coastal zone near Chukchi coast ridging can exceed 5 marks.

*Grounded hummocks.* Underwater parts of the largest hummocks and ridges reach sea bottom and become stamukhas, which are mainly distributed in the fast ice of the southwestern part of the sea (Fig. 2.7.8).



Fig. 2.7.8. Location of grounded hummocks in the south-western Chukchi Sea in the end of winter from data for 1962-1995

### 2.7.3. Sea ice characteristic in period of its melting

*Melting and sea clearing from ice.* Sea clearing from ice starts from regions, adjoining to Bering Strait. Warm current from the Bering Sea facilitate this process, and about 10% of ice in south-western sea region disappears to late May. Alaska polynya is a place of active sea clearing (Chukchi lead). Its area significantly increases under influence of eastern and south-western winds (Fig. 2.7.9, 2.7.10).

Fast ice breaks up in the eastern part of Chukchi Sea coast in May in some years, but from data of polar station Uelen it is known, that fast ice breaks up here more often in third 10-day period of June (Fig. 2.7.9). “Break up wave” sequentially propagates to western coast. Fast ice breaks up most often in first and second 10-day periods of June, but process of ultimate fast ice break up can be delayed till early August (Fig. 2.7.9).

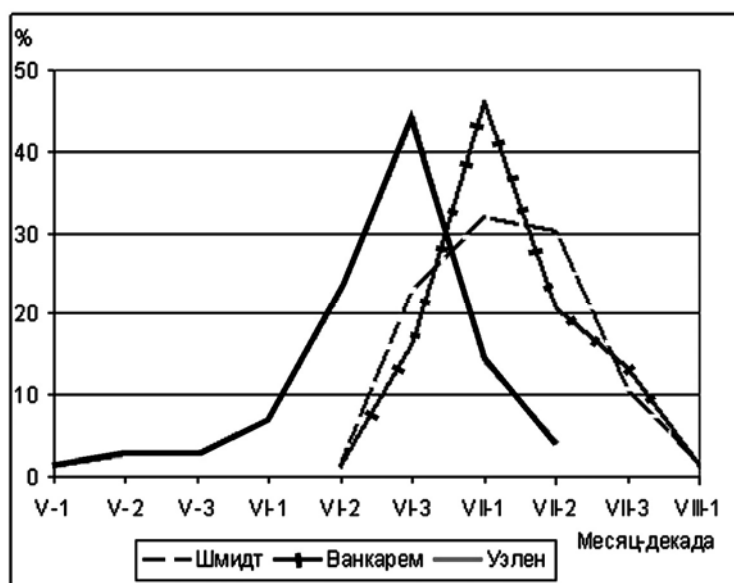


Fig. 2.7.9. Frequency of occurrence of terms of fast ice break up in zones of polar stations in the Chukchi Sea coast

According to polar stations data, fast ice ultimately breaks up in central and western parts of Chukchi Sea coast in July in 81% and 73% of cases, respectively. Near eastern coast in 74% of cases fast ice melts in June (Table 2.7.7).

Table 2.7.7 – Average terms of frequency of occurrence of fast ice break up in the south-western Chukchi in zones of polar stations

Polar stations	Months			
	V	VI	VII	VIII
Schmidt		25	73	2
Vancarem		17	81	1
Uelen	7	74	18	

During melting sea clears from ice on average from Alaska coast north-westwards (Table 2.7.7, Fig. 2.7.10). Sea clears from ice in June and July the most intensively, to late July about 60% of sea basin and its south-western region is free from ice.

Table 2.7.8 – Area of the Kara Sea ice-free regions in the melting period, %

Sea regions	June			July			August			September		
	Decades											
	1	2	3	1	2	3	1	2	3	1	2	3
South-west	11	19	29	39	50	60	68	74	78	83	85	86
All seas	12	20	30	40	48	56	64	69	77	81	82	84

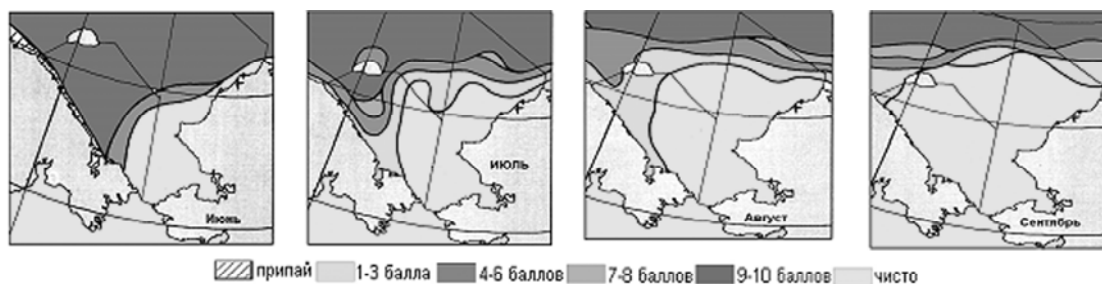


Fig. 2.7.10. Propagation of ice with different concentration in June-September (probability 50%)

When sea is clearing from ice, ice edge moves northwards and north-westwards, in direction of Bering warm water propagation (Fig. 2.7.11). More than 80% of sea basin is ice-free to late September under average conditions (Table 2.7.8).

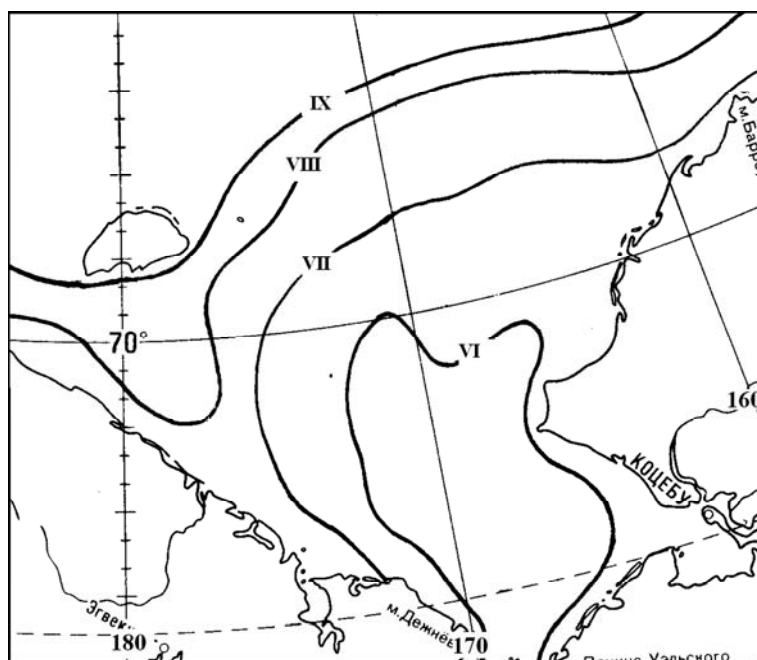


Fig. 2.7.11. Average location of ice edge in the Chukchi Sea in June-September

*Ice massifs.* During process of ice cover melting compact ice (7-10-th) of the Chukchi Sea is located into two ice massifs – the Wranglevsky and Northern Chukchi (Fig. 2.7.12). Gerald branch of Bering current separates the Wranglevsky ice massif, located in south-western sea region, from the Northern Chukchi massif, located in northern sea region. The Wranglevsky massif consists from local first-year ice, but sometimes it includes transported multiyear ice. The Wranglevsky ice massif blocks the eastern approaches to Long Strait in summer months, complicating navigation in June-July. In average years the Wranglevsky massif occupies only about 25% of south-western sea area to late July, and to September its area decreases to 6% (Fig. 2.7.13). However, cases, when in August-September



massif was filled by ice from the eastern East-Siberian Sea, are not rare. Ice is propagated through Long Strait to the east along Chukchi Sea coast and it leads to significant navigational difficulties.

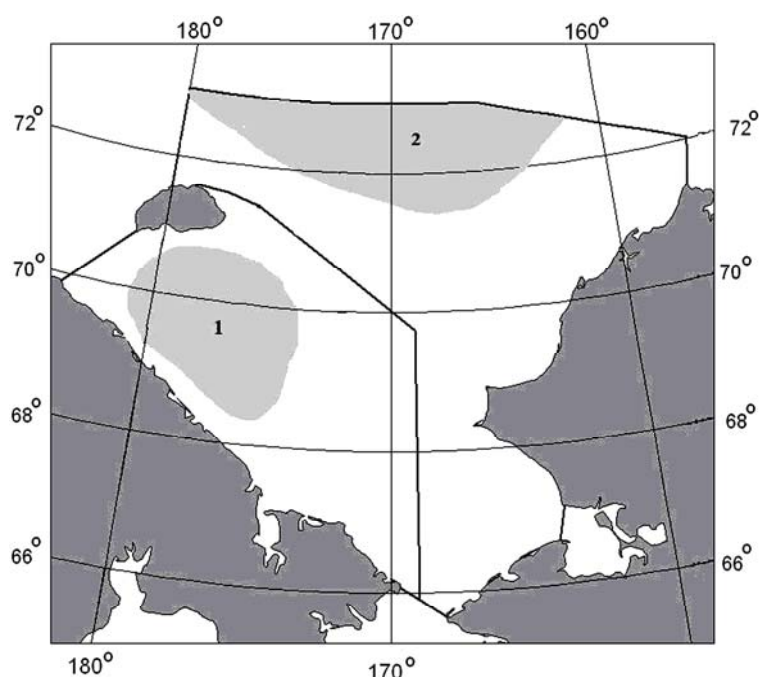


Fig. 2.7.12. Scheme of ice massifs location in the Chukchi Sea. 1 – Wranglevsky and 2 – Northern Chukchi

The Northern Chukchi ice massif is a spur oceanic massif of Arctic basin. Multiyear ice comprises significant part of massif. During summer ice of the Northern Chukchi massif partly melts away and partly is transported out of sea limits. On average about 15% of massif area remained within sea limits before freeze up (Fig. 2.7.13).

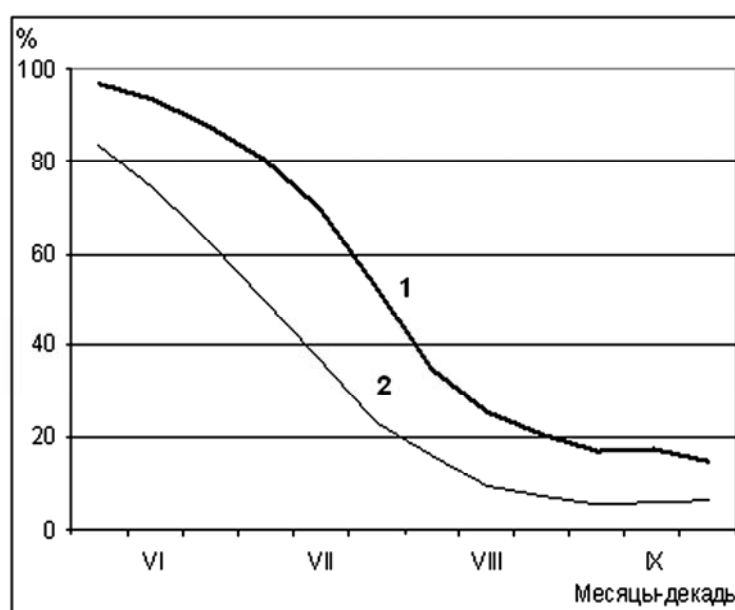


Fig. 2.7.13. Area changes of Wranglevsky (1) and Northern Chukchi (2) ice massifs in June-September, %

During all observations, the Wranglevsky ice massif ultimately disappeared in more than 50% of cases, and in most cases, 36%, occurred in August. Chukchi ice massif is more persistent, in 57% of cases it remained to the end of melting period (Table 2.7.9).

Table 2.7.9 – Number of cases of ice massif disappearance in the Chukchi Sea for 1939-2007, %

Ice massif	Months		
	VII	VIII	IX
Wranglevsky	1	36	16
Northern Chukchi	-	23	20

*Icebergs.* From time to time insignificant amount of small icebergs come from the Beaufort Sea to northern sea regions and to Wrangel Island zone.

## 2.8. Characteristics of ice conditions in the Beaufort Sea

### 2.8.1. General aspects

The Beaufort Sea is distinguished by the most severe ice conditions in entire Arctic. Sea is characterized by rather narrow shelf region. Sharp drop of depth occurs immediately after 100-meter isobath, which is located in 20-40 miles from coasts of Cape Barrow - Herschel Island and increases eastwards up to 60–65 miles north-eastwards from Cape Bathurst. Spur of oceanic multiyear ice massif (from Arctic pack ice) is located in the northern sea. This massif can be dangerous for navigation during most part of the year and in severe years doesn't move from coast. Sea ice drifts clockwise, being saved in this rotation for several years, and only part of it is transported to the west. The most favorable time for navigation is on average period from middle of August to middle of September. Earlier and later navigation can take high risks.

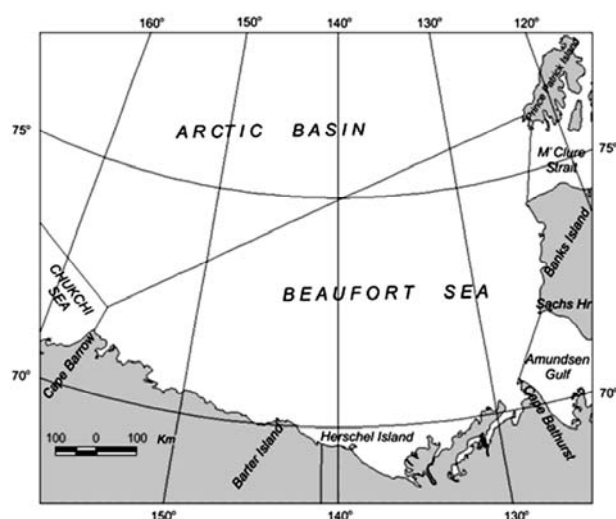


Fig. 2.8.1. The Beaufort Sea borders.

The Beaufort Sea has an open boundary with the Arctic basin in the north and with the Chukchi Sea in the west. In the east its boundary comes by capes and islands Prince Patrick and Banks coast and adjoins continent near Cape Bathurst. Southwards sea coast extends from Cape Bathurst in the east to Cape Barrow in the west (Fig. 2.8.1). Sea area is 480 000 km<sup>2</sup> in accepted sea boundaries.

### 2.8.2. Period of ice cover growth

#### 2.8.2.1 Ice formation and young ice formation

The Beaufort Sea is covered with ice at least nine months a year. Sea freeze-up depends on propagation and location of southern multiyear ice boundary (polar pack ice) in late summer, because new ice formation occurs earlier in ice channels and fractures among multiyear ice of Arctic basin, and then propagates southwards.

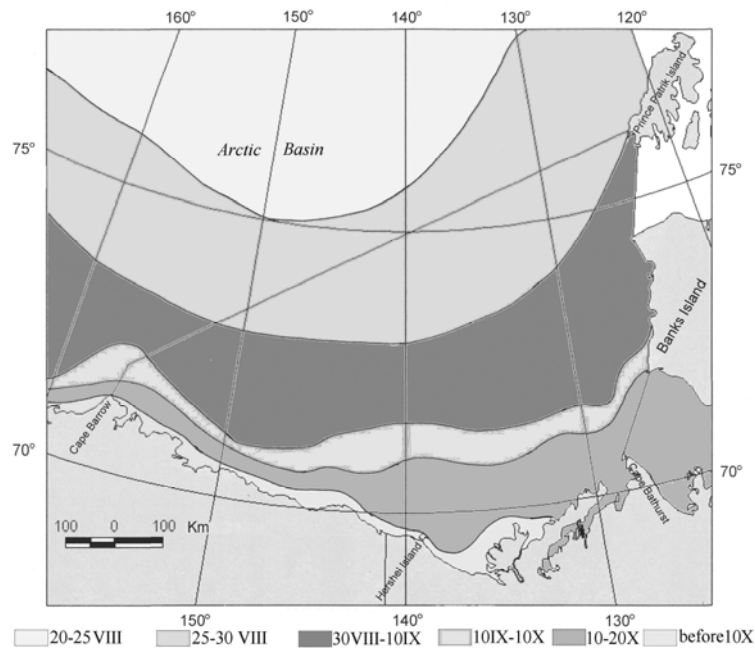


Fig. 2.8.2. Average terms of stable ice formation in the Beaufort Sea regions.

From data of Canadian ice atlas, processes of ice formation starts simultaneously in large zones, located in latitudinal direction (Fig. 2.8.2). In period of August, 20-25<sup>th</sup> initial ice appears in Arctic near northern sea boundary. During next five days ice formation propagates to the northern sea regions. By 10<sup>th</sup> of September young ice is formed in central sea region (Fig. 2.8.2). Then processes of ice formation are getting slower, and rather narrow zone with width about 30-40 miles freezes approximately by 10<sup>th</sup> of October. At the same time, coastal zone of the southern Beaufort Sea between Cape Barrow and Tuktoyaktuk Peninsula freezes up by 10<sup>th</sup> of October (Fig. 2.8.2).

Deep water area between multiyear (pack) ice massif and coastal zone freezes later – on 10–20<sup>th</sup> of October (Fig.2.8.2). Obviously, it can be explained by some heat storage in deep water sea region. In summer warm Bering waters are located along western and northern Alaska coasts, at the same time warmed up waters of Mackenzie river are propagated to the sea north-westwards and north-eastwards by two branches. Water heat storage is formed in deep water region under effect of advection and summer warming up, making slower processes of autumn water cooling in this region. In some years (1958) surface temperature of water in this region reached 5–9°.

In coastal shallow zones near Tuktoyaktuk Peninsula and further eastwards to Gulf of Amundsen ice formation normally starts in the second week of October.

Terms of stable freeze up change from year to year in coastal zones and in zones of drift ice, depending on amount of ice, survived summer melting, its location, water heat storage and terms of autumn cooling. From data before 1974, terms variability of stable freeze up changed within the

range of two months along coast between Capes Barrow and Bathurst (Table 2.8.1).

Table 2.8.1 – Terms of stable ice formation in coastal regions of the Beaufort Sea

Region	Terms of stable ice formation		
	Average	Early	Late
Cape Barrow	20 IX	3 IX	28 X
Barter Island	20 IX	3 IX	28 X
Mackenzie delta	1 X	3 IX	28 X
Cape Bathurst	1 X	3 IX	28 X

#### 2.8.2.2 Propagation and formation of fast ice

Terms of formation and area of fast ice are determined by ice charts of National Ice Centre of the USA (USA NIC) for 1972–2004. Charts are located in Global Digital Sea Ice Data Bank (GDSIDB) by Navy project. According to this data fast ice formation in the Beaufort Sea most often occurs in October. In October 82% of all cases are observed, but at that 44% of cases are observed in the second ten-day period of October. However, there are some cases of early – in September, and late – in early November fast ice formation (Fig. 2.8.3). Early and late terms of fast ice formation are observed after heavy or soft ice conditions previous summer, respectively.

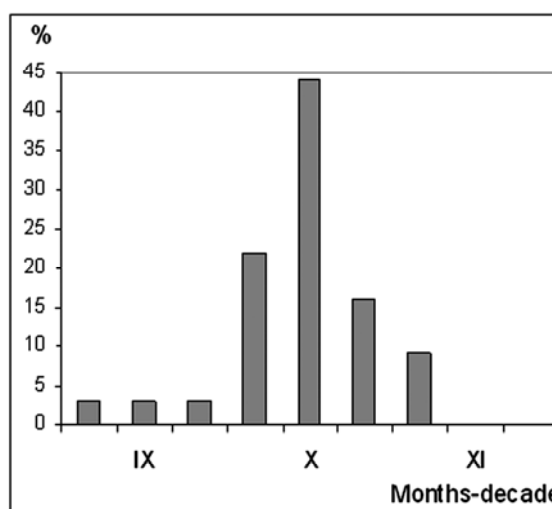


Fig. 2.8.3. Probability of terms of fast ice formation in the Beaufort Sea, %.

Fast ice is normally formed, at first, in zone of Cape Barrow – is. Barter, that occurs in middle of September, then it propagates to the western sea regions (Table 2.8.2).

Table 2.8.2 – Terms of fast ice development at stations of the Beaufort Sea

Station	Fast ice development		
	Average	Early	Late
Cape Barrow	14 X	27 IX	10 XI
m. Barter	16 X	27 IX	3 XI
Mackenzie delta	19 X	3 X	3 XI
Cape Bathurst	31 X	10 X	16 XI

As a result of data processing by USA NIC, data about fast ice area for every decade of its growth and melting for 1972–2004 was received. As it is seen from analyze, fast ice growth on average occurs before April, in severe winters – before May (Fig. 2.8.4). In moderate winters fast ice occupies about 15% of sea area, in severe winters – 25%. In mild winters fast ice area is less than 8% of sea area.

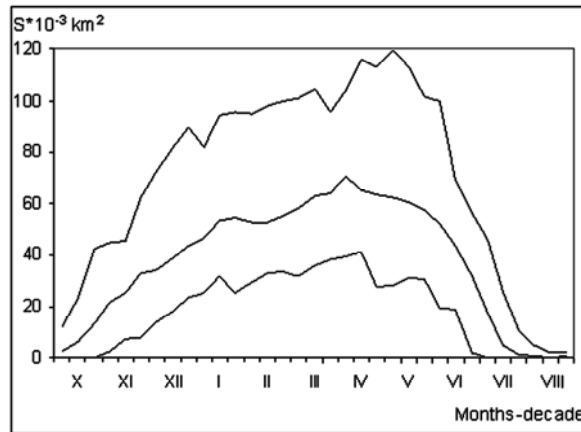


Fig. 2.8.4. Annual mean (curve in centre), maximum (upper curve) and minimum (lower curve) fast ice area (S) in the Beaufort Sea for 1972–2005.

Fast ice is rather level near coast, but it normally includes hummocks. Its amount increases closer to outer boundary.

Fast ice zone usually propagates to 50-60 km from coast within limits of 20-meter isobath. However, as it is seen from data of USA NIC, in 1972–2004 some years were marked, when fast ice width exceeded average value almost two times. It can be seen from Fig. 2.8.5, where probability of fast ice propagation in April is presented. As listed, in this month fast ice normally reaches its seasonal distribution maximum.

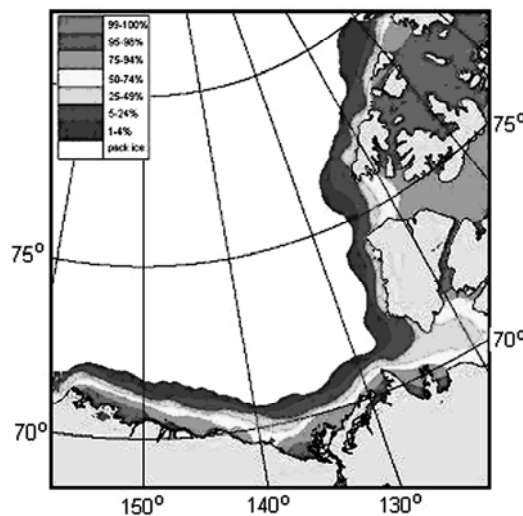


Fig. 2.8.5. Probability of fast ice propagation in the Beaufort Sea, %

Fast ice in the Beaufort Sea significantly differs from fast ice in other Arctic Seas. Its large part includes hummocks ridges, because anticyclonic ice rotation in the eastern Arctic basin and in the Beaufort Sea is mostly accompanied by northern winds, which press drift ice to fast ice zone between Capes Barrow and Parry. Offshore ice drift facilitates fast ice growth along coast line.

In coastal zone on depth up to 2 m fast ice freezes up to bottom. The other part is floating. Propagating from coast, fast ice is held by hummock ridges, settled on the ground on depth of 8–15 m. In late winter hummocks reach bottom on depth further than 20–meter isobath.

Ice rafting and ice piles on coast for distance from 20 to 50 m and sometimes to 100 m are observed during motion of fast ice. Hummocks are formed between fast ice zone and drift ice, settled on the ground on depth of 15–40 m.

Almost in all districts inclusions of multiyear ice are observed in fast ice, and in some years – pieces of small ice islands. During winter fast ice is quasistationary, but under activity of stormy winds, tidal phenomena and air temperature changes sporadic fast ice motion occurs. Near coast fast ice moves within limits of meters, but far from coast fast ice move off can approach tens of meters.

#### 2.8.2.3. Fast ice growth

Thickness of first-year fast ice during winter period increases up to 2 m. On Fig. 2.8.6 seasonal course of fast ice growth in stations of the Beaufort Sea, located in the west (Cape Barrow), in centre of northern Alaska coast (Barter Island) and in the eastern region (Sachs Harbor). Data is referred to 1955–1967, when relatively cold climate was observed in Arctic.

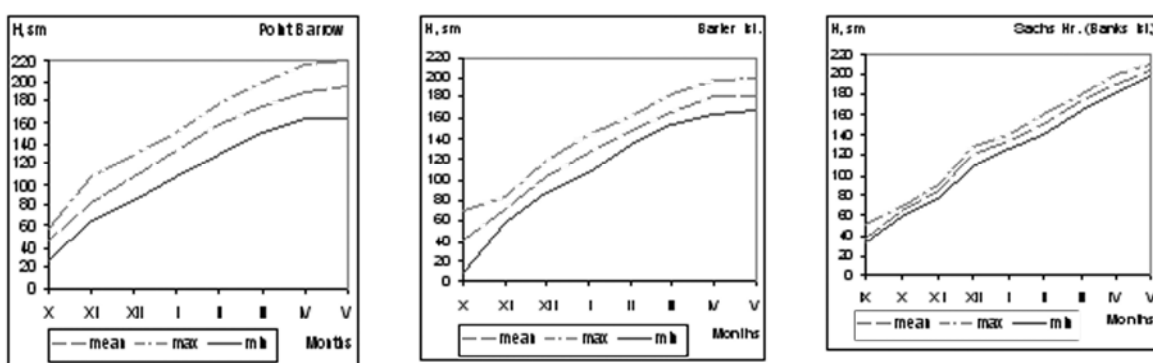


Fig. 2.8.6. Seasonal changes of average, maximum and minimum ice thickness at stations in the Beaufort Sea

As it is seen from Fig. 2.8.6, in coastal region level fast ice reaches age of thin first-year (30–70 cm) in October – early November, in December – medium first-year (70–120 cm), and during January – March ice thickness increases to its maximum values - age of thick first-year ice (more than 120 cm). Multiyear range of fast ice thickness in end of its growth period near

Cape Barrow is 30 cm, then it decreases to 12 cm eastwards from Barter Island, and near Banks Island coast – up to 10 cm.

#### 2.8.2.4. Flaw polynyas

In winter one constant polynya is formed in the Beaufort Sea - Cape Bathurst polynya. It is located between southern extremity of Banks Island and Cape Bathurst along western boundary of fast ice, blocking Gulf of Amundsen (Fig. 2.8.7).



Fig. 2.8.7. Location of Cape Bathurst polynya

Polynya is supplied by eastern and north-eastern winds. When wind transits to western - it closes, but when western winds weaken, it opens again. Like other Arctic polynyas in spring it is a place of heat accumulation and sea clearing from ice. In spring (usually in May), when temperature increases and winds transit to southern, polynya gets wider northwards along Banks Island and further to Prince Patrick Island, and also westwards.

Polynya on bar of river Mackenzie is developed in June, when ice starts melting. In some years its development coincides with Cape Bathurst polynya development. The largest development is observed during their confluence, which is often observed in late June – early July. During intensive confluence, polynyas are finally connected with Chukchi lead polynya in July – August, which propagates from Bering Strait along western coast of Alaska and can move further to Cape Barrow.

In winter and spring local flaw polynyas and open zones episodically occur along entire fast ice boundary. Terms of occurrence of these polynyas are 5-7 days.



### 2.8.2.5. Drift ice

Typical macroscale propagation of ice cover is established after fast ice formation in the Beaufort Sea. Rather dynamic zone is located behind fast ice with prevailing first-year ice. It is “transition” zone, adjoining to region of less movable multiyear ice, which is called Arctic Pack in some Canadian sources (Arctic Pack). Average multiyear location of these zones is shown on Fig. 2.8.8.

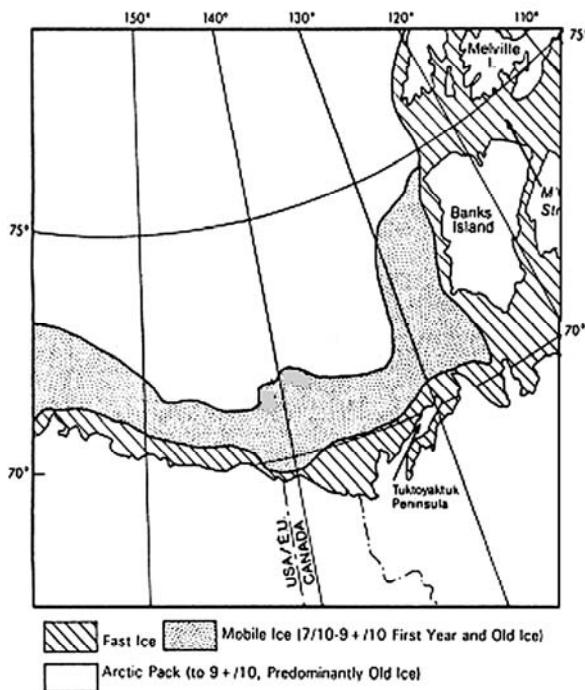


Fig. 2.8.8. Average ice propagation in winter in the Beaufort Sea

Multiyear ice in zone of Arctic pack reaches thickness of 450 cm, constantly moves with currents and winds in Arctic (mostly clockwise) and exists during the whole year (Fig. 2.8.9). Degree of its occurrence in the Beaufort Sea depends on wind regime during the year. On average Arctic pack boundary is located near Cape Prince Alfred (Banks Island), goes down to south-east, comes in 200 km from Hershel Island, then comes westwards in 200 km from northern coast of Alaska. Non-deformed multiyear ice with diameter about 500 m compose about 60% of this zone, some floes reach 10 km in diameter.

During winter sea ice drift is directed from east to west, according to Beaufort Gyre. However, when drift ice comes through eastern Arctic of cyclones and anticyclones, inclinations from general drift are observed. Interannual ice drift velocity is 1,4–4,8 km/day, diurnal speed changes within limits of 2,2–7,4 km/day, the highest speed, ever observed, was 32 km/day.

Ice in “transition” zone constantly moves. General drift direction in this part is - from east to west, similar to Arctic pack zone. Ice motion in zone is accompanied by ridging, channel formation and zones of open water, as a result of drift irregularity and short-term inclinations

from general direction of tidal phenomena.

The largest amount of ice in “transition” zone is observed in February – March. Ice thickness during its normal formation reaches its maximum in April – May, which is 0,9–2,0 m.

Multiyear ice can be observed among first-year ice. It is well defined by size and level hummock ridges. Multiyear ice exists in fast ice and in “transition” zones. Probability of multiyear ice occurrence in fast ice can exceed 15% in middle of winter (January), in drift ice behind fast ice amount of multiyear ice sequentially increases northwards, to boundary of multiyear Arctic pack. Probability of occurrence increases up to 50% (Fig. 2.8.10).

Topography research and research of drift ice depth immersion were made using sonar along section with length 1135 km northwards from the Beaufort Sea coast during middle of May – middle of July in 1991. Immersion depth of drift ice on the cut was 3–6 m. Height of first-year ice above the water level was within 1,5–2 m, multiyear – 2,5–4,5 m. The largest depth of hummocks keel reached 30 m. Several keels approached 32 m.

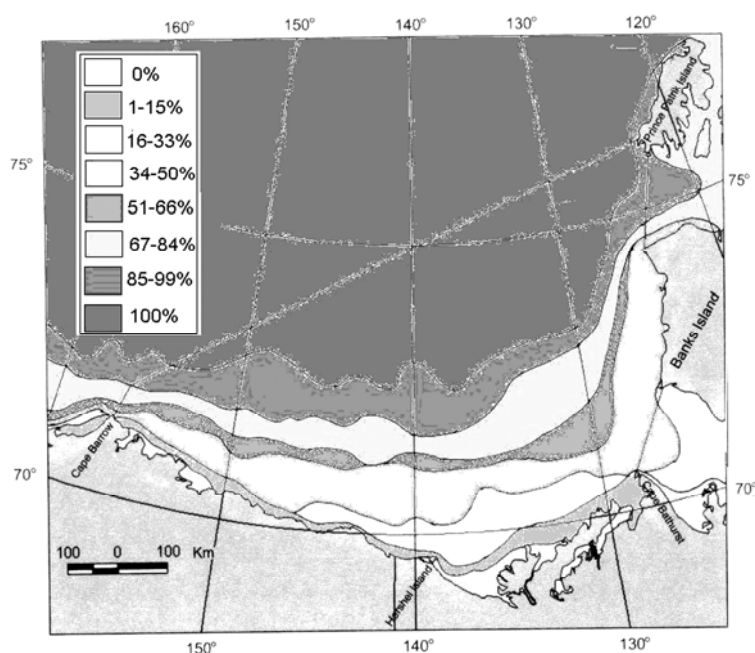


Fig. 2.8.10. Probability of multiyear ice occurrence in January from data for 1971–2000

### 2.8.3. Ice cover in melting period

#### 2.8.3.1 Ice melting and sea clearing from ice

Ice melting in the Beaufort Sea starts in late May – early June. Formation of puddles on ice is the first feature of melting beginning. Puddles are formed under activity of radiation heat in day time before stable air temperature transition through 0° to positive values. According to Table 2.8.3, composed from data and taking into account average ice thickness at Barrow station, ice

melting pattern can be made (Fig. 2.8.6).

Table 2.8.3 – Changes of ice thickness at Cape Barrow in melting period

Time period	Melting value, cm	Ice thickness, cm
1 <sup>st</sup> half of May	–	196
2 <sup>nd</sup> half of May	2	194
1 <sup>st</sup> half of June	3	191
2 <sup>nd</sup> half of June	13	178
1 <sup>st</sup> half of July	18	160
2 <sup>nd</sup> half of July	21	139
1 <sup>st</sup> half of August	24	115
2 <sup>nd</sup> half of August	27	88

As it is seen from Table 2.8.3, intensity of ice melting increases from June to August. In August ice thickness decreases on value, which is total for both June and July, and approaches 51 cm. Just by early September ice thickness decreases on more than 100 cm. Consequently, by this time all young ice disappears in the southern sea part (up to 30 cm), thin first-year ice (30–70 cm) and medium first-year ice (70–120 cm), that has reached thickness of 100 cm.

Ice intensively melts in zones, where polynyas are formed, which in spring accumulate heat from solar radiation. It is polynya of Cape Bathurst - in the eastern sea region, formed behind fast ice northwards the delta of the river Mackenzie. In western part development of large polynya along western coast of Alaska (Chukchi lead) facilitates ice melting and sea clearing from ice in May – early June. Chukchi lead often approaches Cape Barrow and comes further eastwards. On the early stage of ice melting, in June, about 10% of sea area is free from ice.

#### 2.8.3.2. Absolute melting of fast ice

Fast ice break up and decreasing of area partly occur in sea, when ice thickness and its strength decrease during melting. As it is seen from Fig. 2.8.4 (section 2.8.1.2), having reached its seasonal development maximum in April – early May, fast ice starts melting and on average in July disappears. If fast ice sequentially grew in sea during seven months, it would absolutely melt away – during 2,5 months.

According to results of data processing by USA NIC, the earliest terms of absolute fast ice break up occur in the first 10-day period of June, the latest – in the third 10-day period of July. About 80% of cases of absolute fast ice break up occur in July. At that, in the first 10-day period of July fast ice isn't observed in 40% of cases, in the second – 30% and in the third – 10%. In 20% of cases fast ice disappears in June (Fig. 2.8.11).

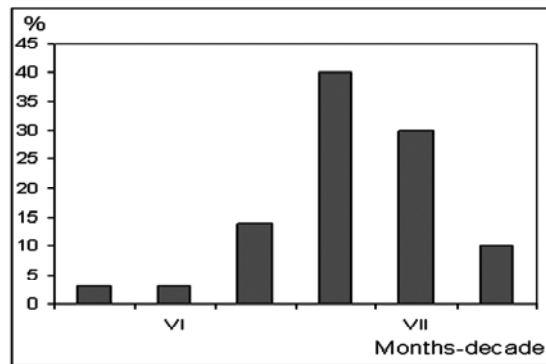


Fig. 2.8.11. Probability of terms of fast ice break up in the Beaufort Sea from data for 1972–2004

Long-term variability of terms of fast ice absolute melting is close to two months (Table 2.8.4).

Table 2.8.4 – Terms of fast ice break up in coastal regions of the Beaufort Sea

Regions	Date		
	Average	Early	Late
Point Barrow – Barter Island	7 VII	10 VI	27 VII
Barter Island – Cape Bathurst	8 VII	17 VI	22 VII

### 2.8.3.3 Sea ice in clearing period

Area of sea ice decreases on about 2% in late May, which is obviously connected with development of polynyas, where young ice hasn't already formed by this time. During June and July sea ice sequentially decreases on about 10% every month. Velocity of ice area reducing insignificantly increases in August – up to 14% and decreases in September to 7,5%. Sea ice area decreases for just about 40% during spring-summer period (Fig. 2.8.12). Ice, survived summer melting, can be observed in 60% of sea water area. Compact ice (7–10-th) composes its most part. This part occupies 40% of sea area, covered with ice, before autumn ice formation (Fig. 2.8.13).

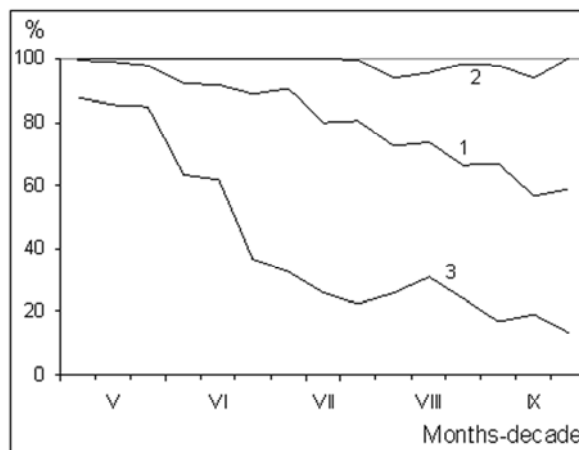


Fig. 2.8.12. Changes of average (1), maximum (2) and minimum (3) ice cover in the Beaufort Sea in spring-summer period, %

In years, unfavorable by hydro meteorological conditions, sea ice propagates to mostly entire sea water area, only about 6% is ice-free from late June to mid-September (Fig. 2.8.13). In contrary, in favorable years sea intensively clears from ice, and ice area reaches about 20% of sea area to late July. Ice melting slows down in August and September, and in late September it decreases up to 13% (Fig. 2.8.13).

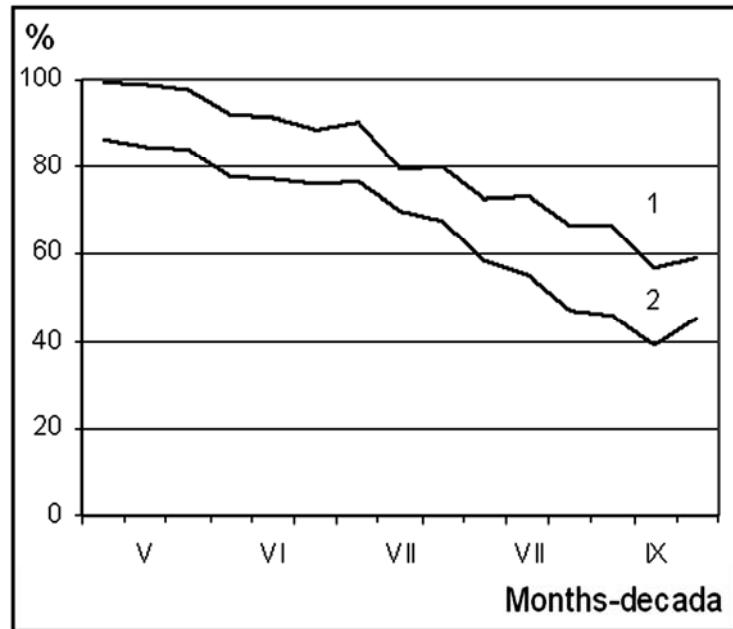


Fig. 2.8.13. Average seasonal changes of ice cover (1) and area of compact (2) ice in the Beaufort Sea

#### 2.8.3.4 Compact ice

During the entire year compact ice dominates in the Beaufort Sea. In Russian (Soviet) science researches ice accumulation with large concentration and thickness within sea boundaries was called ice massif. Massifs have their own names, connected with their location. Ice massifs include ice with compactness 7–10-th. They are the main barrier for navigation in ice. Weather forecasts and location of ice massifs are the most essential data in navigation supplement on the NSR. In Canadian and American studies there isn't any concept of ice massifs, and massif of compact ice in the Beaufort Sea, being mostly a spur oceanic ice massif, doesn't have any name. However, in some Russian sources compact ice of the Beaufort Sea is called Alaska ice massif.

It is necessary to mention, that on average compact ice (7-10-th) doesn't occupy the entire sea area even in winter, compared to other Siberian Arctic shelf seas, due to constant ice motion and formation of polynyas and zones of open water. As seen from Fig. 2.8.14, on average during the whole year only about 12% of ice cover area is open floating ice. Its maximum amount is observed in early September (about 20%), minimum – in middle of November (about 5%).

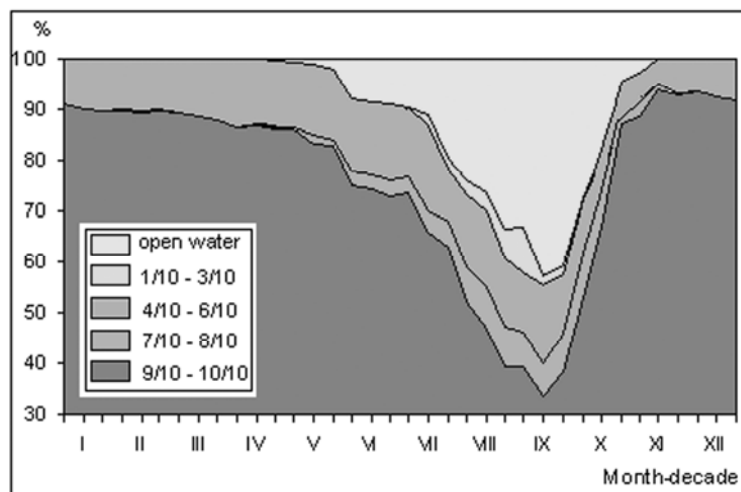


Fig. 2.8.14. Annual mean changes of area of different ice concentration in the Beaufort Sea, %

Before beginning of melting massif of compact ice in the Beaufort Sea includes ice of all age stages, from young ice (in polynyas and leads) to second-year and multiyear ice (Arctic pack in the northern sea regions), and ice on average occupies 86% of sea water area. During May – July its area decreases on 18%. Then velocity of compact ice melting increases, and in August its area decreases on 20% more. In September compact ice area is stable on the level of 40–45%. In late September new ice formation starts among compact ice, and its area sequentially increases (Fig. 2.8.15).

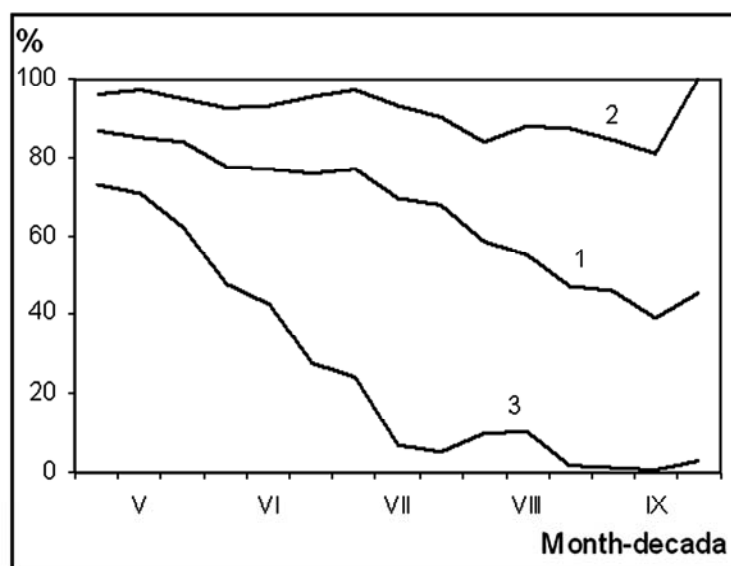


Fig. 2.8.156. Changes of average (1), maximum (2) and minimum (3) compact ice area in the Beaufort Sea (7/10–10/10) in spring-summer period, %

When compact ice melts and then transports out of sea limits, its boundary moves northwards. The most intensive sea clearing occurs in June in the south-eastern region, where Cape Bathurst polynya is developed in spring, which often joins with polynya on bar of the river Mackenzie (Fig.2.8.16). At the same time in zone of Cape Barrow – Barter Island boundary of compact ice locates in 10–15 miles from coast close to 20–meter isobath. In August velocity of

compact ice motion increases northwards. In zone of Cape Barrow – Hershel Island southern boundary is located far from coast (100–120 miles) (Fig. 2.8.16). In September compact ice insignificantly moves northwards, and in late month it moves down to coast.

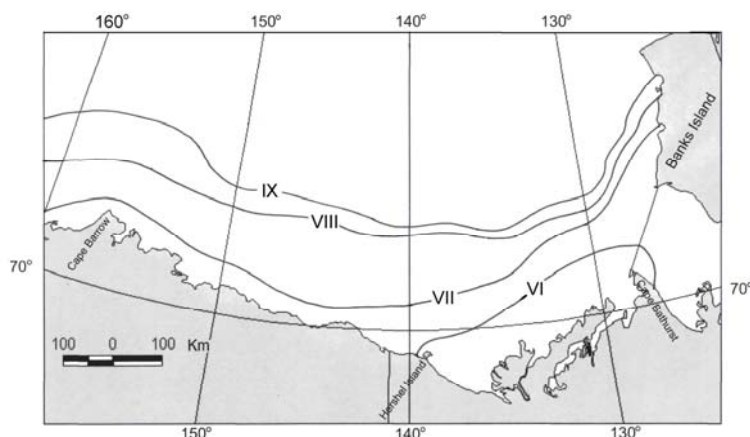


Fig. 2.8.16. Average location of compact ice boundaries (7/10–10/10) in the Beaufort Sea in June – in September from data for 1971–2000

In some years pack ice is transported into the Beaufort Sea water area in summer. Though summer boundary of pack ice normally locates 250 – 300 km from coast, strong winds (stormy) can bring it closer to coastal waters from a few days to a few weeks. Normally this ice includes thick first-year ice, second-year ice and multiyear ice. Concentration of transported ice usually increases during its transportation down to coast. Typical ice thickness of thick ice changes within 1–1,5 m, old ice floes – from 3 to 7 meters. These floes are covered with hummocks, which keels approach 10–20 m. Due to this circumstance, thick ice doesn't come to coast closer than 10-meter isobath.

#### 2.8.3.5. Ice propagation and location of ice edge in June - September

The Beaufort Sea is partly free from ice, when flaw polynyas appear and develop (without ice formation in it), and zones of open water among drift ice also occur. Stable sea clearing starts, when fast ice breaks up and coastal zone clears from floes of broken fast ice. Location of ice edge in ice clearing period (June-September) is shown on Fig. 1.18. Sea clearing starts from delta of the river Mackenzie in the second 10-day period of June, when fast ice isn't absolutely broken, and propagates westwards to Hershel Island and eastwards to Cape Barhurst, then further (through Gulf of Amundsen) to Banks Island to late July (Fig. 2.8.17).

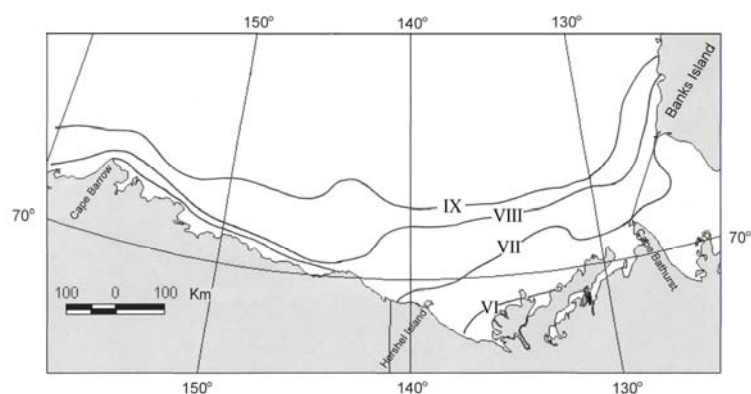


Fig.2.8.17. Average location of ice edge in the Beaufort Sea in June – September from data for 1971–2000

Sea clearing from ice occurs more intensive in August, especially in the south-western sea region. Along Alaska coast ice edge remains near coastal zone. Maximum sea clearing from ice is on average observed in September. At this time ice edge in central region goes up to 72° N, and it has maximum distance from Cape Barrow (35–40 miles).

Chart's fragments of average ice concentration in Canadian-American Arctic in late June – September are shown On Fig. 2.8.18.

According to chart compact ice prevails in sea during all summer months. It occupies 86% of area in June and about 70% in September. At that, area of open water in sea increases from 10% in June to 45% – in September (Fig. 2.8.19).

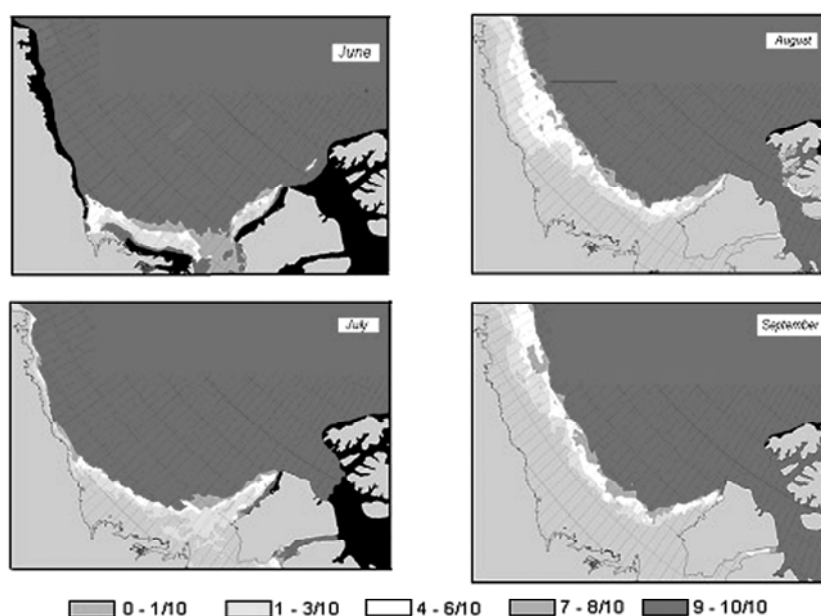


Fig. 2.8.18. Average ice propagation in the Beaufort Sea in late June – late September for 1971–2000



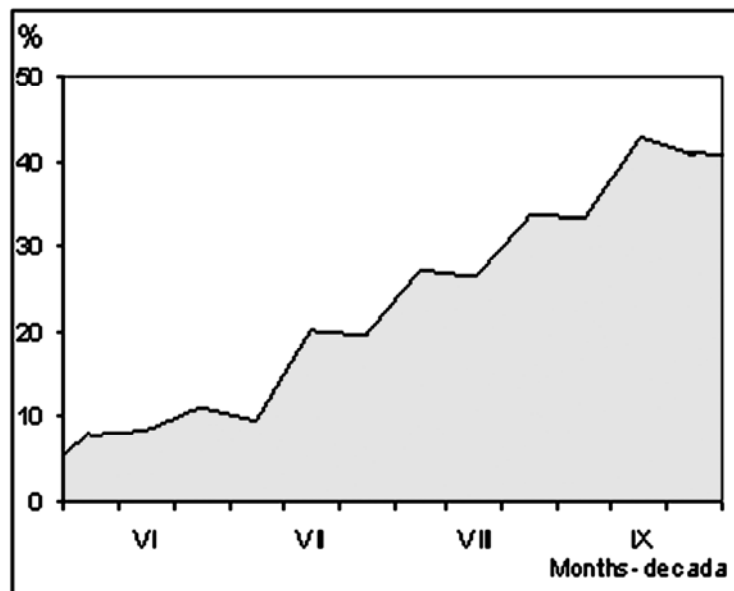


Fig. 2.8.19. Average multiyear changes of open water in the Beaufort Sea in June – September, %

Comparison of ice conditions in August 1998 and 1969 shows long-term variability of ice conditions in the Beaufort Sea (Fig. 2.8.20). In August 1998 the most favorable hydro meteorological conditions were observed in the sea during 1968–2007, and sea ice occupied only about 25% of area. In contrary, in summer 1969 solid compact ice occupied most part of the water area, and only rather narrow coastal part with very open floating ice and open water was ice-free.

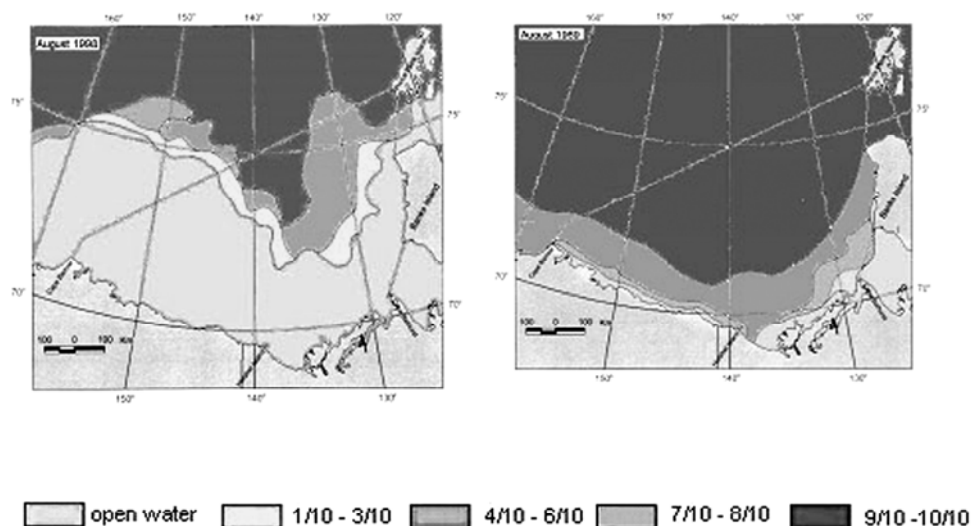


Fig. 2.8.20. Ice conditions in the Beaufort Sea in August 1998 and 1969

Charts on Fig. 2.8.20 are compiled according to archive data of weekly ice charts for navigation months of Canadian Ice service for 1967–2007.

### 2.8.3.6 Hummocks and grounded hummocks

Zones of grounded hummocks and ridging are located further in the Beaufort Sea. This is area of dynamic interaction between rather stable fast ice and drift ice zone. Ice rafting and formation of hummock ridges are observed along outer boundary of fast ice under activity of offshore wind. These ridges reach depth of 8-15 m, and sometimes 25 m, and plays role of sea anchors for fast ice, propagating to 20-meter isobath. Many fractures, polynyas and leads are formed in grounded hummocks area. Grounded hummocks are mostly settled on depth of 15-45 m, some of them remain during entire ice season.

Typical height of hummock ridges of drift ice in winter is 1,5–1,7 m, but sometimes ridges up to 6 m are observed. In case of ice rafting hummocks more than 30 m can be formed. Hummocks keels of multiyear ice floes with thickness 3–7 m, reach 20–25 m. Relation of above water hummock height to their keels is 1:4,5 for first-year ice and 1:3,3 for multiyear ice, respectively.

In 70s of last century study of hummocks was provided in the eastern Beaufort Sea using airplane profilometer. Obtained data (about 7000 of measurements) are summarized by squares of net region (Fig. 2.8.21).

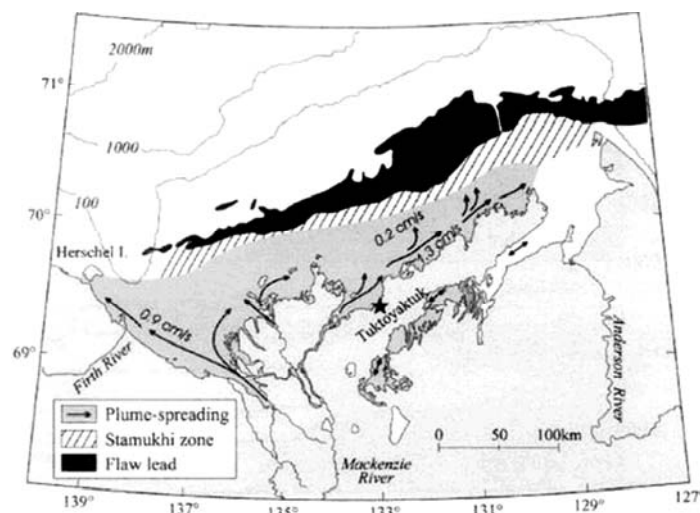


Fig. 2.8.21. Zone of hummocks height measurements in the eastern Beaufort Sea

This data, approximated for all regions, is presented in Table 2.8.5.

Table 2.8.5 – Frequency of occurrence of hummock height intervals in the eastern Beaufort Sea

Interval, m	1,0- 1,5	1,6- 2,0	2,1- 2,5	2,6- 3,0	3,1- 3,5	3,6- 4,0	4,1- 5,0	5,1- 6,0	6,1- 7,0
Frequency of occurrence, %	67,5	20,1	6,6	2,5	1,7	0,9	0,4	0,2	0,1

As seen from Table 2.8.5, 70% of hummocks are mostly less than 1,5 m. In a few cases hummock height approaches 5–7 m.

## 2.9. Characteristic of ice conditions in the Central Arctic Basin

### 2.9.1. Ice drift in the Arctic Basin

In many respects variability of sea ice cover characteristics in the Arctic Basin is determined by ice circulation. The Figure 2.9.1. presents patterns of mean resulting ice drift in the Arctic Basin for the winter and summer periods of the year calculated by means of the corresponding approximation formulas. These patterns agree with earlier published qualitative patterns of general ice drift. They show the presence of the Transpolar Drift Stream (often termed “Transarctic ice flow” in Russian studies) directed to the Greenland Sea between the near-pole area and the northern margins of the Eurasian shelf seas. A large quantity of ice exported from the Russian Arctic Seas joins this flow on the left, while the anticyclonic gyre area with the center approximately at 78°N, 150° E adjoins it on the right.

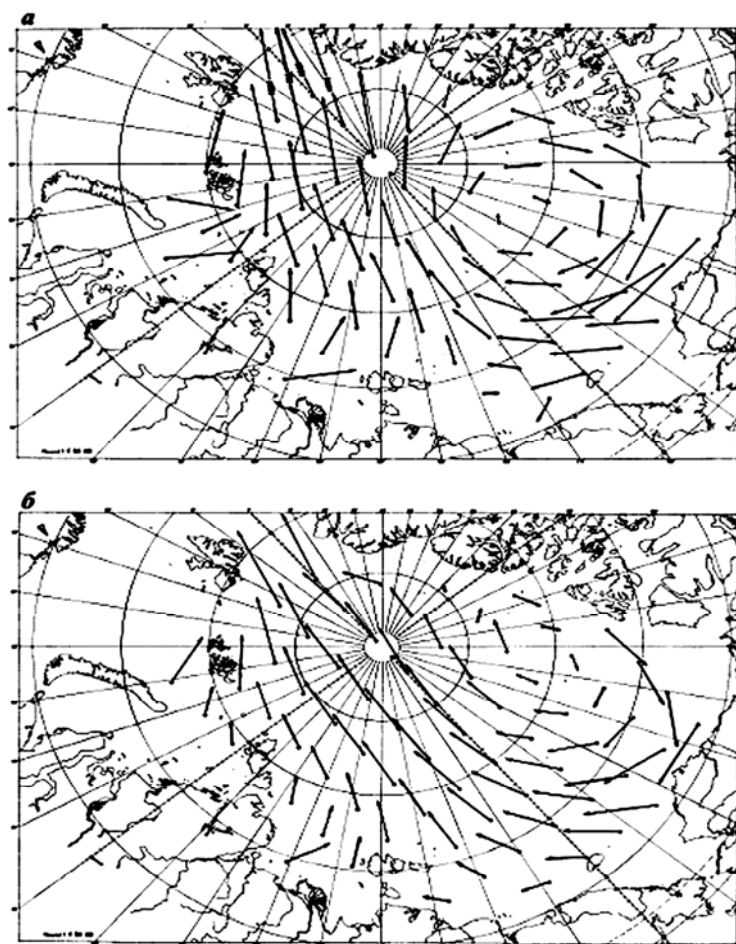


Fig. 2.9.1. Scheme of the average ice drift in October-March (a) and April-September (b)

Ice joining the Transpolar drift stream from the Kara Sea is exported to the Greenland Sea in 1-2 years, from the Laptev Sea – in 2-3 years, from the East Siberian – in 3-4 years and from the Chukchi Sea – in 4-5 years. The period of ice circulation within the anticyclonic gyre changes from 4 to 10-12 years. The lower bound refers to the quasi-circular ice drift area in the

Beaufort Sea and northwards, and the upper – to the trajectories passing across the stagnant region adjoining the north shores of Greenland and the Canadian Arctic archipelago.

In summer, ice from this area is partly transported to the straits of the Canadian Arctic archipelago and further to Baffin Bay. Observational data of ice drift allows determining of probability of drifting objects occurrence into the anticyclonic gyre. From observations data two boundaries were determined, one of them contours a part of the Arctic Basin, from which ice isn't strictly transported to the Greenland Sea. In summer this ice is partly exported to the straits of Canadian Arctic archipelago, but its bigger part remains within the gyre, or, when it is finished, joins the Transpolar Drift. The second boundary determines a region, where ice is transported to the Greenland Sea or melts within marginal seas boundaries, and never gets into anticyclonic gyre. There is a transition zone between listed boundaries, where ice in one case is transported to the Greenland Sea, and in other case – gets into the gyre region. Due to this the ice participating in the gyre can change from 2,5 to 3,5 million km<sup>2</sup> (approximately from 40 to 60% of the Arctic Basin area).

The variability of the general ice drift pattern is also manifested in a significant deviation of some branches of the Transpolar Drift Stream from their usual position. Due to this, closed cyclonic ice circulations occur in some years or seasons in the Laptev Sea and in the vicinity of Wrangel Island, whereas the usually existing export flow from the Kara Sea to the Arctic Basin changes its direction to reverse. Such changes are most frequent in the summertime.

A comparison of the ice drift patterns, presented in Figure 2.9 for winter and summer periods, reveals some specific differences between them. Most noticeable are the differences in the ice drift velocities at the approaches to the Fram Strait, where a velocity increase at approaching the strait is observed in winter. Another regular feature is a displacement of the Transpolar Drift Stream core from Eurasia to America and the corresponding decrease of the anticyclonic gyre area from winter to summer.

Two winter seasons (October-December and January-March) have typical pattern, approximately corresponding to the described annual mean pattern of general drift. At that, location of the Transpolar Drift core, which is usually situated along the northern extremities of the Arctic Seas, can significantly change from year to year, affecting ice outflow from these seas.

In spring period (April-June) ice drift pattern gets simpler: in most regions of the Arctic basin and marginal seas, except of rather small stagnant region northwards of the Canadian Arctic archipelago, ice drifts in direction of the Greenland Sea.

In summer (July-September) deep stream of the Transpolar Drift shifts to the line, connecting Bering Strait and Fram Strait. However, interannual variability of ice drift in this period is clearly expressed. In some years ice drift is typical for winter period whereas cyclonic

system with its center usually located northwards of the Laptev Sea, abnormally develops in other years. These changes significantly influence ice exchange of the marginal seas with the Arctic Basin.

### 2.9.2. Age (thickness) of drifting ice in the Arctic Basin

System of atmosphere and ocean circulation determines duration of ice cover existence, and therefore, prevailing age of the ice in different macrostructural regions. Due to this region with prevailing multiyear ice of increased thickness, specific mesostructure and other properties, is formed in the ocean (Fig. 2.9.2).

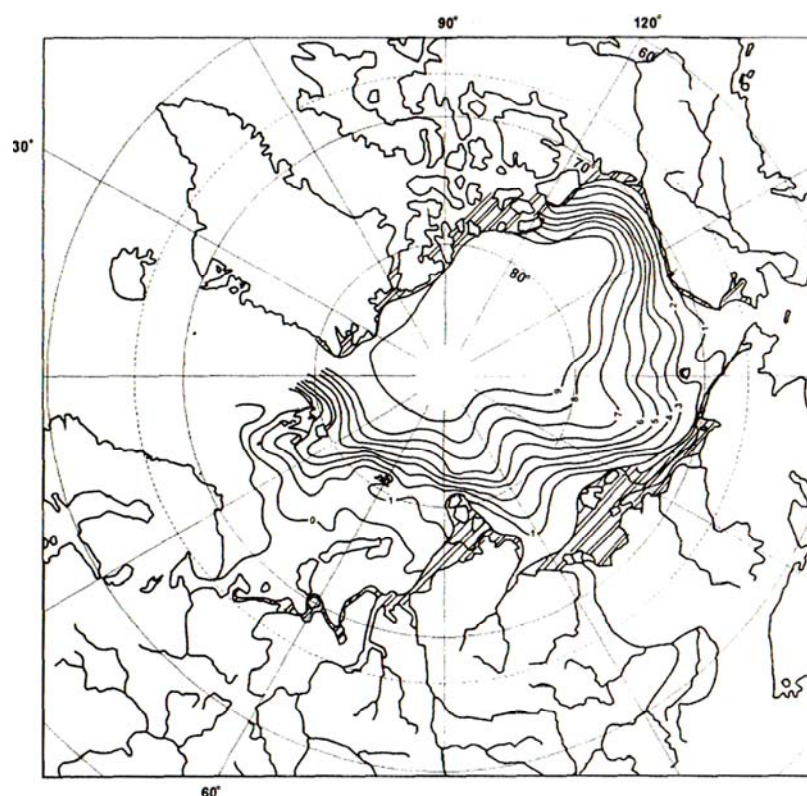


Fig. 2.9.2. Structure of the average field of old ice concentration (marks) and location of fast ice in February

Region, where amount of multiyear ice gradually decreases with increasing distance from the boundary of their relative predominance, is located in its periphery.

Macroscale distribution of multiyear ice corresponds to location of region with increased ice concentration, which forms the oceanic ice massif; its spurs are the major massifs of marginal seas: Svalbard, Kara, Taymyr, Ayon, Wrangel and Alaska.

Increased frequency of occurrence of offshore winds in many seas of the Eurasian shelf, on one hand, and onshore winds – northwards of Greenland and Canadian Arctic archipelago – on the other, contribute to formation of flaw polynyas and ice cover “rejuvenation” in the first region, and intensive ridging and ice accumulation in the second. Together with peculiar features

of thermodynamic conditions it leads to large-scale spatial changes of average ice thickness – its increasing from Siberia coast to Canadian Arctic archipelago and Greenland. Maximum spatial gradients of ice thickness in the end of the winter, occurring due to ice cover “rejuvenation”, are found in most marginal seas of the Siberian shelf.

Ice age in every region of the Arctic Basin is caused by local climate conditions, velocity and direction of general ice drift. Interannual variability of ice distribution by area and age depends on particular region of the Arctic.

The largest amount of multiyear ice is located near the coast of Canadian Arctic archipelago. From this coast it extends to Pole in the north, to Greenland – in the east, and to Alaska coast – in the south-west. Meridians  $180^\circ$  -  $0^\circ$  are its western and eastern boundaries. Thickness of level multiyear ice in this region reaches maximum values of 420 cm. It is necessary to mention, that in places, where Arctic anticyclone is located, ice is covered with thin snow layer. Amount of snowfall is noticeably less here, than in other Arctic regions. Low air temperatures and thin snow-cover are the major factors, causing extreme thickness of level multiyear ice in this region. High ridging plays a significant role in formation of ice thickness.

Annual mean values of ice thickness in the end of winter are the most interesting. Ice of Canadian origin occupies Alaskan, Canadian and western part of Greenland regions. Ice is located in the Transpolar Drift.

Multiyear ice of Canadian origin occupies the entire Arctic Basin, the northern Chukchi Sea and the western East-Siberian Sea. Ice zone of Siberian origin directly borders with Severnaya Zemlya, Franz-Josef Land and Svalbard.

Summarizing direct measurements of ice thickness at drifting stations and calculation results, where age composition of the ice and its ridging are accounted, and also data of sonar observations from submarines, allowed obtaining average ice thickness distribution in the Arctic Basin in the end of winter (Fig. 2.9.3). As it is seen, maximum ice thickness, exceeding 7 m, is observed near the northern coast of Canadian Arctic archipelago, gradually decreasing to 2 m in the Siberian shelf seas.

If ice cover had been immovable, ice thickness distribution in the end of winter would have been determined only by conditions of ice growth, i.e. would have depend on air temperature, water heat content, conditions of heat exchange in air and water. Ice motion noticeably changes ice thickness distribution and its entire meso- and macrostructure. As a result of ice exchange with the Arctic Basin “rejuvenation” of the Siberian Seas ice cover occurs.

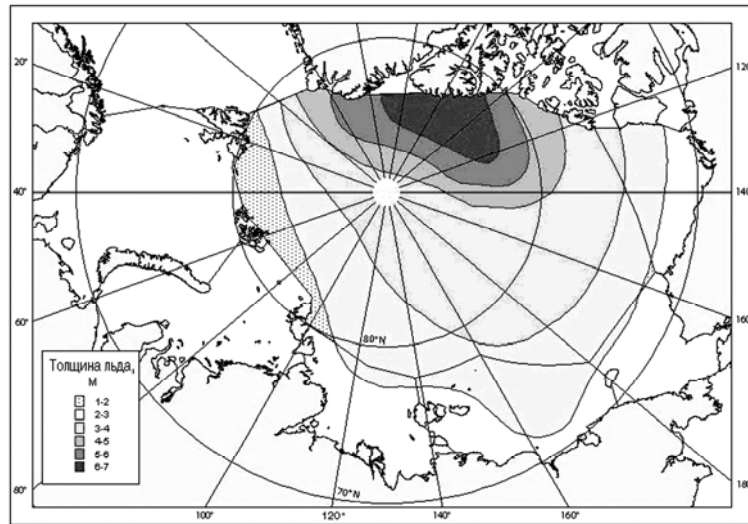


Fig. 2.9.3. Average ice thickness in the Arctic Basin

### 2.9.3. Distribution of level ice thickness along the navigation route in summer period.

Large amount of in-situ data, contained in the database, allows to estimate distribution of sea ice characteristics and changes of navigation ice conditions in summer period (July-September), and to consider regularities of the main sea ice characteristics distribution and operational indicators of ice breaker motion in three sectors of the Arctic Basin:

- 1) sector between 10° E and 100° E;
- 2) sector between 100° E and 150° E;
- 3) sector between 150° E and 165° W.

The southern boundary of these sectors follows the multiyear ice boundary, located in 81-82° N in the first sector, 79-80° N in the second sector and 73-75° N in the third sector.

Hereinafter in the text these sectors referred to as the “Western”, “Central” and “Eastern”.

Figures 2.9.4-2.9.6 show the thickness distribution of ice, directly broken by vessel during its sailing in the Arctic Basin. It is necessary to mention, that only level ice thickness was estimated in observations (outside the hummocks).

As a result of summer melting processes ice thickness distribution from July to September shifts to larger values. Thus, in the Western sector (Fig. 2.9.4) the ice with thicknesses of 120-200 cm, 140-260 cm, and 180-300 cm has the maximum frequencies of occurrence in July (58 %), in August (61 %), and in September (68 %), respectively.

In the Central sector (Fig. 2.9.5) ice with thicknesses of 120-240 cm and 180-260 cm prevail in August (61 %) and in September (60 %), respectively.

Distribution of level ice thickness, recorded by special ice observations in the Eastern sector, is characterized by lower values of prevailing ice thickness (Fig. 2.9.6). In this sector the predominant ice thickness is within the range of 80-180 cm. The relative length of navigation

route in this ice is: 55 % in July, 59 % in August and 63 % in September.

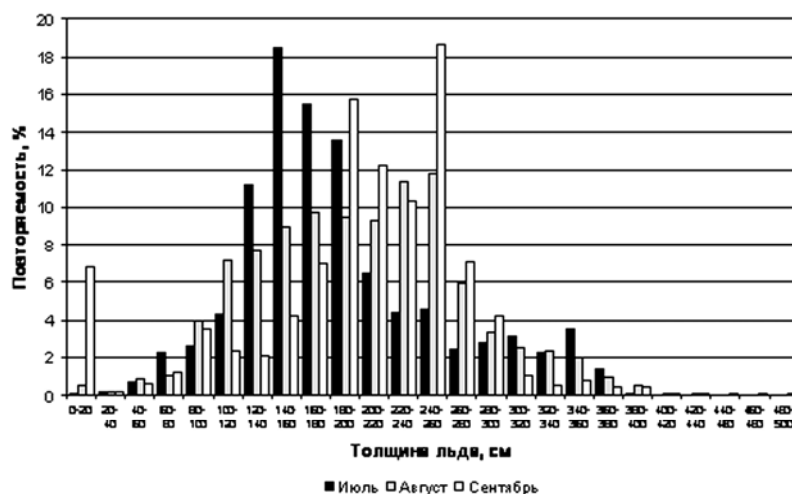


Fig. 2.9.4. Distribution of level ice thickness along the navigation route in the Western sector in the period July-September

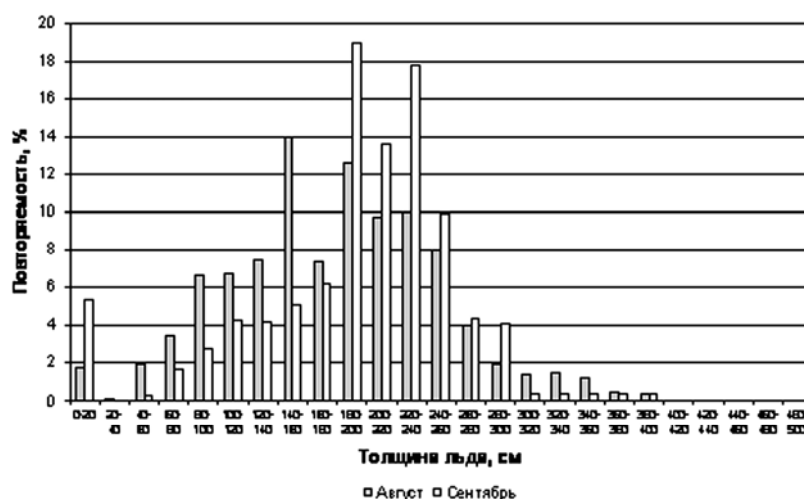


Fig. 2.9.5. Distribution of level ice thickness along the navigation route in the Central sector in the period August – September

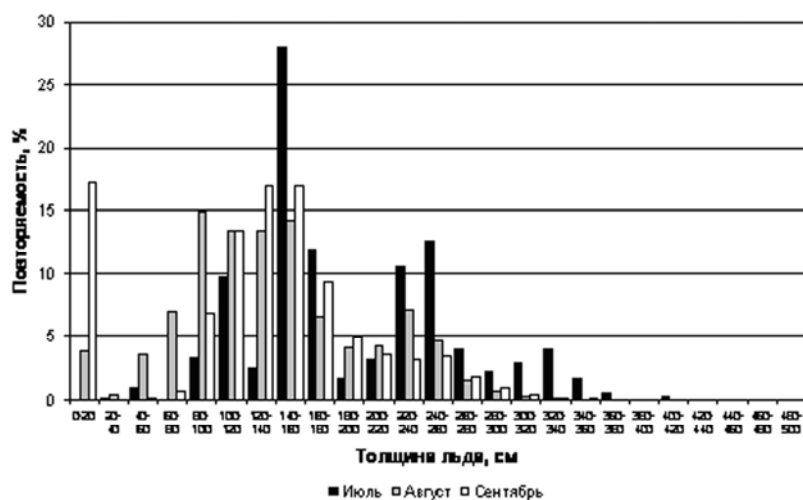


Fig. 2.9.6. Distribution of level ice thickness along the navigation route in the Eastern sector in the period July-September



Selective icebreaker route, when it mostly moves in easier ice conditions and also in thinner ice, affects the ice thickness distribution along the sailing route. Due to this it is reasonable to analyze ice thickness distribution for first-year and old ice separately.

In the western sector prevailing thickness of the first-year ice in July is 140-200 cm (70 %), in August – 100-180 cm (69,5 %), in September – 140-200 cm (61 %) (Fig. 2.9.7). In the western sector prevailing thickness of the old ice in July is 200-260 cm (68 %), in August – 180-260 cm (69 %), in September – 180-240 cm (73 %) (Fig. 2.9.8).

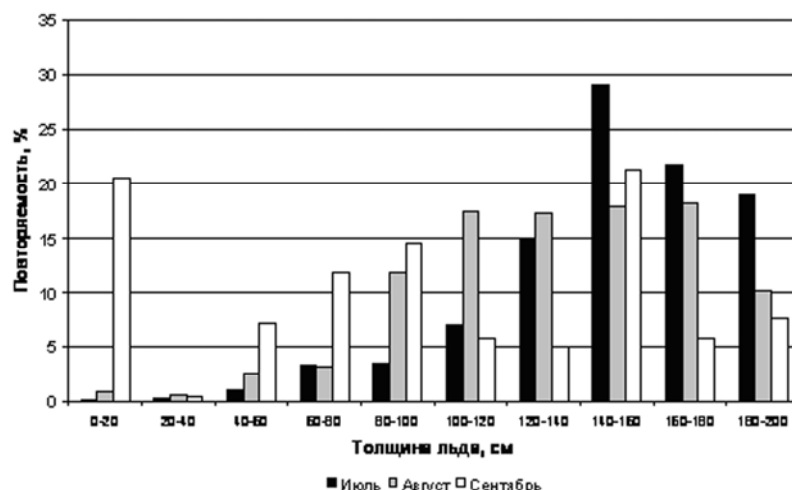


Fig. 2.9.7. Distribution of level first-year ice thickness along the navigation route in the Western sector in the period July-September

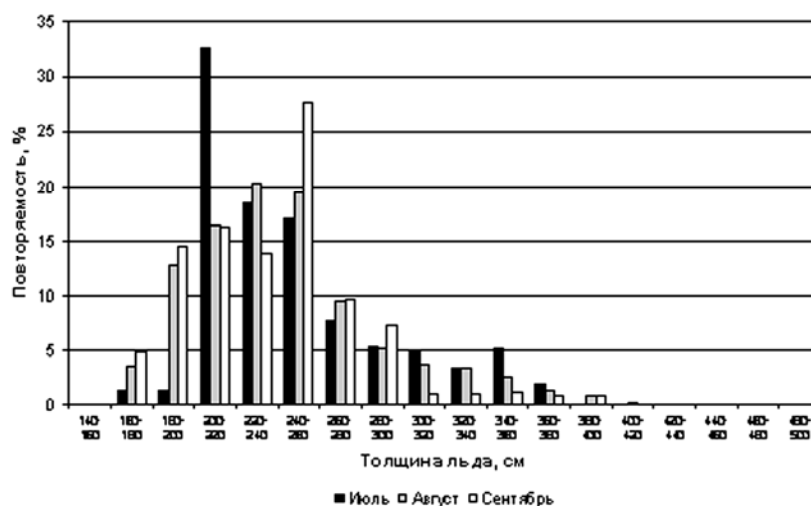


Fig. 2.9.8. Distribution of level thick ice thickness along the navigation route in the Western sector in the period July-September

In the central sector in summer period prevailing thicknesses of the first-year and old ice generally corresponds to their prevailing thicknesses in the western sector (Fig. 2.9.9, 2.9.10).

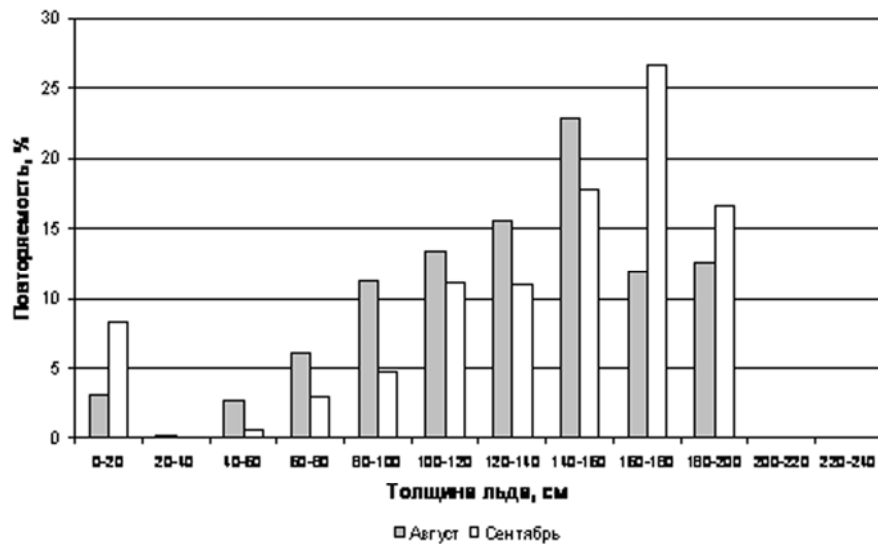


Fig. 2.9.9. Distribution of level first-year ice thickness along the navigation route in the Central sector in both August and September

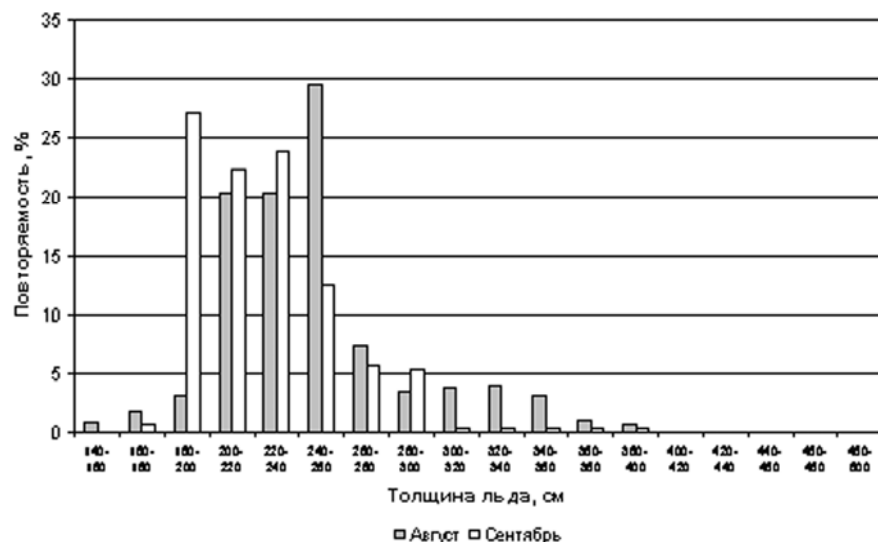


Fig. 2.9.10. Distribution of level thick ice thickness along the navigation route in the Central sector in both August and September

In the eastern sector prevailing thickness of the first-year ice in July is 140-180 cm (67 %), in August – 80-160 cm (77 %), in September – 100-180 cm (66 %) (Fig. 2.9.11). Prevailing thickness of the old ice in July is 220-280 cm (62 %), in August – 180-280 cm (75 %), in September – 180-260 cm (73 %) (Fig. 2.9.12).

#### 2.9.4. Ice melting

With increasing of solar radiation and air temperature in spring snow and then ice start to melt. The mean terms for the onset melting falls on the last 10-day period of May in the Arctic Seas, located to the south of 72° N; in the first 10-day period of June it usually propagates to 75° N, and by the end of the second 10-day period of June it reaches the northern boundaries of the marginal seas, and by late June approaches the near Pole region (Fig. 2.9.13). Standard deviation, which characterizes the interannual variability of ice melting terms, is 10 days.

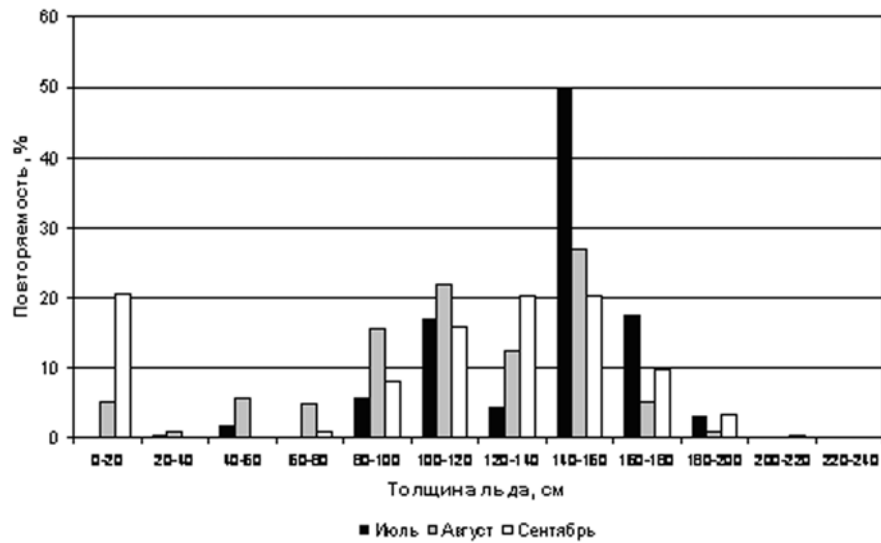


Fig. 2.9.11. Distribution of level first-year ice thickness along the navigation route in both August and September

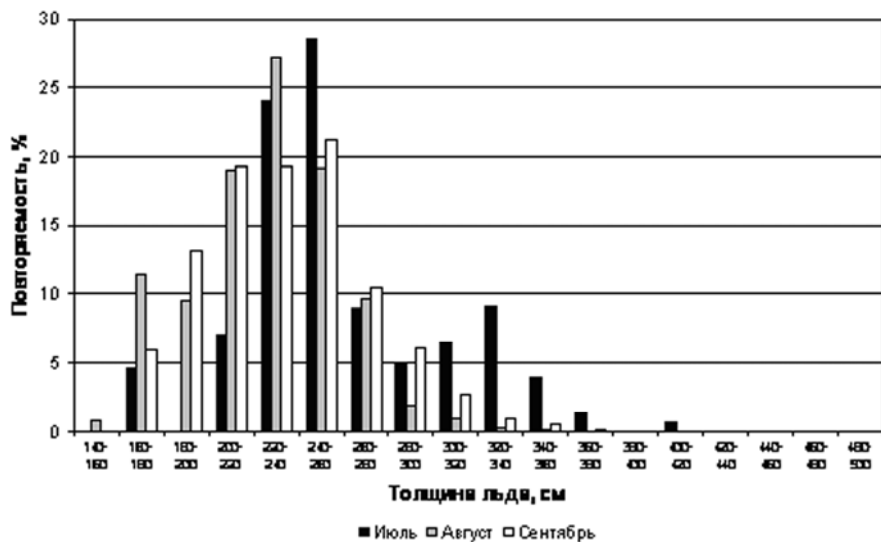


Fig. 2.9.12. Distribution of level thick ice thickness along the navigation route in the Eastern sector in both August and September

Velocity of ice thickness decreasing significantly changes as a result of melting in the Arctic Seas. In the Arctic Basin the mean value of ice thickness decreasing changes during season from 75—100 cm near the northern boundaries of the seas, and to 0—20 cm in the near Pole region (Fig. 2.9.14).

In the period of ice melting essential feature of ice state is estimation of ice decay. Estimation of ice decay is based on accounting external features, which are typical for ice surface changes as a result of its melting: appearance of puddles and their development stage, presence of snow cover etc.

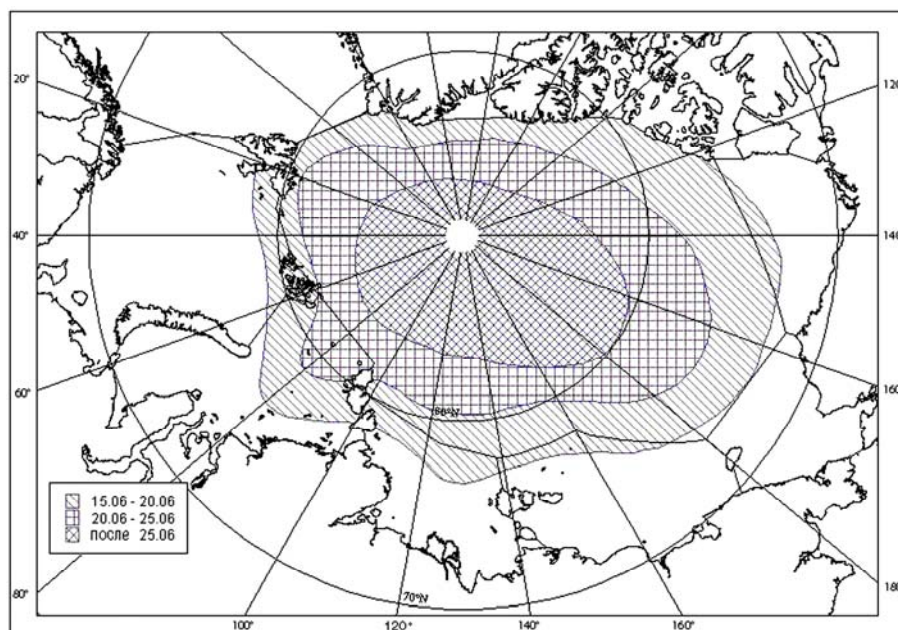


Fig. 2.9.13. Average terms of the beginning of thawing of an ice in the Arctic sector

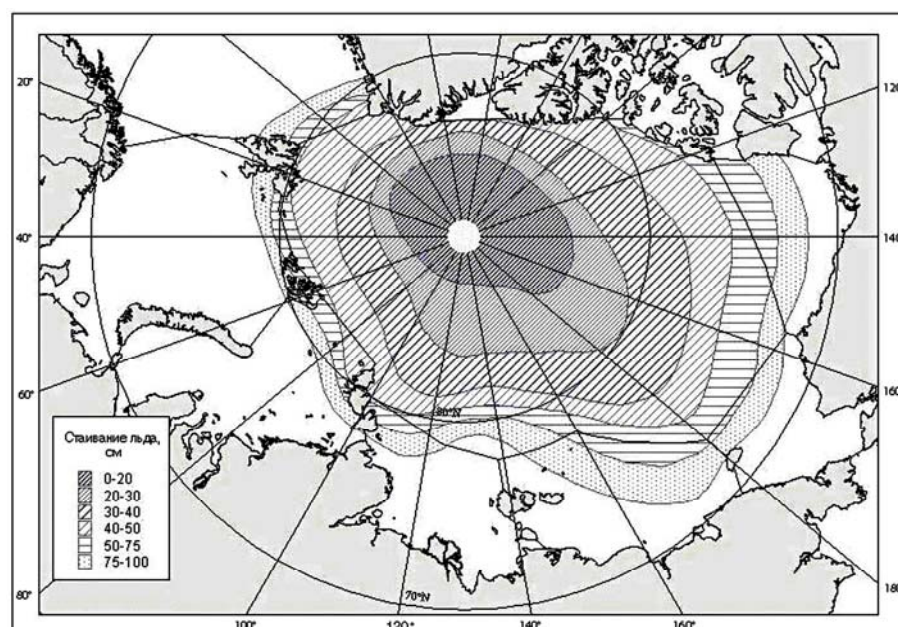


Fig. 2.9.14. Average size of thawing of an ice for a summer in the Arctic sector

It is necessary to mention, that ice decay is characterized with significant interannual and spatial variability. Obviously, ice decay depends on atmospheric processes (air temperature), proportion of different ice types (first-year ice melts more intensive, than old one). Thus, in August 1996 ice with a degree of decay (2-3 marks) typical for these months was observed southwards of 86°, at the same time, northwards of this latitude features of ice melting were absolutely absent, and snow depth amounted to 20-25 cm. This case was observed in all three sectors.

In the western sector the maximum ice decay degree is observed in July – about 50 % of the

ice has a decay degree of 3 marks (Table 2.9.1). In high latitudes in the second half of August freezing of puddles can begin, at this moment a degree of decay conventionally considered to be 0 marks. The Relative length of the route in this ice is less than 7 %. Ice, with a degree of decay of 2 marks has the highest frequency of occurrence in this month. In September in the Western sector ice melting wasn't observed.

Table 2.9.1. Relative length of navigation route in ice of different degree of decay in the Western sector for July-September, %

Month	Ice decay degree, marks					
	0	1	2	3	4	5
July	1,3	13,9	34,9	49,9	0,0	0,0
August	6,7	7,4	63,7	22,2	0,0	0,0
September	100,0	0,0	0,0	0,0	0,0	0,0

In August the most probable value of ice decay degree in the Central sector is 2-3 marks (43 %), however, decay degree of 0 marks was recorded in 37 % of the route (usually it is connected with the end of ice melting). In September melting is observed in 43 % of the route in this sector, and prevalent degree of ice decay is 1 mark (Table 2.9.2).

Table 2.9.2. Relative length of navigation route in ice of different degree of decay in the Central sector in August and September, %

Month	Ice decay degree, marks					
	0	1	2	3	4	5
August	37,2	18,0	18,7	24,0	1,9	0,2
September	56,6	30,1	1,9	11,4	0,0	0,0

Ice of the Eastern sector in July is characterized with a small degree of decay; its values are less than 1 mark (observation data for 1996). In August prevailing degree of ice decay amounts to 1-2 marks (78 %), and in September melting is observed only on 50 % of the route (Table 2.9.3).

Table 2.9.3 - Relative length of navigation route in ice of different degree of decay in the Eastern sector in July-September, %

Month	Ice decay degree, marks					
	0	1	2	3	4	5
July	8,6	91,4	0,0	0,0	0,0	0,0
August	0,1	39,3	38,5	22,0	0,1	0,0
September	49,8	36,6	12,9	0,7	0,0	0,0

### Distribution of snow depth along the navigation route in summer period

Snow depth on ice of the Arctic Basin depends on many factors: amount of precipitation, fallen during previous winter (which in its turn depends on cyclonic activity), wind conditions, air temperature in the melting period and etc. Snow observations from a ship consist of estimating its depth on level ice (outside of hummocks).

In July snow depth on 60 % of the route in the Western sector is less than 10 cm (Table 2.9.4). Nevertheless, in some parts its depth can amount to 55 cm. These snow depth values were recorded in July 1992 in the near Pole region. Obviously, in August snow depth generally decreases due to melting. In this month about half of the sailing route in the Western sector is in the ice without snow. The process of snow accumulation starts in September, after finishing of melting, (see Table 2.9.4). Prevailing snow depth in this month is within the range of 1-20 cm (89 %).

Table 2.9.4 –Distribution of snow depth on ice in the Western sector in July-September, %

Month	Snow depth, cm						
	0	1-10	11-20	21-30	31-40	41-50	51-60
July	15,1	44,5	10,6	16,1	9,6	2,1	1,8
August	49,4	35,2	14,0	1,4	0,0	0,0	0,0
September	2,2	58,3	30,8	7,4	1,0	0,3	0,0

The snow distribution pattern in the Central sector is similar (Table 2.9.5). It is necessary to mention, that ice cover of the Central sector is distinguished by rather larger values of snow depth comparing to ice of the Western sector. This peculiar feature is recorded both in August and in September.

Table 2.9.5. Distribution of snow depth on ice in the Central sector in August and September, %

Month	Snow depth, cm						
	0	1-10	11-20	21-30	31-40	41-50	51-60
August	35,4	33,9	23,9	6,3	0,6	0,0	0,0
September	4,5	30,0	44,3	18,8	2,0	0,3	0,0

In July the prevailing snow depth in the Eastern sector amounts to 20-40 cm (61 %) (Table 2.9.6). In August snow cover is absolutely absent in 57 % of navigation route, though in some areas its depth amounts to 25 cm. In September, after the end melting, newly fallen snow prevails with its depth mostly less than 10 cm (76 %).

Table 2.9.6 - Distribution of snow depth on ice in the Eastern sector in July-September, %

Month	Snow depth, cm						
	0	1-10	11-20	21-30	31-40	41-50	51-60
July	2,7	20,8	10,0	31,1	30,1	5,2	0,0
August	57,2	11,4	24,6	6,8	0,0	0,0	0,0
September	11,5	76,2	12,2	0,1	0,0	0,0	0,0

#### 2.9.6. Distribution of compacting along the navigation route in summer period

Compacting of ice cover is the essential feature of its dynamic processes. An estimation of compacting is qualitative pattern based on external features of changes of some sea ice characteristics – increasing of concentration, formation of new ridges, young ice rafting and etc. One of the most essential features of ice compacting is sharp decrease of ship speed.

In the Western sector compacting is absent along the significant part of the sailing route - 65 % in July, and 75-76 % - in August and September. Weak compacting has the largest frequency of occurrence in summer period, with intensity of 0-1, 1 mark. Relative length of navigation route under strong compacting (1-2, 2 marks) changes from 4 % in July to 2.5 % in September. Very strong compacting (2-3, 3 marks) was not recorded in summer period in the Western sector (Table 2.9.7).

Table 2.9.7 - Relative length of navigation route under compacting of different intensity in the Western sector in July-September, %

Month	Ice compacting intensity, marks			
	0	0-1, 1	1-2, 2	2-3, 3
July	65,2	30,9	3,9	0,0
August	75,8	21,1	3,1	0,0
September	74,8	22,7	2,5	0,0

In the Central sector length of the route without compacting is much higher (by 5 % in August and 15 % in September) comparing to the Western sector – (Table 2.9.8).

In the Central sector compacting frequency of occurrence both in August and September is practically the same. Increasing of navigation route length under compacting with intensity of 1-2, 2 marks, from 1 % in August to 2 % in September is the main distinction.

Table 2.9.8 - Relative length of navigation route under compacting of different intensity in the Central sector in August and September, %

Month	Ice compacting intensity, marks			
	0	0-1, 1	1-2, 2	2-3, 3
August	80,2	18,9	0,9	0,0
September	80,0	18,1	1,9	0,0

In the Eastern sector during summer relative length of navigation route without compacting gradually increases: from 75 % in July to 86 % in September. Along ships route mostly weak compacting with intensity of 1 mark was recorded during ice observations from ships (Table 2.9.9).

Table 2.9.9 - Relative length of navigation route under compacting of different intensity in the Eastern sector in July-September, %

Month	Ice compacting intensity, marks			
	0	0-1, 1	1-2, 2	2-3, 3
July	74,9	23,8	0,0	0,0
August	79,7	19,3	1,0	0,0
September	85,7	13,7	0,6	0,0



### 3.1. Remote sensing observations of ice cover state

Remote sensing – is a process of observations, measurements and recording of energetic and polarization characteristics of self and/or reflected radiation of land, ocean and the Earth atmosphere elements in different spectral bands of electromagnetic waves.

Remote sensing of sea ice is also implemented taking into account physical processes of radiation, reflection and absorption of electromagnetic waves in visible, infrared and microwave wavelength bands. Every band has its own possibilities and limitations for determining sea ice parameters using different regimes of operation, connected with type of radiation – self- or reflected, under controlled conditions of electromagnetic radiation of sea ice.

The final product of remote sensing is quantitative or qualitative description of environment conditions. That is why it is necessary to consider natural component – atmosphere and underlying surface in composition of remote sensing system.

In general remote sensing is considered as a system of natural-technical components and their interactions. It is based on multistage process of information changes and transformation, described by regularity of interacted subsystems.

From the point of view of its composition, special feature of remote sensing system is spatial-temporal division of components (Fig. 3.1.1):

- natural processes in “atmosphere – underlying surface” system;
- sensitive element of remote sensor, located on spacecraft;
- reception and processing facilities and users, located all over the World.

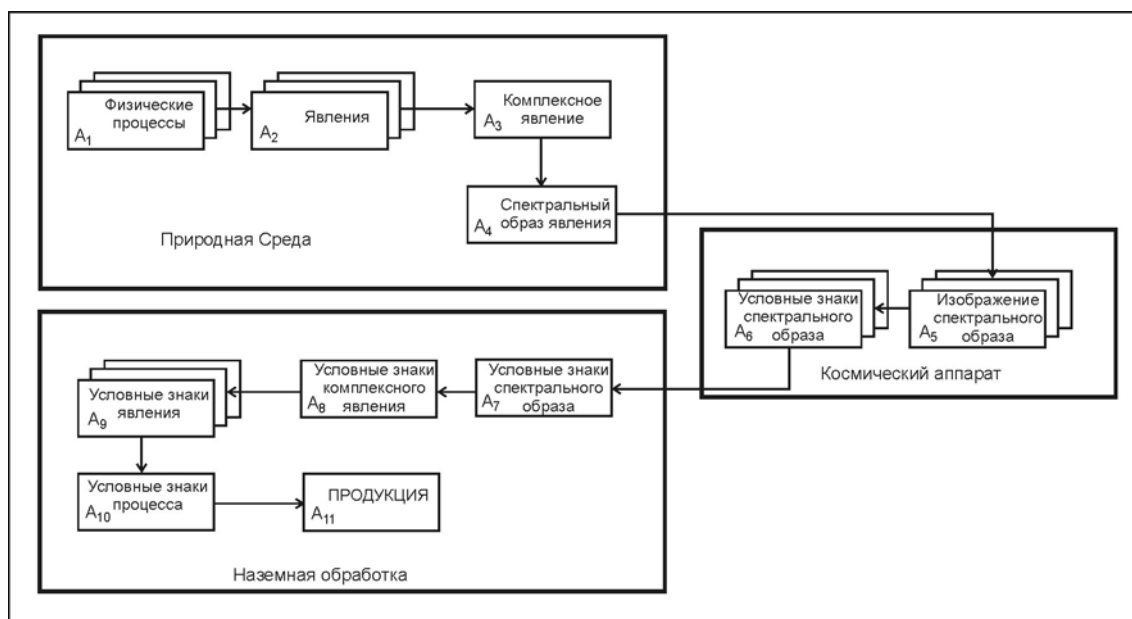


Fig. 3.1.1. Elements of remote sensing system.

Study and description of physical processes in the “atmosphere – underlying surface” system (A1), is an objective of remote sensing. Such processes in sea ice of the freezing seas are:

- process of ice cover formation, determining its type – first-year or multiyear,
- ice drift under influence of atmosphere motion, currents and sea bottom relief,
- ice deformation (breakup, rafting and ridging),
- process of sea ice destruction (melting).

The listed processes proceed according to physical laws, which present objectively existing stable connection between phenomena and properties of material world (objectively existing form of nature expression). Only some processes are observed by remote sensing from all their diversity (A1). Such selectivity is connected with the point, that every natural process influences formation of radiation (or influence some changes) of particular spectrum of electromagnetic radiation. Remote sensors also have selective sensitivity.

Physical processes themselves are not directly observed by remote sensing, they can be discovered only from phenomena observed in the “atmosphere – underlying surface” system, objectively existing characteristics of material world objects. They are indicators of processes (A2), which reflect properties of “atmosphere – underlying surface” system.

Complex phenomena are normally observed by remote sensing. That is why many of spatial-distributed phenomena compose observed complex phenomena (A3).

Complex phenomena in its term produce integrated radiation, which is recorded as a spectral pattern (A4). The listed fact is used in remote sensing in different spectral bands.

Processes and produced by them phenomena in the “atmosphere – underlying surface” system can be observed either by their self- radiation or by changes, that they insert in electromagnetic radiation artificially made under controlled conditions or underlying surface radiation. These changes are determined by heterogeneities (of different nature) of spatial distribution of objects, processes or phenomena. Spatial heterogeneities in their turn can be divided into two main categories:

- heterogeneities, that change radiation by their total volume
- heterogeneities, that change radiation on the interface.

Heterogeneities of the first type include many components (gas molecules, products of condensation, etc.). Size of such particles changes from a hundredth of micron to millimeters, and heterogeneities have large enough range of distribution.

Heterogeneities of the second type are characterized by surfaces with fractal geometrical structure.

Sea ice can be considered as a complex polycrystalline composite, consisting of pure ice with brine and air pockets. It is normally covered with snow. Its backscatter depends on many physical parameters, such as surface roughness, salinity, air inclusions, crystal structure, snow cover and others. This system forms two major mechanisms of scattering:

- surface scattering (scattering from the layer very near the ice or snow surface);
- volume scattering (scattering from the entire ice thickness).

Reflected radar signal significantly depends on surface roughness of different scales. An area consisting of many pieces of broken ice generally gives a higher backscatter than the same ice type with a level surface. Multiple reflections from two or more surfaces nearly perpendicular to each other can give the co-called corner reflection effect, which may enhance the return signal by up to an order of magnitude.

There are also regional differences of the sea ice backscatter values, depending on its location relative to the main ice pack.

Radar image brightness, which is determined by the sea ice and water backscatter, is the principal direct interpretation feature. Based on differences in backscatter, the major ice types can be detected.

Sea ice recently formed on the water surface includes frazil ice, grease ice, slush and shuga. Grease ice inhibits the formation of capillary waves and can be detected by its dark signature, often among bright areas of pancake ice or wind-roughened water surface.

Sensitive element of remote sensor, perceiving incoming radiation (which composition was defined by spectral pattern of phenomena), forms on its output a signal of this pattern (A5). On the output of remote sensor this signal undergoes informational transformation (coding) and is transmitted via radio channel as a multitude of conventional signs of the spectral pattern (A6). Selected system of codes (symbols) describes state of remote sensor signal, expressed in units of radiation field

Received radiosignal contains information about spectral pattern (A7), but distorted by noise of radiochannel. Chosen values of spectral pattern allow estimating values of complex phenomena parameters (conventional signs of phenomena – A8), by which, in its turn, several phenomena parameters can be estimated as well (conventional signs of phenomena A9). Estimation of physical processes, existing in the “atmosphere-underlying surface” system (A10), is made under known connections “process – phenomena”, description of which forms a product of remote sensing (A11).

Informational model of remote sensing system is presented in Fig. 3.1.2.

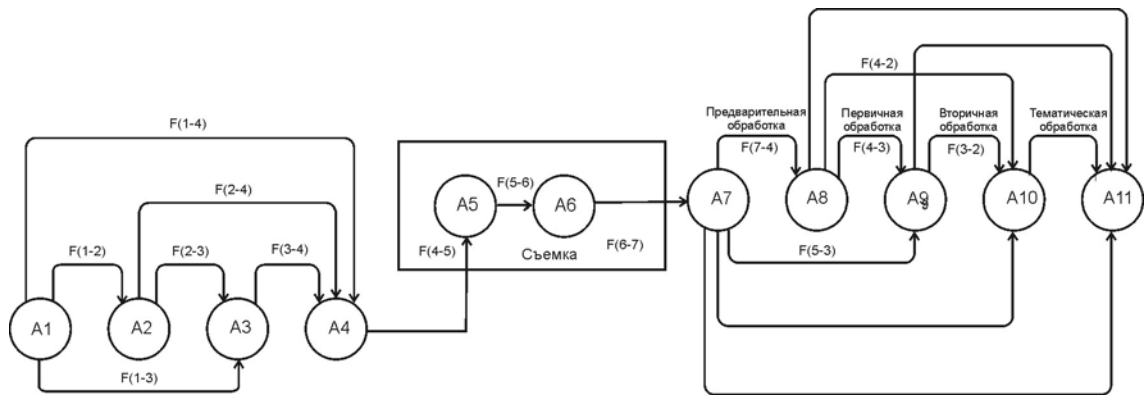


Fig. 3.1.2. Information model of remote sensing

First part of scheme (elements A1 - A4) describes transformations of information about existing processes.

Actions on the stage F (1-2) consist of studying representation mechanisms of manifestation of different processes, occurring in the “atmosphere – underlying surface” system in physical phenomena.

For example, process of vertical displacement of air mass in cyclone leads to water vapour condensation and cloudiness formation. Phenomenon of cloud formation will be an indicator of water condensation process in upwelling air flow. Process of above water surface temperature decreasing to negative values will be accompanied by ice formation phenomenon.

F (1-2) is a process of phenomena determination, as indicators of processes. Process indicator is formation of new objects in the “atmosphere – underlying surface” system and also changes of their state or characteristics.

Actions F (2-3) are directed on studying formation of complex phenomenon, because natural phenomenon is normally observed in complex. Thus, process of cloud formation is accompanied by appearance of new objects (clouds) and changes of water drops size.

Actions F (3-4) consist of studying formation of phenomena and objects spectral pattern, being observed in the “atmosphere – underlying surface” system.

Actions F (4-5), F (5-6), F (6-7) consist of studying transformations in a chain of instrumental changes of radiation, incoming to sensitive element of remote sensor. These changes include both spatial (scanning or survey law) and informational changes (transformation of continuous electric signal to digital coded signal).

Second part of scheme (elements A7- A11) shows actions, produced during ground-based processing and production preparing.

Remote sensing products (A11) are the following:

- results of thematic processing, which describe processes existing in the “atmosphere – underlying surface” system. It is necessary to perform the entire cycle of received information processing (A7) – preprocessing, primary and secondary processing - to obtain these results;
- results of secondary processing, which describe estimates or quantitative characteristics of phenomena, occurring at the moment of observation (conventional signs of phenomena) from the reconstructed values of complex phenomenon (conventional signs of complex phenomenon);
- results of primary processing, describing observed complex phenomenon from the reconstructed values of the spectral pattern (from image of spectral pattern).
- results of preprocessing, accounting for the influence of technical facility (communication channel, structural features of remote sensor, orbit parameters and etc.). Essentially, such phenomena are estimations of integrated radiation, incoming to the sensor from the every footprint (pixel). Preprocessing content F (7-4) consists from accounting regularities of information transformation in chains F (4-5), F (5-6), F (6-7);
- information, i.e. direct recording of signal, received at receiving station.

Identified peculiar features of functioning subsystem of data transformation on spatial distribution of phenomena in the “atmosphere – underlying surface” system shows that processes of spectral image formation and its conventional signs are really significant. First of them is connected with influence of sensitive radiation element on output signal. The second one is connected with peculiar features of signal formation on output of remote sensor.

Methods of observations and processing are used to provide remote sensing of environment.

Observational methods agree with a structure of ballistic group of space system, orbit parameters of spacecraft orbit and set of remote sensors. Ballistic group determines the Earth surface coverage and frequency of receiving and renewing of information.

Selection of satellite orbit is important for Earth survey. Circular orbits are preferable for studying and monitoring of the environment. Due to this, similar scale of images is reached along the entire orbit. Orbit inclination, i.e. angle value, formed by equatorial plane and orbit plane, is significant. Depending on inclination orbits can be equatorial (inclination  $0^\circ$ ), polar (inclination  $90^\circ$ ) and inclined. On to polar (or quasipolar) orbits satellite sensors can view the entire Earth surface. The near polar regions are not observed by the satellite sensors, when orbit inclination is less than  $50-60^\circ$ .

The inclination of satellite orbit is an important parameter, because it determines the range of surveyed latitudes. The satellite orbit can't come out of this latitude range. Thus, swathwidth depends on inclination and height of orbit. There is the direct dependence: the bigger is inclination angle and height of orbit, the wider is swathwidth on the Earth surface. Besides circular orbits, used by meteorological satellites, manned space ships and orbital stations, the

elliptical orbits with large height difference in apogee and perigee, are used for permanent observations of global processes on the Earth. Relative to the Sun or the Earth two types of orbits are separated - geosynchronous and geliosynchronous.

Geliosynchronous orbits are used for survey of Polar Regions, providing repetitive surveys of the same Earth surface areas under similar conditions of light in equal time intervals. Satellite orbits can be divided into three groups by height:

- low-orbit (200 - 400 km) are used in flights of manned space ships and orbital stations,
- medium-orbit (500 -1500 km) – meteorological and resource satellites;
- high-orbit (30000 - 90 000 km) – telecommunication satellites and research stations, intended to space study.

Satellites, located on low- and medium-orbits, are used for Polar Regions monitoring.

The method of signal processing at the receiving station will have to provide receiving of coded signal in user format. Processing in this case consists of signal value presentation in output of remote sensor in form suitable for user. *This stage of processing is called preprocessing.*

When product is information about distribution of radiation intensity, incoming to the remote sensor input (spectral pattern), then processing consists of accounting transformations, implemented in the onboard complex (e.g., scanning laws), radio signal transmission channel, i.e. on the stage of transformation of “sensor - coded signal in the receiving station output” information. *The Listed procedures compose preprocessing stage.* This procedure F (4-3) can be made, if transformation regularities are known F (3-4);

In case, when results of planned works consist of presentation of information about estimation or quantitative characteristics at the moment of phenomena observation, methods of processing, based only on transformation regularities on stages of preprocessing and primary processing, can be used. *Such stage is called stage of secondary processing.* It results in distribution of the spectral pattern of phenomenon. Secondary processing can be made only after finishing stages of preprocessing and primary processing.

Typical task of this stage is determining ice thickness from the infrared images.

The possibility to derive ice thickness from infrared images is mainly determined by the differences in temperature and emissivity of water and ice surfaces in thermal infrared band. The spectral channel of 10,5–12,5 micrometer is the most preferable for sea ice characteristics retrieval. In this channel one can neglect absorption in the atmosphere and assume that the sensor measures radiation emitted by the water, ice and clouds. The radiation power, recorded by the radiometer depends both on the temperature and emissivity of the specific surface.

Infrared emission from sea ice originates in the thin surface layer of ice or snow. Ice, snow and sea water have approximately equal emissivity (0,96–0,99), and therefore surface temperature determines the radiation power of these surfaces.

Determination of sea ice characteristics from infrared images is performed in the process of interpretation, using direct, indirect and logical indicators, the same as for visible images. During winter the thermodynamic temperature of the surface of compact sea ice in the Arctic depends on its thickness. This dependence is confirmed by numerous experimental measurements and calculations using thermodynamic models. However, attempts to find practically acceptable solution to the problem of determining sea ice thickness from satellite IR images were unsuccessful for a long time. Mapping of sea ice thickness is possible only for cloud-free atmosphere in cold period.

If product of remote sensing is description of the processes in the “atmosphere – underlying surface” system, then methods of thematic processing include presentation of the processes on base of implementing the entire previous processing cycle (preprocessing, primary and secondary processing).

In general, fundamentals of practical use of remote sensing for study and monitoring of the environment, including the sea ice, are shown.

## 3.2. Airborne observations. General information

### 3.2.1. Introduction

Nowadays there are two sources of information about ice distribution in the Arctic Ocean and in the Arctic and freezing seas – satellite information and visual airborne observations from airplanes and helicopters.

During last 15 years satellite information came on the first place by volume and possibilities of ice observations on large water areas, as a result of technical progress and development of instruments and equipment. From satellite images with resolution varying from 15 m to 5 km it is possible to derive information about ice distribution during 2-3 days and to accomplish tasks, which earlier could be solved only by means of visual or instrumental ice reconnaissance. At that, it is impossible or really complicated to determine some ice characteristics from satellite images. In winter, the following characteristics can be derived:

- boundaries between thin and medium first-year ice, and medium and thick ice;
- boundaries between old and grey ice;
- boundaries between old and first-year ice in summer.

From the other hand, visual and instrumental ice observations from airplanes and helicopters, covering smaller area, allow to specify satellite ice information. At the present airplanes and helicopters are equipped with the GPS satellite navigation system, which significantly improves accuracy of mapping and significantly changed tactics of ice observations.

### 3.2.2. Observations of sea ice from aircraft and helicopter

At present a great experience of producing ice observations from airplanes and helicopters is accumulated in Russia. It was presented in “Manual of producing airborne ice reconnaissance”. Aircraft ice reconnaissance is a special flight to produce visual or instrumental ice observations in water bodies (sea, river, lake, reservoir and etc.).

Airborne ice reconnaissance is divided into two types according to types of used aircrafts: airplane and helicopter.

Aircraft ice reconnaissance has significant advantages comparing to other systems of information collection, because it allows:

- To observe ice cover state shortly and estimate distribution of all principal characteristics on large area in the freezing seas, lakes, reservoirs, rivers and their estuaries;
- To produce both episodic and regular visual, aerial photo, ice thermal and radar surveys of ice cover, using suitable equipment and devices.
- To carry out all types of ice reconnaissance of pre-defined regions in needed time;



- To support ship steering through ice in operative mode;
- To choose optimal flight altitude for observations;
- To process observation data directly onboard of airplane and to transmit information to users operatively via different communication facilities.

Ice reconnaissance from helicopters is the component of a system of ice information collection. It helps to solve tactical tasks of navigation in ice, operation of hydrotechnical structures, supporting fishing and other trades, selection of ice floes for “North Pole” drifting stations.

The peculiar features of helicopter ice reconnaissance are the following:

- Relatively small flight range and small area of ice observation;
- A possibility to base helicopter on coastal sites, icebreakers, research vessels and platforms;
- Large variations of flight speed and altitude;
- A possibility of detailed ice cover mapping and better accuracy of estimating ice parameters;

Helicopter ice reconnaissance in combination with icebreaker or research vessel operation in the ice is a quite effective tool to study spatial structure of ice cover, interaction of ice floes, processes of ice compacting, ridging and melting. Last years selection of drifting ice floes and organizations of drifting stations in the high-latitude Arctic were carried out using helicopters.

### 3.2.3. Flight time.

*Flight time* of aircraft during ice reconnaissance is calculated from the moment of airplane's take-off to the moment of its landing. Ice observer (expert) composes flight route and calculates flight time. Before the flight its route is passed to navigator, if observations are made from the airplane, and in case of helicopter observations - to helicopter commander, who records it in the onboard GPS. During preparing to flight for AN-26, AN-30 airplanes flight duration is 8 hours with speed 250-300 km/h, and AN-30-D airplane – 10 hours.

While making a route for airplane or helicopter, it is necessary to calculate flight time to approach region of planned observations. It is the time interval, when airplane flies without making observations. Airspeed of helicopter of MI-8 type is 160 km/h.

Flight duration is 2,5 hours without additional fuel tanks, 3,5 hours in case of one additional fuel tank, and 4,5 hours in case of two fuel tanks. During special helicopter ice reconnaissance flights the airspeed should be 100 km/h, allowing detailed mapping of ice cover characteristics.

Airborne ice reconnaissance is classified by purpose and technical tools of observations. Reconnaissance is divided into three types by its purpose: research (survey), science-industrial (operative) and special (Fig. 3.2.1), and by technical means into visual and instrumental. Last-named are carried out using side-looking airborne radar, radar ice thickness measurement device and thermal imager.



Fig.3.2.1. Classification of ice reconnaissance types

### 3.2.4. Classification of ice reconnaissance

#### 3.2.4.1. Research reconnaissance

Research ice reconnaissance (survey) is carried out according to programs of scientific and science-industrial Roshydromet departments. Its purpose is studying spatial-temporal changes of ice cover and development of long-term and short-term ice forecasts. As a result of flights, periodically made along standard routes (Fig. 3.2.2 and 3.2.3), in the period 1950-1996 observational ice charts were composed, which allow to estimate general sea ice conditions in seas, lakes, reservoirs and rivers of Russia and to study its changes. Results of this reconnaissance flights were reported to national economic organizations for solving operative tasks of ship navigation, fishery and other practical needs.

Frequency of survey ice reconnaissance depends on intensity of ice cover temporal changes and is determined by organization, which plans reconnaissance, carry out researches and prepare forecasts. Survey ice reconnaissance is normally divided into *monthly and ten-day*. Survey ice

reconnaissance are carried out more frequently on rivers, lakes, reservoirs and some sea areas in the period of ice floating and freezing-over.

Monthly survey ice reconnaissance in the Arctic Seas was carried out in December-May, August, when sea is mostly covered with ice.

Apart from collecting information about concentration, distribution, ridging, ice type and forms program of ice reconnaissance also includes observation of fractures (channels, leads and polynyas) to find out stage of its mechanical disintegration, and also snow cover, pollution, ice thickness and other parameters. Programs of survey ice reconnaissance often included conducting special experiments, testing new observational methods, devices and etc. Some flights in the Arctic included radar (December, May) and ice thickness measuring survey. Results of these surveys were used either for solving research tasks or for direct support of navigation.

Survey ten-day ice reconnaissance in the freezing non-Arctic seas were carried out in winter, and in the Arctic Seas – in summer.

In spring and autumn survey ice reconnaissance in rivers and their estuaries, reservoirs and lakes is reasonable to conduct in short time intervals (3 and 5 days), because ice processes develop very fast.

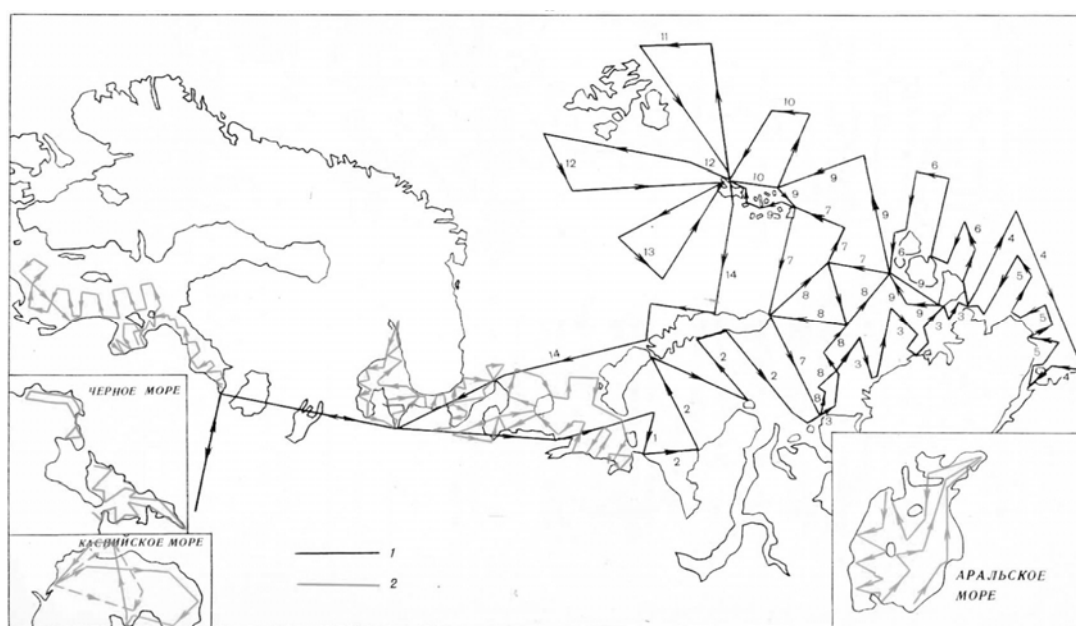


Fig.3.2.2. Standard scheme of monthly survey ice reconnaissance routes. Standard scheme of ice reconnaissance routes. 1— routes in third ten-day period of March; 2 — routes in January, February and March.

Fig.3.2.3. Routes of monthly survey ice reconnaissance in the Kara and Barents Seas in winter.

#### 3.2.4.2. Science- industrial ice reconnaissance

Ice reconnaissance of this type is operational and it is the most important type of ice information collection in seas, rivers and reservoirs for direct support of navigation, fishery and other economical purposes. Ice reconnaissance is conducted according to agreements and programs of production organizations in areas, where and when it is necessary. Science-industrial ice reconnaissance is divided into *operative and tactical* by its purpose.

*Operative* airborne ice reconnaissance is conducted to determine location of ice massifs and ice edge, its concentration, type and other characteristics describing navigation conditions.

In the Arctic Seas and river estuaries *operative* ice reconnaissance were conducted in periods of preparation and implementation of marine operations (Fig. 3.2.4).

*Tactical* airborne ice reconnaissance is carried out in the parts of the route with heavy ice conditions to choose the optimal course of ship sailing (Fig. 3.2.5). As a rule, this reconnaissance is performed episodically, when there is a practical need. A task for ice reconnaissance and its planned route are elaborated before the flight and can be specified in its implementation.

Tactical ice reconnaissance is divided into the following types: areal survey (Fig. 3.2.4), selection of sailing route (Fig. 3.2.5) and barraging.

### 3.2.4.3. Areal survey.

This type of reconnaissance is performed for detailed observation of the route section, where ship steering or expedition works take place. Flight route in this case is several “U-shaped” traverses with a distance of 10-20 miles between them (Fig. 3.2.4).

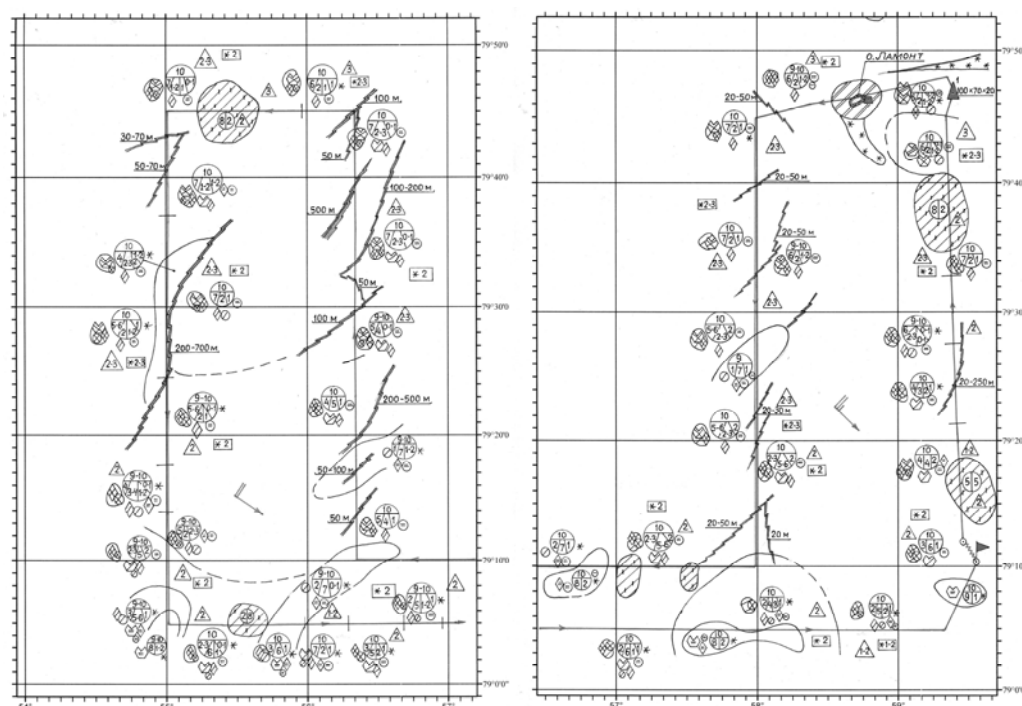


Fig.3.2.4. Area ice reconnaissance in the Barents Sea for 16<sup>th</sup> of April, 2007

The goals of ice reconnaissance, conducted on 16<sup>th</sup> of April, 2007 during the expedition onboard diesel icebreaker «M. Somov» in the Barents Sea (Fig. 4) consisted of the following: determination of the southern boundary of prevailing medium first-year ice (with partial concentration of 5-7/10-th), identification of large ice breccia floes of medium and thin first-year ice (for performing expedition work), detection of leads and fractures for sailing to the north-east, and also icebergs and bergy bits.

#### 3.2.4.4. Selection of sailing route.

This type of ice reconnaissance using helicopters is the most essential for icebreakers and research vessels sailing in the Arctic and Antarctic. During planning of ice reconnaissance ship captain determines general route and, consequently, direction of ice reconnaissance. In case of availability of a satellite receiving station onboard vessel (icebreaker) and in cloud-free conditions leads and fractures can be identified from images and used for sailing. In this case route of helicopter flight is planned beforehand, and ice reconnaissance task is only to specify their location using helicopter GPS and to determine; limiting route parts, such as joints of large floes, and their bypassing ways. Ice expert onboard helicopter directly maps leads and fractures and operatively reports their turning points to icebreaker or ship by radio. The variant, when satellite information is absent and direction of channels and fractures don't match with general sailing route is the most complicated. In this case it is impossible to plan flight route beforehand. After taking off ice expert chooses zig zag route above 10-100 m wide leads, which can deviate from general route on 20-90° and possibly transit into zones of broken ice between large floes. Thus, the main purpose is to select a sailing route to bypass large ice floes. It is necessary, because ship (icebreaker) speed decreases to 1-3 knots when she crosses ice floes, whereas in channels and fractures it equal to 6-8 knots, and in broken ice between floes – to 4-6 knots. At that it is necessary to account wind direction and the selected route must always be from leeward side of floes to avoid ship “wedge” in to joints of floes after leaving lead fracture, or broken ice zone. Ice reconnaissance, presented on Fig.3.2.5, shows the flight for selection of recommended sailing route with general course of 40° in channel, covered by nilas and grey ice.

#### 3.2.4.5. Barraging

This ice reconnaissance is performed in very complicated conditions, when direct ship steering needs uninterrupted sea ice observations and giving recommendations to ship by radio-telephone or showing the optimal sailing route through ice isthmus by airplane (helicopter) evolutions. In case when airplane (helicopter) is within the field of view of ship navigator – barraging is performed by escorting method. When airplane (helicopter) controls ship motion on

longer route and is not always in the field of view of ship navigator - barraging is performed by guidance method.

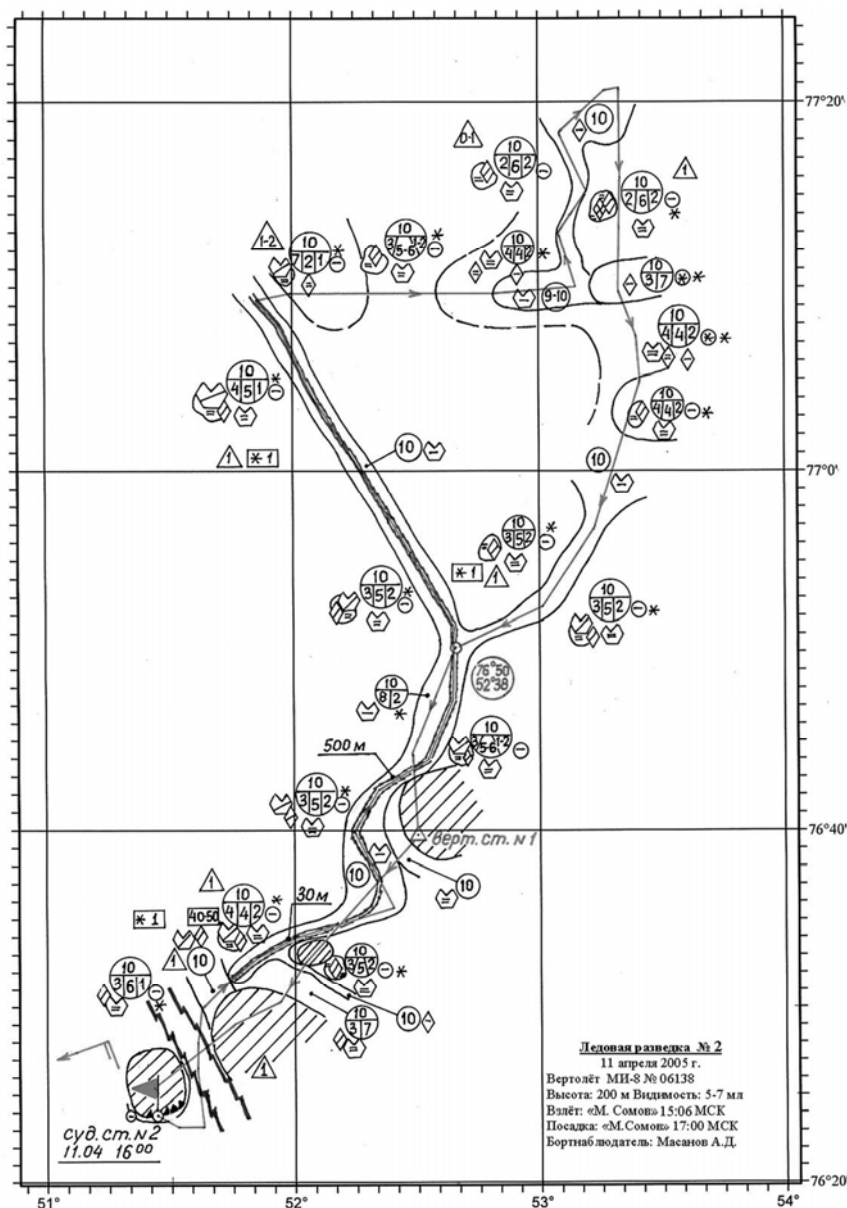


Fig.3.2.5. Tactical ice reconnaissance for selection sailing route for 11<sup>th</sup> of April, 2005 in the Barents Sea

### 3.2.5. Special ice reconnaissance

Special airborne ice reconnaissance is performed to solve search and experimental-research tasks, and also for support of other economical needs (road routing on ice, observations of ice condition in zone of hydro meteorological constructions and etc.).

Special ice reconnaissance is performed episodically by one-time demand, which depends on given purposes, and observes small ice areas. At that, high accuracy of observations and maximum detailing of some ice cover parameters, listed in the task, are necessary. Two types of

special ice reconnaissance are identified at present: searching and polygon surveys (Fig. 3.2.6 and 3.2.7).

#### 3.2.5.1. Searching ice reconnaissance

Searching ice reconnaissance is organized by either research institutes or national economical organizations for detection of:

- ice floes suitable for organization of runways and “North Pole” (NP) drifting stations;
- ice floes suitable for landing of airplanes for conducting scientific (oceanographic, ice research, geophysical and other) studies, and also for deployment of hydrometeorological automatic stations and other objects on drifting ice;
- ice floes with people and equipment, drifting to the open sea;
- places of winter ship anchorage;
- ice islands;
- routes for constructing winter ice roads.

In 2003 during conducting expedition work onboard diesel icebreaker «M. Somov» it was necessary to perform searching ice reconnaissance to select floes of thick first-year and second-year ice brecchia for further morphometric and ice research measurements. These floes were preliminary selected from satellite «NOAA-15» image (Fig. 3.2.6), and then searching ice reconnaissance was performed with landings and control drillings to determine ice thickness (Fig. 3.2.7).

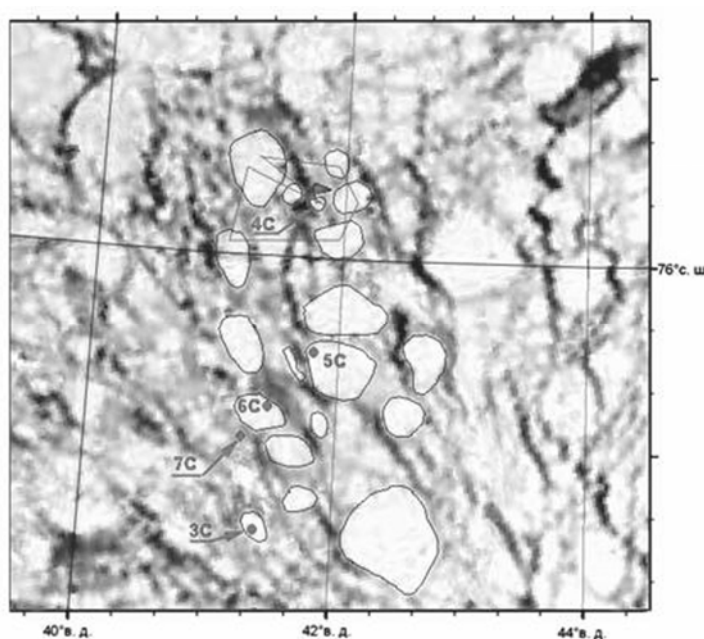


Fig.3.2.6. NOAA-15 Satellite image (6<sup>th</sup> of May, 2003). 3-7C – ship stations (conducting complex of morphometric and ice research observations);  
Line – route of helicopter flight.

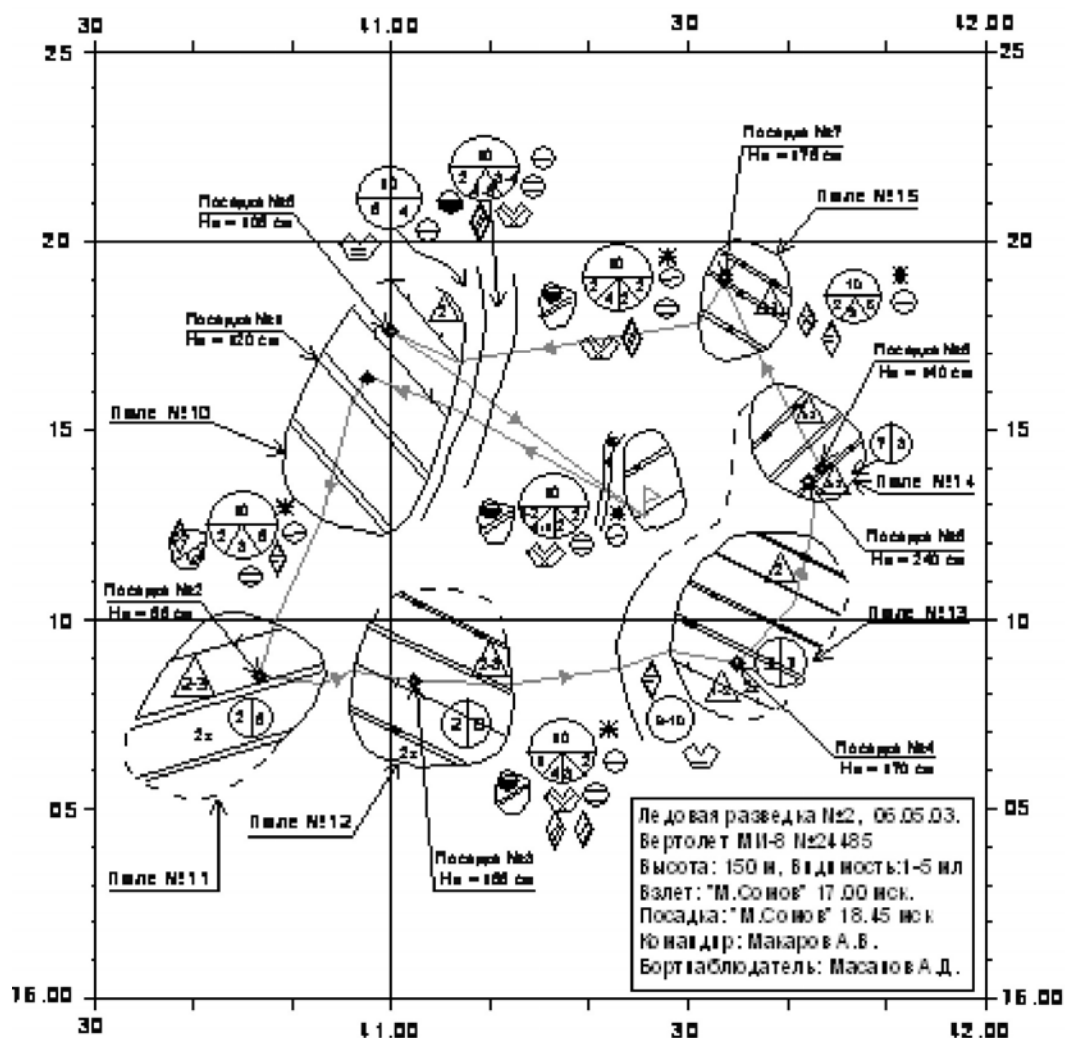


Fig. 3.2.7. Searching ice reconnaissance on 6<sup>th</sup> of May, 2003

### 3.2.5.2. Ground Polygon surveys

Polygon surveys are intended to study thermodynamic processes and ice drift. The tasks of the polygon surveys are the following: detailed mapping of some ice cover parameters (concentration, forms, disintegration orientation and size of leads, cracks etc.) to study destruction and formation of ice cover, motion drift etc.

In 2006 hydro meteorological support of drilling was provided in point XXXX XXXXX as a part of Swedish expedition «ACEX-2004» (Fig.3.2.8). The task of NIB «Soviet Union» consisted of breaking multiyear ice floes to pieces less than 100 m, and icebreaker «Oden» broke them to pieces less than 20-30 m. Icebreaker «Vidar Viking» made drilling and could move, comparative to point of its location, on distance less than 50 m, pushing off separate ice pieces. Areal ice mapping was performed in the 20x20 miles area to provide safe drilling and to determine time of their finishing in case of ice conditions deterioration (appearance of large



floes, which can't be destroyed in 1-2 hours). Flights with parallel traverses on a distance of 2,5 miles between them were performed for this purpose.



Fig. 3.2.8. Location of icebreakers during drilling works (leftmost – NIB “Soviet Union”, central – icebreaker “Oden”, rightmost – “Vidar Viking”).

Methodic of preparing and performing flights was elaborated after three flights. This methodic includes route composition on a distance of 2,5 miles by means of PC. Special computer program for calculation of turning points coordinates was compiled for this purpose. It simplified process of preparing to flight and its conducting. Before the flight forecasters determined ice drift direction for next 12 hours. Using PC the flight route was calculated in such a way, that all observational traverses had to be perpendicular to the forecasted drift direction (Fig. 3.2.9). Then, the route was given to a pilot (as a file) and further it was saved in memory of helicopter GPS. During flight pilot controlled helicopter location relatively to calculated route using GPS monitor. Accuracy of pilotage wasn't worse than 50-100 m. Ice expert mapped all floes along route. If they were more than 2-3 miles, each floe was flied around, and then helicopter returned on its route.

In this section all types of airplane and helicopter ice reconnaissance are presented. In spite of large possibilities of satellite information visual ice reconnaissance hasn't lost its actuality.

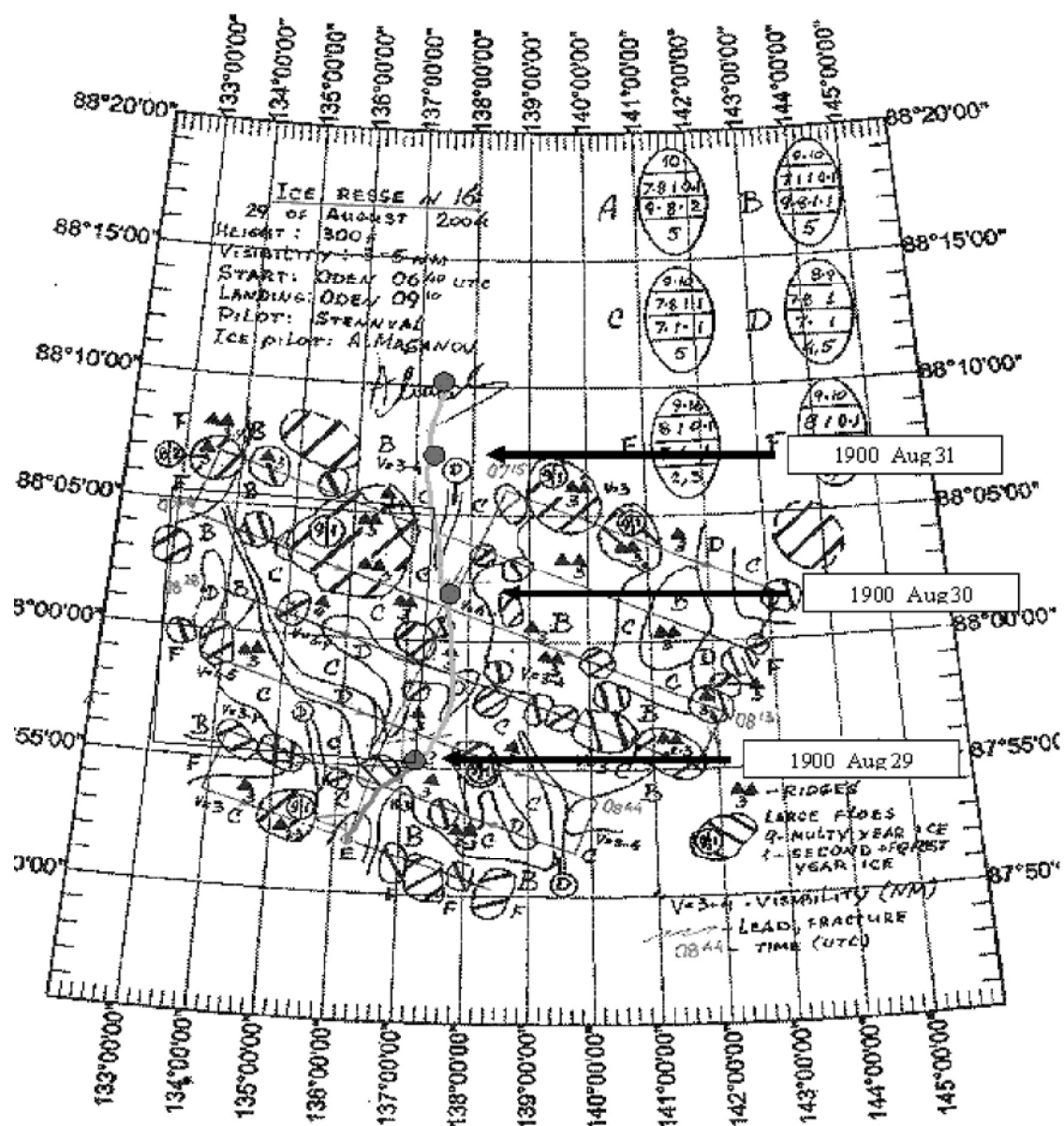


Fig.3.2.9. Polygon ice reconnaissance on 29<sup>th</sup> of August, 2004. Ovals and numbers – sea ice concentration according to international nomenclature; 4. 08-44 time of helicopter turn on route.

### 3.3. Ice observations from the ship

#### 3.3.1 Types of ice observations from the ship.

Large amount of material from ship expeditions has been accumulated for a long period of studying and exploring Arctic. A whole series of most essential parameters of state and evolution of ice cover can't be measured due to transition from airplane ice observations to remote sensing methods (monitoring of ice conditions using satellite). These parameters are the following: ice thickness, ice ridging, melting stage, compacting and etc. Observation materials, accumulated for previous years, and data of ship observations at present time, are the only sources of information on these parameters. Modern technology of ice cover monitoring can be based on them.

The sources of the ship data are the following:

- Special ship observations (small-scale characteristics of ice cover elements and operational indicators of ship motion);
- Navigator's observations, stored in dispatcher's report, duty log, voyage reports of captains and ship hydrologists;
- Summary ice charts of routes (sea operations), placed in expedition's reports, similar to composite ice charts by their spatial resolution;
- Ice observations, provided by foreign specialists.

#### 3.3.2 Special ice observations from the ship.

Purpose of special ice observations from icebreaker is to obtain new natural data to detect regularities of small-scale variability of ice parameters, which significantly influence navigation efficiency, and to account ship operation characteristics during its motion in different ice formations.

Special ice observations have complex pattern, which allow to use obtained natural data for solving both practical and scientific tasks.

Main tasks of special ice observations are the following:

- a) Detailed observations of ice cover characteristics' distribution along the ship route, which essentially influence efficiency, safety and reliability of ship sailing;
- b) Measurement of operation indicators of ship motion in main ice formations with small discreteness;
- c) Natural data obtaining about functioning of the system "ice/ship" and "ice/ convoy of ships";

In period 60s – 90s AARI specialists quite regularly conducted special ship observations of sea ice characteristics distribution along the navigation route and their effect on ship motion.

Regularities, obtained from the observations, formed the basis for ice cover description in the freezing seas as an environment for navigation, and for creating method and empirical model of quantitative accounting of ice navigation difficulty.

Further development of ice cover research, as an environment for navigation, and perception of laws of the system “ice/ship” functioning are connected with studies of influence of spatial-temporal variability of ice cover on the navigation efficiency and safety, development of risk estimations and ice navigation reliability algorithms, and verification of information from modern remote sensing facilities (ERS, RADARSAT high- resolution satellite images, and also passive microwave data from SSM/I and etc.).

In spite of significant amount of special observations, accumulated during previous years, the past capabilities of navigation equipment and technical instruments of ship motion control were not always corresponded to determination of spatial variability of ice cover elements along the navigation route, and visual ice observations were qualitative. Data, obtained in experiments, conducted during icebreakers and ship tests on special testing grounds (mostly in level fast ice), was an exception.

Modern observations are directed to obtain large, and at the same time, detailed information, using new instruments of recording ice cover parameters, and methodic principles, which are traditionally used in work by specialists of AARI. Such approach is substantiated by necessity in comparative analyze of ice and operational indicators, which were obtained during planned tests with data from previous years.

Special visual ice observations are carried out according to two connected directions:

1) estimation of standard complex of ice cover parameters on homogenous parts by both navigation region (within limits of horizontal visibility), and directly along the navigation route (along the ship route in a stripe with a width of sixfold, and with a length of threefold length of ship hull).

The following parameters are estimated in the navigation region:

- Total ice concentration;
- Relative areas, occupied by different ice types;
- Dominant forms of each ice type gradation;
- Dominant degree of ice ridging;
- Dominant ice rafting;
- Orientation types of leads relative to general course of the ship motion (channels, leads and fractures in the ice).

Practice of hydrometeorological support of navigation in the NSR in winter (period of maximum ice propagation) allowed detecting, that one of the most significant ice parameters for navigation is orientation type of leads relative to general course of icebreaker.

Five main types of leads are found:

- Type A – zone of “orientated leads”, where dominant orientation of lead system and general icebreaker course coincides or differ at most for 30°. Icebreaker moves steadily and mostly in leads, sometimes crossing joints of ice floes and rough edges of channels and fractures;
- Type B – zone of “non-orientated leads”, where lead orientation is chaotic or dominant lead orientation differs from general icebreaker course more than for 30°. Icebreaker motion there is less stable, than in zone A and combines sailing in channels with necessity to cross compact ice isthmus (big floes and ice brecchia) during transition from one lead system to another;
- Type C – “zone of higher ice crushing”, where sailing is stable and in the orientated zone, usually with prevalence of broken ice forms (WMO code 1-4);
- Type D – “zone of lead absence”, where icebreaker moves in close ice with concentration of 10/10-th and prevalence of ice floes. Icebreaker motion in this area is determined by combination of “traditional” ice parameters (thickness, ridging and etc.);
- Type E – “zone of decreased ice concentration”. In this zone clearly defined leads are absent, icebreaker moves in ice, which is homogenously distributed in water area, with concentration of 8/10-th or less. This type is typical for edge regions and sailing in spring (period of ice melting).

The following parameters are estimated during navigation:

- Total ice concentration;
- Relative area occupied by different ice types;
- Prevalent forms of each ice type;
- Range of level ice thickness for every ice type;
- Total ridging of ice cover;
- Total melting (decay) of ice cover;
- Depth of snow for every ice type;
- Occurrence and intensity of compacting in ice cover;
- Orientation of compacting axis in ice cover;
- Condition of channel, made by icebreakers (width, tortuosity, ice floes sizes in channel).

Observations are conducted according to “Instruction for ice observations from ship”, elaborated at AARI in 1975.

2) To reveal regularities of small-scale variability of ice parameters, which significantly influence navigation efficiency, in the course of expedition additional observations of the following parameters are conducted:

a) ridging:

- Maximum sail of hummocks;
- Average sail of hummocks;

b) leads:

- Average width of leads;
- Length of sailing route in leads within the limits of homogenous ice zone;
- Time of icebreaker/ship motion in leads, with a width comparable to the beam athwartship.

c) compacting:

- Compacting type (compacting “block”, “joint”);
- Route length in compact joints of ice floes within the limits of homogenous ice zone.

These set of ice parameters is determined for homogenous ice zones. Zone is considered to be homogenous, when all ice parameters change within the limits of accuracy of usual observations.

Measurements of linear characteristics of ice cover are conducted using satellite navigation instruments of new generation (GPS) and ship radar.

### 3.3.3 Recording of ship motion operative indicators

Several operational characteristics, describing ice/ship system functioning, are recorded at the same time with ice parameters for every homogenous zone:

- Time and coordinates of beginning/end of homogenous ice zone to determine its length;
- Convoy warrant order (in case of steering);
- Type of autonomous ship motion (uninterruptedly, with run);
- Time of work with runs;
- Number of runs;
- Time of blocking (in case of ship blocking);
- Type of ship motion in convoy (independent, in tow);
- Time spent on ice breaking around the ship and ship towing;
- Used power of icebreaker’s power installation system;

- Scheme of control panel of icebreaker's power installation system.

Recording of geographical coordinates of ship location (GPS-data) is made on the HD of PC with small discreteness (~ 1 minute) during the entire period of sailing in the ice. This type of information allows receiving pattern of ship velocity distribution in main ice formations and homogeneous ice zones, coefficient of navigation route meandering.

#### 3.3.4. Meteorological observations.

Meteorological observations from ship/icebreaker consist of observations of the following parameters:

- Air temperature;
- Direction and velocity of wind;
- Atmospheric pressure;
- Horizontal visibility;
- Type and nature of atmospheric phenomena.

Meteorological observations are made using automatic weather station. Data of weather station is automatically recorded on HD of PC, and also is recorded once a watch (4 hours) or when any weather parameter sharply changes. Observations of horizontal visibility are visually and constantly made.

Ship observations are conducted around the clock from the bridge (6 watches, each for 4 hours).

Change of geographical location of ship (drift) is determined every hour during icebreaker/ship station to conduct experiments on ice.

#### 3.3.5 Navigator's ice observations.

Ice observations, conducted by navigators, consist of generalized data (for particular time interval, (usually for one watch) about main ice parameters in navigation zone with geographical coordinates and time (date) of beginning/end of navigation in this area. In case of abrupt changes in ice conditions – strong compacting, ship approaching ice edge or near edge divergence and etc., navigators record time of ice phenomena and its geographical coordinates.

Navigator's ice observations usually include information about the following ice parameters:

- Total ice concentration;
- Ice type composition;
- Dominant forms for each ice type;
- Total ridging of ice cover;

- Total degree of destruction (melting) of ice cover;
- Compacting and its intensity in the ice;

The operation factors, shown in the recording of navigator's observations, are the following:

- Time and coordinates of generalized area beginning/end;
- Convoy order (in case of steering);
- Type of autonomous ship motion (uninterruptedly, with runs);
- Time of blocking (in case of ship blocking in ice);
- Type of ship motion in convoy (time, spent on ice breaking around the ship, its towing and etc);
- Used power of icebreaker's power installation system;
- Scheme of control panel of icebreaker's power installation system.

Meteorological observations include observation of the following meteorological parameters:

- Air temperature;
- Direction and velocity of wind;
- Atmospheric pressure;
- Horizontal visibility;
- Type and nature of atmosphere phenomena.

These observations are obligatory recorded in the duty log, and are also included in dispatcher's reports.

### 3.3.6 Ice observations, made not by methodic of AARI.

Ice observations, made not by methodic of AARI, contain generalized data, for predefined time interval (normally for 1 or 3 hours), about ice parameters complex in the navigation region with geographical coordinates and time (date) of beginning/end of navigation in this zone. A set of observed ice parameters in different expeditions can significantly change. Nevertheless, it usually contains data about the most important parameters: total concentration and ice type composition in the region of ship navigation, ridging characteristics, leads and puddles, ice thickness and snow depth, compacting and etc. Apart from that, this type of observations contains data about velocity and type of ship motion, indicators of ship power installation work; meteorological data and notes.

This type of observations is more detailed analogue of navigator's observations.



### 3.3.7 Other data.

When ship ice observations were not conducted or observational data is not available, there is data that in some cases allows estimating difficulty of ice navigation in the Arctic Basin. Information about time and geographical coordinates of ship (with discreteness of 1-10 minutes), received from satellite navigation system of the new generation (GPS), can be referred to this data.

Regularities of spatial-temporal variability of ice cover elements, discovered in the course of ship observations, and their influence on ship motion (convoy of ships) are used for:

- Adaptation of empiric model of quantitative estimation of ship navigation difficulty in ice;
- Development of empiric-analytic model of ship motion (convoy of ships) in real ice, based on theory of ice resistance to ship motion and empirical relations;
- Development of algorithms of reliability and risk assessment for navigation of different ship types in the ice;
- Development of algorithms of computer simulation marine transport system functioning;
- Creating a real base for special meteorological support of marine navigation – choice of optimal variants of navigation, development of new methods of specialized ice forecasts and etc.;
- Verification of modern remote sensing (satellite) data about ice parameters distribution along the navigation route, especially of those that cannot be detected from satellites at present (compacting, ridging, rafting, ice thickness, decay and etc.);
- Analysis of tensometric measurements of loads distribution on tanker hull in different ice conditions.

### 3.3.8 Recording of observation data

Ice observation data is recorded on the following carriers:

- Observation log. It is filled during observations in accordance with a set form.
- Digital observation log. Development of digital version of observation log is carried out at the moment at AARI. This log consists of program complex, which interface allows ice expert to record ice parameters values on computer HD in real time, and hardware complex, which includes PC and receiving indicator of GPS.
- Digital tables (database)

### 3.3.9. Database composition (structure)

Database of ice navigation conditions was formed for storing, systematization and analysis of ice observations from ships. Database is permanently renewing and consists of results of ship observations in the Arctic and other freezing seas and in the Arctic Basin

The database consists of two blocks:

Block A – special ice observations from the ship.

- Element (line) of database is homogenous ice zone with fixed geographical coordinates and time (date) of beginning/end of sailing in it;
- Element (line) contains: ice cover parameters, separately for the sailing region, and separately directly along the sailing route, operation indicators of ship motion; notes.
- Values of characteristics (indicators) of database can be observed (measured), calculated, absent (or non-observed).

B) Ship ice observations, conducted by navigators and other specialists and carried out not by methodic of AARI.

- Element (line) of database is generalized characteristics of navigation ice conditions for particular time interval (watch, one hour and etc.), with fixed geographical coordinates and time (date) of beginning/end of sailing in this zone;
- Element (line) contains: ice cover characteristics – by zone of navigation (within limits of horizontal visibility); operation indicators of movement; meteorological conditions of navigation, notes;
- Values of characteristics (indicators) of database can be observed (measured), calculated, absent (or non-observed).

### 3.4. Ship telemetering system for ice thickness recording

Ship telemetering system is related to systems of image perception and consists of television camera, images processing and representation devices to obtain ice floes parameters, e.g. their size.

Known device, used for exploratory survey of ice thickness during ship motion, is a measuring rod on line. The rod is a wooden desk with a length of 50 cm and a width of 7-10 cm, divided into decimeters. Rod sections with length of 1 dm are alternately colored in black and white, or in white and red. A hole for the line is made in the middle of rod, “knop” is tied on the reverse side. This device has the following usage: rod is thrown on the ice, where it serves as a scale for visual determination of ice floes thickness, which are turned near perpendicular at the shipboard. Low accuracy of ice thickness determination is the disadvantage of this method.

Ice meter by Tsurikov and Pervakov, determining ice thickness during ship motion, is also known. Ice meter (Fig. 3.4.1a) consists from a metal bar 1 (length 60 cm). Bracket 2 is fixed at the end of the bar with a short tube 3, parallel to the bar. Movable clip 4 is placed on the bar with a supporting screw 5. Metal frame 6 with transparent plate (14×22) is fixed to the clip. Straight-line grid with 2 cm scale division is put on the plate. One section of the grid is divided to smaller scale divisions - every 4 mm. 1 cm scale divisions are put on the bar.

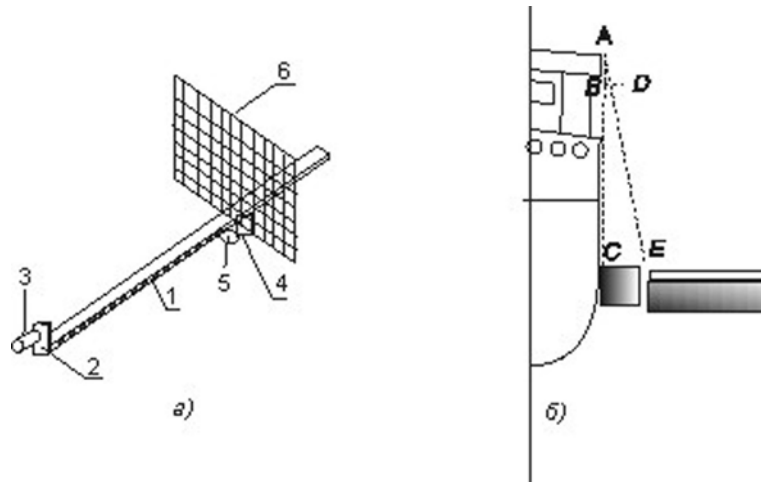


Fig. 3.4.1. An exploratory survey of ice thickness during ship motion

Zero of this scale coincides with the top end of the tube, which is put to observer's eye. Rubber eye shade is worn on the tube to protect observer's eye from contact with cold metal. Ice thickness measurements by ice meter are based on solving of similar triangles (Fig. 3.4.1b), big cathetus are distance from observer's eye to measured object – near-perpendicular turned ice floe AC and the distance from observer's eye to frame AB, and small cathetus are measured thickness CE and its projection onto grid BD.

Unknown ice thickness CE can be found from equation (1):

$$CE = \frac{AC \cdot BD}{AB} \quad (1)$$

Height of observer eye above ice surface AC must be known for measurements. When ice floe is located abeam, a number of grid divisions BD, corresponding to ice floe thickness CE, is marked. The only disadvantage is a quick observer's eyes tiredness during the work, which limits quantity of received information.

Measurement of ice floe thickness in ship telemetering system is carried out by means of calculating distance between two markers in the images of near-perpendicular turned floes. For this purpose television camera, digital to analog converter and manipulator ("mouse", trackball and etc.) are included in the composition of known device, using which light markers, marking start and end of interval, are located in the image.

The essence of this device is illustrated by drawing, presented in Fig. 3.4.2. It explains connections between television camera, digital to analog converter, manipulator, processing and imaging devices.

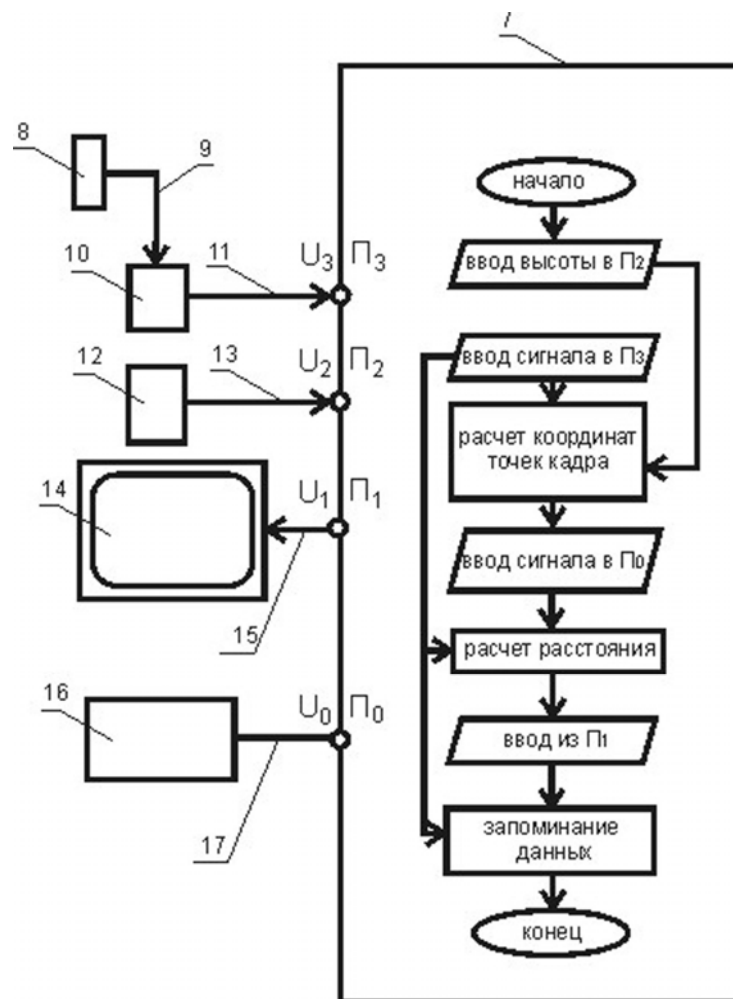


Fig. 3.4.2. System work scheme

$\Pi_0$ - $\Pi_2$  – input/output port of the processing device,  $U_0$ - $U_2$  – corresponding input (output) signals.

Television camera 8 is connected by cable 9 with the analogue-digital converter 10, which output signal  $U_3$  by cable 11 comes to connector  $\Pi_2$  of the processing device 7. Data about camera height on the ship bridge as a signal  $U_2$  are set into its input connector  $\Pi_3$  using input device 12. Processing device 7 is connected with a monitor 14 by cable 15 and with manipulator 16 by cable 17.

Working principal of this device is the following.

Television camera is located on the ship bridge in the position of sea surface sighting (point "A" on Fig. 3.4.1 б). Values of height above sea surface and inclination angle of optical axis of camera are recorded. Signal  $U_2$  about corresponding data using data input devices 12, representing a keyboard, comes to input  $\Pi_2$  of the processing device 11 by cable 13. Digital signal of perspective image  $U_3$  as a matrix of digital brightness values on output of analogue-digital converter 10 by cable 11 comes to input  $\Pi_3$  of the processing device 7, which calculates a distance between points, formed on monitor 14 as light markers, depending on camera height and position of matrix elements of digital signal  $U_3$ , which correspond to the location of markers. Image, combined with marker, comes to the monitor screen 14 as a signal  $U_1$  through output  $\Pi_1$ . Digital matrix of image signal and values of distance between markers – ice floes size comes to data recording device under command from the data input device 12.

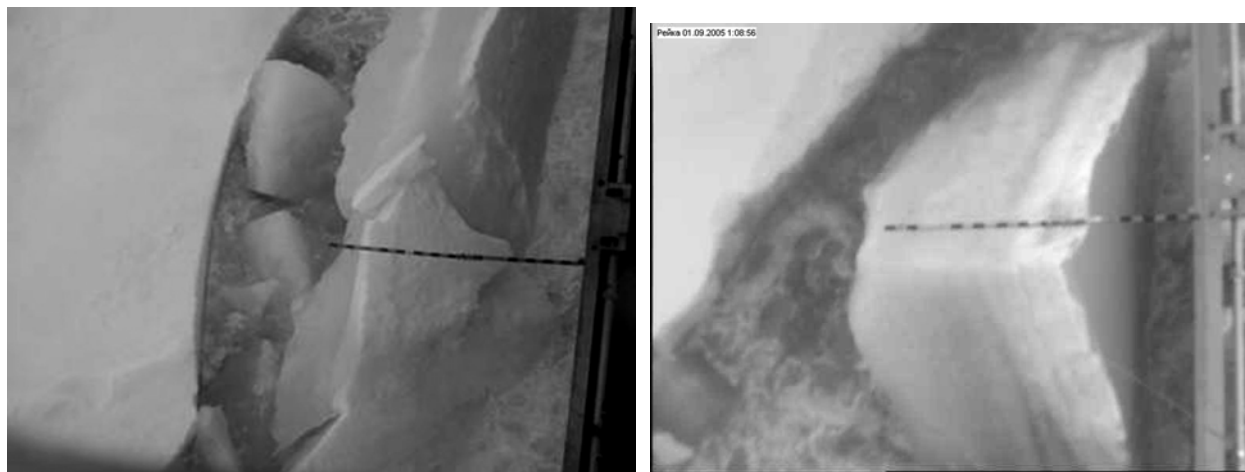


Fig. 3.4.3. Types of near-perpendicular turned ice floe a) and image on monitor б)

Long-term exploitation of the ship TS in 2004-2005 (21<sup>st</sup> and 23<sup>rd</sup> voyages of R/V «Academic Fedorov»), in 2006 onboard diesel icebreaker «Norilsk Nickel» (April), NIB «Yamal» (5 voyages, May-August), in 2007 onboard NIB «Rossiya» (2 voyages, May-June), R/V «Academic Fedorov» (26 voyages, July - September), in 2008 onboard tanker «Vasily Dinkov» (1 voyage, March), NIB «50 years of Victory» (2 voyages, July), NIB «Yamal» (2

voyages, August), R/V «Academic Fedorov» (28 voyages, August-September), showed both its efficiency and reliability during operation in extreme conditions (temperature changes, humidity, vibration) and high mobility and simplicity in operation, which allowed untrained staff to work with it. Photos of reversed ice and its image on the monitor are shown in Fig. 3.4.3

Necessary to mention, that in 2004-2005, when the first version of the telemetering system was in operation, amount of information was significantly less, than in 2006-2007. It can be explained, firstly, that in 2006 TS was renewed – black and white low-resolution camera was placed by a color high-resolution camera.

Material, received during this time, consists of more than 20000 measurements of ice thickness in 2006 (5 voyages of NIB «Yamal»), in 2007 - about 5000 (voyage of NIB «Rossiya»), more than 20000 in the 26<sup>th</sup> voyage of R/V «Academic Fedorov», in 2008 - 2000 images (voyage of tanker «Vasily Dinkov»), more than 20000 (voyages of NIB «50 years of Victory», «Yamal»), more than 10000 in the 28<sup>th</sup> voyage of R/V «Academic Fedorov».

This data bulk (more than 70 thousand images during 3 years of STS operation (2006-2008)) is of great scientific and practical interest. Receiving of such data massif by contact methods (ice drilling) is practically impossible, though its processing must be made by people with special interpretation skills and is quite time consuming.

Processing of the TS recordings consists of the following stages:

1. Archiving of program buffer «Tayfun» into files \*.arv for every 4 recording hours, i.e. 6 archive files per day.
2. Selecting informative frames from archive files, their conversion and recording in \*.jpeg format.
3. Writing a comment to the archive file for its further recording in “TS database”.
4. Registering and recording in file information about ship operation «with runs» (number of runs, single and total duration).
5. Registering and recording in file information about ship motion along fractures in close ice (time of beginning and end of fracture).
6. Recording and formation of database about biota accumulation under the ice.
7. Recording and formation of database about animal traces (bear, seal and etc.) on the ice.
8. Measurements of ice thickness and snow (firn) depth in images (\*.jpeg files) with their automatic recording to the thickness database.

At that, clauses 2, 4-7 are made simultaneously with archive browsing.

It is necessary to mention, that clauses 2 and 8 are the most laborious, because with a recording discreteness of 1 frame/s, an operator must browse almost 14,4 thousand frames during processing of one archive file (4 hours). Even if speed of browsing is 2-3 frames per second,

only browsing of daily recording will take from 8 to 12 hours, not accounting time necessary for identification of “inversion” and saving frame as \*.jpeg file.

During processing average number of informative frames only by ice thickness (not accounting other parameters) amounted to almost 100 recordings per hour in some days. E.g., on 27.07.08 the total number of frames, selected for ice thickness estimates, amounted 1816, in some days of 2007 during motion in close ice – more than 2500 frames per day. Totally, this circumstance increases processing time minimum twice.

Speed of processing mostly depends on either operator’s qualification or experience of processing.

85% of STS recordings from four polar voyages of NIB “50 years of Victory” and “Yamal” were preprocessed (clauses 1-2 in processing description), and 20075 information frames were selected during 28<sup>th</sup> voyage of R/V «Academic Fedorov».

Total volume of recordings in expedition «Arctic-2008» for 19 days of motion in close ice is equal to 224 hours (0,8 million frames, Table 3.4.1).

Apart from that, materials about accumulation of carotinoids under the ice during the expedition «Arctic-2007», were prepared and passed to VNIRO specialists from the recordings of STS.




The reason for system modernizing was prepared in 2008 from analyzes of operation notices and suggestions about STS work in 2006-2007.

As a result, main component blocks and materials, necessary to construct a new system, were obtained by the early August, 2008, including:

1. Television camera CNB AP800 with remote control function.
2. Program «Tayfun», version V147.0 with electronic switch HASP (3 sets).
3. Frame of image grabber «Tsunami -4» to connect with 4 cameras.
4. Thermal case AWH32 with cleaner and washer.
5. Support rotating device AiPT45.
6. Telemetering signal receiver RTS-9.02M.
7. Control console MG-K102 with a function of control of support rotating device inclination/turn, zoom/focus of television camera, switch on/off of cleaner/washer of thermal case.
8. Deck plate of support rotating device.
9. Power cable, signal cable, coaxial cables for switching devices.

After the principal scheme of commutation of the system devices was developed by specialists of research laboratory of ice navigation of the department of ice regime and forecasts, it was assembled and checked in the laboratory.

Table 3.4.1 – Composition of TS data archive in the expedition «Arctic-2008»

№	Date	Time of file start	File	Work characteristic of TC	Preprocessing				Notices	
					Ice (number of images)	Runs (number)	fractures (total time)	GPS	 full recording	
									 partial recording	
									 thickness processing	
	Expedition "Arctic-2008", 28 <sup>th</sup> voyage of R/V "Academic Fedorov", Arkhangelsk - Wrangel Island- NP-36 - Arkhangelsk									
1	23.08.08	0:00	230808-00-04.arv							
2		4:00	230808-04-08.arv							
3		12:00	230808-12-16.arv							
4		16:00	230808-16-21.arv							
5	28.08.08	8:00	280808-08-12.arv							Survey of Wrangel Island 08-09
6		16:00	<b>280808-16-21.arv</b>							<b>Adjustment SW 1625-1655</b>
7	29.08.08	0:00	290808-08-12.arv							
8	30.08.08	8:00	300808-08-12.arv							
9		12:00	300808-12-16.arv							
10		16:00	300808-16-21.arv							
11		20:00	300808-20-24.arv							
12	31.08.08	4:00	310808-04-08.arv							
13		8:00	310808-08-12.arv	<b>10.19 clock was put 10 min forward. Before clock was always slow</b>						
14		12:00	310808-12-16.arv							
15		16:00	310808-16-21.arv							
16		20:00	310808-20-24.arv							
17	01.09.08	0:00	010908-00-04.arv							
18		4:00	010908-04-08.arv							
19		8:00	010908-08-12.arv							
20		12:00	010908-12-16.arv							
21	02.09.08	4:00	020908-04-08.arv							
22	05.09.08	8:00	050908-08-12.arv							СП-36, ice by shipboard
23		12:00	050908-12-16.arv							СП-36, ice by shipboard
24	06.09.08	8:00	060908-08-12.arv							Panorama
25	08.09.08	8:00	080908-08-12.arv							
26		12:00	080908-12-16.arv							
27		16:00	080908-16-21.arv							
28		20:00	080908-20-24.arv							
29	09.09.08	0:00	090908-00-04.arv							
30		4:00	090908-04-08.arv							
31		8:00	090908-08-12.arv							
32		12:00	090908-12-16.arv							



33		16:00	090908-16-21.arv						
34		20:00	090908-20-24.arv						
35	10.09.08	0:00	100908-00-04.arv						
36		4:00	100908-04-08.arv						
37		12:00	100908-12-16.arv						
38		16:00	100908-16-21.arv						
39	11.09.08	0:00	110908-00-04.arv						
40		4:00	110908-04-08.arv						
41		12:00	110908-12-16.arv						
42		16:00	110908-16-21.arv						
43		20:00	110908-20-24.arv						
44	14.09.08	12:00	140908-12-16.arv						
45		16:00	140908-16-21.arv						
46		20:00	140908-20-24.arv						
47	15.09.08	0:00	150908-00-04.arv	00.44 – inconsistency for 9 min – corrected for 00.53					
48		4:00	150908-04-08.arv						
49		8:00	150908-08-12.arv						
50		12:00	150908-12-16.arv						
51		16:00	150908-16-21.arv						
52		20:00	150908-20-24.arv						
53	16.09.08	20:00	160908-20-24.arv						
54	17.09.08	0:00	170908-00-04.arv						
55		4:00	170908-04-08.arv						
56		8:00	170908-08-12.arv						
57		12:00	170908-12-16.arv						
58		16:00	170908-16-21.arv						
59		20:00	150908-20-24.arv						
60	18.09.08	0:00	180908-00-04.arv						
61		4:00	180908-04-08.arv						
62	19.09.08	16:00	190908-16-21.arv						FJL region, test survey
<b>Total 56 files arv (224 recording hours) for 19 days</b>									<b>0,806 mln of frames</b>
		1 file	Program calibration						
		5 files	Panoramic survey						

Further assembly and adjustment works of STC-M was conducted during the 28<sup>th</sup> voyage onboard R/V «Academic Fedorov».

Experience of STC-M operation during the expedition «Arctic-2008» showed, that this modification is efficient; and simplifies work of personnel (watch of crew SHEMA on the bridge). Going out to the bridge to clean a box windscreen became unnecessary due to remote control of washer and cleaner. Camera positioning to zone, selected for survey, zoom adjustment and focusing can be made by one operator using the control console.

Apart from that, possibility to control local system using remote access allows to control work of system and partly control it by the net.

Implementation of support rotating device in the system made possible remote control for operational pointing and survey of any objects within 180° sector horizontally and from +20° to -80° vertically by ship starboard. Camera has optical zooming of 26× and automatic focusing, thus, quality of received image is quite high.

At present usage of remote control in corpore is impossible due to technical limitations of telemetering signal receiver. Only focus adjustment and optical zooming are available in the given band (2×10×). Function of camera control will be available in corpore after hookup of second receiver. Flowchart of STC-M and general view of main system components are presented in Fig. 3.4.4 – 3.4.6.

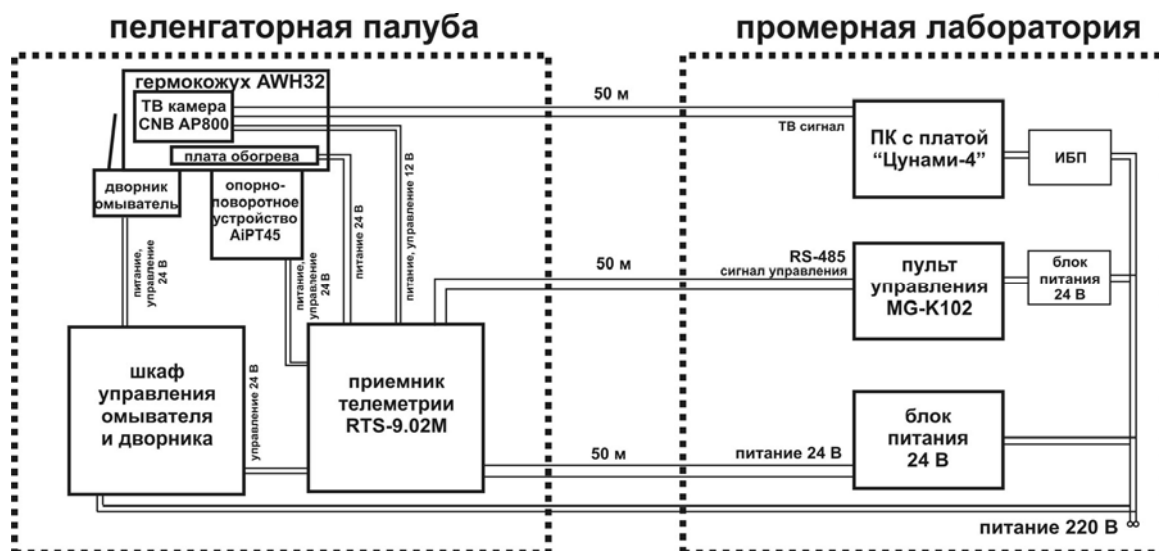


Fig. 3.4.4. Flowchart of ship telemetering system STS-M



Fig. 3.4.5 General view of STS-M

1 – thermal case Wizebox AWH32; 2 – windscreen wipers and washer of thermal case; 3 – Support rotating device AiPT45 on special piece; 4 – case for control of washer and cleaner; 5 – telemetering signal receiver RTS-9.02M



Fig. 3.4.6. Thermal case with cleaner and washer, fixed on the support rotating device

### 3.5. Dangerous ice phenomena and ice formations

#### 3.5.1. Types of dangerous and unfavorable ice phenomena

*Dangerous ice phenomena (DP)* – is hydrometeorological phenomenon or complex of hydrometeorological values, which can be dangerous for people due to their size, intensity or duration. It can also significantly damage economical objects and population.

*Unfavorable hydrometeorological phenomenon (UHP)* – is hydrometeorological phenomenon, which significantly complicates or impedes activities of individual enterprises and sectors of economics.

Presence of sea ice causes serious risk during conducting any type of work on drifting ice and fast ice. Safety and efficiency of navigation, marine work, functioning of hydrotechnical constructions depend on ice cover state.

Generally, value of sea ice impact on objects is defined by amount, concentration and thickness of ice, parameters of its motion, and ice strength.

Ice phenomena can't be dangerous or safe, they pose a threat only within limits of their impact on particular objects and influence on certain types of work. Ice conditions and ice phenomena can passively influence or actively impact on industrial objects, threatening people's safety, transport, hydrotechnical constructions and work realization.

There are two categories of potential threat to productive activity in connection with ice cover impact:

- *Dangerous ice phenomena (DIP)* of active impact of drifting sea ice, which are formed by dynamic factors, occur suddenly, operate in limited region and in limited time interval;
- *Unfavourable hydrometeorological phenomenon (UHP)* of passive effect of drifting ice and fast ice are determined by presence and state of the ice cover, which is mostly formed by thermal factors, occurs gradually and exists in large region during long time period.

Influence of unfavourable ice conditions and impact of dangerous ice phenomena directly determine level of safety and degree of economical efficiency of navigation, transportation on fast ice, work of offshore above-water platforms, pipelines and terminals for uninterrupted tanker fueling. Diverse influence of the sea ice on safety and efficiency of building hydrotechnical constructions is especially significant. Each object is specific, and due to this differently react to different ice impact.

*Navigation.* Efficiency of ice navigation mostly depends on thickness and concentration of drifting ice. The limiting parameters of ice are determined according to type and ice class of ships.

Ships can spend plenty of time traversing ridges. Thus, ridges in drifting ice decrease economical efficiency of cargo transportations approximately proportional to their concentration.

In straights and along coasts quite rarely occurs a strong local ice flow (“ice river”), which can complicate maneuverability of ship and cause emergency.

The most significant decrease of cargo transportation efficiency is caused by ice compacting. Average cruising speed of ship normally decreases under often and long ice compacting on the navigation route. Most emergencies, ship damage and even their wreck occur under very strong compacting.

In autumn and winter, when the air temperature is below  $-10^{\circ}\text{C}$ , ice adherence to a ship hull and icing of deck-erections can occur when ship sails near more or less large areas of young ice or open water. Partial decrease of ship speed and maneuverability or even their complete loss occurs when ice adheres to the ship hull.

*Works on the fast ice.* Efficiency and safety of works on the fast ice mostly depend on thickness and strength of ice, which corresponds to the melting stage of ice cover. Its limiting parameters are presented in the documents, providing safe works on the fast ice. These parameters are determined for particular type of works taking into account static pressure and dynamic impact of carriers.

Constructive strength of the near edge part of the fast ice is important during unloading on the fast ice. This part of the fast ice is less stable. Thus, presence of ridges and barriers of hummocks, which are partially grounded, reinforces constructive strength of the near edge part of fast ice.

*Offshore above-water platforms and terminals, placed on the ground.* These constructions are the most important during oil and gas exploration. Platforms and terminals can be effected by more or less significant pressure from drifting ice at the sea level. The value of pressure is proportional to the ice drift velocity, and total ice mass, interacted with construction. At that, the total ice mass, interacted with the construction, depends on thickness, concentration, and ridging of homogenously moving ice. Results of forces are mostly determined by strength and size of ice floes, and also by morphometric peculiar features of engineering objects location and peculiar features of dynamic effect of their interaction with ice cover.

*Buried constructions for oil and gas exploration.* This construction isn’t effected by force of drifting ice at the sea level. Underwater parts of moving icebergs, floebergs, large hummocks and dragging of large floes piles on the bottom, which are formed during pressing of large drifting ice masses, can be dangerous for them. Traces of contact of these ice formations and piles with the sea bottom are furrows of bottom exaration. Unfavorable effects of covering underwater metallic constructions with the ice, can’t be excluded.

*Year-round uninterrupted fueling of tankers.* Concrete constructions of terminals can resist ice drift pressure. However, it doesn't mean that they can fuel tankers. Probably, large piles of broken ice can be formed around the terminal during ice pressure from different directions, which can be grounded like stamukhas, when sea depth is less than 20 m. It can be supposed, that this phenomenon can prevent tanker fueling for a long time. However, probability of terminal blockage by broken ice can widely change for different regions.

*Navigation channels.* If terminal is located in shallow fast ice zone (for protection from drifting ice pressure) with one or several navigation channels, connecting it with the sea area, there will be a danger of filling these channels with broken ice during rafting of drifting ice on the fast ice edge. Such phenomenon can probably prevent ship approaching to terminal or coast for a long time. However, its probability can change significantly in different regions.

*Underwater pipelines laid in the ground.* Underwater parts of moving icebergs, floebergs and large ridges, and also dragging of crushed ice against sea bottom over the pipeline during formation of grounded hummocks, as well as their subsequent effect are of great danger for the underwater engineering constructions. Furrows with different sizes (result of ice exaration) are observed during sonar observations of the sea bottom in many sea ice regions. Intensive erosion of the sea bottom around grounded hummocks and intrusion of their keels for 1-2 m into the bottom was found during their underwater observations.

*Coastal constructions and constructions near the coast.* In some regions of the Arctic coast piling of young ice on the shore is observed in autumn. During piling ice can cause exaration impact on the bottom of the coastal shoals and on the shore at a distance up to 100 m from the shore line. This ice piling on the shore can be dangerous for coastal buildings.

In autumn-spring period intensive storm can produce strong impact of ice floes in shallow coastal zone, if broken fast ice with thickness of about 1 m and hummock pieces are observed occur near the coast. This "ice storm" can be dangerous for coastal constructions.

*Building of hydroengineering constructions.* It is supposed, that building of hydroengineering constructions is carried out if the working area is totally free from fast ice and drifting ice. At that, the efficiency of construction work is influenced not only by dangerous ice phenomena, but mainly by unfavorable ice phenomena. Information about ice-free period duration, terms of water area clearing from ice, terms of ice formation beginning and young ice growth up to values of 10-15 cm and 25-30 cm are extremely significant for effective planning and implementation of construction works. Duration of ice-free period in the Arctic Seas is very short and annual terms of clearing and freeze-up change within wide limits. Orientation on average terms can be economically unprofitable.

Analysis of typical effect of ice cover in the freezing seas on navigation and ice impact on engineering constructions allows selecting dangerous ice phenomena (Table 3.5.1) and unfavorable ice conditions (Table 3.5.2). Danger of ice phenomena is taken into account in connection with their impact on particular engineering objects and influence on conducting particular type of work. Thus, when new specific hydroengineering constructions and type of work emerge, these lists can be specified and supplemented.

Table 3.5.1. List of dangerous ice phenomena

Ice phenomena	Hazard
Ice piling and pressure	Damage of above-water, buried and bottom constructions.
Moving ridge	Threat for buried and bottom constructions.
Strong ice compacting	Emergencies, damage of ships and above-water constructions
Intensive ice drift, including «Ice river»	Emergency situation for ships due to loss of maneuverability.
Ship hull covering with ice	Decreasing of ship velocity up to full stop. Emergency situations.
Ship icing, hydro technical construction icing	Loss of ship stability. Statistical tensions on elements of engineering constructions.
Ice floes and fast ice destruction under outer load	Collapsing of airplanes, helicopters and ground vehicle under the ice. People death.
Separation of fast ice in places of work	Emergency situation during unloading on the fast ice. Threat to people, ground vehicle and cargoes.
Ice piling	Shore line exaration. Threat to coastal buildings.
“Ice storm”	Shore line exaration. Threat to coastal buildings.

Table 3.5.2. List of unfavorable ice conditions.

Ice phenomena	Hazard
Drift ice condition (large thickness and etc.)	Direct influence on exploitation velocity of transport vessels.
Easy and heavy ice compacting	Decreasing of exploitation velocity of transport vessels.
Results of ice rafting, breaking and piling	Blockage of approaches to terminals and ship channels by broken ice
Late terms of ice remaining in water area	Late terms of navigation without icebreakers, constructing or repairing works. Small economic efficiency of work.
Early terms of ice remaining in water area	Early terms of navigation without icebreakers, constructing or repairing works. Small economic efficiency of work.

Organization of specialized system of monitoring and forecasting ice conditions is necessary to minimize ice impact on marine transportation system at the stage of operation. Ice

cover monitoring provides regular acquisition, processing, analysis and distribution of the current sea ice information in the terminal area and along the sailing route to support navigation safety and conducting tie down operations, as well as for ecological safety of water area.

Ice formations (big floes of multiyear ice, ridges, grounded hummocks, icebergs and etc.) can have a dangerous and unfavorable impact on different types of productive activity. The list of dangerous and unfavorable ice formations is presented in Table 3.5.3.

Table 3.5.3. List of dangerous and unfavorable ice formations

Ice formation	Hazard
Giant and vast ice floes of deformed or multiyear ice	Damage of above-water, buried and bottom constructions. Complicated occurrence of tie-down operations.
Ridges and floebergs	Threat to buried and bottom constructions. Complicated occurrence of tie-down operations.
Stamukhas	Statistic load. Dynamic load under level fluctuations. Influence on under-water pipeline.
Icebergs and bergy bits	Emergency situation, when iceberg crashes vessels, above-water and under-water constructions.

Ice phenomena and ice formations become dangerous for productive activity during implementation of concrete productive activity, when they arrive to definite criterion. Thus, criterion must be précised, taking into account local ice conditions, and agreed with producing activity of served organizations.

### 3.5.2. “Ice river” phenomenon

*Analysis of hydrometeorological conditions and phenomenological description of “Ice river” phenomenon*

For a long time researchers of the Arctic Seas were interested in increased velocities of currents and especially ice drift. Ice, drifting in these local rapid flows, complicates navigation of ships and icebreakers in the freezing seas due to occurrence of huge, ice mass, “attached” to ship, which sometimes can cause emergencies and even catastrophes. At the same time ice floes, moving with a current, are excellent “tracers” for systematic airborne observations using aerial photosurvey. It is impossible to carry out these measurements using direct instrumental methods, because ice, drifting with high velocity, often presences a mixture of ice cake and small ice cake sometimes during compacting.

High velocities of ice drift were confirmed last decades as a result of instrumental observations. Extremely high velocity of ice drift often caused critical situations and emergencies during navigation in the Arctic. Ships of ice class and even of icebreaking type



were powerless in conditions of extreme ice drift with compacting. Thus, at the present moment it is impossible to counteract against catastrophic phenomenon of “Ice river”. Danger degree of phenomenon should be dependant on current velocity in flow and mainly on ice concentration and compacting. Water flow with broken ice can overcome almost every ship. However, big ships, powerful icebreakers, and even nuclear icebreakers can’t sail in slow flow of ice cake and small ice cake with concentration of 9–10/10-th. At that they are playthings of nature for rather long time. Drift of nuclear icebreakers “Sibir”, “Arktika” and icebreaker “Kiev” in the region of Yugor Shar Strait in March-April of 1980, and also drift of icebreaker “Captain Sorokin” in the Yenisey Gulf in November of 1977, can be given as example. “ICE RIVER” (ICE JET) – is a non-stationary jet flow of close floating ice cake and small ice cake, drifting with high velocity and sometimes with compacting, in straits, gulfs or in open areas of freezing seas near the fast ice boundary or slow-moving ice massif.

Analysis of known cases of this dangerous phenomenon allows its detailed examining. High velocity of current and ice occurrence in flow are the determining factors for identifying this phenomenon as a very dangerous. At that presence of drifting ice, especially along fast ice boundary, when this phenomenon is accompanied by compacting, complicates navigation even under very small velocity of “ice river” current (0,5–1 knots).

Under its compacting ice, moving with the current makes resistance for ship motion which is several times more, than that of water flow itself. It is necessary to take into account that horizontal turbulent vortexes sometimes occur in such flow. Their spatial and temporal scale is determined by bends of fast ice boundary, ice thickness near its edge, size of ice floes and horizontal gradient of velocity in the stream itself. Horizontal and vertical velocity gradients are peculiar features of dynamic instability of non-stationary current under non-linear interaction of different fluctuations in jet flow. “Ice river” phenomenon often occurs on the background of steady or periodic currents, as multiple acceleration of this flow in the surface layer.

Current acceleration in straits with presence of drifting ice (with high denivelation of the sea level on opposite sides of the straight) should be related to the listed phenomena. Though a mechanism of extreme velocities formation often differs from mechanism of “ice river” formation in the open Arctic Seas, they are connected by one significant circumstance. This is a complication of ship motion in flow of drifting ice, causing emergencies. Existence of the fast ice boundary in straight, which narrows a surface current, can cause conditions for the current acceleration. That is why, under appropriate winds ice edge “works” as a wall with local (near edge) denivelations of the sea level on the background of general level inclinations in the straight. Local denivelation of the sea level is always formed by surge wind near the coast and also wind near the ice boundary (fast ice or slow-moving ice massif) in the sea with mixed layers

on liquid ground. Level gradients facilitate formation of extreme currents, which form phenomena like “ice river”, if drifting ice is present. Currents are accelerated especially significant in narrow straights, like Yugor Shar Straight, near Krestovskiye Islands in the Yenisey Gulf and others, even if ice edge is absent.

Formation of “Ice river” phenomenon occurs under definite conditions, which are defined by geographical, morphological, meteorological, ice and hydrophysical conditions.

*Geographical factors.* “Ice river” most often occurs in the Arctic straights independently on their location (regardless of some scientists opinion). These phenomena can be observed in narrow gulfs, where rivers flow, e.g. the Yenisey Gulf, Ob’skaya Bay and others, open parts of the Arctic Seas near coast with presence of fast ice boundary or close slow-moving floating ice massif.

*Morphometric factors.* The stated factors are narrowing of funnel-shaped coastline near straights, sea depth reduction, that is often summarized with effect of coast line narrowing, influence of configuration (sharp bends) of boundaries of fast ice or close slow-moving floating ice massif.

*Meteorological factors.* The meteorological factors, influencing formation, existence and weakening of “Ice river” phenomenon are the following:

- distribution of surface baric field gradients, i.e. surface wind, transmitting its kinetic energy to underlying ice surface due tangential stress as external exciting and supporting force;
- sustained effect of strong wind of the same direction;
- thermal processes as indirect factor of ice formation and melting;
- sharp and significant increase of air temperature in the cold season with strong frosts on the background, facilitating formation and outflow of brine from the ice, and as a result – significant salination of the water surface;
- hard frosts, facilitating rapid freeze-up of brine in young ice and desalination of the water surface .

*Ice conditions.* The ice conditions, facilitating formation, existence and weakening of “Ice river” phenomenon are the following:

- existence of drifting ice, often ice cake and small ice cake of different concentration, which joins this motion under the influence of current or wind, or under their combined unidirectional influence due to tangential stress at its lower and upper surfaces;
- existence of quite lengthy boundary of fast ice or close slow-moving floating ice massif, relatively to which ice cake with different concentration can join local motion due to effect of current and wind;

- formation of jammed brash barrier at the fast ice edge during compacting, which becomes multi meter deep wall for the surface water column often down density jump layer;

- reconstruction of local ice conditions under the influence of wind in narrow zone, when during compacting near the boundary of fast ice or massif, consisting of older thicker ice, strong ice breaking occurs. At the same time size regrouping of ice cake occurs due to different windage of ice floes;

- increase of roughness parameter with corresponding increase of wind drag coefficient of ice drift due to decrease of ice floe size, when its horizontal size becomes comparable to its vertical size during breaking;

- appearance of local sections, separating areas of different ice drift conditions, under opposing motion of drifting ice flows, which were caused by different reasons, occurred in different time, and some of them are indicators (“prints”) of past “Ice rivers”;

- formation of polynyas and leads in ice massifs.

Presence of drifting ice and increasing of roughness parameter are very important for jet flow formation, because small-sized floes join motion faster. Periodical compacting leads to ice floes regrouping, if ice is strongly broken and convergence is absent. As a result, narrow stripe of ice cake and small ice cake is formed along the boundaries of fast ice or ice massif, which plays role of “coast” for “Ice river”, when it was formed. The second - opposite coast is ice massif, composed from medium floes and small floes, which under favorable (for phenomenon formation) wind and current would be practically stable due to its rather large inertia relatively to ice cake and small ice cake due to their bigger windage. The more ice is broken near the edge, the more probable is formation of “Ice river” under appropriate wind and current.

If “ice river” flow is initiated by wind (“from above”), ice concentration in the flow must be maximum. If the flow was mainly initiated by hydrological reasons (“from below”), ice concentration of ice cake and small ice cake in the flow can be arbitrary. Though when concentration is small, the phenomenon is not “Ice river”, but just jet stream.

*Hydrophysical factors.* This is the most complicated and little-studied aspect of hydrometeorological conditions of the phenomenon under study formation.

The following factors can be related to these conditions:

- a). Total or local denivelation of daturence surface  $\partial\zeta/\partial n$ , created by surging wind, when large gradients of the sea level facilitate formation of strong gradient currents and their acceleration, if vectors of external and internal forces coincide;

- b). Presence of constant periodical – tidal and non-periodical currents, which accelerations under effect of other forces contributes to appearance of maximum velocities of jet flows;

- c). Driving of flows to the boundaries of fast ice or ice massif under the impact of Coriolis force;
- d). Occurrence of surface desalinated water layers with large static stability, divided by thin interlayer with high gradients of density  $\partial\sigma/\partial z$  – effect of “Dead water” (during motion of upper layer relative to the lower layer);
- e). Rapid ice heating under sharp and significant increase of air temperature, resulting in rapid abnormal desalination of the ice, salinity increase in the surface water layer, and formation of thin layer with high negative density gradients under it ( $-\partial\sigma/\partial z$ ) – instability of inversion type;
- f). Increase of salinity in the surface water layer during ridging in the winter period ( $S\% \rightarrow \max$ ).

Considering first three aspects, it is necessary to mention, that motion in flow is supported by tangential stress of wind  $w$  and strongly developed baroclinicity due to large denivelation of level  $\partial\xi/\partial n$  at opposite boundaries of straights, or may be polynyas or leads. Constant current and strong tidal current, forming jet flows, are often present a common background.

Last three aspects determine thickness of “Ice river” layer  $\Delta h$ , and, consequently, speed of its joining into motion and flow velocity. At that, listed processes, making effect of “Pure sliding”, create lubricant layer directly on ice bottom, and water isn’t practically join the motion.

Classification of all factors, determining conditions of “Ice river” formation, is presented in Fig. 3.5.1.

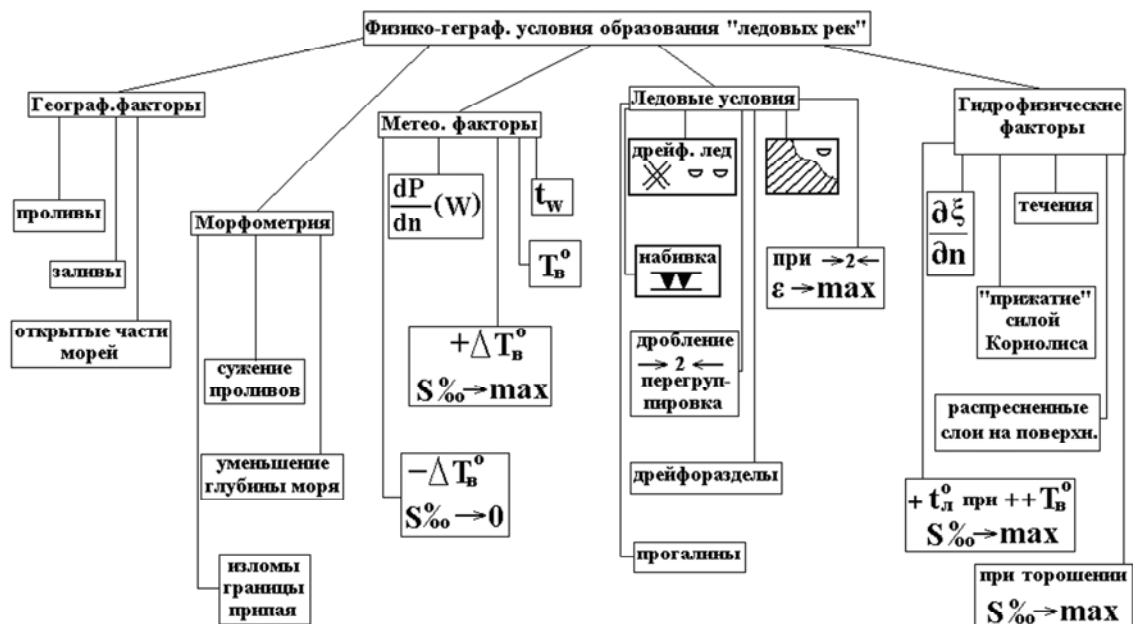


Fig. 3.5.1. Scheme of conditions, determining “ice rivers” formation.

Name of phenomenon (“Ice river”) is conventional, so using sea dynamics terminology it can be defined as extreme ice drift in boundary stream currents in a sea with strongly mixed layers, making an effect of “Pure sliding” in layer of density jump and surge effect with compacting along boundaries of close floating ice or fast ice in open regions of the freezing seas, gulfs and straights.

This complex of hydrometeorological conditions and their variability in the Arctic Seas exist quite often. Thus, total probability of “Ice river” formation is quite high, especially under at least partial combination of the listed hydrophysical factors.

Probably this phenomenon occurs quite often and visual information about it can be found on ice, as a “remained trace” of past “Ice rivers”. It means that sections, separating areas with different ice drift fields, which present frozen-up ridges of ice cake and small ice cake, located along coastal boundaries of fast ice or directly at the edges of large close ice formations, are often observed from airplane or ship, and visually look like boundaries of “Ice river”. Probably, this phenomenon occurred in other regions, but ice material was prepared for “Ice river” formation during quite long period. However, it is more probable, that this process occurred with beginning one of the hydrophysical factors (Fig. 3.5.1).

Anyway, sections, separating areas with different ice drift fields, are the indicators of high flow velocity in the past, because their typical feature is elongation (rectilinear) for several kilometers, and sometimes for tens of kilometers. Above all, large ice breaking degree after compacting and presence of (like “buffer” zone) near the ice edge point to phenomena like “Ice river”, which happened in the past.

Attendant hydrometeorological features in the entire history of the Arctic navigation are mentioned and recorded quite rarely. It can be explained by two psychological reasons.

Firstly, sailors were careless in recording attendant hydro meteorological conditions and especially in measuring their characteristics, after they had happily overcome a dangerous phenomenon.

Secondly, sailors unconsciously avoided regions, where “ice rivers” could occur.

Analyze of materials shows that normal duration of “Ice river” existence is directly proportional to its spatial scale, and is inversely to flow velocity. Scales of horizontal vortexes depend on heterogeneity size: internal waves on frictional boundary of density jump layer, sizes of sharp bend of ice massif or fast ice boundaries, ice floes distribution by size.

Scheme of flow velocity interactions in “Ice river”  $v$  with the listed meteorological and hydrophysical factors is presented on Fig. 3.5.2. Scheme of “Ice river” flow velocity dependence on meteorological and hydrophysical factors is presented in Fig. 3.5.2. Values of appropriate features, known from observation archive, are located in exponential stripe. The shown

dependence is qualitative and gives correspondence of scale of listed factors changes, because they are mostly evaluative and non-instrumental. Apart from that, the other vertical axes do not directly depend on horizontal axes. They are only directly proportional to each other.

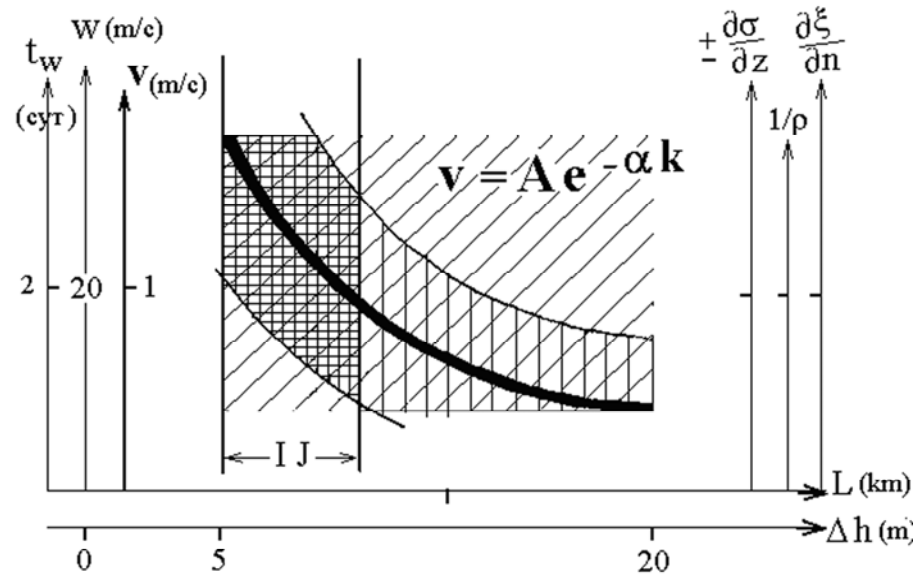


Fig. 3.5.2. Dependence scheme of flow velocity  $v$  in “ice river” (IJ) from wind force  $w$ , duration of wind activity  $t_w$ , water density gradient  $\sigma$ , level denivelation  $\xi$ , ice floes breaking value  $\rho$ , flow scale  $L$  and flow depth  $\Delta h$ .

Parameters of the factors, given on Fig. 3.5.2 from incomplete data archive, in general corresponds to the listed scheme, though they should be specified theoretically and experimentally. It is obvious, that “Ice river” boundaries (IJ – Ice Jet) are diffused according to all listed in the Figure parameters, because they were specified heuristically. General scheme of ice and wind conditions, and flow itself (IJ) in the “Ice river” region is presented in Fig. 3.5.3. and Fig. 3.5.4. (1, 2) points ( $d, e, g$ ).

Vertical structure of “Ice river” should be considered – its vertical profile along the motion axis under one force and wind direction  $W_r$  for two variants (1 and 2) of salinity and water density distribution and lubricant layer thickness of  $\Delta h$ .

Water density distribution  $\sigma$  in the left part of (1) in Fig. 3.5.4. according to hydrophysical factors corresponds to point ( $d$ ) and this process occurs in summer-autumn period. Processes, connected with sharp changes of air temperature and winter ridging are shown in the right part of Fig. 3.5.4 (2) and correspond to hydrophysical conditions of salinity maximum and minimum in surface under-ice layer according to points ( $e$ ) and ( $g$ ). All this takes place in autumn-winter period. The largest amount of originating “Ice rivers” fall on this autumn-winter-spring period (points ( $d, e, g$ )). Other cases of “Ice river” origination (IJ) (points ( $a, b, c$ )) can take place in any season under appropriate hydrometeorological conditions.

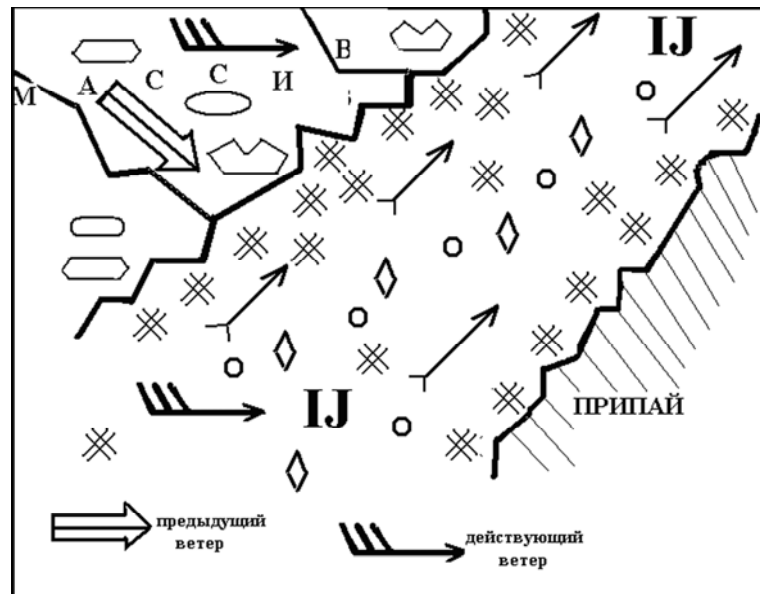


Fig. 3.5.3. General scheme of ice regime in the region of “ice jet” activity.

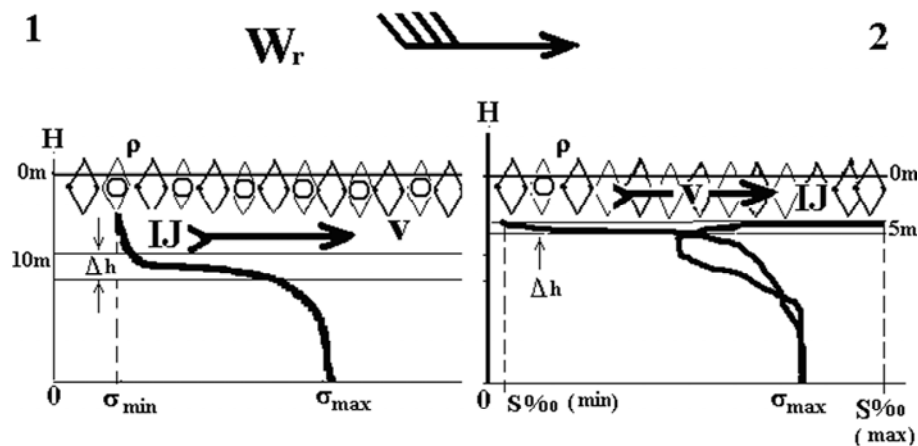


Fig. 3.5.4. Scheme of different variants (1) and (2) of “ice river” formation conditions (IJ) according to aspects ( $z$ ,  $\partial$ ,  $e$ ) of hydro physical list in described before classification.

Water density distribution  $\sigma$  in the left part of (1) on Fig. 3.5.4 according to hydrophysical factors corresponds to point (d) and this process occurs in summer-autumn period. Processes, connected with sharp changes of air temperature and winter ridging are shown in the right part of Fig. 3.5.4 (2) and correspond to hydrophysical conditions of salinity maximum and minimum in the under-ice layer, according to points (d) and (g). All this take place in autumn-winter period. The largest amount of originating “Ice rivers” fall on this autumn-winter-spring period (points (d, e, g). Other cases of “Ice river” origination (points (a, b, c)) can take place in any time of the year under appropriate hydro meteorological conditions.

Above all, the thinner is lubricant layer  $\Delta h$ , the higher is “ice river” velocity (IJ) under other conditions being equal in any seasons, i.e. there is inverse proportional dependence  $v \sim 1/\Delta h$ .

Scheme of “Ice river” flow velocity connections  $\mathbf{v}$  with the listed meteorological and hydrophysical factors is presented (Fig. 3.5.4). Scheme of “Ice river” flow velocity dependence on meteorological and hydrophysical factors is presented in this figure. Values of corresponding characteristics, known from observation archive, are located in exponential stripe. This dependence is qualitative and gives correspondence of scales of changes of the listed factors, because they are mostly evaluative and non-instrumental. Apart from that, other vertical axes are not in direct dependence on horizontal axes. They are only proportional to each other.

Parameters of factors, which are given on Fig. from incomplete data archive, in general correspond to the listed scheme, though they should be specified theoretically and experimentally. It is obvious, that “Ice river” boundaries are diffused according to all parameters, presented in Figure, because they were specified heuristically. On Fig. 3.5.5 a chart of probable “Ice river” formation is presented under particular synoptic conditions as an example.

According to evidences of captains of diesel and nuclear icebreakers, participated in transport ships steering in the western sector of the Arctic during last years “Ice rivers” quite often significantly complicate navigation operations. Navigation is especially complicated in the regions of Yugor Shar Strait, Kara Gate and approaches to Dixon Island (mostly from the south), in the straits of Nordenskjold archipelago and others.

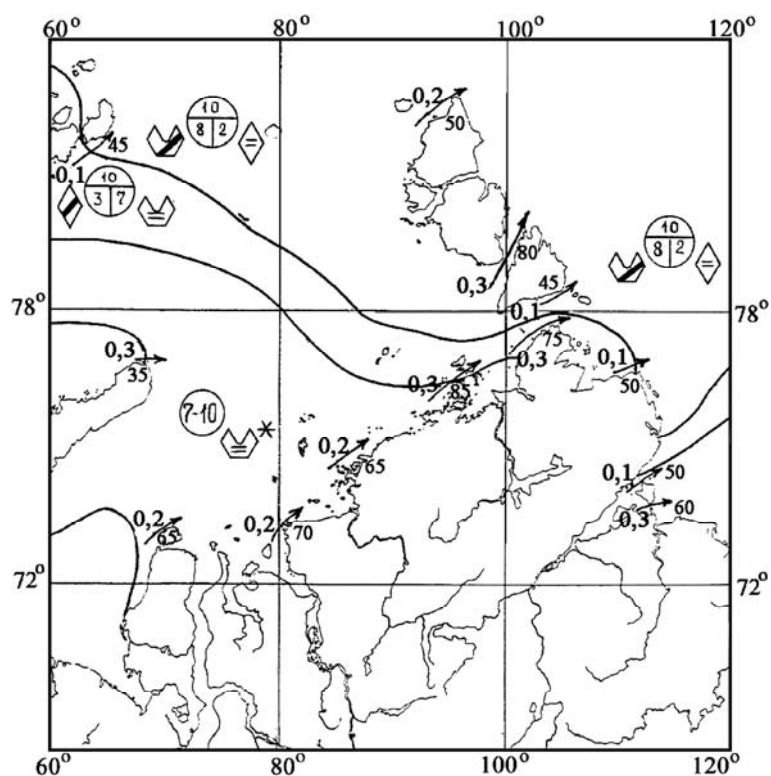


Fig. 3.5.5. Probability chart (0-1) of “ice river” formation in the Kara Sea under strong south-western wind in autumn. Two-digit numbers (35 – 80) - probabilities (per cent) of (IJ) occurrence in local regions.



### 3.5.3. Snow-ice “pillow” adhesion with a ship hull

Snow and ice adhesion with a hull of icebreakers and transport ships during their sailings in autumn-winter period is a typical phenomenon. It is rarely observed in spring, only in cases of new ice (grease ice, nilas and grey ice) formation in polynyas and fractures.

During summer period of navigation this phenomenon usually is not observed. Process of snow-ice “pillow” adhesion to a ship hull consists of two stages:

1. Adhesion of crushed ice-snow conglomerate to a ship hull and rapid growth of its mass to length and width (contact of the surfaces ice – steel).
2. Freezing of ice pieces together in the entire monolith, composing body of snow-ice “pillow” (contact of the surfaces ice – ice).

Typical features of ice adhesion to a ship hull are suddenness of snow-ice “pillow” formation, and its avalanche-like increase and large force of ice adhesion to a ship hull.

The largest frequency of occurrence of adhesion is observed at the ship bow, where stress is stronger. Snow-ice “pillow”, formed near stem, propagates along shipboards to the midship. Cases, when ice adheres along the entire shipboard are observed very seldom. Frequencies of adhesion occurrence from the port side and from the starboard are approximately equal. Adhesion size on the port side and on the starboard can be different. Adhesion width can reach 15 m on one side, and less than 1-2 m on another at the same time.

Adhesion intensity is estimated by different features, which accounts spatial-temporal scale of phenomenon and force of ice adhesion to a ship hull.

- Weak adhesion – episodic adhesion, occurring once in 10-15 minutes on small areas of shipboard (1-2 m width and 3-5 m length). If snow-ice “pillow” hits channel edge during motion, it easily and completely separated from the ship falls off.
- Average adhesion. It is formed every 5-10 minutes and its size is 2-4 m width, and 5-20 m length. Ice is separated from the ship only after repeated reverses.
- Strong adhesion. It is formed continuously, along the entire shipboard, and its width is more than 4 m. After reverses it doesn’t completely separate from the ship.

Typical ice conditions, when adhesion is observed, are divided into three main types.

- Jammed brash barrier from grey and grey-white ice, occurred when compacting is up to 2 marks. Adhesion is intensive, and width of snow-ice “pillow” is in the range from 2 to 10 m.
- Ice brecchia of jammed brash barrier, ice cake, small ice cake, thin and medium first-year ice with snow depth more than 15-30 cm. Adhesion is intensive, and width of snow-ice “pillow” is more than 4-5 m.

- Thick first-year ice with snow depth more than 20-40 cm. Adhesion is of short duration and weak if compacting is absent. If compacting is up to 2 marks, average adhesion is possible.

The strong and average adhesion is observed for the following characteristics of ice conditions: ice concentration is 10/10-th, ice thickness is 30-70 cm, ice ridging is 2-3 marks, ice compacting is up to 2 marks, and snow cover depth on the ice is 30-40 cm and more.

Phenomenon of icebreakers and transport vessels adhesion essentially determines technical capabilities of their operation.

Adhesion with average intensity reduces velocity of “Moskva” type icebreakers up to 1-3 knots during their sailing in grey-white ice. When adhesion is absent, its velocity is about 10 knots in the same ice conditions.

Typical example of snow-ice “pillow” formation at the board of icebreaker “Kapitan Dranitsyn” during its sailing in the Laptev Sea is shown in Fig. 3.5.6.



Fig. 3.5.6. Example of icebreaker hull “Kapitan Dranitsyn” covering with ice in the northern Laptev Sea (coordinates  $79^{\circ} 15' \text{ N}$ ,  $125^{\circ} 47' \text{ E}$ ) on the 2<sup>nd</sup> of September, 2003 with nilas. Top view, along the board. Intensive white part along left bow of icebreaker – snow-ice pillow.

Ice adhesion to the ship hull limits technical capabilities of icebreaking and transport fleet operation, as well as lead to emergencies. Sudden stop of icebreaker is a typical situation, when adhesion begins. It presents a real threat of collision with a steered ship, which can't avoid piling. This danger is aggravated by ice compacting during adhesion, i.e. when steering distance is suddenly reduced (distance between hulls of ships). Number of emergency cases due to ice

adhesion to ship hull amount to 10% of the total number of crashes, caused by ice conditions. Strong and average ice adhesion to ship hull is regarded as dangerous ice phenomena, due to its influence on navigation safety.

In order to remove a “pillow”, adhered to the ship hull, a navigator has to use reverses and engage a trimming system. Nevertheless, most “favorable” conditions for snow-ice “pillow” formation occur during “forward – back” motion in a channel with crushed small ice cake. Thus, ships less suffer from adhesion effect during sailing in undisturbed ice parallel to a channel, than in the channel filled with crushed small ice cake.

Intensity of snow-ice “pillow” formation, according to natural observations, depends on technology of making channel in compact ice. When icebreaker speeds up in compact ice, it “gets stuck” by waterline perimeter. It makes favorable conditions for snow-ice “pillow” formation. Thus, practical resume can be made: to reduce possibility of ice adhesion during making a channel, it is necessary to work as “chopper” or make a channel, as wide as possible, limiting icebreaker’s path by reducing its power.

State of hull surface (its deterioration) significantly influences adhesion process, i.e. roughness degree of connecting surfaces. If roughness increases, ice adhesion to hull increases.

Using probability maps of strong and average ice adhesion to ship (icebreaker) hull provide for estimation of typical ice conditions for its formation.

Natural studies of ice “pillow” formation conditions were carried out during voyages of icebreakers “Lenin”, “Sibir” and “Arktika” in different regions of the Kara Sea. The results showed, that in spite of differences in morphological ice characteristics and thermohaline structure of surface water layers, a thick shuga layer or intrawater ice layer of several meters thick, consisting of small isometric crystals not more than 5 mm in diameter, always persist under ice during formation of this phenomenon. As a result of ice drilling it was found that the thickness of snow-ice “pillow” itself can reach 6-8 meters, and 80-90% of it consists of these crystals, which hold large ice pieces on its surface.

Based on the studies of this ice formation phase composition it was concluded that the mechanism of ice adhesion to a ship hull origin must be connected with dynamic conditions of ice formation, providing formation of shuga or intrawater ice layer under the ice cover. This conclusion is confirmed by fact, that in most cases this process is observed during lead formation due to dynamic motion of the ice and formation of open water areas. The Northern Sea Route passes through the marginal areas of drifting ice massif and areas of flaw polynyas, where the most intensive formation of intrawater ice and shuga is observed, and therefore the equal probability of the ice adhesion phenomena occurrence along the entire route looks reasonable, which is confirmed by long-term statistical data.

Results of the long-term laboratory experiments and natural studies allowed making several conclusions about conditions of ice adhesion to icebreakers and ships in the Arctic Seas:

1. Beginning of ice adhesion phenomenon can take place under different hydrometeorological and ice conditions.

2. Lack of changes in vertical distribution of temperature gradient along the ship hull and values of electric potentials difference under its interaction with the ice at the moment of ice “pillow” formation evidences that these two physical parameters can’t be the first cause of the phenomenon under study.

3. Thermohaline stratification of intrawater ice and shuga in the under ice layer can significantly facilitate occurrence of ice adhesion phenomenon.

4. Mechanism of contact occurrence of intrawater ice and shuga with a ship hull, causing ice “pillow” formation, must correspond well with observational results:

a) if icebreaker speed increases, ice contact with metal disappears;

b) absence of intrawater ice and shuga crystals freezing between itself, and with pieces of the ice and icebreaker hull in ice “pillow”;

c) asymmetry of ice “pillow” formation during work even in the same part of ice cover;

d) ice compacting facilitates ice “pillow” formation, and its fracturing and break up destroys it.

Map of the Kara Sea, where natural tests (measurements of snow-ice “pillow” parameters) in different sea regions in different years were carried out from the nuclear icebreakers “Lenin” and “Arctic” is presented in Fig. 3.5.7.

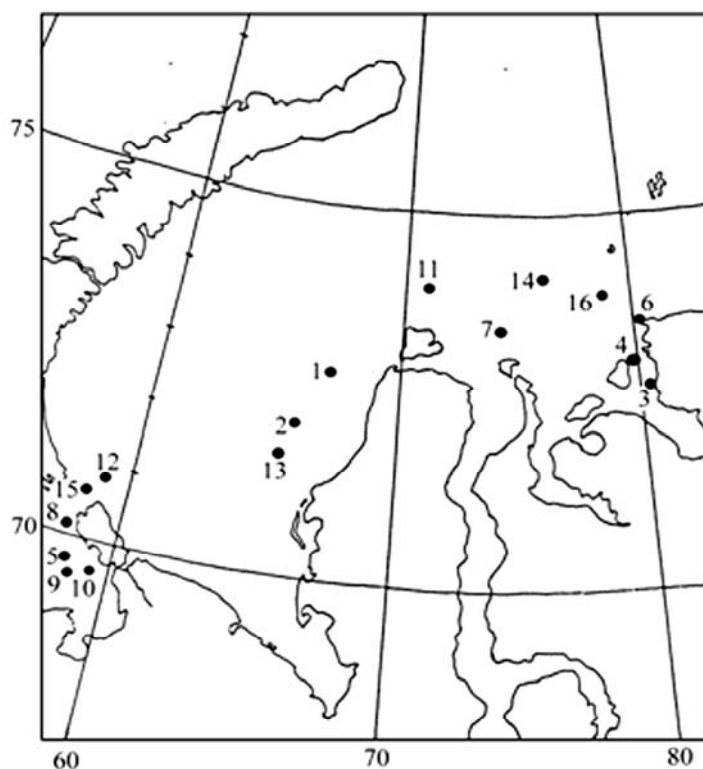


Fig. 3.5.7. Location of points, where field observation of NIB “Lenin” hull covering with ice occurred in December-January, 1987-88 (points 1-10), and NIB “Arctic” in December-January, 1988-89 (points 11-16).

Since in ice brecchia of thin and medium first-year ice with thickness of 50-100 cm, where ice “pillow” is formed most often, the icebreaker moves with speed not more than 5-6 knots, the value of dynamic flow pressure amounts to 0,004 MPa. It is almost half of the force of ice crystals film interaction with icebreaker hull, which for the listed conditions can amount to 0,008 MPa. However, in the period of field observation conducting, in two cases from 16 (points 7 and 12 in Fig. 3.5.7) works were carried out on ice brecchia of grey-white and thin ice with a thickness of 30-35 cm, under which even shuga layer with a thickness of 2,5-3,0 m was observed. During icebreaker motion in it with a speed of 12 knots ice adhesion was not observed. Only typical motion of ice pieces along hull on distance of 5-10m was observed. When the icebreaker reduced a speed to 5-6 knots, ice “pillow” was formed, and icebreaker lost speed completely. When it started motion using full power the similar picture was observed.

Thus, conducted field observations completely approved an influence of water flow specific pressure on formation of initial layer of ice “pillow”, which had to be formed with increasing value of this parameter up to 0,019 MPa.

### 3.6. Ice effect on engineering constructions

#### 3.6.1. Vessel classification.

Observations of creation and implementation of rules and recommendations of vessels projecting and operation are regulated by “Rules of projecting and classification of vessels”. Special classification organizations look after their compliance: English Lloyd, American Bureau of navigation, Norwegian VERITAS, German Lloyd and Russian Marine Navigation Register. At first these classification organizations (except of RMNR) were established as national insurance companies. Then, vessels classification on the basis of many features became necessary to fix insurance premium due to development of navigation and shipbuilding. It's incorrect to fix the same rate of insurance payment for loss/damage of cargo or ship itself for vessels, which size differs a lot. The most essential feature for ships of transport fleet is their displacement, which approximately determines amount of transported cargo.

Another essential feature is a ship construction, which mostly determines ship hull strength, possibility of safety navigation in rough sea, cruising range, and finally terms of ship exploitation. This is particularly important for ships navigation in ice. Any ship, designed to navigate in the ice, must have appointed ice class of Register or other classification organization. This class establishes requirements to amount of ship hull strengthening due ice impact to correspond the necessary level of ship hull strength, which is additional to that for ships without ice class. There are other requirements to screw propeller strength, power capacity, etc., but the main one is to the ship hull strength.

Technical detail design of the ship is presented to the Register for technical examination and approval before ship constructing. The Register inspection employees observes constructing works, and ship can't be delivered to customer for exploitation, and further it can't put to sea without special examination and permission of Register, attesting appropriate technical condition of a ship, which guarantee its safe exploitation. RMNR is not only an insurance company (as other foreign classification organizations), but ship must obligatory receive the Register class to negotiate an insurance contract and obtain insurance payments for loss/damage of cargo or ship. Ship, which wasn't registered in any classification organization, would be some kind of «*Flying Dutchman*», with a difference that this hypothetical ship physically did not exist, but threatened with its non-material phantom. Thus, our hypothetical ship can exist physically, but either sea administrations or cargo owners won't “see” it without having a juridical person.

Ship classification and rules of their construction have a long history of more than 200 years. History of projecting, building and operation of engineering constructions for the sea shelf

is much shorter. The first “Rules of classification, building and equipping of floating drilling constructions and marine stationary platforms” by RMNR were published in 2001.

The clause 3.10.1.2 in chapter 3.10 “Ship strengthening for navigation in the ice” of the Rules of Register (edition of 1990), states: «These rules regulate a minimum necessary strength level under effect of calculated ice load and ship construction depending on sign of the category mark of ice conditions in symbol of its class”. At that, it means that ship owner would operate a ship according to its passport, developed by competent organization, which specifies condition of safe ship operation in the ice, depending on sign of the category of ice strengthening, ice conditions and icebreaker support”. As it follows from the text, RMNR provides minimum margin of projecting/building safety for ships in these rules. Other competent organizations, firstly, AARI (presented by its main structural subdivision – department of ice states of ships) develop recommendations of safe navigation regimes in specific ice conditions.

Theoretical tasks to determine forces, occurring during ship push on the ice, solved at AARI in the 60s of XX century, allowed calculating ice loads for different types of contact at a good theoretical base. Levels of construction strength were set to efficiently resist loads. Ship hull strength to ice impact became a new field of studies. At the same time semiempirical method to calculate ice resistance to ship motion was developed, using possibilities of model experiment in the ice basin, and the independent field of hydromechanics – ship motion in the ice was established.

Peculiar features of operation and designing ships for navigation in the ice are exceptionally caused by ice cover existence in the Arctic Seas, at that, in several regions of the Arctic Ocean ice is observed all the year round.

Two directions of studies, described above – ship hull strengthening and ship motion in the ice are based on analysis of the processes of ship hull interaction with the ice. Classification of ice conditions as an environment for ship sailing was developed based on these results. It is different from the ice nomenclature, and depending on deformation type and ice melting, it can be subdivided into three categories: close ice, medium floes, small floes and ice cake.

Close ice is understood here as fast ice or floes of drifting ice, which are destructed during ship motion as a result of flexural strain. Depending on ship speed and ice thickness, minimum floe size was determined, which ship overcomes as “close ice”, i.e. when floe isn’t split by cracks.

Ice cake is an ice floes accumulation, and they cannot be destroyed by flexural strain due to their small size even with their relatively large thickness. Ice is just separated apart by ship hull and partly sunk. In this case main components of ice resistance to ship motion are components of ice floes separating and sinking.

Small floe – is ice, where ship motion is characterized by processes, typical for both close ice and ice cake.

Naturally, methods of ice resistance calculation to ship motion in listed conditions were developed, i.e. methods of ship velocity calculation in these conditions – ship motion in the ice. It is essential, that ice loads on ship hull and construction response – ice strength - were calculated for cases of ice motion in these conditions.

Important nomenclature characteristic of drifting ice, which should be taken into account in the calculations, is concentration – the ratio expressed in tenths describing the amount of the sea surface covered by ice as a fraction of the whole area being considered. Compact drifting ice has a concentration of 10/10-th and no water is observed. Close ice is a drifting ice with a concentration of 7-8/10-th, composed from ice floes, contacting with each other. Open floating ice is a drifting ice with a concentration within 4-6/10-th with large amount of fractures; ice floes don't generally contact with each other. The next in the nomenclature is very open floating ice (1-3/10-th) and open water – less than 1/10-th.

Very important phenomenon is also ice compacting, which is related to dangerous ice phenomena and significantly complicates navigation in the ice. It obliges a designer to strengthen midship according to requirements of RMRN. Classifying, unfortunately, is qualitative and by external features and is estimated by three-point scale.

### 3.6.2. Typical regimes of ship operation in the ice.

#### 3.6.2.1. Uninterrupted motion in compact ice.

This regime is typical for icebreakers and ships of active ice navigation, i.e. ships, which have relatively high ice class. In this regime (due to icebreaking form of bow line) ice is destroyed by flexure due to occurring vertical forces. Ice loads at that are not large and can't be determining in the calculation of hull construction strength. However, this regime (regime of uninterrupted motion in the ice) most accurately characterizes ship passability through the ice – its ability to overpass the ice. Only during motion in level compact ice three main parameters can be rather accurately measured: ice thickness, power of energy installation and velocity of stable ship motion under these conditions. Curves of ship passability through the ice can be drawn based on these three parameters. Maximum ice thickness, which ship overpasses by uninterrupted course with stable velocity about 2 knots, is accepted to term as maximum ship passability through the ice.

The maximum ship passability through the ice is a passport characteristic of a ship, though in real conditions compact level ice is rarely observed.



### 3.6.2.2. Ice destruction by runs.

This regime is typical for icebreaker operation, when it can't move continuously. At that, the largest ice loads occur, when icebreaker pushes the ice, but doesn't destroy it, only crushing ice floe edge.

### 3.6.2.3. Motion in channel behind icebreaker.

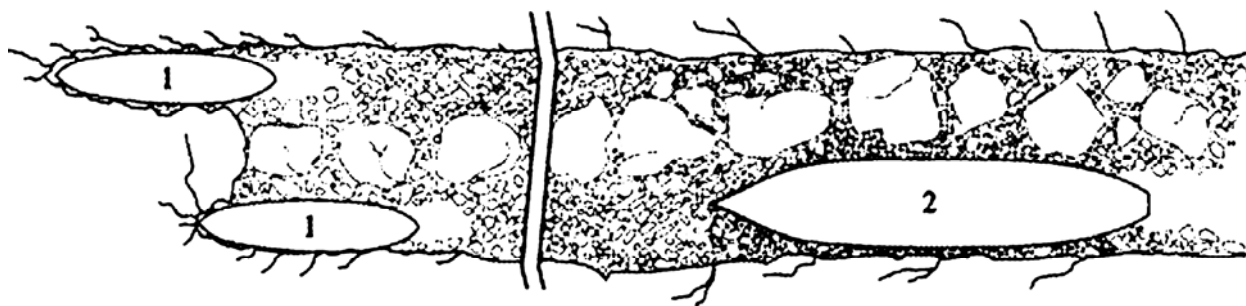
It is one of the most important regimes of transport ships navigation under icebreaker steering. At that medium floes and ice edge in channel hit the hull of steered ship. In the last case ice loads can be high, what is approved by results of multiple natural tests of hull strength and analysis of ship damage, due to her piling on edge of ice floe. The variant of reflected blow in the channel edge, when ship is thrown from one safe edge of the channel to another, is the most dangerous.

	«Ермак»	«Мудьюг»	«Калитин Драгунцов»	«Арктика»	«Гайдак»
Длина, м	134,84	88,49	129,02	148,00	149,70
Ширина, м	26,05	21,17	26,50	30,00	28,87
Осадка, м	11,0	6,5	8,5	11,00	9,00
Тип энергетической установки	дизель- электрич.	дизельная	дизель- электрич.	атомная	атомная
Мощность ЭУ, МВт	30,462	9,560	18,240	55,000	36,800

Fig. 3.6.1. Main types of the icebreakers

In this case, its value increases due to increase of cosine of resultant ice load direction. Ship steering by icebreaker is used in close drifting ice. In this case channel edge is formed by ice floes moved apart and broken by icebreaker. Taking into account, that they can be quite thick, and speed is quite high, blows in channel edge can also be dangerous.

◆ Движение под проводкой двух ледоколов (в случаях, когда ширина судна существенно превышает ширину ледокола)



Расположение судов в караване (1 – ледоколы, 2 – судно)

Fig. 3.6.2. Icebreaking convoy

#### 3.6.2.4. Ship motion in drifting ice.

This regime is typical for both icebreakers and ships of all ice classes. Ship motion in floes of drifting ice can be quite similar to motion in the compact ice.

Navigation in drifting ice, depending on its concentration, has its own peculiar features, which should be carefully studied. Navigation in compact floating and close floating ice (when ice floes mostly contact with each other) is generally determined by ship passability through the ice and depends on engine power and hull shape. As a rule, considerable ice loads aren't observed, because ship (in regime of autonomous motion) can't develop high speed in thick ice, causing large ice loads. In thin drifting ice the situation is opposite. Under quite high speed, loads, destroying ice, are not large and aren't dangerous for ship hull. Open floating ice is quite another matter. Ship can make quite high speed due to presence of fractures between ice floes. Sometimes navigator can't reduce speed or turn aside from oncoming ice floe, which can be thick enough to have grave consequences.

Methods for determining maximum ship passability through ice should be presented separately. As mentioned, it is a passport characteristic of any ship. The only reliable method to determine it - natural testing of constructed ship in real operation conditions. It is necessary to mention, that in the 50s of XX century by special decision of Council of Ministers of USSR AARI was appointed a directing agency to be responsible for designing icebreakers and ice class vessels, designed and constructed for USSR on foreign and domestic shipyards. In the 60s USSR

Ministry of Marine Fleet issued an order, stating that every lead ship of the ice class series must be tested in natural conditions, under the direction of AARI and according to program, prepared at AARI. Special time and ships (often distracted from main voyages) were fixed for these testing. At that one of the main tasks was determination of the maximum ship passability through the ice.

Level ice floes were chosen for testing (it is desirable in several thickness ranges). On every ice floe ship started to move using engine operative mode with step change of power. Each operative mode was changed, when ship passed not less than three lengths of its hull with constant speed using fixed power (in rudder position of “rudder straight”), i.e. motion regime was considered stable. Ice thickness, accompanying meteorological conditions and ship speed were recorded with the most possible accuracy. As a rule power and number of rudder revolutions were recorded from ship instruments. It was desirable to study several operative modes on each testing area, characterizing dependence of speed on power for given ice thickness. But it depended on thickness of level ice in the testing area: investigators received one or two points for ice thickness values, which are near the maximum for a given ship. The maximum ship passability through the ice, determined in this way, was both certificate ship characteristic and test of development work, which specified ice characteristics of the ship on stage of its designing.

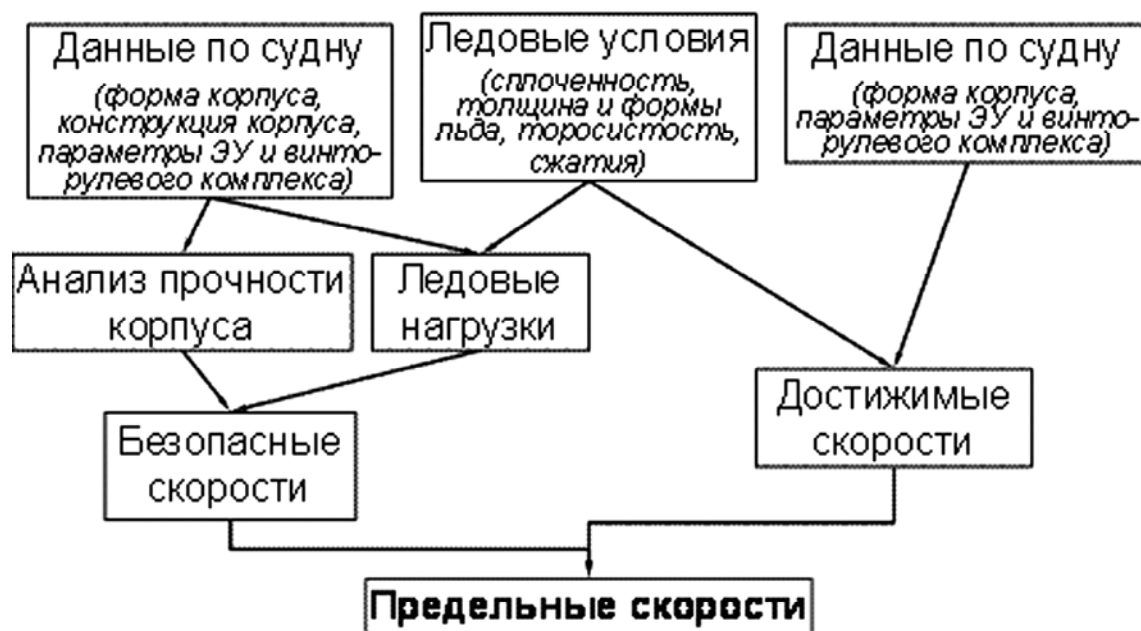


Fig. 3.6.3. Calculation of the ship velocity in ice conditions

The other method of ice characteristics of ships determination is the method of model testing in the specific ice tank. This method could be used after bringing into operation of the specific ice tank at AARI in 1955 – the first ice tank in the world. At the same time a methodic of ice

modeling in this ice tank was developed. In compliance with the similarity theory, this methodic provided for compliance of geometric, kinematic and dynamic similarity criteria, which gave satisfying convergence of experiment results with nature.

The method is good in a way, that model testing is conducted on the projecting phase, and designer, accounting the experiment results, can correct the project and improve ice characteristics of the ship under construction. Accuracy of the of experiment results recalculations for nature depends on methodic of modelled ice formation, used in this ice tank. Shape of ship hull is optimized to reach maximum ship passability through the ice, based on the results of these tests. Minimum acceptable power of energy installation is established to provide specified ship passability through the ice; variants of rudder and screw propeller protection from ice are investigated. Shape of hull, ship passability through the ice, power and variants of screw propellers protection were worked out for both icebreakers and transport ships at the AARI ice tank. Model testing of transport ships (“Amguem” type) takes the special place in testing. Due to long series of model testing, ships of this type have better passability through ice, comparing with the more powerful (on 17%) prototype (diesel icebreaker “Lena”). Shape of “Amguem” type hull is admitted to be classic. More than 15 ships of these series were built. For many years they transported cargoes to the most distant settlements of the Russian Arctic in heavy ice conditions.

It is necessary to mention, that the first in the world ice tank of AARI became a prototype for designing and constructing many foreign experimental ice tanks. Similar tanks (in different variants of construction) were built in Finland, Germany, the USA, Canada and Japan. The International ice towing tank committee (ITTC) was established in 1970s. A series of comparative control testing of the same ship model were carried out in all ice tanks by ITTC initiative. The purpose was to inspect testing methodic in different ice tanks and methodic of model testing results recalculation to natural conditions. The results of testing in the AARI ice tank were admitted to be one of the best.

Possibility to check out the results of theoretical developments by model and natural testing data significantly advanced two main directions of providing ice characteristics of ship: ship passability through the ice and ice strength. In early 1970s an idea of ship “Ice certificate” was developed and realized in the department of ice characteristics of the ships. This idea was based on combined usage of ship passability through ice calculations, calculations of ice loads, analysis of hull reactions to these loads and calculations of safe speeds for ship motion in different ice conditions. Ice passport is a collection of recommendations to choose safe regimes of motion in different ice conditions for different ship types.

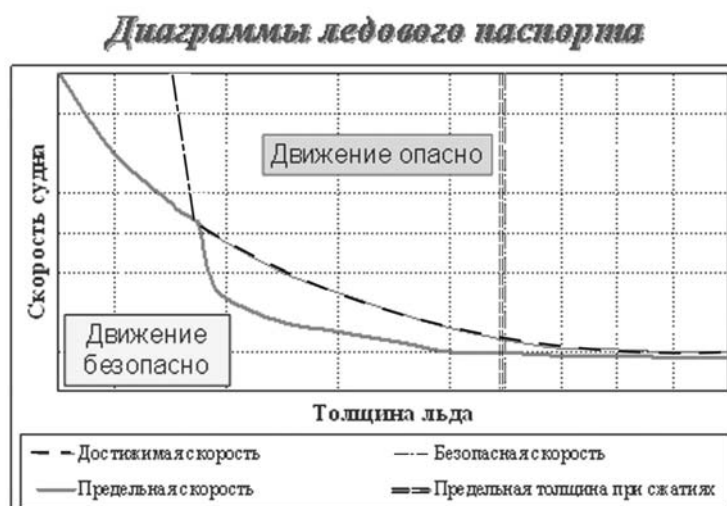


Fig. 3.6.4. Diagram of ice passport

First ice passport was developed by request of Murmansk Shipping Company for ships of “Pioneer Hero” series in 1974. There were already 10 ships of this series and significant part of cargo transportations in the NSR was provided by them. Natural testing was necessary for verification of calculation models of assessable and safe motion speeds. They were carried out in summer of 1973 onboard the motor ship “Shura Kober” during her Murmansk – Dixon – Tiksi – Igarka voyage. Tensometric testing of ship hull and ship passability through the ice were made during this voyage. In autumn testing was continued onboard “Tonya Bondarchuk”, which is of the similar ship type, in level young ice in the Yenisey Gulf and in the Kara Sea. Ice passport was developed and given to customer in 1974 on the base of testing. In fact, beginning from 1974 by requests of ship owners – Murmansk, Northern, Far Eastern and Primorsk Shipping Companies, one ice passport for particular type of ships was annually developed. Totally, ice passports were developed for more than 30 types of domestically produced and foreign ships.

## **Conclusion**

Observation of natural phenomena and summarizing of obtained results are the most widespread methods either for studying natural environment or implementation of economical activity under unfavorable natural conditions. Observations allow finding general regularities and lead to them.

Complex of theoretical aspects was considered in training manual, connected with providing observations of ice cover. Uppermost, for their analyze it was necessary to present general features of ice conditions in freezing seas in their connection with observation methods.

Specialists, trained during this course in 2007-2008, took part in studies during the International Polar Year, organization of series of “North Pole” drifting stations and in other work on hydro meteorological support in the freezing seas of Russia.